THE UNIVERSITY *of* EDINBURGH

Transition Metal Complex-Based Molecular Machines

by

Dhassida Sooksawat

Degree of Doctor of Philosophy

School of Chemistry

The University of Edinburgh

October, 2014

Lay Summary

Inspired by the performance and evolutionarily-optimised natural molecular machines that carry out all the essential tasks contributing to the molecular basis of life, for example, ribosomes, large and complex molecular machines that make proteins from amino acids within all living cells, chemists aim towards fabricating synthetic molecular machines that mimic biological nanodevices with potential applications in catalysis, drug delivery, electronic materials and sensing. The use of rotaxanes, compounds that consist of a dumbbell-shaped molecule or a thread surrounded by a ring molecule and terminated by bulky groups that prevent disassembly, as a prototype for molecular machines has emerged as a result of their ability to undergo translational motion between two or more stations within the thread. Although biological machines are capable of complex and intricate functions, their inherent stability and operational conditions are restricted within living organisms. Synthetic systems offer a limitless number of building blocks and a range of interactions to be manipulated. Transition metal-ligand interactions are utilised as one strategy to control the directional movement of submolecular components in artificial machines due to their well-defined geometric requirements and significant strength.

This thesis presents new externally addressable and switchable molecular elements for transition metal complexed-molecular machines involving a common chemical reaction with acid-base. The proton input that induces changes to platinum complexes can be exploited to control exchange between different coordination modes of platinum complexes either 2+2 or 3+1 square planar donor sets. The development of the pH-switchable metal-ligand motif for the stimuli-responsive platinum-complexed molecular shuttle based on a rotaxane structure has also been explored. The metal-directed self-assembly of tubular complexes were studied in order to develop self-assembled rotaxanes. A series of metal building blocks was explored to extend the scope for a tube self-assembly.

Table of Contents

Abstract

Inspired by the performance and evolutionarily-optimised natural molecular machines that carry out all the essential tasks contributing to the molecular basis of life, chemists aim towards fabricating synthetic molecular machines that mimic biological nanodevices. The use of rotaxanes as a prototype for molecular machines has emerged as a result of their ability to undergo translational motion between two or more co-conformations. Although biological machines are capable of complex and intricate functions, their inherent stability and operational conditions are restricted to *in vivo*. Synthetic systems offer a limitless number of building blocks and a range of interactions to be manipulated. Transition metal-ligand interactions are utilised as one strategy to control the directional movement of submolecular components in artificial machines due to their well-defined geometric requirements and significant strength.

This thesis presents new externally addressable and switchable molecular elements for transition metal complexed-molecular machines involving an acid-base switch. The proton input that induces changes to cyclometallated platinum complexes can be exploited to control exchange between different coordination modes. The development of the pH-switchable metal-ligand motif for the stimuli-responsive platinum-complexed molecular shuttle has also been explored. The metal-directed self-assembly of tubular complexes were studied in order to develop self-assembled rotaxanes. A series of metal building blocks was explored to extend the scope for a tube self-assembly.

Declaration

The scientific work described in the present thesis was carried out in the School of Chemistry at the University of Edinburgh between November 2010 and June 2014. Unless otherwise stated, it is the work of the author and has not been submitted in whole or in part for any other degree or professional qualification at this or any other University or institute of learning.

Signed:……..

Date:……..

Meetings Attended and Presentations Given

1. Organic Research Seminars, School of Chemistry, University of Edinburgh, UK, 2011-2014.

Oral presentations:

a) *Transition Metal Complex-based Molecular Machines*, December 2011.
b) *Transition Metal Complex-based Molecular Machines*, January 2013.
c) *Transition Metal Complex-based Molecular Machines*, May 2014.

2. School of Chemistry Visiting Speaker Colloquia, School of Chemistry, University of Edinburgh, UK, 2010-2014.

3. RSC Perkin Division 39th Scottish Regional Meeting, University of Edinburgh, UK, December 2010.

4. RSC Perkin Division 40th Scottish Regional Meeting, University of Strathclyde, UK, December 2011.

5. School of Chemistry, Organic Section Firbush Symposium, Firbush Point Centre, University of Edinburgh, UK, April 2012.

Poster presentation: Towards Molecular Machines based on Platinum(II)-Complexed Rotaxanes

6. 14th International Seminar on Inclusion Compounds, Heriot-Watt University, UK, August 2013.

7. RSC Macrocyclic and Supramolecular Chemistry Meeting, University of Glasgow, UK, December 2013.

Poster presentation: *Acid-base Responsive Switchable Platinum Complexes*.

8. RSC Perkin Division 42st Scottish Regional Meeting, Heriot-Watt University, UK, December 2013.

Acknowledgements

First of all, I would like to express my sincerest gratitude to my supervisor, Dr. Paul Lusby, who has given me the opportunity to work in his group and supported me throughout the four years of my PhD journey with patience and encouragements. Without his input, guidance and enthusiasm, I would have struggled and this thesis would not have been completed. I am proud to be student number four who graduated from this powerful and energetic group.

When I first came to the group, Dr. Oleg Chepelin and Dr. Paul Symmers helped me settled down and were always willing to lend their hands when needed. They were also my moral and intellectual supports and we became good friends over my four years in Edinburgh. So, many thanks to both of you for your precious friendship. I am also grateful to David August and Michael Burke, whom I considered more than colleagues. It has been my pleasure to work and play with them over the past two years. Also, I would like to acknowledge Matthew Edwards, my project student last year who recently became a new member of the group.

I would like to extend my thanks to the School's support staff: Dr. Lorna Murray and Dr. Juraj Bella who always make sure all the NMR spectrometers run smoothly 24/7; Alan Taylor for the mass spec service; Annette, Amanda, Rona and Denise for their help with administrative matters; and Tim, Raymond, John, Sigita, David and Martin from the stores for ensuring that all the chemicals and supplies were available.

When I first came to Edinburgh I moved in with a wonderful Thai friend, Dr. Chaweewan Sapcharoenkul, who helped me adjust to the freezing cold and windy autumn, showed me around, cooked me food and always gave me support for the first two years. Thank you Wow, you are the best flatmate ever.

I would like to thank the rest of the corridor and other chemistry people for creating such a nice environment to be in and for making my time in Edinburgh so memorable; Matt, Nina, Emily, Georg, Tracy, Rachel, Marjorie, Verónica, Maddie, Dharmesh, Sara and others whom I have failed to name.

Special thanks to Paramita Punwong and Watsamon Phusakulkajorn for being the best friends ever, always looking out for me and having my back in times of need. I also

thank Pojanut Suthipinittharm for her friendship and her excellent English skills in proofreading parts of my thesis.

Being a Thai student in the UK for several years has brought me in contact with a Thai community that support each other and help relieve homesickness. I would like to thank everyone I met here and will continue to be a friend to them when back in Thailand: New-Nad, Krieng, Kung, Amm, Goh, Gift, Wa-Mod, Kwang-Art, Kuichai-Trev, Eat-Oak, Mui, Bong, Arm, Lek, Sit, Tee, Noi, Tong, Dee-Aim, Pooh, Pom, Pete and many more.

Thanks are owed also to my sponsor, the DPST programme, which gave me the opportunity to pursue my study to the highest level abroad. I am grateful to all the staffs at DPST and OEA-UK.

Last but by no means least, I would also like to thank my parents, Dhoopdhorng and Wirat Sooksawat and my little sister Nartthisa Sooksawat for their encouragements, help and love through every step of my education. This thesis is dedicated to you guys. My family have also been extremely supportive throughout my PhD and I thank them for following my progress with such pride from the beginning and even when times were difficult. They always provided encouragements and have always believed in me.

Abbreviations

12[ane]S_4	1,4,7,10-tetrathiacyclododecane
3,5-lut	3,5-lutidine
aq.	aqueous
bipy	2,2′-bipyridine
Boc	*tert*-butoxycarbonyl
CAN	Cerium ammonium nitrate
CD	Cyclodextrin
C^N	Bidentate ligand coordinating through a carbon and a nitrogen atom
C^N^C	Tridentate ligand coordinating through a carbon, a nitrogen and another carbon atom
COSY	Correlated Spectroscopy
CSA	(+)-camphor-10-sulfonic acid/ camphorsulfonate
CuAAC	copper(I)-catalysed alkyne-azide cycloaddition
CV	Cyclic voltammetry
d	day(s)
DCE	1,2-dichloroethane
dec.	Decompose
DEA	Diethylamine
DIPEA	*N*,*N*′-diisopropylethylamine
DMAP	4-dimethylaminopyridine
DMF	*N*,*N*-dimethylformamide
dmbipy	5,5'-dimethyl-2.2'-bipyridine
DMSO	Dimethylsulfoxide
DNA	Deoxyribonucleic Acid
DOSY	Diffusion-Ordered Spectroscopy (NMR)
EDTA	Ethylenediamine tetraacetic acid
en	ethylene diamine
eq	equivalent(s)
Et_2O	Diethyl ether
EtOAc	Ethylacetate
EtOH	Ethanol
ESI	Electrospray ionization (MS)
FAB	Fast Atom Bombardment (MS)
h	hour(s)
H_2**L¹**	2,6-diphenylpyridine
HPLC	High Performance Liquid Chromatography
L	Ligand
m/*z*	mass to charge ratio
MeCN	Acetonitrile
MeOH	Methanol
min	minute(s)
MS	Mass Spectrometry
nESI	nano-Electrospray Ionisation
NMR	Nuclear Magnetic Resonance

NOESY	Nuclear Overhauser Effect Spectroscopy (NMR)
OTs	*p*-toluenesulfonate
P_1-^{t}Bu	Phosphazene base P_1-^{t}Bu
PEPPSI	[1,3-Bis(2,6-Diisopropylphenyl)imidazol-2-ylidene](3-chloropyridyl)-palladium(II) dichloride
Ph	Phenyl
Py	Pyridine
RNA	Ribonucleic Acid
rt	Room temperature (23 °C)
TBACl	Tetrabutylammonium chloride
TBAF	Tetrabutylammonium fluoride
TBDMS	*tert*-butyldimethylsilyl
TBTA	Tris[(1-benzyl-1H-1,2,3-triazol-4-yl)methyl]amine
TCE	1,1,2,2-tetrachloroethane
terpy	2,2′,6′,2″-terpyridine
TFE	2,2,2-trifluoroethanol
THF	Tetrahydrofuran
TLC	Thin-Layer Chromatography
TMS	Trimetylsilyl
TsOH	*p*-toluenesulfonic acid
TTF	tetrathiafulvalene
TRISPHAT	*Δ*-tris(tetrachloro-1,2-benzenediolato)phosphate(V)
UV	Ultraviolet
Vis	Visible
VT	Variable Temperature (NMR)

NB: Conventional abbreviations for units and physical quantities are not included.

General Remarks in Experimental Data

Unless stated otherwise, all reagents and solvents were purchased from commercial sources without further purification. Dry DCM, CH_3CN and THF were obtained by passing the solvent (HPLC grade) through an activated alumina column on a PureSolv™ solvent purification system (InnovativeTechnologies, Inc., MA). All reactions were carried out under a nitrogen atmosphere, unless stated otherwise. Column chromatography was carried out using Geduran® Silica 60 (particle size 40-63 μm, Merck, Germany) as the stationary phase, and TLC was performed on precoated silica gel plates (0.25 mm thick, 60 F_{254}, Merck, Germany) and observed under UV light.

All ^{1}H, ^{13}C and ^{19}F NMR spectra were recorded as stated on either the Bruker AV 500, AV 400 or AV 600 instrument at a constant temperature of 298 K, unless otherwise stated. All DOSY experiments were performed on either Bruker AV 400 or AV 500 (Topspin 2.1) using bipolar gradient pulses for diffusion with two spoil gradients (ledbpg2s.compensated) pulse sequence. The data was processed using Bruker Topspin 2.1. Chemical shifts (δ) are reported in parts per million and referenced to residual solvent peaks (CD_2Cl_2: ^{1}H δ 5.32 ppm, ^{13}C δ 54.0 ppm; $CDCl_3$: ^{1}H δ 7.26 ppm, ^{13}C δ 77.2 ppm; $C_2D_2Cl_4$: ^{1}H δ 6.00 ppm, ^{13}C δ 73.8 ppm; MeOD-d_4: ^{1}H δ 4.87 ppm, ^{13}C δ 49.0 ppm; DMSO-d_6: ^{1}H δ 2.50 ppm, ^{13}C δ 39.5 ppm; THF-d_8: ^{1}H δ 3.58 ppm, ^{13}C δ 67.6 ppm; DMF-d_7: ^{1}H δ 8.03 ppm, ^{13}C δ 34.9 ppm; D_2O: ^{1}H δ 4.79 ppm). Coupling constants (*J*) are reported in hertz (Hz). The *J* value given per chemical shift, unless stated otherwise, refers to *J-J* spin coupling through three bonds (^{3}J). Standard abbreviations indicating multiplicity were used as follows: m = multiplet, t= triplet, dd = doublet of doublets, td = triplet of doublets, d = doublet, s = singlet, bs = broad singlet, p = pentet.

Mass spectrometry (MS): FAB and ESI was carried out by the MS services at the University of Edinburgh. Melting points (m.p.) were determined using a 1102D Mel-Temp® apparatus and are reported uncorrected.

Layout of the Thesis

This thesis explores a strategy of achieving control over the relative positions of submolecular components with respect to one another for transition metal complexed-rotaxanes. Attempts towards the synthesis of acid-base switchable platinum(II) complexed rotaxanes and utilising self-assembly approach for a construction of molecular shuttle are also discussed. A brief review of the literature is given in Chapter I, describing the background information concerning the rotaxanes synthesis methodologies, examples of stimuli-responsive molecular shuttles and some functional applications of molecular machines. Self-assembly molecular systems are also described. Chapter II focuses on the investigation of an acid-base induced changes to cyclometallated platinum complexes with different denticity of ligands to be able to develop a stimuli-responsive bistable [2]rotaxane. Chapter III describes the determination of a platinum(II) complexed-[2]rotaxane construction using various strategies. Chapter IV contains the construction of self-assembled tubular complexes and the endeavour to develop a self-assembled rotaxane. The outlook contains closing remarks about the work that has been presented and ideas for its applications.

Chapter I

Transition Metal-Complexed Rotaxanes: From Dynamic Systems to Functional Molecular Machines

Acknowledgements

Dr. Paul Lusby is gratefully acknowledged for proofreading this and the following three chapters.

1.1 Background

Molecular machines can be defined using a similar concept to their macroscopic counterparts - as devices in which the component parts display change in their relative position as a result of some external stimulus. Molecular machines operate through chemical reactions and need to be fed by an energy source.[1] Nature uses molecular machines to perform a large number of essential functions including energy conversion, cell division, intracellular displacement and muscle contraction. The studies of biological machines have been investigated in detail; with advancing development in the field, it has been possible to visualise the movement of such systems, in some cases while they are in action. The three most important and well-known examples are ATP synthase[2], a rotary motor responsible for the synthesis of ATP, the actin-myosin complex[3] of the muscles, which behaves as a linear motor, or kinesin and dynein[4], essential super family proteins which walk along a microtubule tracks. Another example of a linear biomolecular machine is RNA polymerase[5], which moves along DNA while carrying out transcriptions. Much of the inspiration to construct molecular machines comes from these outstanding biotic exemplars. At the same time, synthetic and in particular supramolecular chemistry has flourished, opening unlimited possibilities concerning design and construction of artificial molecular machines.[6]

Most of the artificial systems constructed so far are based on interlocked molecules, such as catenanes and rotaxanes.[7] Rotaxanes are chemical structures in which one or more macrocycles are mechanically prevented from dethreading from a linear unit by bulky "stoppers", while in catenanes two or more macrocycles are interlocked. Their interlocked structure provides them with high degree of freedom, thus allowing tunable movement. The large amplitude submolecular motions achieved from catenanes and rotaxanes can be divided into two classes: pirouetting of the macrocycle around the thread (rotaxanes) or the other ring (catenanes) and translation of the ring along the thread, shuttling (rotaxanes) or around the other macrocycle (catenanes) (Figure 1.1). The relative position of the components in interlocked molecules is often referred to as a "co-conformation". The translation and rotation envisaged in rotaxanes suggest that they be useful prototypes for the construction of both linear and rotary molecular machines.

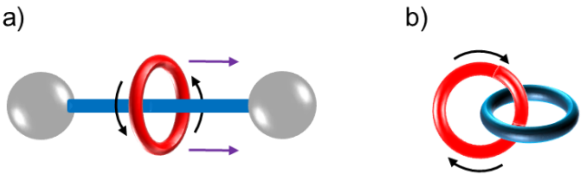

Figure 1.1 Schematic representations and possible large amplitude modes of movement for one component relative to another: a) Rotaxane; b) Catenane.

1.2 Synthesis Strategies of Rotaxanes

The first report of a rotaxane synthesis was described by Harrison and co-workers in 1967.[8] The synthesis relied not on any favourable intercomponent interactions but the statistical probability that a finite amount of thread would be encapsulated through the macrocycle. Through several treatments of the resin-bound macrocycle with thread precursor solution, followed by extraction of unwanted reagents, the product was hydrolysed from the solid support with an extremely poor 6% yield. However, this approach established the proof of concept that rotaxane architectures were a synthetic possibility.

Non-covalent intermolecular interactions (*i.e.* electrostatic, hydrogen bonding, π-π stacking interactions, hydrophobic effects, metal-ligand interactions) have been used in the preparation of rotaxanes and catenanes. There are various ways for making rotaxanes by supramolecular synthesis.[9] They can be self-assembled using template-directed synthesis methods[10] using "threading-followed-by-stoppering" or "capping" where the axle is threaded through the macrocycle, followed by attachment of the stoppers; "clipping" *via* a preformed thread coordinated to a U-shape which is closed or clipped around the thread; or "slipping" in which the preformed macrocycle slip into the preformed thread strategies (Figure 1.2). The template induces the assembly of specific product by preorganising the reactants in a favourable orientation for the formation of the covalent bonds.

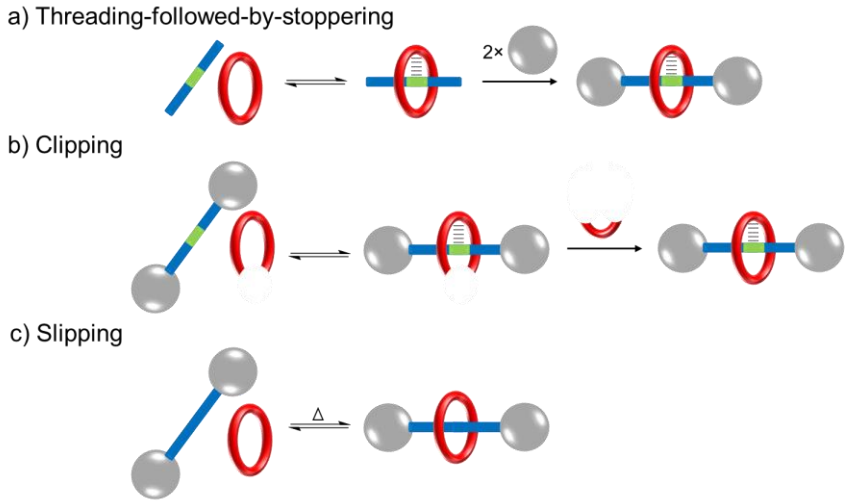

Figure 1.2 Schematic representation of synthetic approach to rotaxane formation: a) Threading-followed-by-stoppering, b) Clipping, c) Slipping.

1.2.1 Non transition metal template

1.2.1.1 Aromatic interactions

Stoddart and co-workers successfully synthesised the first catenane promoted by π-π stacking interactions between electron deficient bipyridinium units and an electron rich diphenol motif in an extraordinary 70% yield in 1989.[11] They also utilised the same motif for the construction of rotaxanes. The first example of a molecular shuttle $\mathbf{1}^{4+}$ was obtained using a clipping technique.[12] Stabilising dispersive forces between bipyridinium units of the diphenol stations on the thread including π-π stacking of the donating and accepting unit brought the subcomponent in the appropriate direction and proximity such that cyclisation took place to give $\mathbf{1}^{4+}$. Unbiased temperature-dependent shuttling of the macrocycle between the two degenerate diphenol stations was observed by a series of variable temperature (VT) NMR experiments.

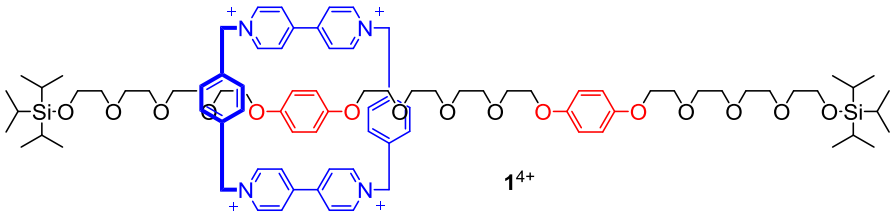

Figure 1.3 The first reported molecular shuttle $\mathbf{1}^{4+}$.

Similar pseudorotaxane $\mathbf{2}^{2+}$ was obtained using the slippage approach.[13] The macrocyclic and the thread were heated together in MeCN solution at 55 °C. Upon cooling the reaction

mixture, the slipped ring remained threaded on the dumbbell thread as a result of the thermodynamic trap provided by stabilising π-π stacking interactions.

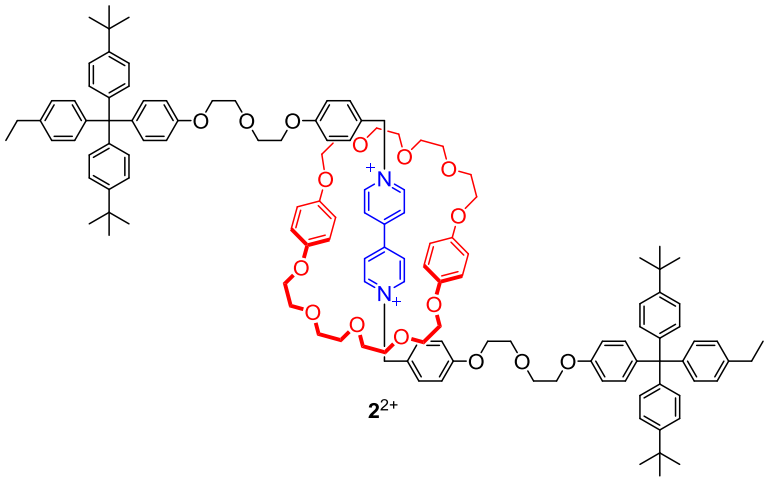

$\mathbf{2}^{2+}$

Figure 1.4 [2]pseudorotaxane $\mathbf{2}^{2+}$ synthesised by slippage methodology.

Stoddart and co-workers have pioneered the art of building interlocked architectures using the π-π interaction between bipyridinium-based macrocycle and an electron-rich aromatic ring guest motif, and *vice versa*[14] and have described a wide range of different structures and uses featuring this motif.[15]

1.2.1.2 Hydrophobic interactions

The most extensively studied rotaxanes formed by exploiting the hydrophobic effect are those containing cyclodextrins (CD). Cyclodextrins have been known to form inclusion complexes with a variety of aromatic hydrocarbon guests since the 1960s,[16] the first rotaxane was prepared by Ogino group in 1981, a β-CD-based rotaxane $\mathbf{3}^{4+}$ which was afford in low yield (Figure 1.5).[17]

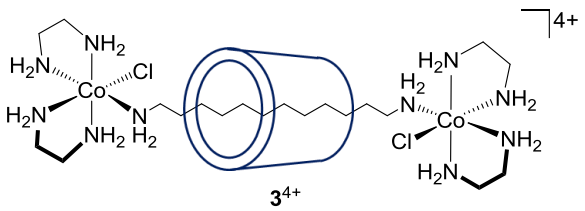

$\mathbf{3}^{4+}$

Figure 1.5 Ogino's cyclodextrin-based [2]rotaxane.

The first photoswitchable rotaxane was reported by Nakashima and co-workers in 1997.[18] A cyclodextrin-based [2]rotaxane $\mathbf{4}^{4+}$ featuring an azobenzene moiety in the thread capped with 2,4-dinitrobenzene was prepared in aqueous solution in 30%.

Shuttling of the CD ring was achieved through photoisomerisation of a central azobenzene group. In *trans*-**4**$^{4+}$, the azo-linkage resides within the cavity of the cyclodextrin unit (Figure 1.6). Irradiation at 360 nm caused isomerisation of the double bond to generate *cis*-**4**$^{4+}$. NOE NMR experiments suggested that upon formation of the *cis* co-conformer the CD ring translates to a secondary, ethylene spacer moiety. The original *trans*-**4**$^{4+}$ co-conformer was regenerated upon irradiation at 430 nm to complete the switching cycle.

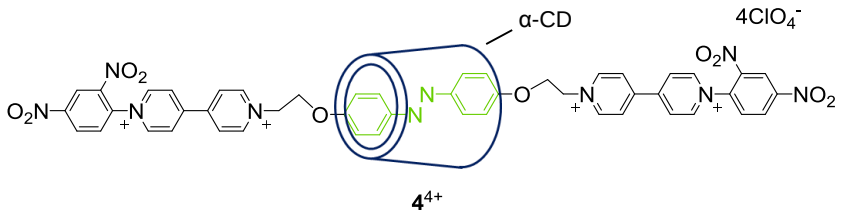

Figure 1.6 Photoresponsive single station shuttle **4**$^{4+}$ based on azobenzene unit.

1.2.1.3 Hydrogen-bonding interactions

Although hydrogen bonds are a lot weaker than covalent bonds or metal-ligand bonds, multiple recognition sites with high level of preorganisation brings about an effective hydrogen-bonding template. Hydrogen bonding has been used to synthesise peptido[2]rotaxanes in Leigh's group by the condensation of appropriate aromatic diacid chlorides and benzylic diamines in the presence of dipeptide derivatives, which template the formation of benzylic amide macrocycles through a five-molecule, hydrogen bond directed "clipping" strategy.[19]

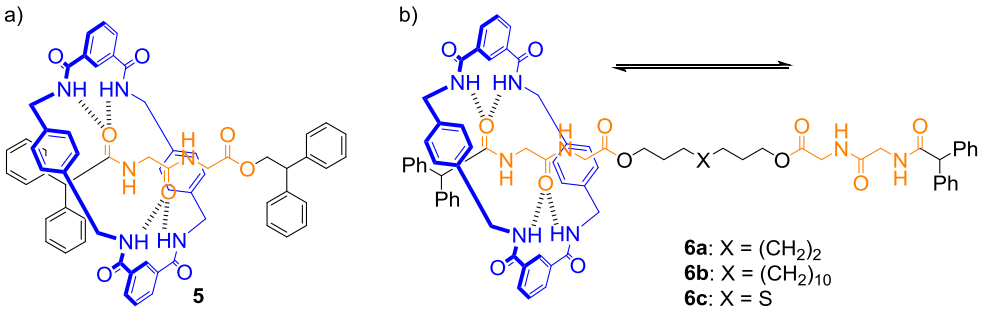

Figure 1.7 a) Hydrogen bond directed-assembled peptide-based [2]rotaxane **5**; b) peptide-based degenerate molecular shuttles **6a-c**.

Such rotaxanes have been elaborated into shuttles by combining two hydrogen bonding peptide units with additional lipophilic spacer in a thread to provide a simple route to multistationed, hydrogen bond-assembled molecular shuttles.[20] In $CDCl_3$, the macrocycle

in **6a-c** shuttles between the two degenerate peptide stations rapidly at room temperature. In the hydrogen bond accepting solvent, DMSO-d_6, the interaction between the benzylic amide macrocycle and peptide units was broken resulting in the macrocycle positioned primarily at the central polarphobic station while the two stations were solvated.

Rotaxanes **7**·H^{3+} were the first switchable molecular shuttles reported using secondary ammonium and crown ether macrocycle units.[21] The dibenzocrown ether is bound to the ammonium cation by means of N^+-H···O hydrogen bonds as well as weaker C-H···O bonds from α-methyl adjacent to nitrogen atom. Deprotonation of the ammonium centre with base was used to turn off these interactions, resulting in shuttling to a second bipyridinium station (**7**$^{2+}$).

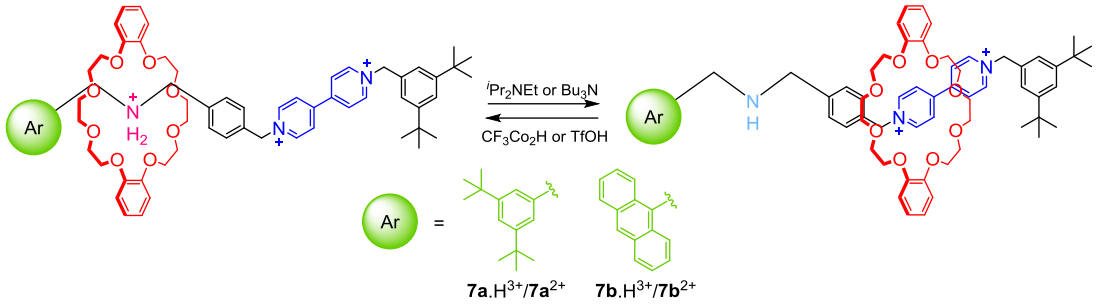

Scheme 1.1 A pH-responsive bistable molecular shuttle displaying good positional integrity in both chemical states.

1.2.2 Transition metal templates

Metal-ligand coordination is very attractive in the field of supramolecular assemblies due to the well-defined geometries of metal complexes allow for angles that cannot be approached in linear hydrogen bonding in natural systems or σ-, π-hybridisations in covalent synthesis to be obtained.

A wide range of metals with preferences for different coordination geometries have been used with numerous ligands to template the formation of interlocked architectures. Figure 1.8 shows different transition metal-ligand coordination geometries used in a passive-metal template strategy.

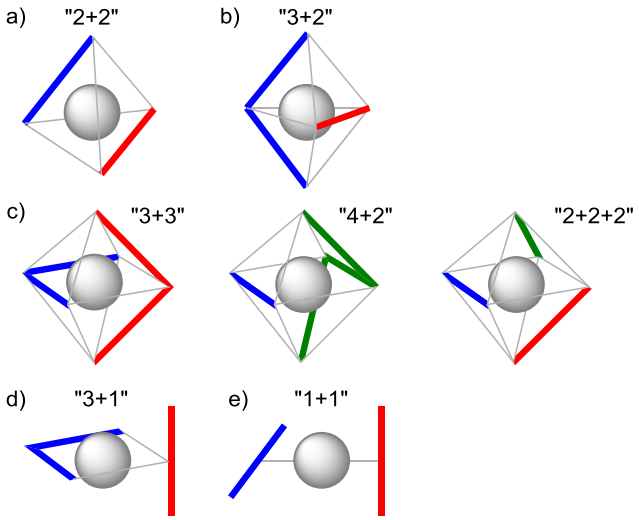

Figure 1.8 The range of transition metal-ligand coordination geometries exploited in the synthesis of mechanically interlocked architectures: a) three-dimensional tetrahedral, b) trigonal bipyramidal, c) octahedral, d) two-dimensional square planar and e) one-dimensional linear motif.[22]

1.2.2.1 Tetrahedral Cu(I) template

In 1983, Sauvage and co-workers achieved the first metal-templated synthesis of a [2]catenane.[23] They employed the preferred tetrahedral geometry of Cu(I) to organise two bidentate phenanthroline ligands in a mutually orthogonal manner creating a crossover point that directs the subsequent macrocyclisation reaction. In the initial two papers, Sauvage used this motif to construct catenates, that could be subsequently demetallated using KCN to afford the catenands.[23-24]

The first synthesis of a rotaxane based on the same Cu^{I} template was reported by Gibson and co-workers in 1991.[25] The rotaxane **9** was produced in 42% by reacting the threaded copper complex $\mathbf{8}^{+}$ with a bulky iodo compound (stopper). The stopper prevents dethreading after subsequent demetallation.

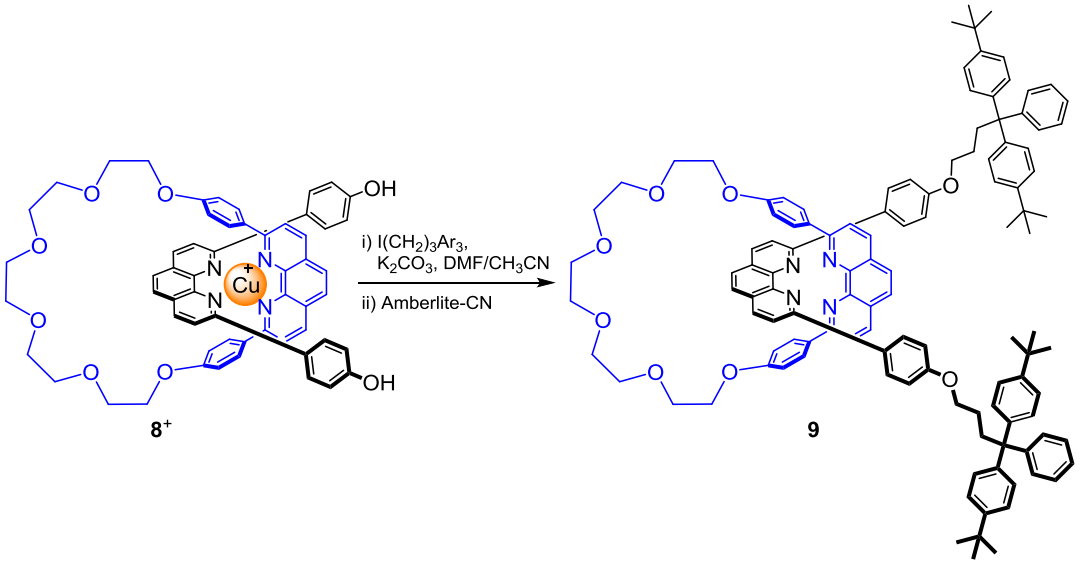

Scheme 1.2 Gibson's Cu(I)-phenanthroline based rotaxane synthesis.

Recently, Leigh and co-workers have reported the assembly of a [2]rotaxane **14** through imine bond formation around Cu(I) ion between a picolinaldehyde **11**, and amine **12** and a bipyridine macrocycle **10** following the copper(I) template system introduced by Sauvage and co-workers.[26] The assembly was simple and effective. The reactions proceeded with high yields within a few minutes at ambient temperature and it can be extended to form a [3]rotaxane **15** by simply replacing monoamine **12** with diamine **13** (Scheme 1.3).

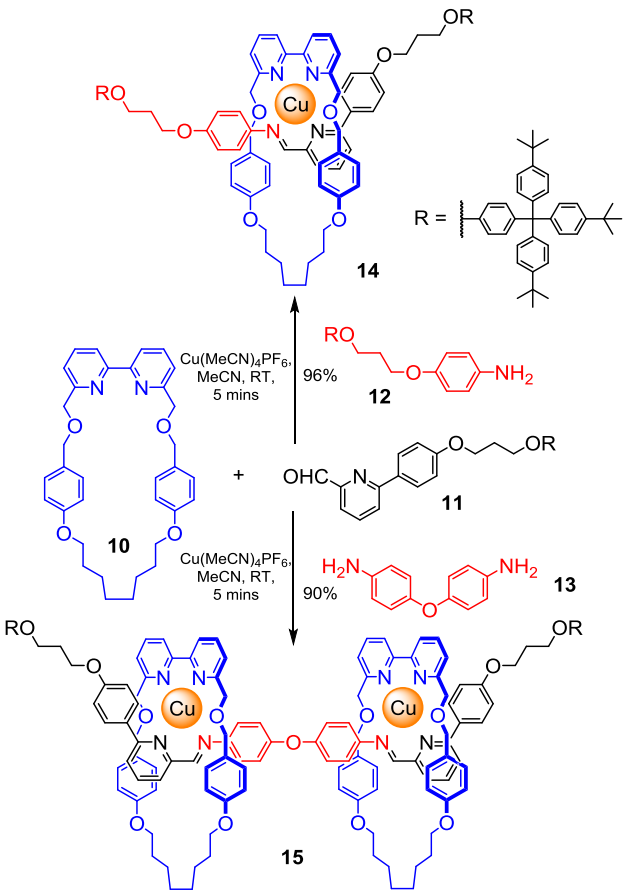

Scheme 1.3 Cu^{I}-mediated assembly of [2]rotaxane **14** and [3]rotaxane **15**.

1.2.2.2 Octahedral templates

[2]Rotaxanes can be efficiently formed using a general ligand system of ions that prefer octahedral coordination metals. Leigh and co-workers have reported rotaxane formation by reacting a preformed bis-amine macrocycle **16** with 2,6-diformylpyridine **17** and stopper aniline **18** to form imine bonds with an appropriate divalent metal ion in good yields (57-99%) (Scheme 1.4).[27]

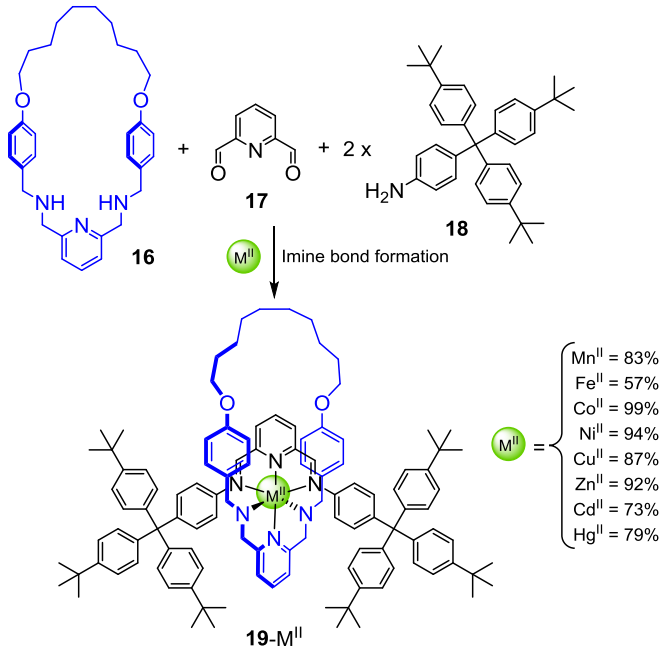

Scheme 1.4 Octahedral amine/imine-based [2]rotaxane **19**-M^{II} formed through imine bonds.

The same basic scaffold could be modified to work with harder, trivalent metal ion templates such as Co^{III} by using 2,6-pyridinedicarboxamide coordinating motif (Scheme 1.5).[28] The thread was first bound to labile Co^{II} followed by oxidation of Co^{II} to Co^{III} to lock the ligands in place and underwent RCM to generate the [2]rotaxane **20**-Co^{III}.

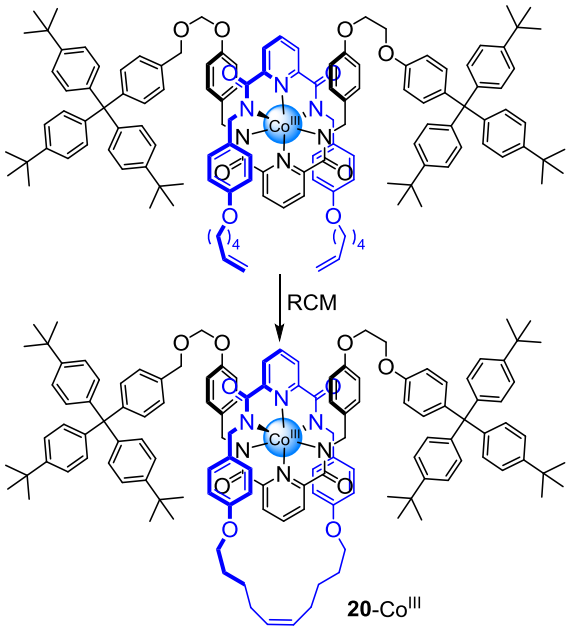

Scheme 1.5 Co^{III} template synthesis of [2]rotaxane **20**-Co^{III}.

An octahedral "4+2" donor ligand set has been used for the template synthesis of rotaxanes by Sauvage's group in 2003 (Scheme 1.6).[29] The reaction of Ru^{II} complex **21**

and macrocycle **22** that incorporates a 2,2'-bipyridine ligand in ethyleneglycol afforded pseudorotaxane, which was then capped with stoppers by Williamson ether synthesis to form [2]rotaxane **23**-Ru^{II} in 56% yield.

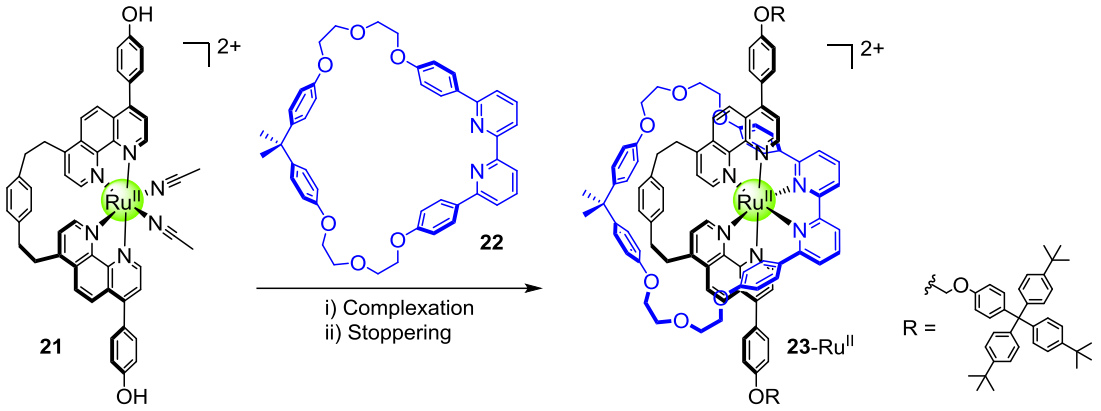

Scheme 1.6 Sauvage's octahedral construction of rotaxane **23**-Ru^{II}.

1.2.2.3 Square-planar geometries template

The two-dimensional arrangement of donor atoms in a square-planar geometry might be unsuitable for the assembly of a three-dimensional scaffold. However, in a "3+1" donor ligand set,[30] the steric demands of the tridentate ligand can force the monodentate ligand to be perpendicular in order that the cross-over point can be generated[22] then this can be used to generate a three-dimensional interlocked structure from a two-dimensional template.

Sauvage and co-workers first described an example utilising a palladium square planar "3+1" strategy towards the synthesis of a Pd-pseudo-rotaxane complex.[30] A year later, the first synthesis of [2]rotaxane using square-planar template system was prepared by Leigh and co-workers in 2004.[31] The rotaxane design based on the palladium chemistry developed by Hirao and co-workers[32] consists of a tridentate 2,6-di(benzylamid)pyridine macrocycle precursor and either a 2,6- or 3,5- disubstituted pyridine counterpart (monodentate ligand) (Scheme 1.7). The synthesis commenced by reacting tridentate ligand with $Pd(OAc)_2$ in acetonitrile to generate Pd^{II} complex **25** in which labile acetonitrile ligand can be displaced with suitable monodentate ligand. However, ring closing olefin metathesis (RCM) followed by hydrogenation (Scheme 1.7 step c) gave the rotaxane **28a** in 77%. Although **27b** and **27d** were formed, no [2]rotaxane was produced after step c. This was attributed to 3,5-substitution pattern macrocyclisation preferentially occurs without encircling the thread, forming a non-

interlocked ring-on-thread-complex resulted in free macrocycle **30** and thread. The X-ray crystal structure of **29a** confirmed the interlocked architecture and the pseudo square-planar geometry of the palladium.

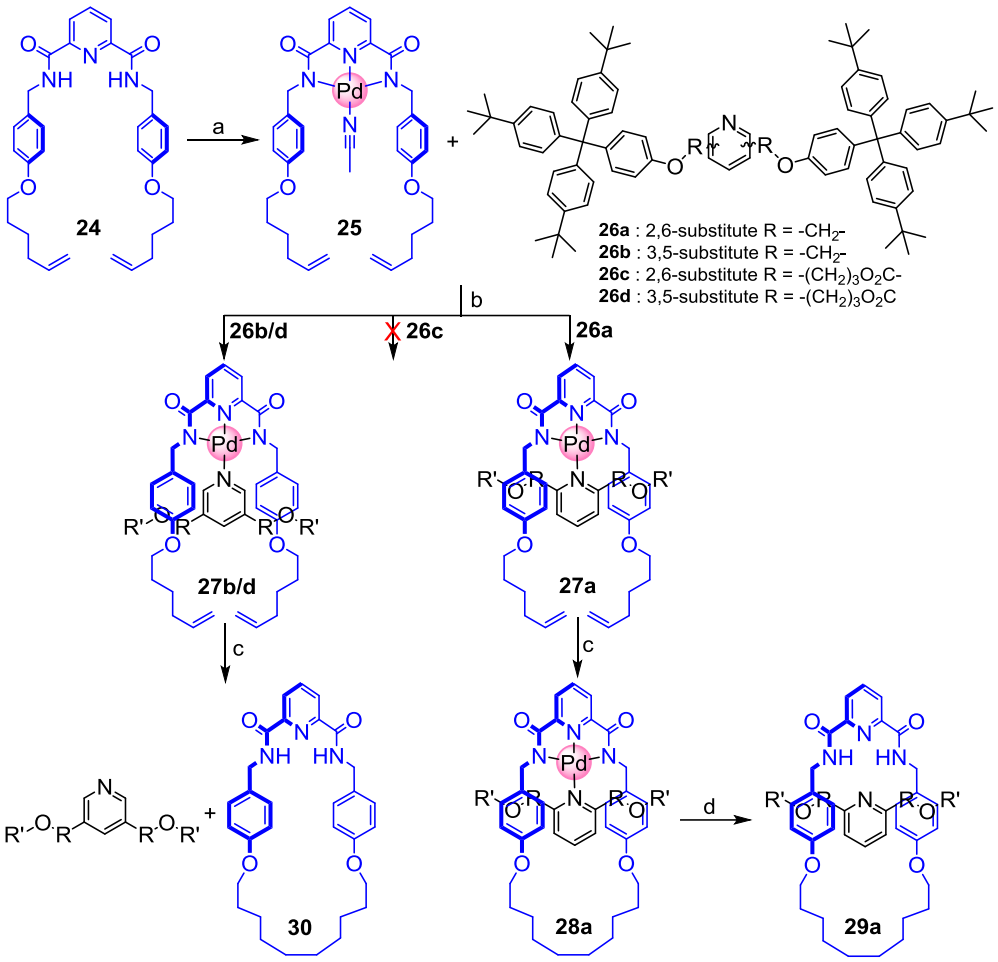

Scheme 1.7 Palladium template directed synthesis of rotaxane **29a**. Reagents and conditions: a) $Pd(OAc)_2$, MeCN, 76%; b) $CHCl_3$, 50 °C, **27a** = 63%, **27b** = 96%, **27c** = 0%, **27d** = 97%; c) i) Grubb's 1st Gen. Catalyst, CH_2Cl_2, ii) H_2, Pd/C, THF, **28a** = 98%, **26b**+**30** = 69% (over 2 steps); d) KCN, CH_2Cl_2, 20 °C, 1 h then 40 °C, 0.5 h, 97%.

The same "3+1" approach of rotaxane synthesis was also reported later by Takata and Hirao, and Chiu using a similar Pd^{II}-macrocycle motif.[33] In this example, pseudorotaxanes with terminal hydroxyl groups in the thread were reacted further with isocyanate stoppers to furnish [2]rotaxanes. More recently, it has also been demonstrated that the Pd^{II} centre is capable of successively catalysing hydroamination reaction of propargyl or allyl-urethane moieties within the thread, transforming into oxazolidone and oxazolidinone units respectively.[34]

The robust nature of the square-planar Pd^{II} methodology was used in the synthesis of [n]rotaxanes using just a single template site on the thread **31** (Scheme 1.8).[35] The method involved the repetitive coordination, macrocyclisation and demetalation to iteratively generate [2], [3] and [4]rotaxanes. It would appear that the only limiting factor in the synthesis of higher order rotaxanes is the length of the thread.

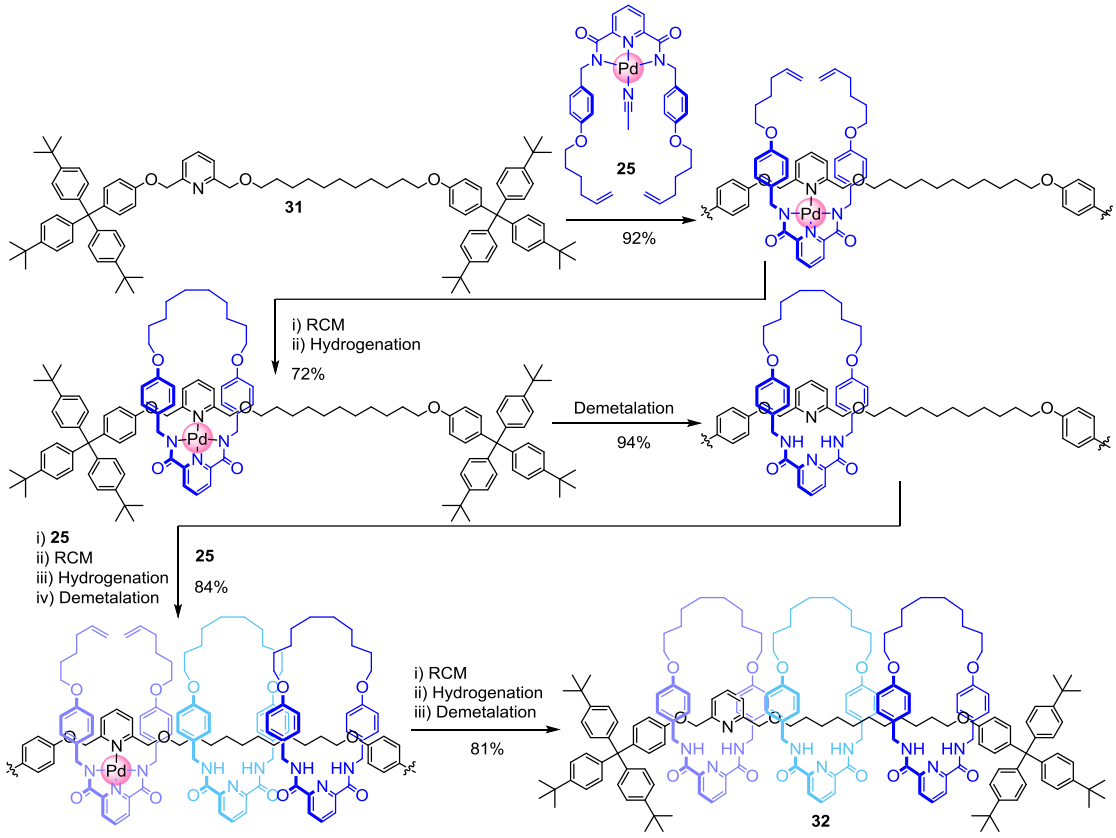

Scheme 1.8 Synthesis of [4]rotaxane **32** by the repetitious use of a single templates site of the axle.

The concept was extended to produce precisely controlled sequence isomerism in a rotaxane through constitutionally different macrocycles being sequentially added (Figure 1.9).[36]

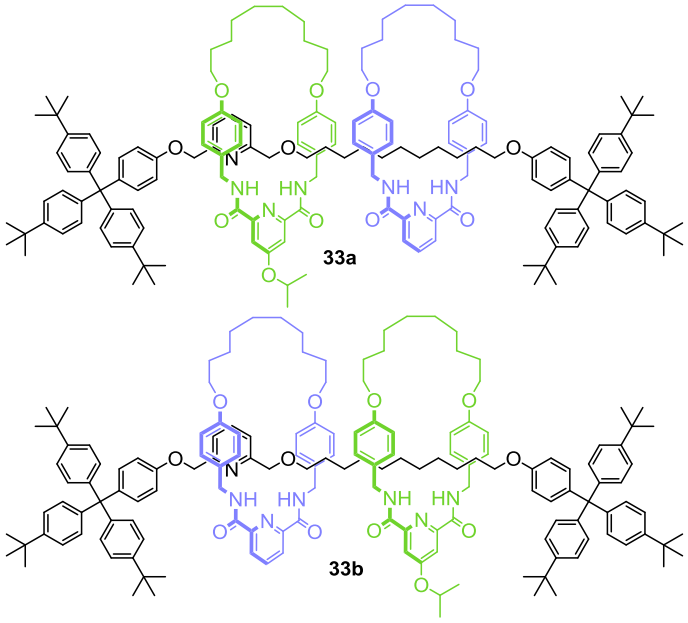

Figure 1.9 Sequence isomerism in [3]rotaxanes. Diastereomers **33a** and **33b** are constitutionally identical.

Recently, Nitschke and co-workers have developed a square-planar Pd^{II}-bis(imino)pyridine motif and used to prepared a range of metallosupramolecular structures by self-assembly (Scheme 1.9).[37] Pd^{II} ions have been combined with amines and 2,6-diformylpyridine instead of former reported 6-coordinate metals. Macrocycles, [2]rotaxanes and [2]catenanes have been shown to form with high yield in one pot synthesis.

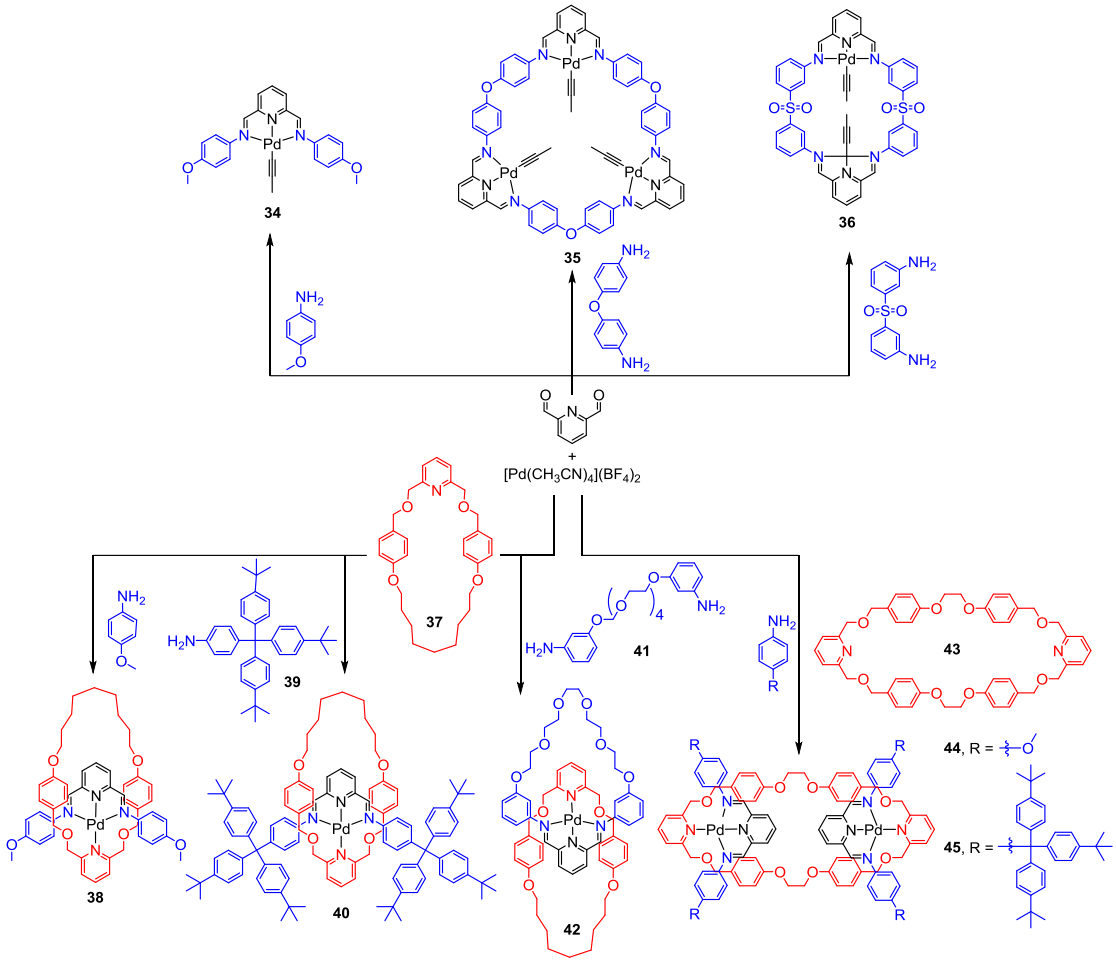

Scheme 1.9 Synthesis of a range of metallosupramolecular architechtures from 2,6-diformylpyridine, Pd^{II} ions, different mono-and diamines, and ancillary ligands.

1.2.2.4 Active metal template

As has been shown, the metal templated approach provides access to increasingly sophisticated interlocked architectures. However, these strategies have one common feature in that they require stoichiometric quantities of the metal template. The role of the metal is essentially a glue to hold the reactive fragments together in an orientation that favours interlocking. Inspired by well-documented principles of transition-metal catalysis, a new strategy has been introduced in which the metal not only induces preorganisation, but also plays an active role in the bond formation. This strategy, developed by the Leigh group, is known as the active metal template approach (Figure 1.10).[38]

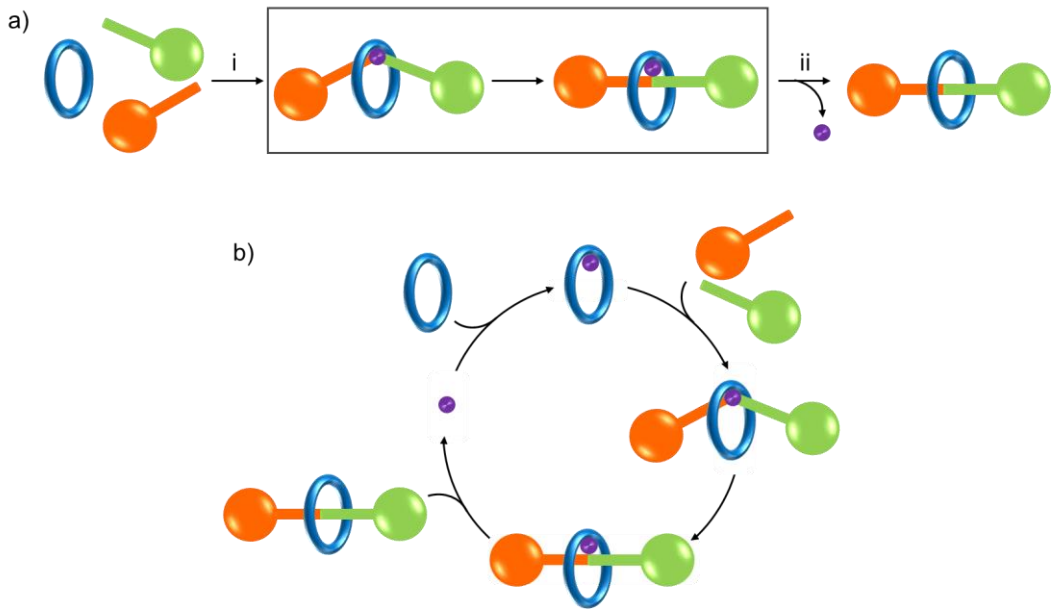

Figure 1.10 Schematic representation of the active metal template synthesis. a) Stoichiometric active-metal template synthesis of a [2]rotaxane: i) template assembly and covalent bond forming catalysis, ii) demetalation; b) Catalytic active-metal template synthesis of a [2]rotaxane.

The concept was first demonstrated in 2006 by Leigh and co-workers by using the Cu(I)-catalysed 1,3-dipolar cycloaddition of organic azides with terminal alkynes (CuAAC) "click" reaction to form a disubstitute triazole ring from half-thread **46** (alkyne) and **47** (azide) through the cavity of pyridine-containing macrocycle **48** (Scheme 1.10).[38]

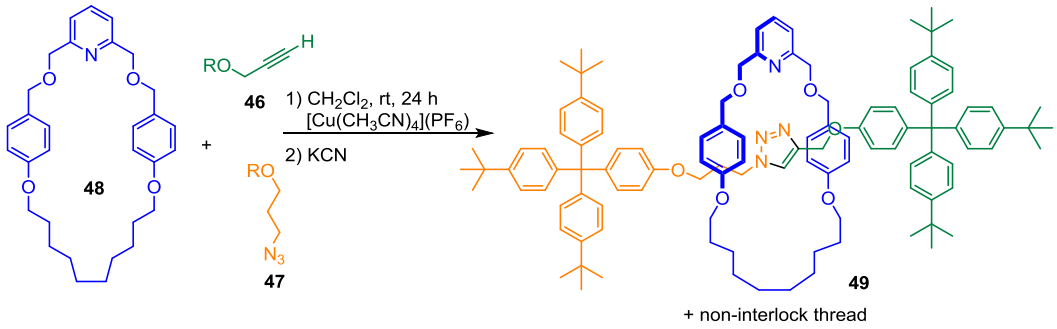

Scheme 1.10 Active-metal template synthesis of the [2]rotaxane **49** *via* CuAAC reaction.

Treatment of an equimolar solution of the three components with a stoichiometric amount of Cu^{I} salt afforded the [2]rotaxane **49** in 57%. Improved yields of 94% were observed when 5 equivalents of **46** and **47** were employed with prolonged reaction time to 72 h. The addition of pyridine to the reaction mixture as a competing ligand caused the Cu^{I} catalyst to turn over furnishing rotaxane **49** in 82% yield using only 4 mol% of the metal catalyst relative to half-thread **46** and **47**. Additionally, a series of analogous

[2]rotaxanes were formed with the range of the systemic variation of the reaction parameters. The unexpected formation of [3]rotaxane **50** while varying the ratio of macrocycle to Cu^{I} from 1:1 to 10:1 has implications for the mechanism of the CuAAC reaction shown in Scheme 1.11.[39]

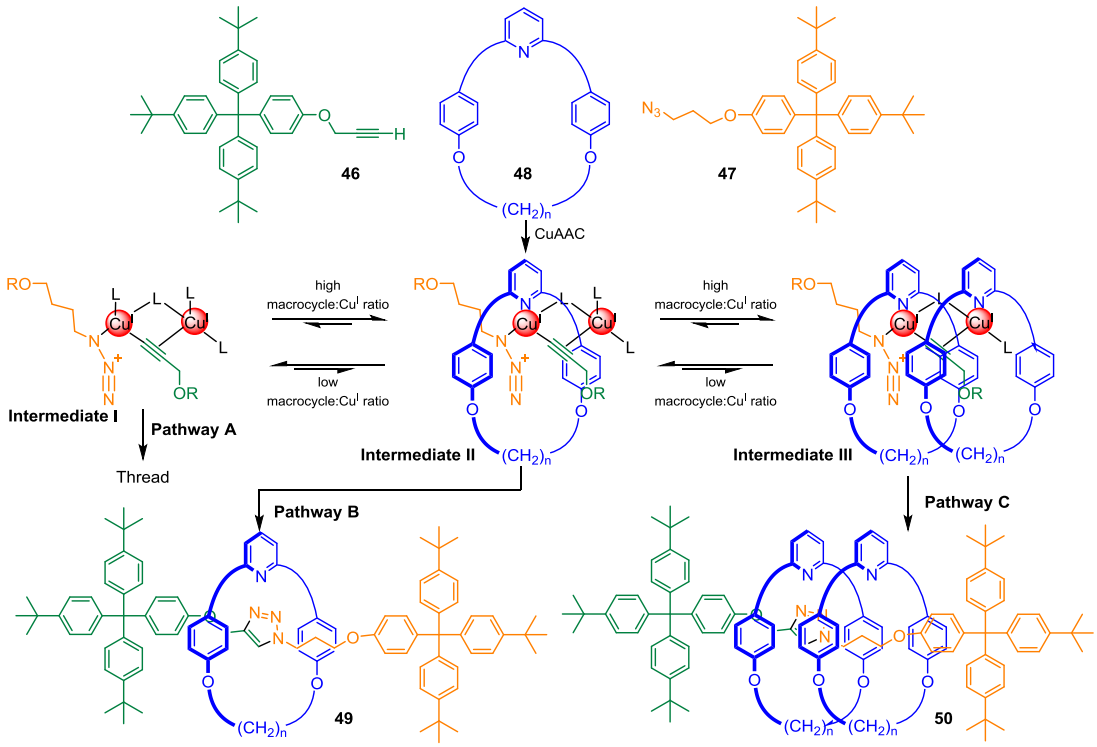

Scheme 1.11 Mechanism of the CuAAC active template synthesis of [2] and [3]rotaxanes.

More recently, Goldup and co-workers have extended the active template CuAAC strategy to prepare small rotaxane by reducing the size of macrocycles which allowed access to small functionalised rotaxanes based on commercially available materials in excellent yields.[40] Their group also demonstrated the first synthesis of rotaxanes under aqueous conditions a few years later.[41] Moreover, Goldup group have extended the AT-CuAAC concept to prepare planar chiral rotaxane in high enantiopurity without any used of chiral separation techniques.[42]

Other copper-based active template reactions were developed after the successful demonstration of CuAAC active template. Saito and co-workers utilised Cu-mediated Glaser diyne coupling and Ullmann C-S bond formation in active template rotaxane formation.[43] Leigh group has also developed a Cu^{I}-mediated alkyne-alkyne heterocoupling using a modified Cadiot-Chodkiewicz procedure which produces rotaxane with unsymmetrical axle.[44]

Combining the previous powerful square-planar Pd strategy with active metal template strategy, Leigh and co-workers have investigated synthesis of the interlocked structures using Pd^{II} in the active-metal template strategy. The use of palladium-catalysed alkyne-alkyne bond formation in rotaxane formation was developed. Both stoichiometric and catalytic quantities of Pd^{II} resulted in good conversion of alkyne-functionalised stopper to [2]rotaxane.[45] The Pd(II)-catalysed oxidative Heck cross-coupling over Pd(0) has been developed in the active metal template synthesis of [2]rotaxanes.[46] [2]Rotaxane was prepared in 73% from bipy-based macrocycle, arylboronic acid and vinylic ester in the presence of benzophenone and atmospheric oxygen. The reaction proved tolerant to a variety of coupling partners.

The Pd(II)-mediated Michael addition has been used to assemble rotaxanes with excellent efficiency.[47] Reaction of Pd^{II}-macrocycle complex **51** with ethyl cyanoacetate **53** leads to Pd complex **54**. Ethylcyanoate becomes activated to deprotonation by *N*,*N*-diisopropylamine (DIPEA) and still bound within the cavity of the macrocycle allowing two successive Michael addition of the vinyl ketone half-thread **52** to both sides and forms [2]rotaxane complex **55**-Pd^{II} in 99% yield. (Scheme 1.12).

Demetallation with KCN gave metal-free rotaxane H_2**55** in which the amide macrocycle shuttles between the two ketone groups of the thread.

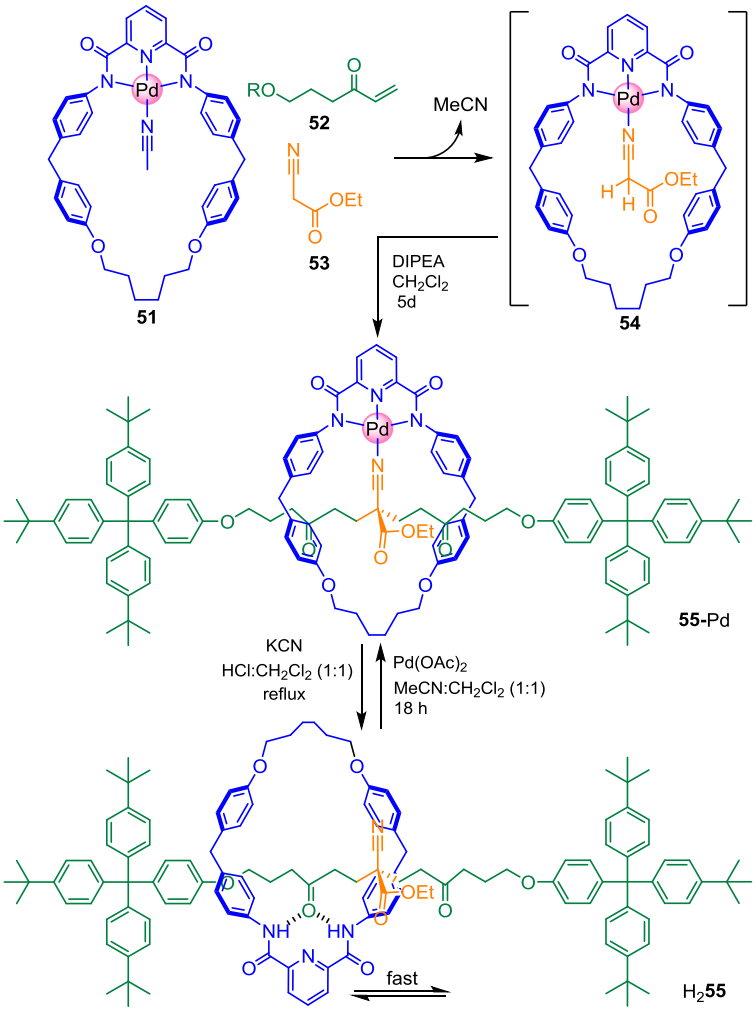

Scheme 1.12 Pd(II) promoted Michael addition for the preparation of rotaxane **55**-Pd, and its decomplexation to hydrogen-bonded molecular shuttle H_2**55**.

1.2.3 Rotaxanes containing metal ions in their framework

In 2006, Wisner and co-workers reported the synthesis of a [2]rotaxane *via* first- and second-sphere coordination in which the metal centre acted as both an organising template and as covalent attachment points between the components.[48] *trans*-Bis-benzonitrile palladium(II) dichloride was coordinated with isophthalamide-based tetralactam macrocycle *via* hydrogen-bonding between Cl and amide hydrogens in the macrocycle. The replacement of the two labile benzonitrile molecules by stronger-coordinating pyridine stoppers gave the Pd-containing rotaxane **56** in 89% yield (Figure 1.11). The authors later extended this strategy replacing halides with thiocyanate ligands[49] which afforded dissymmetric binding geometries of the rotaxane by coordination with the macrocycle *via* the nitrogen atoms. This suggests SCN moieties act as a ratchet between two degenerate stations as supported by VT ^{1}H NMR experiments.

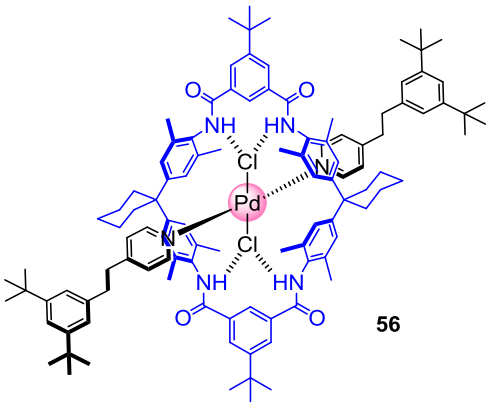

Figure 1.11 $PdCl_2$-containing rotaxane **56**.

A novel threading-followed-by-shrinking strategy was introduced by Asakawa and co-workers in 2004.[50] The secondary diallylammonium salt **57** threads through a crown ether incorporating salophen macrocycle **58** forming a pseudorotaxane **59**. Addition of $Pd(OAc)_2$ afforded the corresponding rotaxane **60**-Pd in 30% by shrinking the macrocycle around the thread (Scheme 1.13).

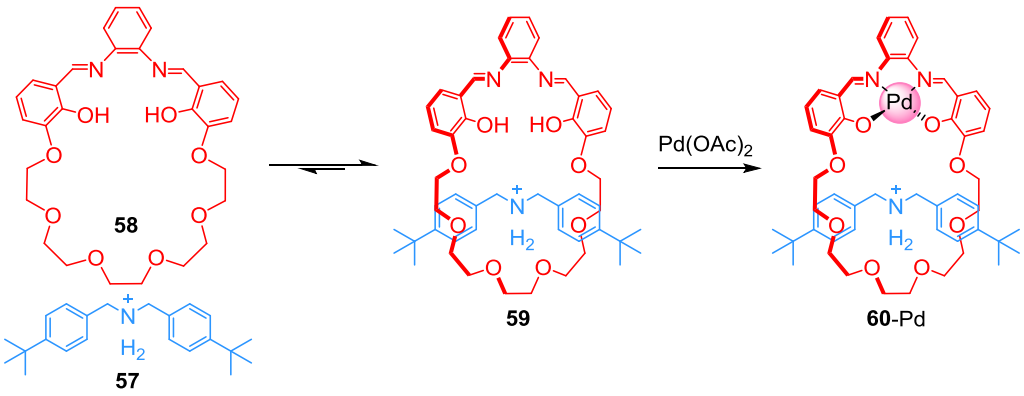

Scheme 1.13 Synthesis of [2]rotaxne **60**-Pd.

A hybrid organic-inorganic rotaxane was reported by Leigh , Winpenny and co-workers in 2009.[51] The design is based on the observation that a heterometallic Co-Cr ring bridged by fluoride and alkyl/aryl carboxylate formation is templated by various organic cations. The rotaxane was synthesised by reacting secondary amine thread incorporating bulky stoppers at each end with a mixture of Cr^{III} and Co^{II} solutions in pivalic acid. The [2]rotaxane **61** was produced in 23% yield. The X-ray structure showed the eight metal centres in each heterometallic wheel to be almost perfectly coplanar. This methodology was extended to prepare [3] and [4]rotaxanes and molecular shuttles in which the ring undergoes random thermal motion between two ammonium sites on the thread.

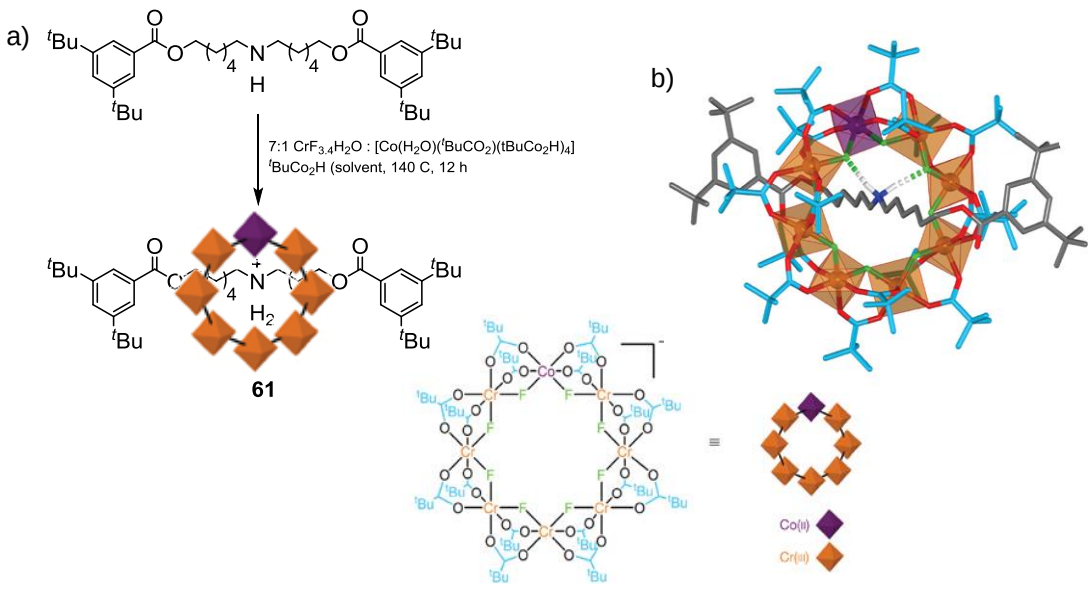

Scheme 1.14 a) Synthesis b) X-ray crystal structure of hybrid organic-inorganic [2]rotaxane **61**. Reproduced from ref. 50.

In 2010, a rotaxane based on a metal cage and a bisanionic thread was reported by Clever and Shionoya.[52] The assembly **62** consists of a Pd^{II}-mediated molecular cage surrounding an anionic thread as a result of two binding principles: metal coordination for assembly of the cage and ion-pair interactions for guest binding.

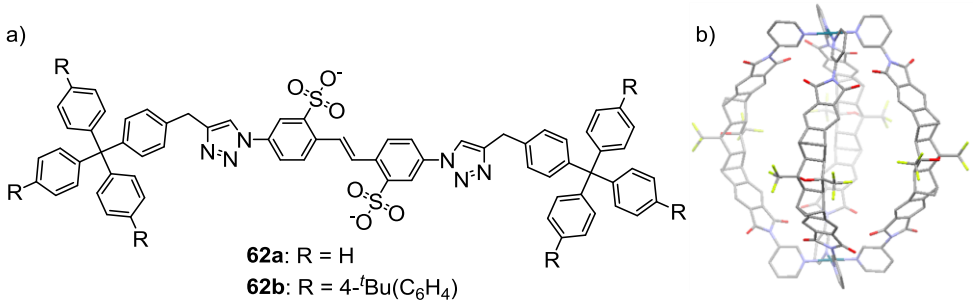

Figure 1.12 a) Structure of bisanionic thread; b) X-ray structure of cage.

1.3 Stimuli-Responsive Molecular Shuttles

A rotaxane can be designed and synthesised with two or more recognition sites within its axle component. If two identical stations are arranged, a degenerate, co-conformation equilibrium state is obtained in which the macrocycle spontaneously shuttles back and forth between two sites as discussed above for Stoddart's first molecular shuttle (Section 1.2.1.1). A rotaxane will exist as two different equilibrating co-conformations if the two recognition sites are different. The populations of each station reflect the strengths of the

two different sets of non-covalent binding interactions. If the macrocycle affinity between two stations is appropriately large, the macrocycle resides predominantly in one co-conformation. In stimuli-responsive molecular shuttles, an external stimulus does not induce directional motion of the macrocycle, but rather changes the non-covalent intercomponent interactions. The binding strength of the less-populated station is increased and/or the initially preferred binding site is destabilised to the extent that the second binding site becomes energetically more favoured, causing shuttling of the macrocycle to the second station. The system can be returned to its original state by using a second chemical modification (Figure 1.13). A biased Brownian motion arises from a difference in the activation energies for movement in different directions, not from the difference in energy minima.[53] In suitably designed rotaxanes, the switching process can be controlled by reversible chemical reactions (protonation-deprotonation, reduction-oxidation, isomerisation) from chemical, electrochemical or photochemical triggers.

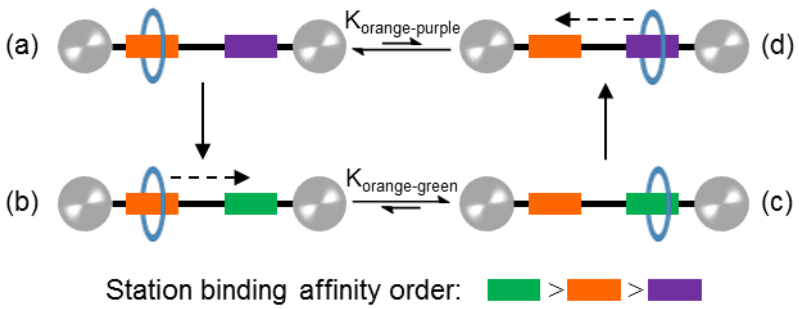

Figure 1.13 Translational submolecular motion in a stimuli-responsive molecular shuttle: a) the macrocycle initially resides on the preferred station (orange); b) a reaction occurs (purple→green) which changes the relative binding potentials of the two stations such that, c) the macrocycle "shuttles" to the now-preferred station (green). If the reverse reaction (green→purple) now occurs (d), the components return to their original positions.[53]

1.3.1 pH induced molecular shuttles

The first bistable switchable molecular shuttle which could be considered as an example of a molecular Brownian motion machine was reported by Stoddart and co-workers in 1994 (Scheme 1.15).[54] The electron-accepting tetracationic cyclophane in **63**$^{4+}$ was shown to rapidly shuttle between both potential π-electron donor sites, hydroquinol and benzidine, at room temperature but upon cooling to 229 K the macrocycle was found to reside over benzidine satation in a ratio of 21:4 as evidenced by ^{1}H NMR spectroscopy. Protonation of the benzidine residue with trifluoroacetic acid destabilises its interaction

with the ring and it moves to reside on the secondary hydroquinol station to generate [**63**·2H]$^{6+}$. The system can be restored by adding pyridine-d_5 to neutralise the system.

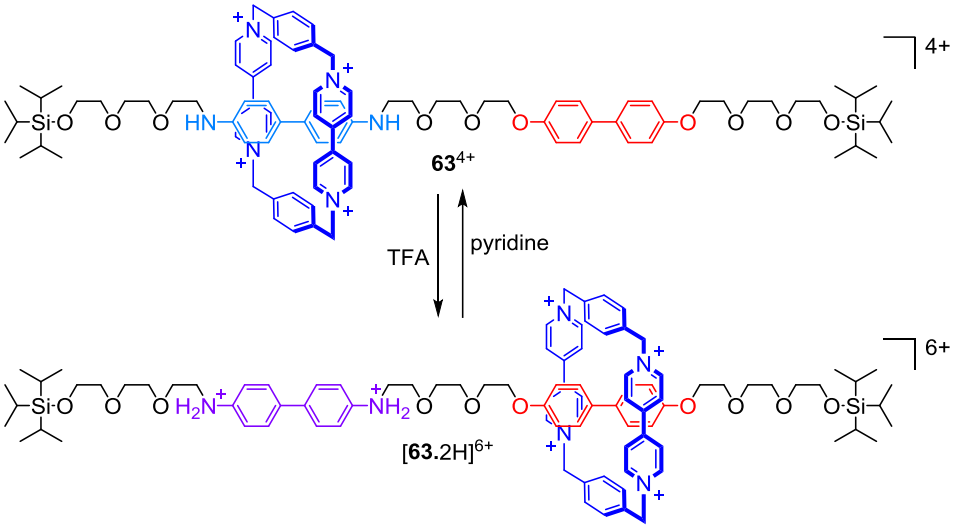

Scheme 1.15 The first non-degenerate shuttle **63**$^{4+}$.

Rotaxane [**7**·H]$^{3+}$ (as shown in Section 1.2.1.3) was another example of acid-base switchable rotaxane that exhibits good macrocycle positional integrity in both chemical states. Stoddart, Balzani and co-workers have generated a so-called "molecular elevator" by incorporating the architectural feature of [**7**·H]$^{3+}$.[55] This molecule, [**64**·3H]$^{9+}$ consists of a tripod thread component containing an ammonium centre and a bipyridinium motif in each leg which is interlocked by a platform-liked tritopic macrocyclic host (Scheme 1.16). The macrocycle initially resided at the ammonium site (upper level). Upon adding over three equivalents of base, the ammonium centres were deprotonated and as a result, the platform moved to bipyridinium (lower level) stations. Subsequent treatment with acid restored the ammonium stations, the macrocycle moved back to the upper level. The "up and down" motion corresponds to a quantitative switching and can be repeated many times

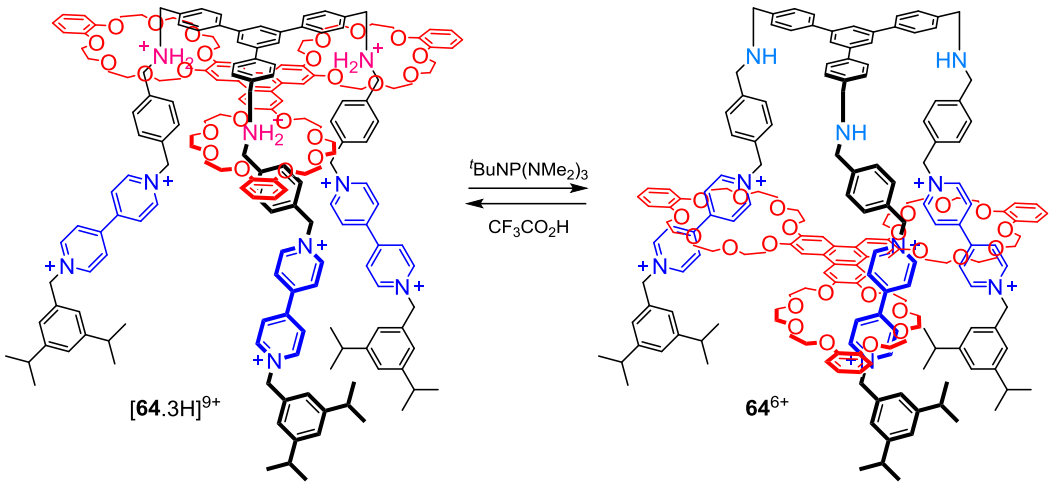

Scheme 1.16 Chemical structure of a "molecular elevator" [**64**.3H]$^{9+}$/**64**$^{6+}$

A pH-responsive switch that exploited hydrogen-bonding interactions to anions was reported by Leigh and co-workers in 2004.[56] The rotaxane **65** is formed from a hydrogen bonded benzylic amide macrocycle and succinimide peptide containing thread. The thread also contains a cinnamate derivative. In the neutral state, the macrocycle resides exclusively on succinamide station due to poor hydrogen-bond of phenol moiety. Deprotonation in DMF-d_7 results in the macrocycle binding to the phenolate anion. Reprotonation of the phenol returns the system to its original state. The shuttling is extremely solvent-dependent and it usually performs best in non-competing solvents.

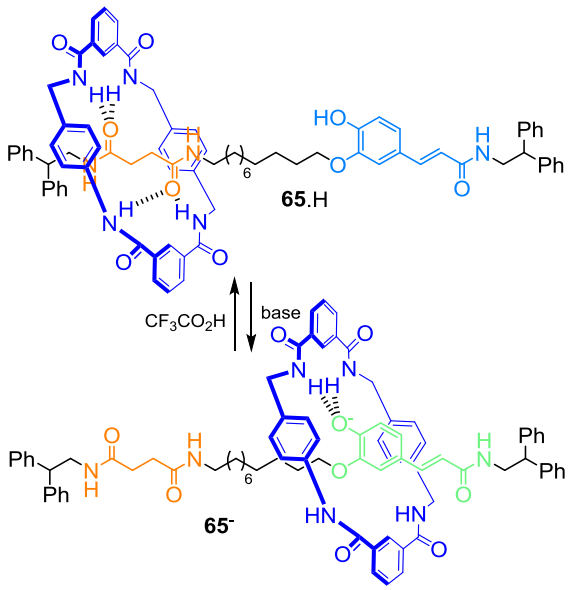

Scheme 1.17 pH-switched anion-induced shuttling in hydrogen-bonded [2]rotaxane **65**·H/**65**$^-$ in DMF-d_7 at rt. Bases that are effective include LiOH, NaOH, KOH, CsOH, Bu_4NOH, ^{t}BuOK, DBU and Schwesinger's phosphazine P_1 base.

Leigh and co-workers have reported the assembly and operation of a pH-responsive Pd(II)-complexed molecular shuttle.[57] The rotaxane **69** consists of a palladium complexed bis-carboxamide pyridine macrocycle and a thread with DMAP and pyridine stations. The thread **67** or **68** was then reacted with macrocycle **66** in a ligand exchange reaction, leading to the kinetically trapped pseudorotaxane which was subsequently subjected to Mitsunobu reaction with a stopper to obtain rotaxane **69**-Pd.

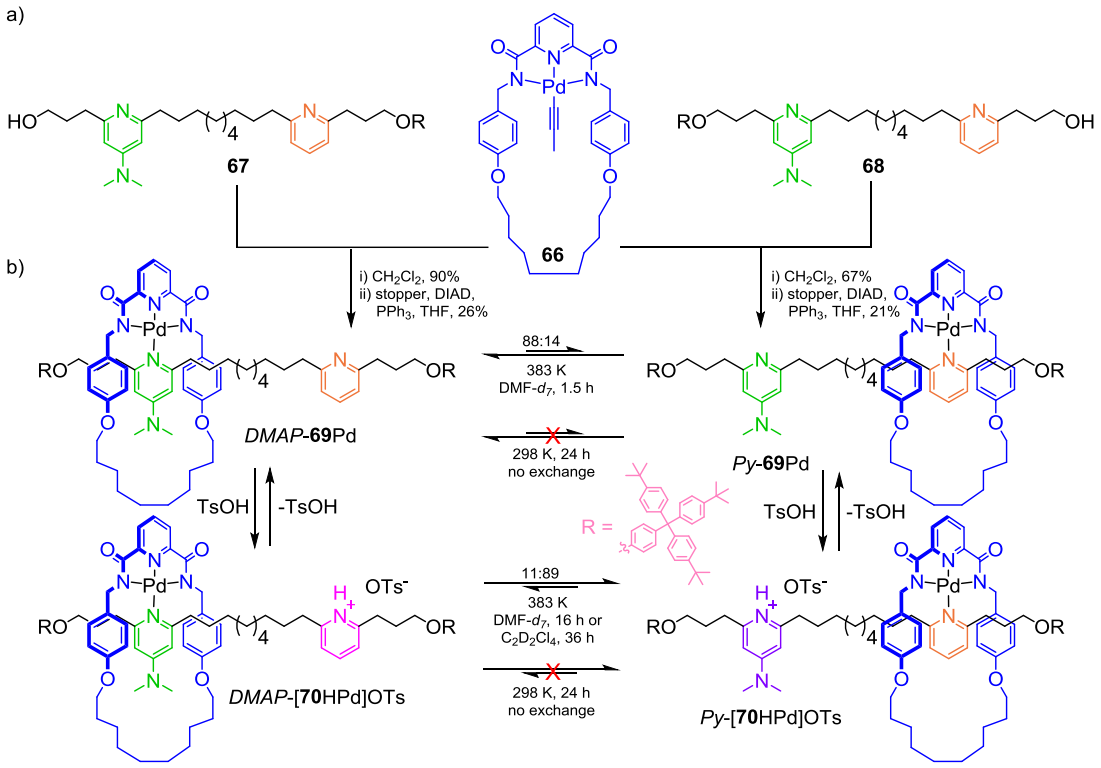

Scheme 1.18 a) Synthesis of Palladium-complexed molecular shuttle **69**-Pd; b) operation of the palladium-complexed molecular shuttle **69**-Pd.

Translocation of the palladium-complexed macrocycle between two monodentate stations was achieved as a function of basicity. Switching of the macrocycle in *DMAP*-**69**-Pd was attempted upon treatment with 1 equivalent of TsOH. The metastable co-conformer *DMAP*-[**70**HPd]OTs was formed but the macrocycle remained bound to the DMAP station. The ^{1}H NMR spectrum showed no shift of the DMAP signals over several days indicating that the co-conformer is stable at ambient temperature. However, upon heating *DMAP*-[**70**HPd]OTS at 383 K, positional switching of the palladium macrocycle was observed reaching an equilibrium of 89:11 ratio of *Py:DMAP*-[**70**HPd]OTs after 16 h (DMF-d_7) or 36 h ($C_2D_2Cl_4$). Deprotonation of this isomeric mixture of [**70**HPd]OTs (Na_2CO_3, CH_2Cl_2, 30 min) generates the neutral co-conformers. Heating either pure *Py*-

69Pd or the non-equilibrium 11:89 mixture of *DMAP*/*Py*-**70**Pd at 383 K in DMF-d_7 for 90 min reversed the coordinative bias of the metal to complete the cycle with an equilibrium ratio of 86:14 *DMAP*/*Py*-**70**Pd.

A second generation Pd(II)-complexed molecular shuttle, **71**-Pd (Figure 1.14) was reported three years later[58] featuring a change to the size and shape of the macrocycle. A significant increase in the shuttling rates and more pronounced positional discrimination in both chemical states (neutral and protonated) was observed. It has been suggested that the larger macrocycle in the second generation shuttle provides a less sterically demanding environment around the metal and thus better accommodates the incoming coordinationg solvent molecule or OTs^- anion, in turn gives a faster shuttling rate. In the protonated state, the better positional bias of the Pd(II) macrocycle suggests that the Pd-(bis-anilide) ring binds less strongly to the thread than the Pd-(benzylic amide) while in neutral condition, the bias arises from a subtle balance of solvation, metal-ligand coordination and π-stacking interactions.

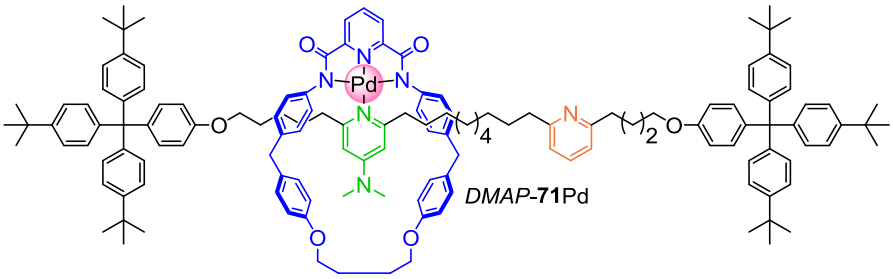

Figure 1.14 Second generation Pd(II)-based pH-responsive molecular shuttle **71**-Pd.

1.3.2 Electrochemically induced molecular shuttles

In the pH-switchable shuttle **63** (Scheme 1.15), the translation could also be achieved by electrochemical oxidation of the benzidine station to give the radical cation; the macrocycle shuttles to the biphenol station.[54] However, the use of redox-active stations based on tetrathiafulvalene (TTF) brings about a series of redox-active shuttles in Stoddart group. In the ground state of $\mathbf{72}^{4+}$ (Scheme 1.19) the tetracationic cyclophane mostly resides on the more electron-rich TTF station. Chemical or electrochemical oxidation of the TTF to either its radical cation or dication results in a shift of the cyclophane to the dihydroxynaphthalene station.[59]

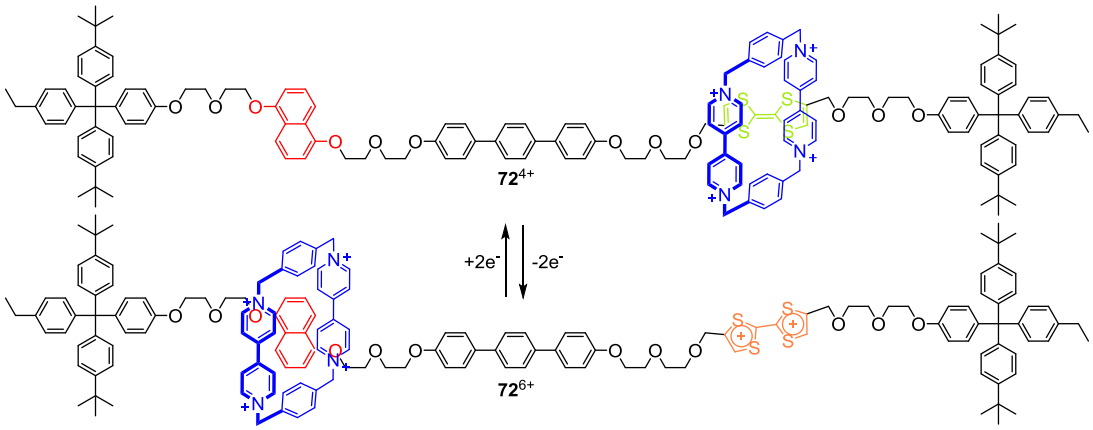

Scheme 1.19 Redox-switchable molecular shuttle $\mathbf{72}^{4+}/\mathbf{72}^{6+}$. The redox reactions may be carried out either chemically or electrochemically.

An electrochemical switchable amide-based [2]rotaxane **73** including two potential hydrogen-bonding stations, a succinamide (*succ*) and a redox-active 3,6-di-*tert*-butyl-1,8-naphthalimide (*ni*) reported by Leigh and co-workers (Scheme 1.20) is one of the molecular shuttles with the highest reported positional loyalty (*ca.* 10^6:1 in one state; *ca.* 1:500 in the other).[60] The neutral naphthalimide moiety is poor H-bond acceptor thus does not hold the macrocycle efficiently, as a result, macrocycle binding at *succ* station tightly in $CDCl_3$, CD_3CN, and THF-d_8. One-electron reduction of naphthalimide to the corresponding radical anion, results in a substantial increase in electron density on the imide carbonyls with an accompanying increase in hydrogen-bond acceptor strength. This leads to a co-conformation *ni*-$\mathbf{73}^{\cdot-}$. Subsequent reoxidation to the neutral state restores the original binding affinities and the macrocycle returns to *succ* station.

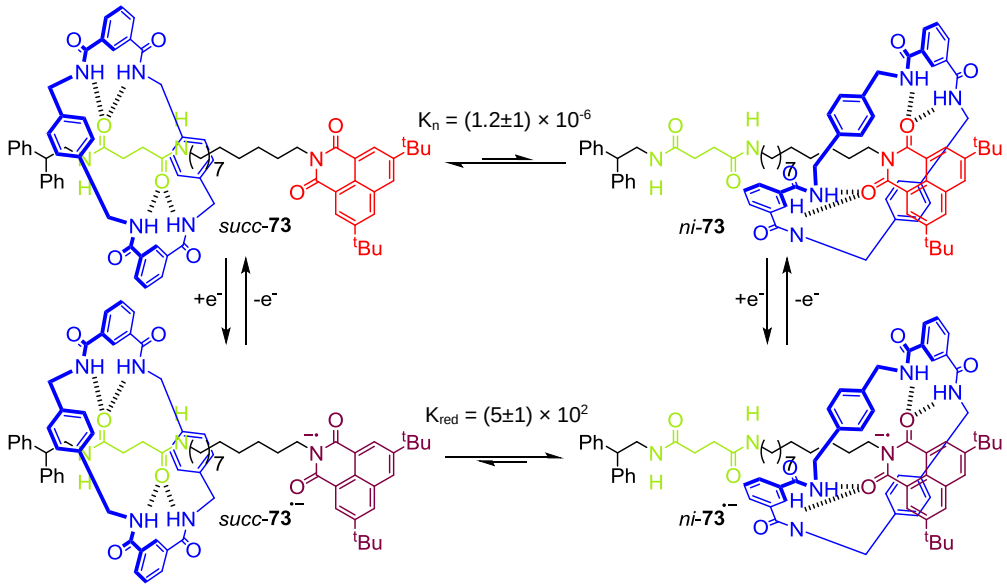

Scheme 1.20 A photochemically and electrochemically switchable hydrogen-bonded molecular shuttle **73**.

The electrochemically-induced translation of a macrocycle in the copper-based rotaxane **74**$^{+}$ (Figure 1.15) has been reported by Sauvage and co-workers in 1997.[61] This system functions on the same principle as that of the first switchable [2]catenane, published three years earlier.[62] The [2]rotaxane **74**$^{+}$ posseses a tridentate 2,2',6',2"-terpyridine (terpy) and a bidentate 2,9-diphenyl-1,10-phenanthroline (dpp) in the thread and the macrocycle has only dpp. The electrochemical properties of copper complexes were used to set the system in motion, utilising the oxidation states +1 and +2 which show differences in the preferred coordination number (CN): CN = 4 for copper(I) and CN = 5 (or 6) for copper (II). The interconversion between both co-conformations is electrochemically triggered and results in the "sliding" of the ring along the thread. Although the system was set in motion using a redox signal (Cu^{II}/Cu^{I}), the gliding motions are slow on the CV time scale.

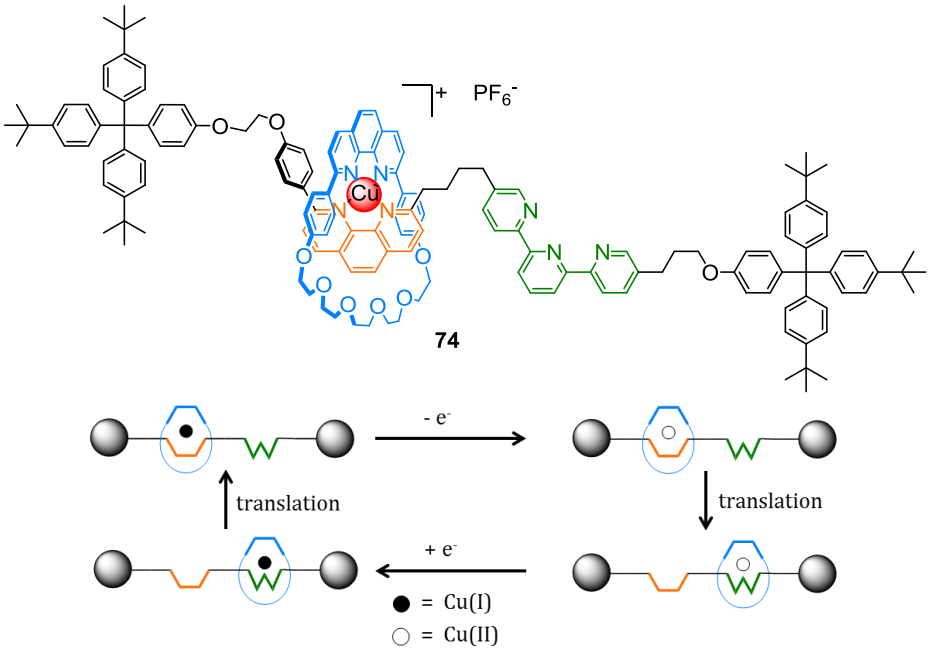

Figure 1.15 The first copper-based molecular shuttle **74** and schematic in shuttling process.

Subsequently, new shuttles have been designed within the Sauvage group incorporating the wide and non sterically hindering dpbiiq (8,8'-diphenyl-3,3'-biisoquinoline) macrocycle (**75**) and its corresponding rotaxane (**76**$^{+}$) compared to a dpp-based analogue (**77**$^{+}$) (Figure 1.16). † The behaviour of these two Cu-rotaxanes has been investigated by CV. The rate constant for the conversion of $\mathbf{76}_4^{2+}$ to $\mathbf{76}_5^{2+}$ is approximately 2 s^{-1}. By contrast, after oxidation of $\mathbf{77}_4^{+}$ to $\mathbf{77}_4^{2+}$, the thermodynamically

† The subscript indicates coordination number of the complexes.

unstable form of the complex seems to be stable for several hours, also showing that the rigid purely aromatic connector between phen and terpy is much less favourable to fast translation than the flexible axis used in **74**$^{4+}$. The opposite motion observed in 5-coordinate rotaxanes is relatively fast for both shuttles with the half-life of the 5-coordinate Cu(I) species being below 20 ms for the dpiiq-containing system **76**$_5^{+}$ and below 1 s for the dpp-based molecule **77**$_5^{+}$.[63]

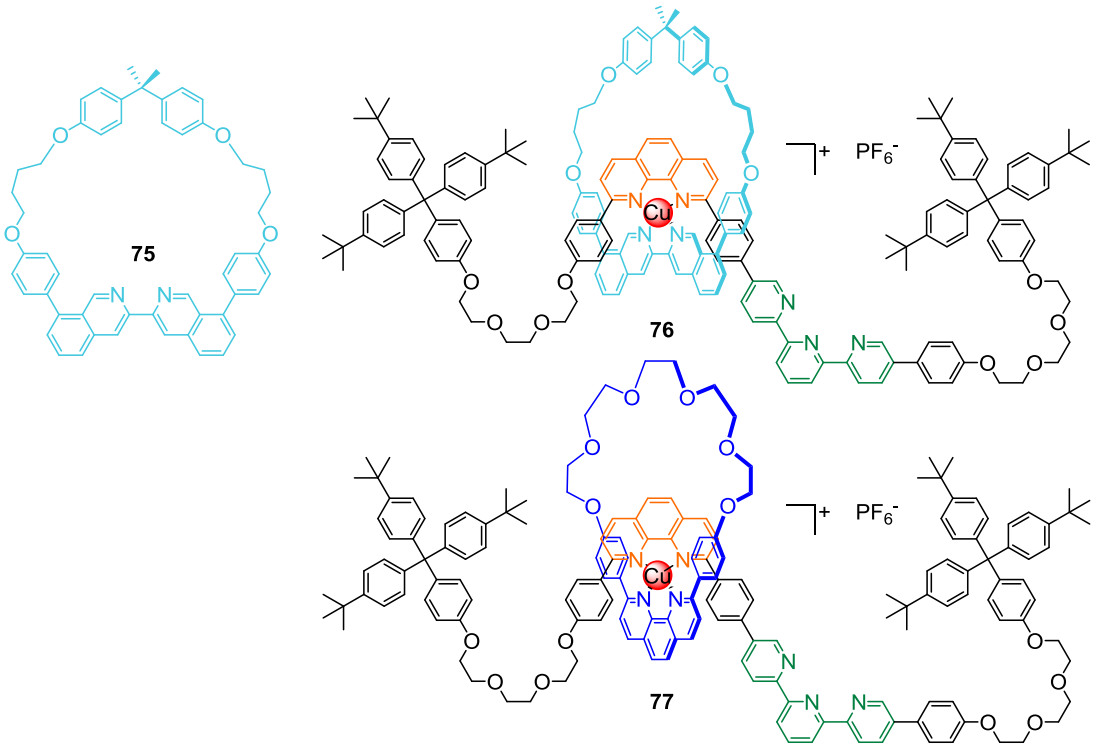

Figure 1.16 New design macrocycle **75**, containing a dpbiiq unit, its corresponding rotaxane **76** and dpp-containing rotaxane **77**.

1.3.3 Light-induced molecular shuttles

Reversible *cis-trans* photoisomerisation of stilbene and azobenzene motifs have been widely exploited for realising translation in rotaxane-based systems.[53] One example is shown for a cyclodextrin-based [2]rotaxane **4**$^{4+}$ by Nakashima (Section 1.2.1.2). The same author has varied ethylene spacer length between the stopper and aromatic unit in the rotaxane structures and showed that the shuttling process can be driven by light, heating and solvent polarity.[64]

A molecular shuttle based on [2]rotaxane **78** containing α-cyclodextrin macrocycle, azobenzene, biphenyl chain and two different fluorescent naphthalimide units was

reported by Tian and co-workers (Scheme 1.21).[65] Reversible motion of the CD macrocycle between azobenzene and biphenyl station takes place after irradiation at 360 and 430 nm, respectively. The CD macrocycle locates over the azobenzene unit in *trans*-form and it moves to the biphenyl site when the azo motif undergoes isomerism to the *cis*-form. This net translational displacement is accompanied by reversible changes in fluorescence intensity of the two stoppers which increase when the CD reside in the close proximity and decrease when CD is away.

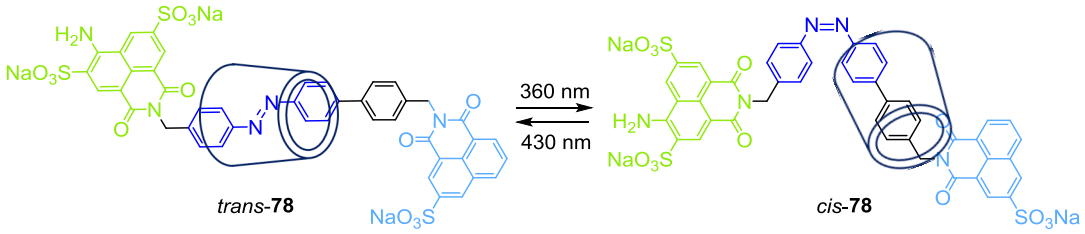

Scheme 1.21 A light driven molecular shuttle based on CD-[2]rotaxane **78**.

Similar shuttling has also been observed when stilbene was used as a photoresponsive unit (Scheme 1.22).[66] Isophthalic acid stopper was found to form hydrogen-bond interactions with the CD macrocycle and prevent the shuttling motion. Upon treatment with base, the shuttling is enabled. The reaction progress was monitored by ^{1}H NMR spectroscopy and fluorescence spectrophotometry.

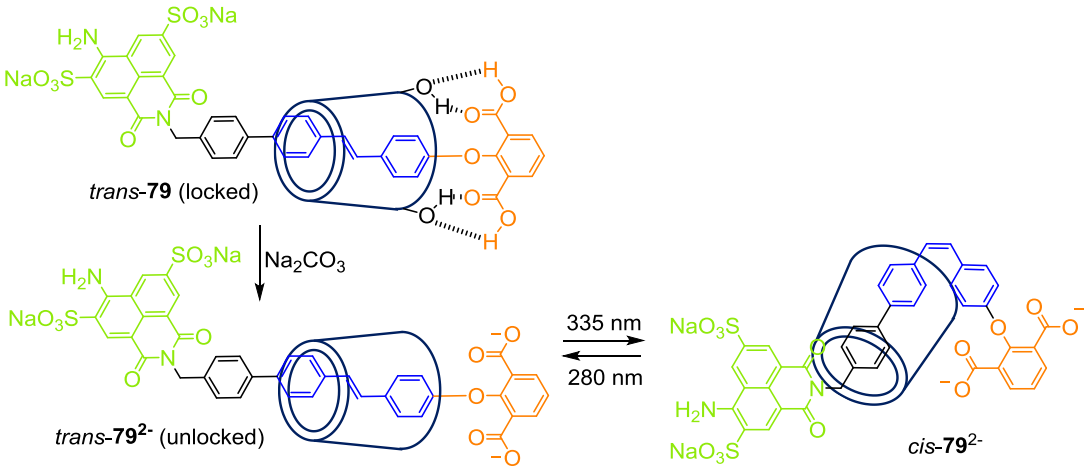

Scheme 1.22 The strong hydrogen-bonding between the OH groups in CD and two carboxyl groups in the isophthalic acid unit locks the photo-driven motion of CD. The addition of Na_2CO_3 destroys the H-bond, unlocking the shuttling motion.

Anderson and co-workers demonstrated unprecedented directional shuttling of an asymmetric cyclodextrin macrocycle (smaller 6-rim *vs* larger 3-rim) along a symmetric organic axle featuring a stilbene moiety (Scheme 1.23).[67] In *trans*-**80**, a rapid gliding motion of the CD ring along the thread was observed by 2D NMR spectroscopy. Irradiation at 340 nm led to *trans*-*cis* isomerisation to afford *cis*-**80**. In the *cis*-conformer, the stilbene unit of the thread is located in close proximity to the 6-rim of the CD ring whilst the wider 3-rim is able to better accommodate the bulky "stopper" group. The molecular switching cycle between the two co-conformers was completed upon irradiation of *cis*-**80** at 265 nm.

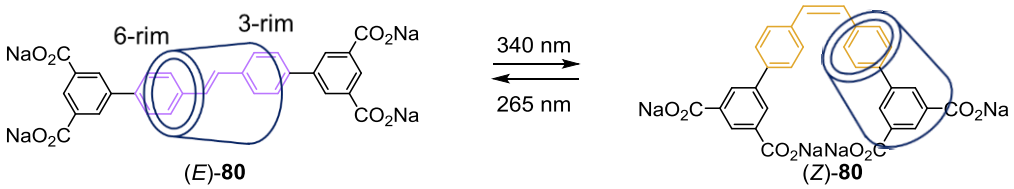

Scheme 1.23 Photoresponsive single-station shuttles **80** based on stilbene units.

The Leigh group has reported the shuttles that utilise the interconversion of fumaramide (*trans*) and maleamide (*cis*) isomers of the olefin units by photochemical and thermal stimuli (Scheme 1.24).[68] Fumaramide groups are excellent biding sites for a benzylic amide macrocycle[69] with ideal positioning of *trans* hydrogen-bond acceptor sites for interactions with the ring. Irradiation of fumaramide rotaxane (*E*)-**81** at 254 nm produces the corresponding *cis*-maleamide rotaxane (*Z*)-**81** which reduces the number of intercomponent hydrogen bonds and so the macrocycle changes position to the succinamide station. This translational form is stable until a new stimulus (heat) is applied to re-isomerise the maleamide unit back to fumaramide.

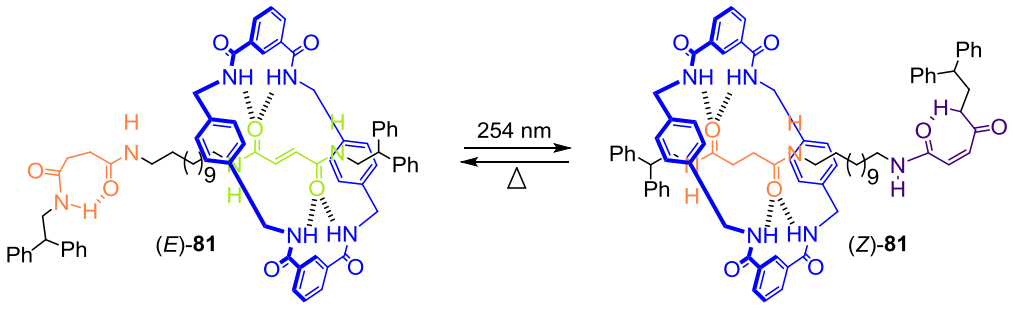

Scheme 1.24 Bistable light and heat responsive molecular shuttle **81**.

Rotaxane **82**$^{6+}$ was designed to achieve photoinduced ring shuttling in solution by Balzani, Stoddart and co-workers.[70] The operation to obtain abacus-like movement

starts with light excitation of the photoactive unit ruthenium(II) tris(bipyridine) complex followed by the transfer of an electron from the excited state to the 4,4'-bipyridinium station, which is surrounded by the macrocycle, with the consequent deactivation of this station. This photoinduced electron-transfer process has to compete with the intrinsic decay of the metal center excited state. The ring moves from the reduced 4,4'-bipyridinium station to the 3,3'-demethyl-4,4'-bipyridinium unit, a step that has to compete with the back electron-transfer process from reduced 4,4'-bipyridinium station (still encircled by the ring) to the oxidised unit Ru^{3+}. A back electron-transfer process from the free reduced bipyridinium station to the oxidised Ru^{3+} unit restores the electron-deficient bipyridinium station. As a consequence of the electronic reset, the ring moves back from the dimethyl-bipyridinium station to the bipyridinium station. It has been shown that the absorption of a visible photon by $\mathbf{82}^{6+}$ can cause the ring movement. A full mechanical cycle that does not generate any waste products is illustrated in Scheme 1.25b. $\mathbf{82}^{6+}$ performs as a "four stroke" autonomous artificial linear motor working by an intramolecular mechanism powered by visible light.

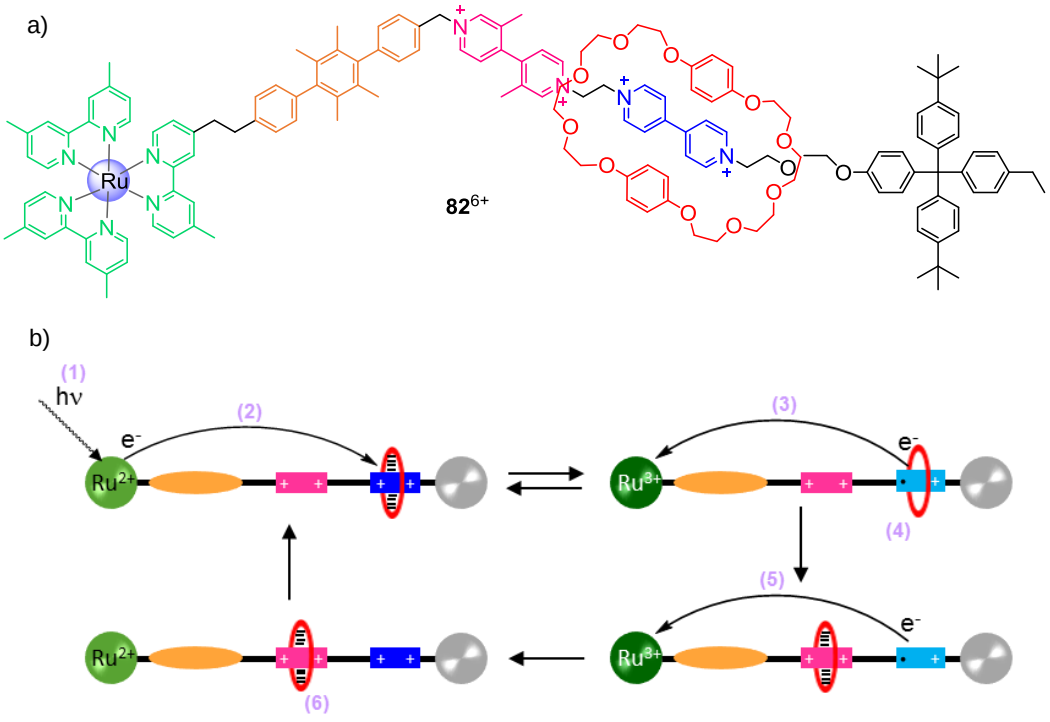

Scheme 1.25 a) Chemical formula of the rotaxane $\mathbf{81}^{6+}$; b) Operation of rotaxane $\mathbf{81}^{6+}$ as an autonomous "four stroke" molecular shuttle powered by light.

In addition, photoinduced translational motion in [2]rotaxane **23**-Ru^{II} has been realised by Sauvage and co-workers in 2005.[71] The Ru(II) metal centre was preferred to endo-coordinate to the thread by tuning the size of ligands of the macrocycle to obtain

rotaxane **23**$^{2+}$. By irradiating a solution of **23**$^{2+}$ in 1,2-dichloroethane at 470 nm and in the presence of a large excess of Cl^-, a clean photochemical reaction takes place, two coordination sites of Ru(II) were filled by chloride ligands which caused dissociation of the macrocycle to permit the translation along the thread.

1.3.4 Molecular shuttles powered by metal ions

A molecular shuttle that can be switched upon the addition of lithium ions was produced by the Sanders and Stoddart groups.[72] The co-conformation of [2]rotaxane **83** with the macrocycle sitting over the naphthaldiimide station is dominant in the charge neutral form, but rather than one electron reduction to change the macrocycle bias to the pyrimellitic diimide station, addition of Li^+ ions also results in the movement of the ring. Two lithium ions can be complexed between the crown ether macrocycle and the carbonyl of the diimide moieties with a significantly stronger interaction in comparison to naphthaldiimide (Scheme 1.26). The system was reset by addition of a large excess of [12]crown-4.

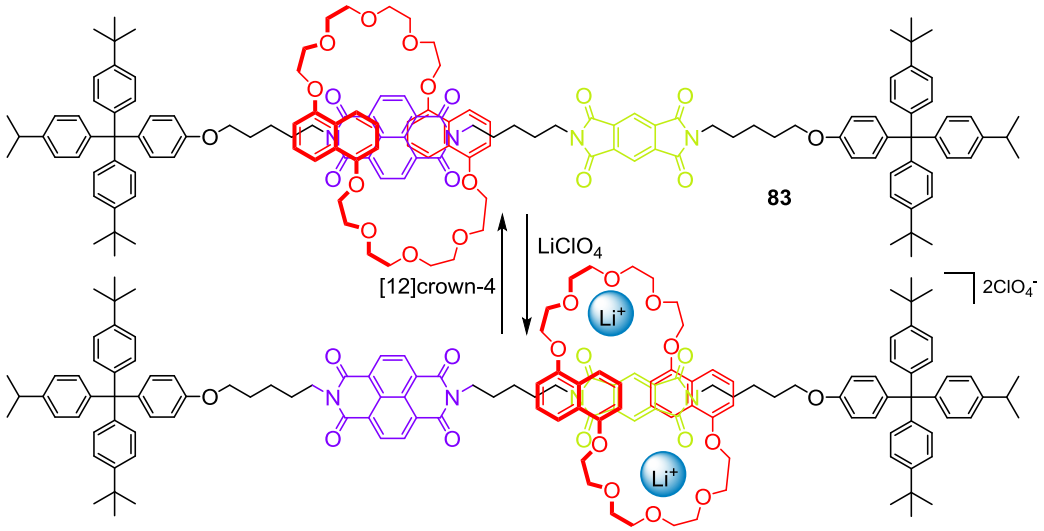

Scheme 1.26 Cation-induced shuttling based on lithium-ion complexation and decomplexation in **83.**

Metal-ion binding can be used to destabilise the binding of the macrocycle at one site, and cause translational motion to the other station through two distinct mechanisms as reported by Leigh and co-workers in 2006 (Scheme 1.27).[73] The macrocycle in rotaxane H_2.**84** preferable resides over the glycylglycine derivatised station with a bis(2-picolyl)amino stopper. Upon addition of one equivalent of $Cd(NO_3)_2.4H_2O$, a complex in which the metal ion is bound to the carboxamide carbonyl oxygen on the thread and

three nitrogen of stopper is produced and the macrocycle still rests at the same position. However, deprotonation of the adjacent peptidic station causes the metal to wrap itself up to form the [Cd**84**(NO_3)(H)] complex, thus switching off the interaction with the macrocycle. The macrocycle then shuttles to the succinic amide ester station. The process is fully reversible: removal of Cd^{2+} ion with excess cyanide and *in situ* reprotonation of the amide nitrogen with NH_4Cl quantitatively regenerates H_2.**84**. In the case of rotaxane **85**, Cd^{2+} ions are only chelated to the three nitrogen atoms of the stopper. As the two pyridyl units have to adopt a coplanar conformation, this causes a steric hindrance and destabilises the interaction with the macrocycle. The macrocycle is thus forced to move to the weaker succinic amide ester site. The shuttling is fully reversible on demetallation of [Cd(NO_3)$_2$(**85**)] with cyanide.[74]

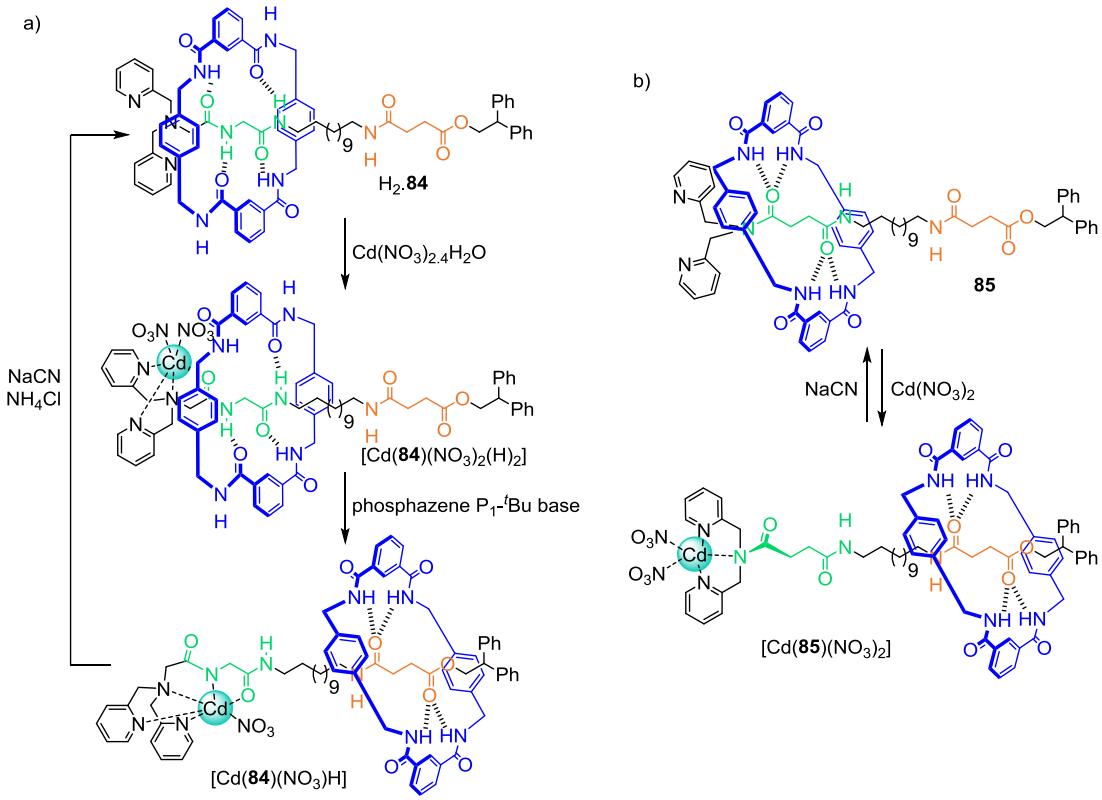

Scheme 1.27 (a) Shuttling of **84** through stepwise competitive binding. (b) An allosterically regulated molecular shuttle **85**.

A molecular machine that nominally mimics the function of actin/myosin linear motors has been constructed by Sauvage and co-workers.[75] The system is based on a symmetrical doubly threaded topology and is able to contract or stretch under the action of an external chemical signal. Each filament contains both a bidentate and a tridentate chelate contributing to the copper-complexed rotaxane **86**$^{2+}$, Figure 1.17. The rotaxane

dimer $\mathbf{86}^{2+}$ was set in motion by exchanging the complexed metal centres. The free ligand obtained by reacting the stretched isomer, 4-coordinate Cu(I) with an excess of KCN was then subsequently remetallated with $Zn(NO_3)_2$ affording the 5-coordinated Zn^{2+}-complex $\mathbf{86}^{4+}$ in the contraction form. The reverse motion could be induced upon addition of excess $Cu(CH_3CN)_4^+$.

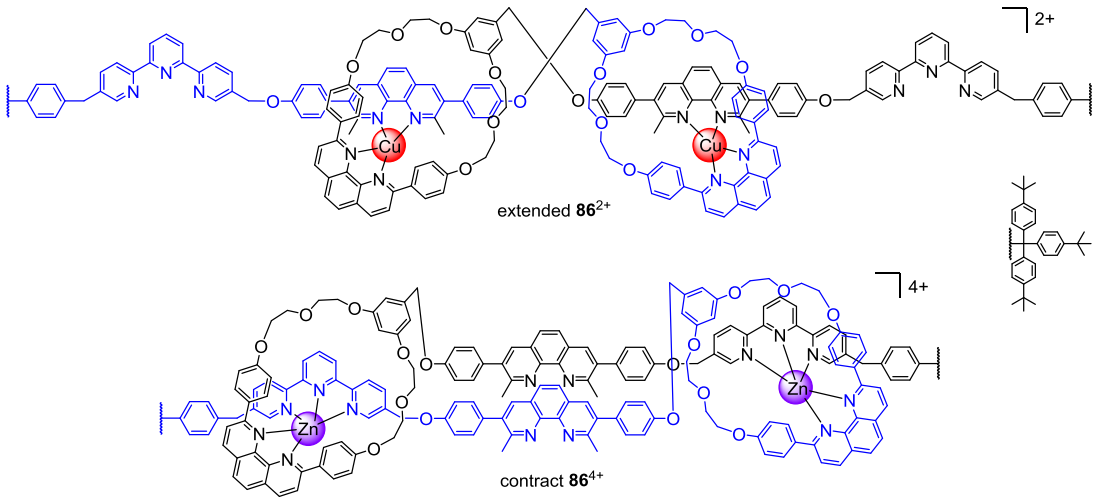

Figure 1.17 The two states of the muscle-like molecule **86**.

The group of Sauvage has reported a [3]rotaxane $\mathbf{87}^{2+}$ representing the first example of an adaptable receptor based on an interlocked compound (Scheme 1.28).[76] Two porphyrinic "plates" are able to glide along the track that threads through the macrocycle. Starting from the copper-free [3]rotaxane **88**, metalation of the coordination sites will induce a translational motion of the threaded rings and the porphyrins will come into closer proximity. As a result, a flexible substrate, **89** trapped in between these two porphyrins will be compressed whereas the rigid substrate, **89** will be destabilised and possibly expelled from the receptor.

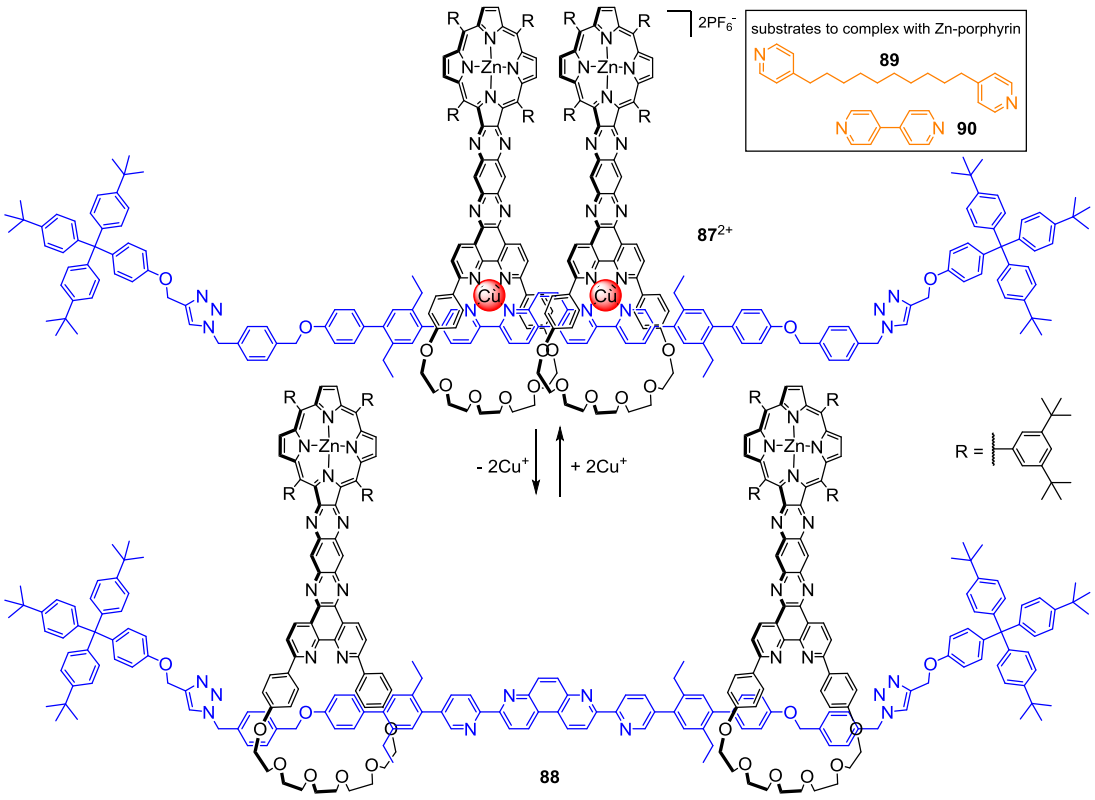

Scheme 1.28 The copper(I)-complexed [3]rotaxane **87**$^{2+}$ and free [3]rotaxane **88**.

1.3.5 Anion driven molecular shuttle

Leigh and Lusby have established an example of an anion switchable molecular shuttle **91** based on a bistable palladium(II)-containing [2]rotaxane (Scheme 1.29).[77] Up to this point, palladium(II) has been used to play the role of prearranging the subcomponents of the rotaxanes or catenanes for the interlocking step. Here, the rotaxane **91** was covalently captured using the CuAAC reaction, whilst the palladium-chloro macrocycle complex was residing over the benzyl-pyridinium position of the track due to ion pairing and secondary interactions of the macrocycle with the track components. The resultant triazole unit served as a secondary station for the palladium(II)-based macrocycle. To switch to the other station, the chloride anion was removed with a silver(I) salt, and the coordinative unsaturated palladium macrocycle translocated to the triazole unit. The process could be reversed upon treatment with Bu_4NCl.

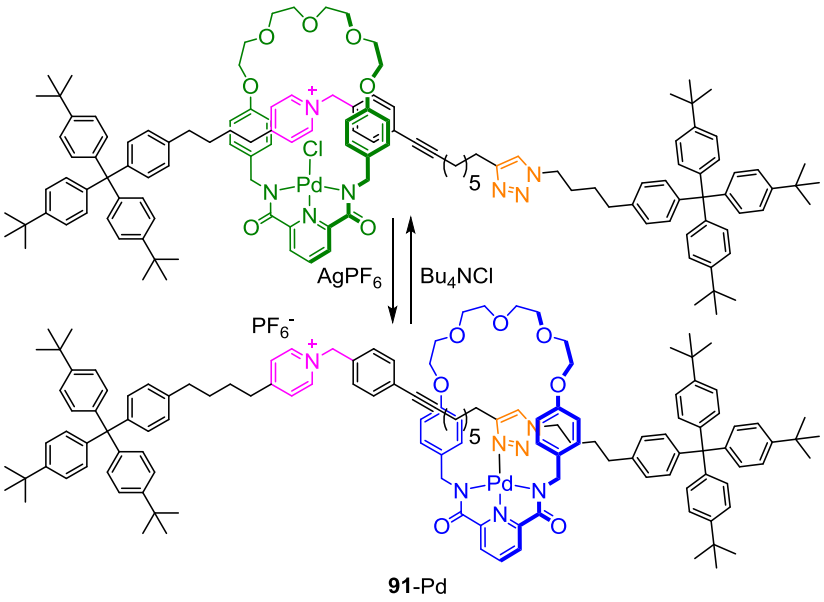

Scheme 1.29 Operation of chloride-switchable molecular shuttle **91**-Pd.

1.4 Compartmentalised Molecular Machines

To create artificial Brownian machines, control over the kinetics for exchange of the substrate between two sites of the machine, which is recognised as ratcheting, must be introduced.[53] In doing so, resetting the Brownian machines does not undo the work it has carried out or the task performed.

In 2006, Leigh and co-workers produced rotaxane **93** which was developed from rotaxane **92** (Scheme 1.30a) featuring fumaramide and succinamide stations separated by a bulky silyl ether gate that prevents a macrocycle from shuttling (Scheme 1.30b).[78] The system was prepared as a single positional isomer with the macrocycle residing over fumaramide station. When the kinetic barrier provided by the silyl ether group was removed, the machine was statistically balanced (85% of the macrocycle on the fumaramide station, 15% on the succinamide station). The balance was broken by light-induced *E*→*Z* photoisomerisation, which concomitantly reduced the affinity of the macrocycle for site closest to the diphenyl stopper generating a new equilibrium with 56% of the macrocycle over the succinamide station (the photostationary state from irradiation at *trans*-fumaramide unit at 312 nm is 49:51 ±2% *E*:*Z*). Applying an unlinking stimulus, by addition of a silyl group, stop the exchange between two compartments. Thermal *Z*→*E* isomerisation was then used to reset the system and make it thermodynamically unbalanced, unlinked, and not in equilibrium. After a single

operational cycle of the machine (balanced-unlinked, unbalanced-unlinked, unbalance-linked and reset to initial unlinked state), 56% of the macrocycles were located on the succinamide station. In this system, the thread performed a task of directionally changing the net position of the macrocycle, moving it energetically uphill.

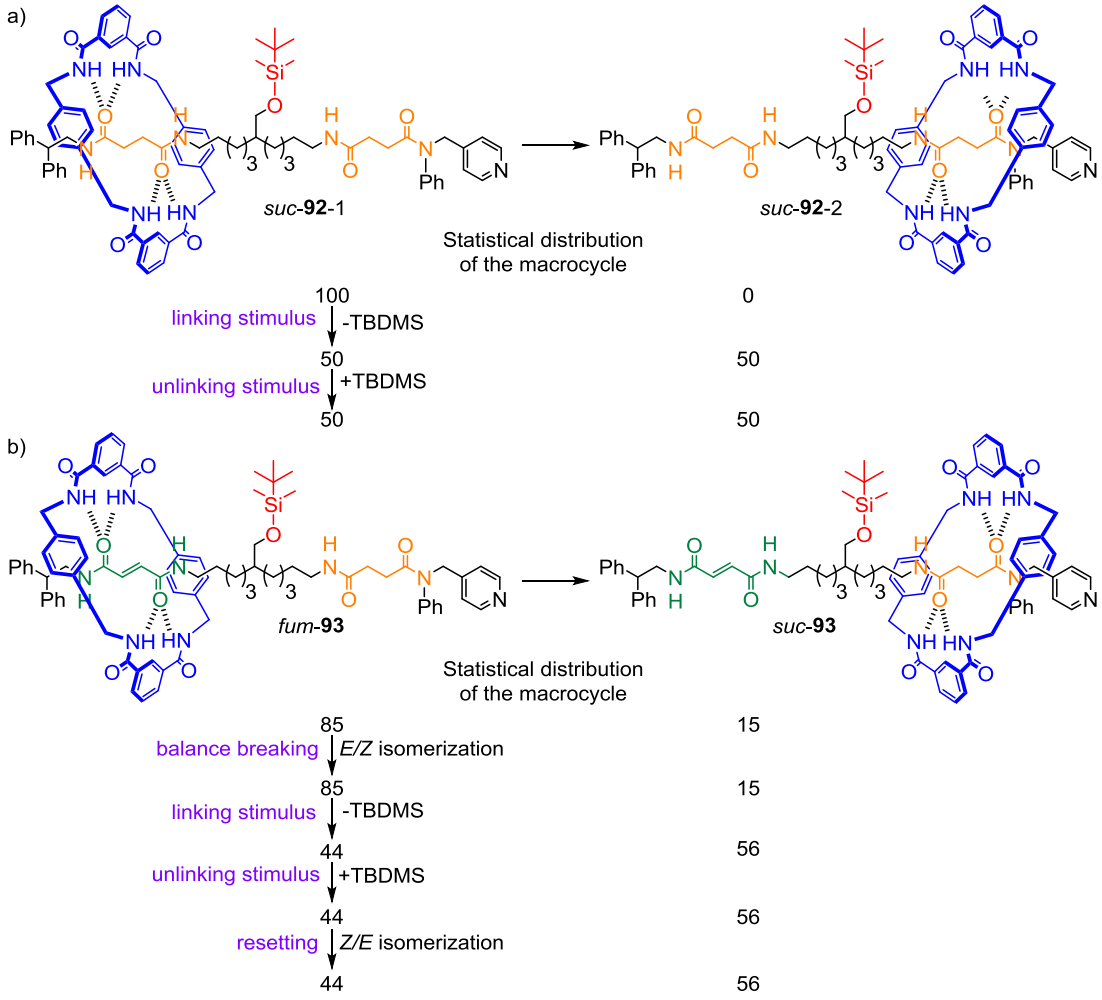

Scheme 1.30 a) Operation of a compartmentalised Brownian molecular machine **91** that act as an irreversible switch; b) Operation of a compartmentalised molecular machine **92** that transports a particle (macrocycle) energetically uphill.

In 2007, Leigh and co-workers published a photo-operated molecular information ratchet based on rotaxane **94,** which consists of a dibenzo crown ether based macrocycle mechanically interlocked onto a thread containing two secondary ammonium stations separated by an α-methyl stilbene group (Scheme 1.31).[79] This stilbene group acts as a gate that either permits (*E*-configuration) or prevent (*Z*-configuration) the macrocycle from shuttling between the dibenzyl ammonium compartment (dba, left) and monobenzyl ammonium compartment (mba, right). The gate is mostly closed upon

irradiation in the presence of an external benzil photosensitiser. However, the benzophenone associated with the macrocycle can undergo energy transfer, which is distance dependent, to induce *Z*→*E* photoisomerisation, thus opening the gate. Significantly, the macrocycle can only signal its positon when it is in the left compartment and close to the gate. Following translocation to the mba station, the macrocycle is far from the gate, and the benzil sensitised reaction dominates and the gate remains closed. This operation can drive the macrocycle distribution away from its equilibrium value (when the gate remains open) of 65:35 *dba*-**94**:*mba*-**94** to a maximum ratio of 45:55.

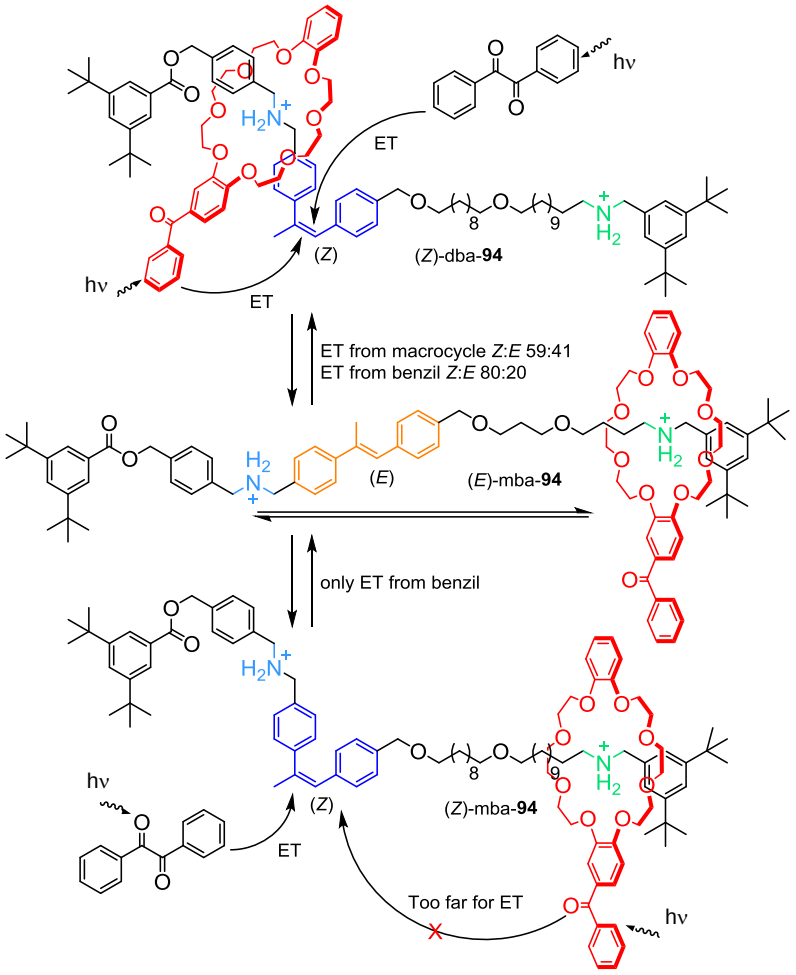

Scheme 1.31 A light-powered molecular information ratchet.

Chemically-driven information ratchet, rotaxane **95** was demonstrated by Leigh and co-workers in 2008 (Scheme 1.32a). The parent, unfunctionalised symmetrical bis(fumaramide) rotaxane has an equal macrocycle distribution between the two fumaramide groups. A chiral acylation catalyst was used to drive the system from its equilibrium ratio of 50:50 *left*-**95**:*right*-**95** to an unequal populations of 33:67. The chiral

catalyst is able to discriminate between the two pseudo-enantiomeric co-conformers of **95** and reacts more rapidly when the macrocycle is on the same prochiral fumaramide side. Use of the catalyst's chiral antipode gave the expected equal and opposite ratio of 67:33 *left*-**95**:*right*-**95**. This unequal distribution corresponds to a decrease in entropy (the energy for this is probably offset by the consumption of the chemical reagents), but the enthalpy of macrocycle-thread interaction is unaffected.

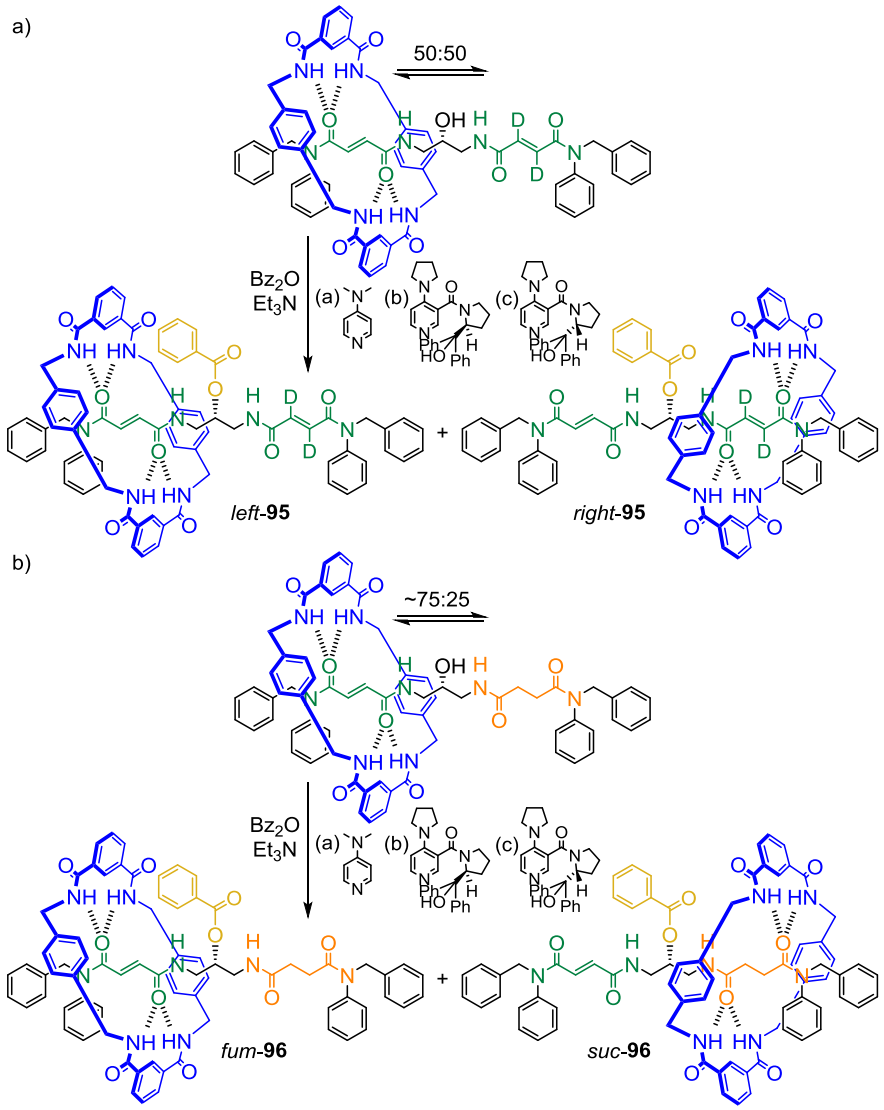

Scheme 1.32 a) A chemically fuelled molecular information ratchet; b) A chemically fuelled molecular information ratchet capable of ratcheting a Brownian particle enthalpically uphill.

The same approach was employed for the non-symmetrical rotaxane **96** containing one fumaramide group and one succinamide group (Scheme 1.32b). The equilibrium between these two stations is ~75:25 *fum*-**96**:*suc*-**96**. Benzoylation with (*S*)-catalyst reduced the population ratio to 63:37, corresponding to a transportation of approximate

15% of macrocycle from the energetically favourable fumaramide station to the less-favourable succinamide unit.

Recently, Leigh and co-workers have developed a three-compartment molecular information ratchet **97** using the similar chemical-information-ratchet concepts (Scheme 1.33).[80] The macorocycle ends up predominantly on one of the two chemically equivalent end compartments, as determined by the handedness of the catalyst.

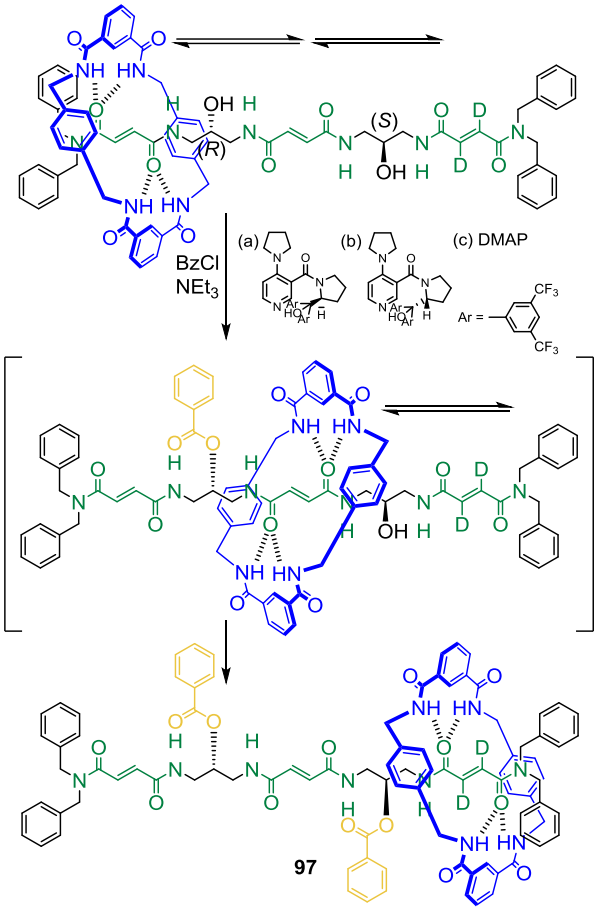

Scheme 1.33 Directonal transport of a macrocycle within a [2]rotaxane three-compartment chemical information ratchet **97**.

1.5 Functional Molecular machines

1.5.1 Sequence-Specific Peptide Synthesis by Artificial Molecular Machines

Recently, Leigh and co-workers described a molecular machine that nominally mimics the ribosome by joining amino acids in specific sequence to produce a short oligopeptide.[81] The structure of the molecular machine **98** is based on a rotaxane including the thread (which bears the amino acid monomers as reactive phenolic esters), and a macrocycle that features a terminal amine and a cysteine unit capable of mediating native chemical ligation (Figure 1.18). The amino acid phenolic esters act as gates that prevent the macrocycle from moving further along the track. However, the macrocycle can react with the first station, producing an intermediate thioester and transfer it to amino terminus. The removal of the amino acid from the first gate also allows the macrocycle to slip over this and onto the second phenolic ester. The process continues until the last amino acid on the thread is transferred and the macrocycle detaches from the strand. HPLC, ^{1}H NMR spectroscopy and mass spectrometry were used to confirm the identity of desired product, in particular that the machines works processively to produce a single amino acid sequence.

A year later, the Leigh group reported a machine that was more efficient by changing the rotaxane forming strategy from "final-step-threading" to "rotaxane capping" which enables a longer amino sequence track. The new approach can join up to four amino acids in sequence featuring up to a 20-membered ring native chemical ligation transition state.[82]

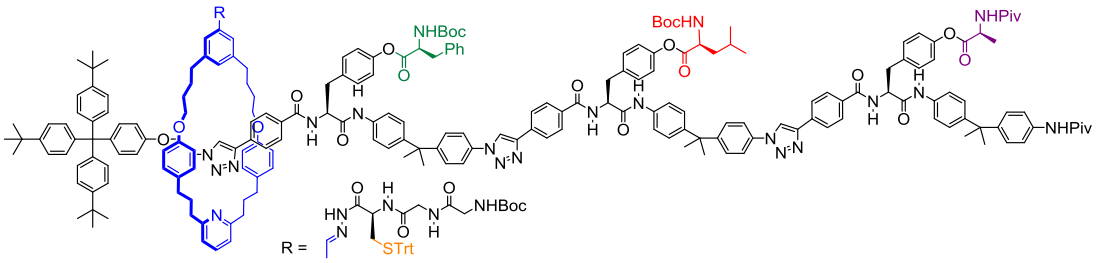

Figure 1.18 [2]Rotaxane based molecular machine **98**.

1.5.2 Metal complexes molecular biped

A bimetallic molecular biped **99** was developed by the Leigh group recently.[83] This molecular walker features a palladium and platinum complex "feet" (based on tridentate

pyridine-2,6-dicarboxamide motif used in previously described catenanes and rotaxanes) linked together using CuAAC chemistry (Scheme 1.34). The palladium foot can be selectively stepped between DMAP and Py sites *via* reversible protonation while the kinetically inert platinum complex foot keeps the complexes remains attached to the track. Operational control of stepping mechanisms is based upon carefully alternating the stimuli-induced with consideration of the thermodynamics and kinetics of each step.

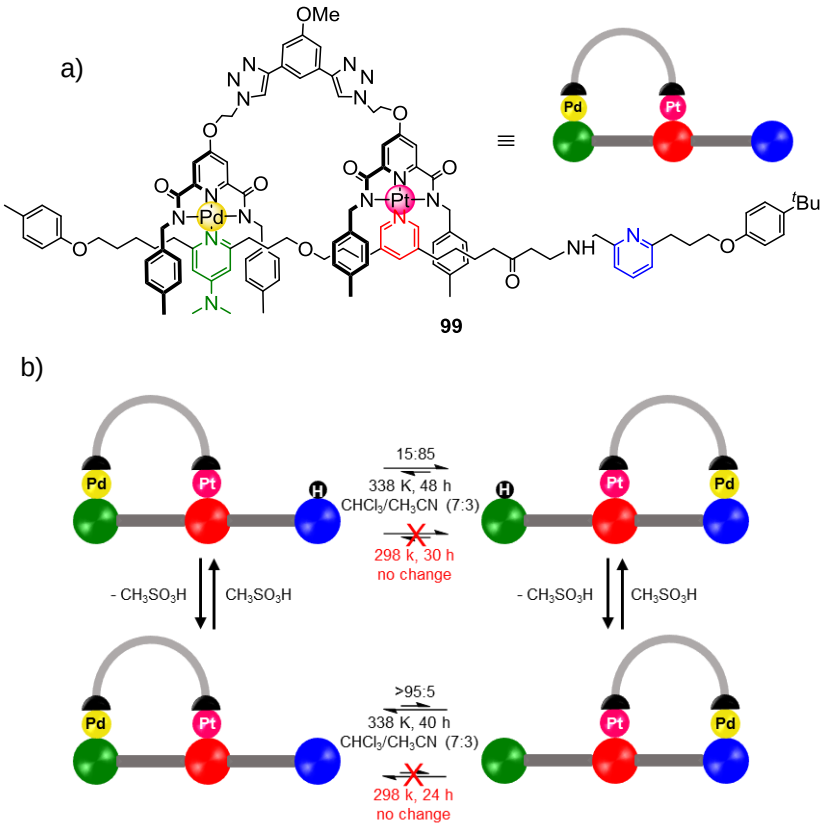

Scheme 1.34 a) Chemical structure of bimetallic walker-track complex **99**; b) Stepping of a Pd(II)/Pt(II)-complexed molecular biped.

1.5.3 Rotaxane-based switchable organocatalyst

Recently, a study of the reactivity of a rotaxane acting as an amino catalyst for the functionalisation of carbonyl compounds was published by Leigh and co-workers.[84] The rotaxane **100** consists of a dibenzo crown ether based macrocycle trapped onto a thread containing a dibenzylamine and a triazolium ring (Scheme 1.35). The catalytic activity can be switch "off" or "on" by acid-base stimuli-induced change of the position of the macrocycle on the thread. The rotaxane **100** showed an effective performance in iminium, enamine, tandem iminium-enamine and trienamine catalysis.

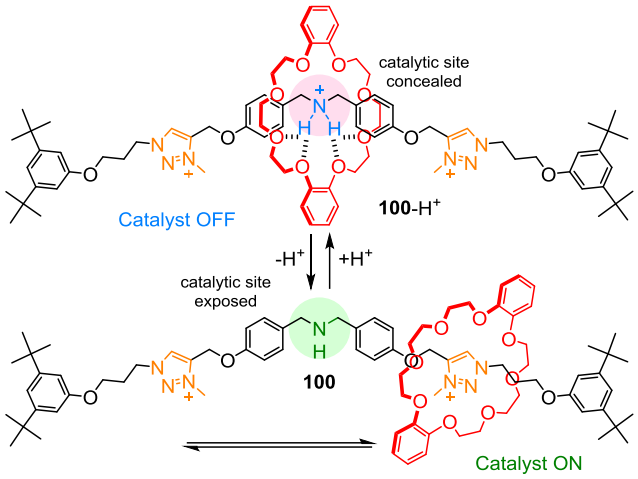

Scheme 1.35 Rotaxane-based switchable organocatalyst **100**/**100**-H⁺.

1.6 Self-assembly molecular systems

Nature uses supramolecular self-assembly strategies to generate useful functional systems, including all of the examples biomotors. The approach can be used to overcome limitations arose from multistep covalent synthesis for nanodevices. The covalent-bond based synthesis has proved successful in making molecules with useful functions, whereas the ability to make supramolecular assemblies with applications are poorly recognised.[85] As the number of components included in a self-assembly process increases, the tendency to self-sort[86] leads to the formation of several product arises and that obstructs the development. To achieve useful function, in particular those that involve mechanical movement any self-assembly system would need i) to exhibit high fidelity of the self-assembling interactions that will allow information-rich components to selectively assemble, ii) an ability to direct self-assembly along a kinetically preferred pathway, with the products displaying pronounced kinetic stability such that mechanical motion rather than dynamic host-guest exchange can be observed.[85b] From this perspective, coordination assemblies, and in particular those that feature multiple relatively strong metal-ligand interactions appear promising as elements of molecular machinery as they exhibit pronounced cooperative stability such that they could be considered non-equilibrium systems.[87] There are some other examples known, based on non-interlocked coordination assemblies[88] that undergo the molecular motion.[51, 89]

1.6.1 Tubular coordination complexes

Fujita and co-workers has studied a coordination approach to create discrete tubular structures. A wide range of pyridine-based molecular strands have been used to assemble tubular architectures through non-covalent metal-ligand interactions, in particular, with *cis*-protected square-planar building blocks such as [(en)Pd(NO_3)$_2$] (**101**). By adjusting the length of strand-like ligands, they envisaged an approach to precisely control the length of self-assembled tubular objects. A family of rectangular molecular panels **102**-**107** was designed in order to assemble them into several tubular structures of various sizes and shapes (Figure 1.19). Oligo(3,5-pyridine) panels **102**, **103** and **104** contain three, four and five binding sites, respectively. Molecular panels **105** and **106** contain six binding sites from two terpyridine linked by an alkyl chain or biphenyl unit. Molecular panel **107** featuring four terpyridine podands on a benzene-tetracarboxylate scaffold has twelve binding sites.

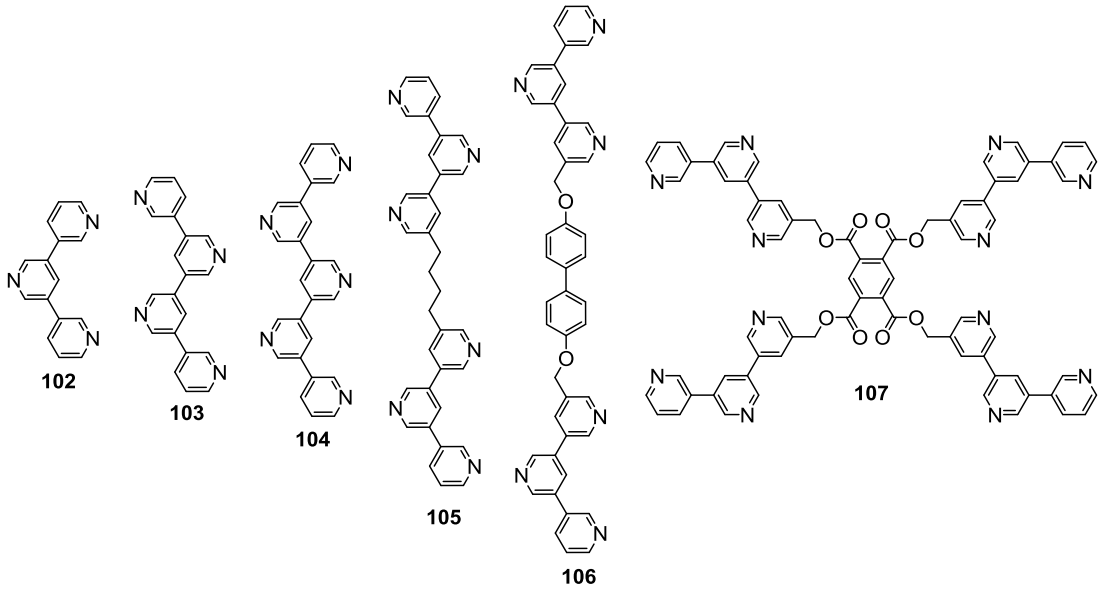

Figure 1.19 Rectangular ligand **102**-**107**.

The Fujita laboratory has shown quantitative formation of coordination nanotubes from ligand **102**-**104** and Pd^{II} **101**.[90] In the case of pentakis(3,5-pyridine), coordination tube **110** should be assembled from four molecules of **104** and ten molecules of **101**. However, this formed only in the presence of a rod-like template molecule, 4,4'-biphenylenedicarboxylate **111** (Figure 1.20). Similarly, tubes **108** and **109** were also obtained with the aid of templates and were characterised by NMR and cold-spray-ionisation mass spectrometry (CSI-MS).[91] The inclusion of **111** inside **110** was revealed

from the highly upfield signals in ^{1}H NMR due to shielding from the aromatic panel ligands. Moreover, other rod-like molecules such as biphenyl and *p*-terphenyl were effective whereas large molecules such as adamantyl carboxylate did not show any template effect and in the absence of template tubes were not formed effectively, even after a week at 60 °C. It was also found that the formation of these tubes was reversible. The formation of two isomer **109a** and **109b** was observed in a *ca*. 1:1 ratio.[90b] NMR measurement showed a very slow interconversion between isomers. The tubular structures of **108**, **109a** and **110** were confirmed by X-ray crystallographic analysis. The crystal showed π-π and CH-π interactions between templates and pyridine frameworks.

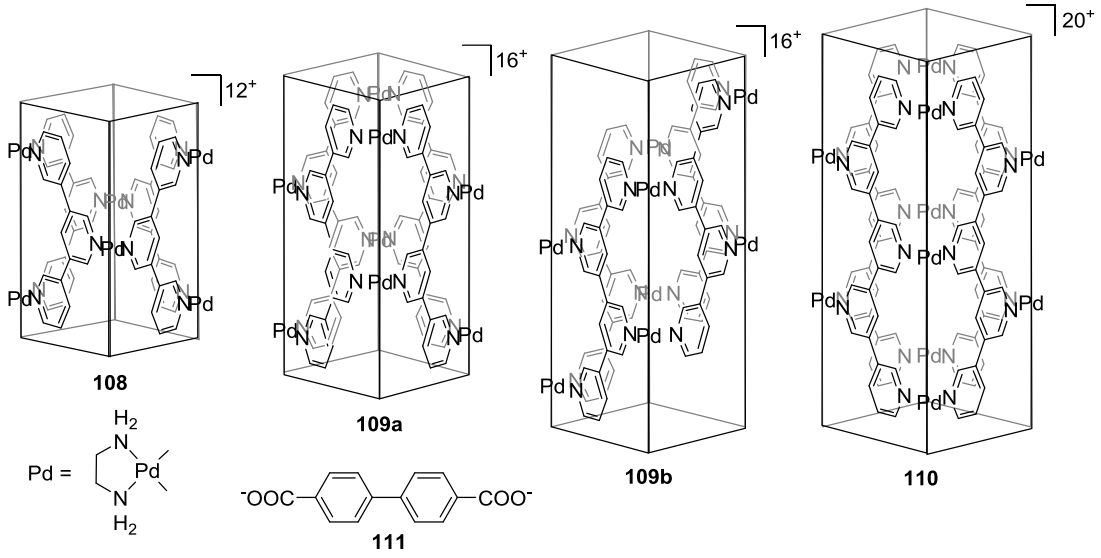

Figure 1.20 Self-assembly of coordination tube **108**, **109** and **110**. The template **111** included in the cavity of the tubes is omitted for clarity

In 2002, Fujita and co-workers published the studies on the dynamic behaviour of the guest molecules inside the cavity of tubular assemblies.[92] Unsymmetrical biphenyl derivative **112** was used as a template for tube **110** which desymmetrise the host framework. VT NMR experiments explained the guest molecule is trapped and unable to flip at room temperature, spin around its long axis make the four sides of the framework equivalent, it is able to escape from the tube, symmetrising the host environment at high temperature. The dynamic movements of the guest can occur *via* two possible pathways. If [G]/[H] <1, the guest molecule self-dissociates *via* an empty intermediate. When [G]/[H] > 1, the guest can be replaced by the second guest *via* a concerted pathway (Figure 1.21). The preferential binding of anionic guest **110** over a neutral guest, 4-methylbiphenyl was shown as it was displaced immediately upon addition of **112** which

suggested electrostatic interaction between the tube and the template is also important for the host-guest complexation in addition to aromatic interactions.

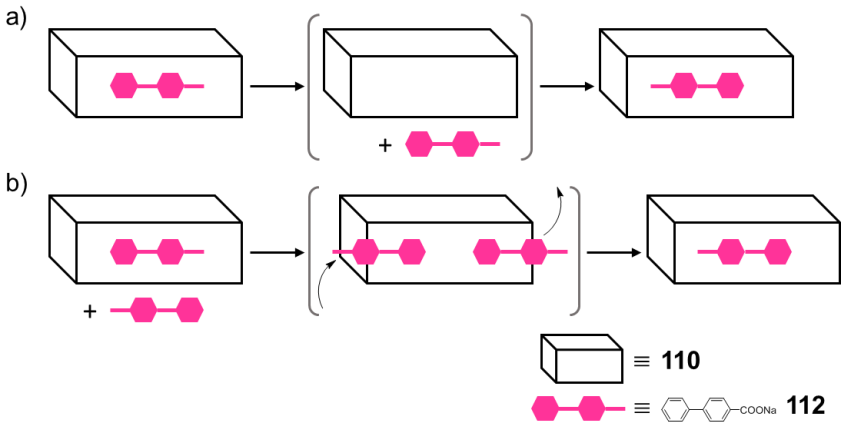

Figure 1.21 Mechanism of guest exchange at a) [G]:[H] = 1:1 and b) [G]:[H] = 2:1.

In 2003, the assembly of a stable nanotube **113** with an empty cavity was achieved by mixing a hexapyridine ligand **105** and **101** without any template molecule.[93] The ligand adopts a U-shape conformation due to its flexibility upon coordinating with Pd^{II}. The tubes were found to encapsulate aliphatic guests such as cyclohexane and octane.

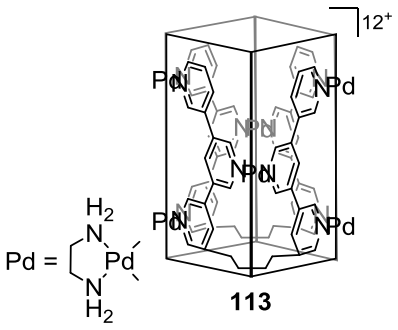

Figure 1.22 Structure of tube **113**.

To construct a long coordination nanotube, the Fujita team used ligand **106** to accomplish the self-assembly.[94] The ligand is connected with a rigid biphenyl unit to avoid unfavourable intramolecular coordination. A 3.5 nm tube **114** was achieved using **115** as a template. The high yield was achieved when **118** was used as template for the tube. After removal of **118**, in contrast to all previously described assemblies except **113** which was formed without any template molecule, the tube framework remained unchanged at room temperature. Empty tube **114** possesses considerable kinetic stability due to the twenty four cooperative Pd^{II}-pyridine interactions. Templates **116-118**, which are different lengths, were shown to efficiently promote the assembly of tube

114 in high yield.[95] Competitive experiments were examined for the guest binding when the templates were mixed in the assembly reaction. The result indicated the effectiveness of the guests in the order of **116** > **117** > **118**. Moreover, unsymmetrical guests **119** and **120** were investigated to obtain some insight into the dynamics of guest binding by VT NMR experiments. The results suggested **120** was accommodated within the tube more tightly than **119**. Redox-active guest **121** with two tetrathiafulvalene (TTF) linked by an oligo(ethyleneoxide) spacer was used to template tube **114** to examine the dynamic behaviour of the tube under redox conditions.

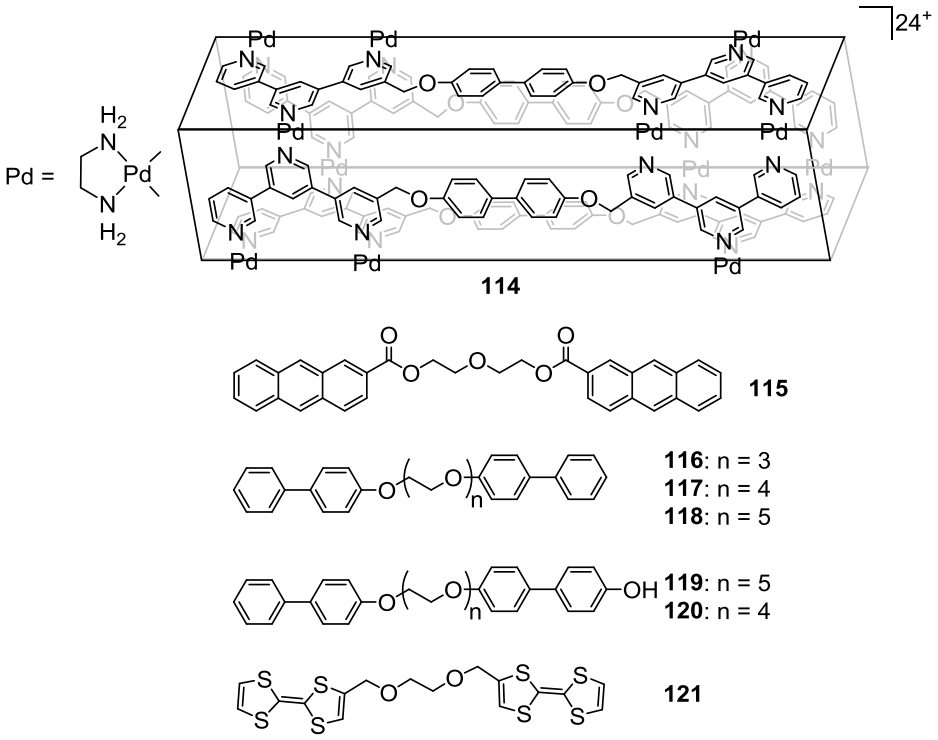

Figure 1.23 Self-assembly of coordination nanotube **114** and the different structures of templates molecule **115**-**121**.

Ligand **107** was expected to assemble into the mono-end-capped coordination tube **122** upon complexation with **101** in the presence of an appropriate guest as seen in tube **113**.[96] In addition to the expected structure **122**, the complexation of **101** and **107** also gave rise to the double open tube **123** which was observed only at higher concentrations as a minor component. Tube **123** did not convert into **122** at lower concentration which indicated that both structure are kinetic traps on the potential surface. The assembly of tube **122** was accomplished by the templating effect of guests such as 4,4'-dimethylbiphenyl **124**. As expected, two methyl groups of **124** accommodated in **122** were clearly discriminated by ^{1}H NMR spectrum. Asymmetric guest **112** was efficiently

accommodated in a unidirectional fashion. Only one isomer, in which the hydrophobic biphenyl group was included within the tube and the hydrophilic carboxylate group was exposed outside, was formed. Dicaboxylate guest **111** which was bound in open tube **108** was not included in **122**, showing that the end-capped site of **122** provides an efficient hydrophobic pocket.

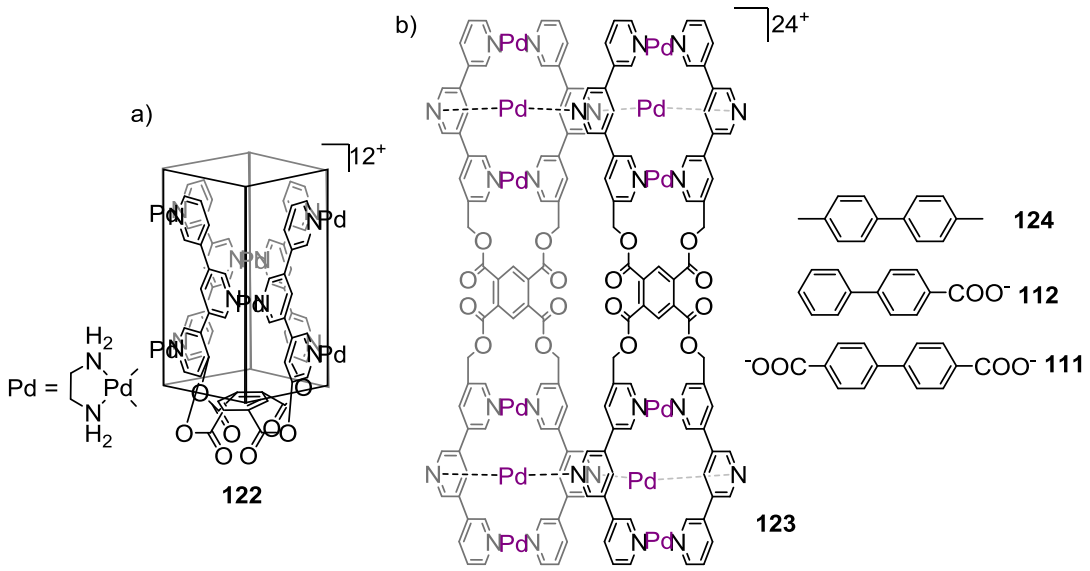

Figure 1.24 Self-assembly of a) mono-end-capped tube **122**, and b) double open tube **123**. The template molecules are omitted for clarity.

1.6.2 Self-assembled of tubes from other metal building blocks

Similar discrete coordination nanotubes were also studied by zur Loye and co-workers.[97] A neutral tetranuclear nanotube $[Hg_4Cl_8(bbimms)_4]$ (**126**) assembled from $HgCl_2$ and the semirigid ditopic ligand 1,3-bis(benzimidazol-1-ylmethyl)-2,4,6-trimethylbenzene **125** which is capable of adopting either the *syn* or the *anti* conformation. When Hg^{II} (that favours bent coordination environments) was treated with bbimms, it was observed that the ligand inevitably bridges the ions in an *anti* conformation to form discrete tubular tetramers (Scheme 1.30). The molecular tube exhibits relatively high thermal stability and is capable of encapsulating guest molecules such as DMF or DMSO in its two rectangular compartments.

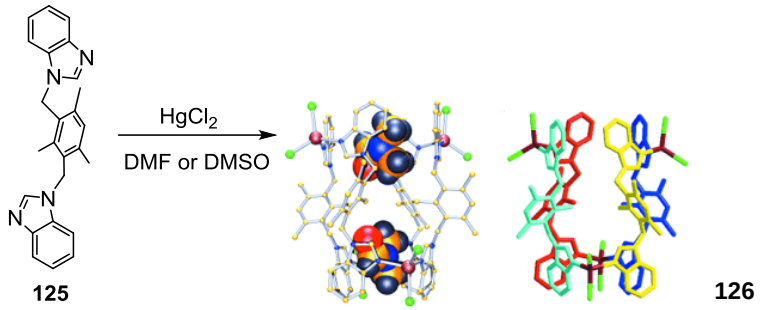

Scheme 1.36 Self-assembly of tube **126**. X-ray structure reproduced from ref. 97.

Zhang, Su and co-workers have reported the self-assembly of coordination tube Ag_6L_6 **128** based on the T-shaped 4-(3,5-bis(diphenylphosphino)phenyl)pyridine) ligand **127** (Scheme 1.37).[98]

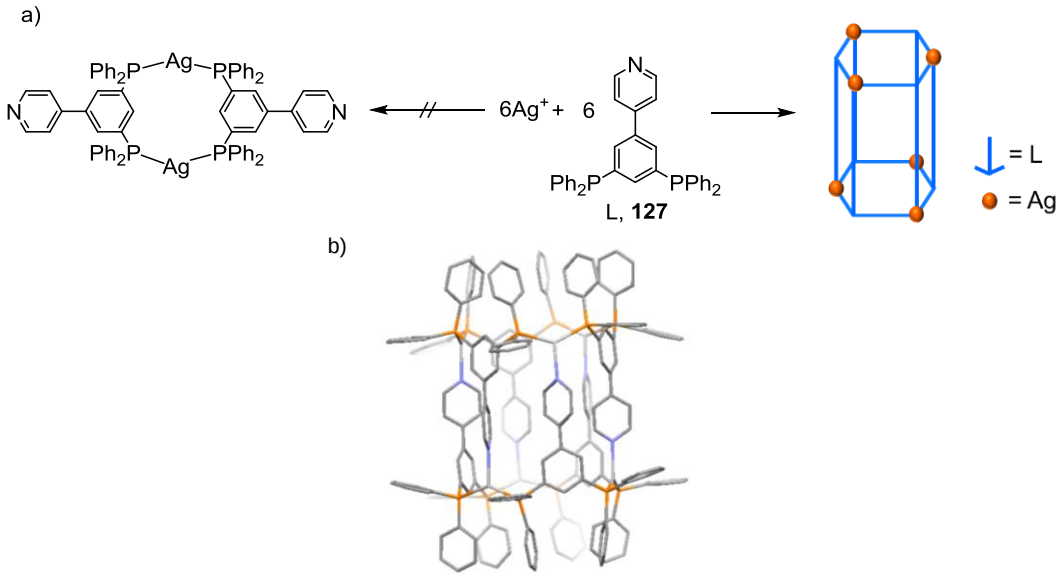

Scheme 1.37 a) Self-assembly of **128** tubular structures; b) X-ray crystal structure of the tube complex **128**.

Recently, Gagliardi, Cramer, Nitschke and co-workers have described the construction of M_8L_4 tubular complexes *via* self-assembly of Cu^I or Ag^I ions and elongated tetraamines with two 3,5-diaminophenylene moieties connected by a suitable spacer and 2-formylpyridine (Scheme 1.38).[99] The tubes were often observed as equilibrium of D_4-symmetric or D_{2d}/D_2-symmetric isomers. Variation in ligand length, substituents, metal ion identity, counteranion and temperature influenced the equilibria. The D_{2d}/D_2 isomer is stabilised by the elongation of the ligand or the introduction of an offset between tube ends while the D_4 isomer, which more stabilised in the presence of PF_6^- counteranions, is

the only one that exhibits guest binding properties. Substitution of $Ag(CN)_2^-$ for $Au(CN)_2^-$ resulted in the formation of $Ag(Au(CN)_2)_2^-$ as the optimal guest through transmetalation.

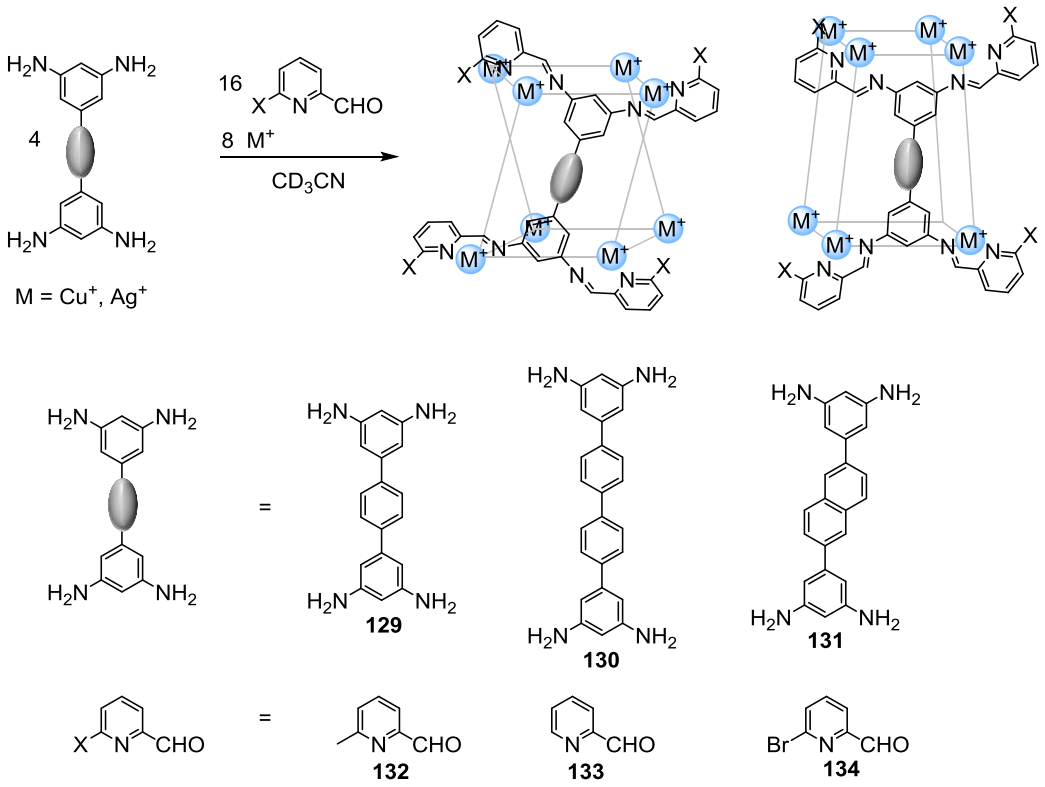

Scheme 1.38 Synthesis of M_8L_4 tubes.

1.6.3 Self-assembled molecular shuttles

The acid-base responsive-helix-rod complexes based molecular shuttles were reported by Huc, Jiang and co-workers.[89] This work was one of a few examples, to date that showed molecular motion in dynamically assembled systems without disassembly during operation. The shuttles consist of oligomeric aromatic amide molecular tapes that fold into very stable helices incorporating a cylindrical cavity with high affinities for complementary rod-like guests. An alkyl-chain guest terminated with bulky stoppers cannot thread into the cavity but instead slowly forms a complex with the oligoamide helical host winding around it. Increasing strand length adjusts the distance between the anchor points along the helix axis and tunes the time scale of helix unfolding-refolding dynamics. A range of different lengths of the guests were prepared to match the helix length. 1:1 stoichiometry of the host-guest complexes were assessed in the solid state (X-ray crystallography), solution (NMR spectroscopy) and the gas phase (mass spectrometry). The host-guest complexes between the shortest oligomer **136** and **137**

and their respective guests form readily at 25 °C which make them not suitable to be shuttles as refolding will be fast or may be faster than the shuttling rate. The complex **135**⊃**138** forms at 25 °C over 30 min, which gave an estimated kinetic constant of dissociation slower than 2 d^{-1}. High host-guest stability and slow formation kinetics in the **135**⊃guest hint at even slower kinetics of complex dissociation encouraged further studies of the molecular shuttle.

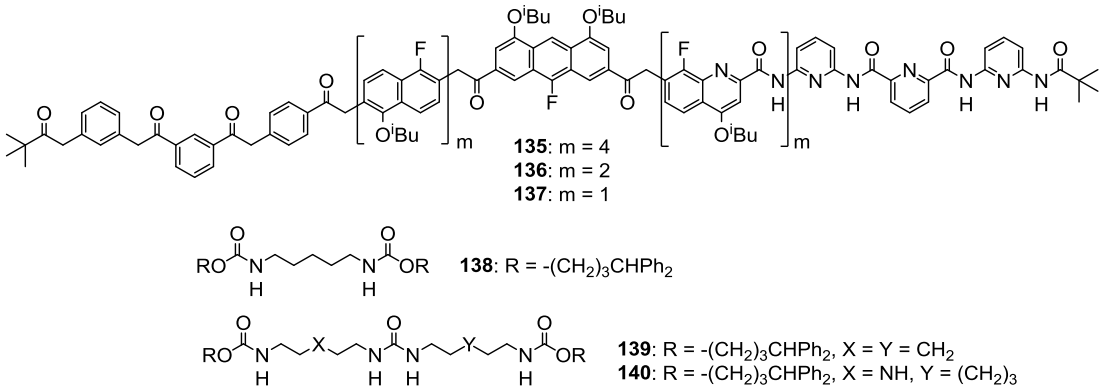

Figure 1.25 Host-guest components for assembly.

Rod-like guest **139** possess three hydrogen-bond acceptors and thus contains two degenerate stations, which can bind only one helix at a time because of the proximity. Exchange spectroscopy NMR experiments showed clear correlation resulting from the motion of **135** between the two stations of **139**. The rate of this motion was calculated to be between 2 and 4 min^{-1} at 25 °C, a time scale considerably smaller than that of host-guest complex dissociation, implying that **135** exchanges between the two stations of **139** *via* a sliding (shuttling) process and not *via* a dissociation (unfolding)-association (refolding) mechanism.

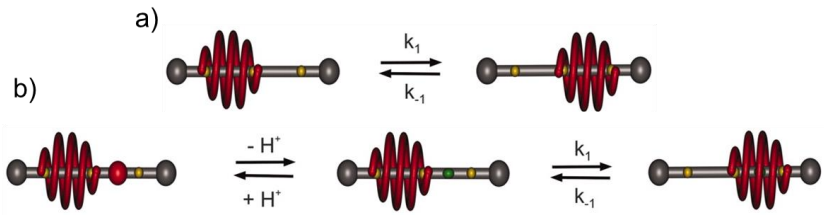

Scheme 1.39 a) Degenerate helix shuttling along a symmetrical guest **137** of helix **133**. The yellow dots mark hydrogen bond acceptors; b) Helix **133** sliding along a nondegenerate guest possessing a station that can be blocked or unblock upon protonation or deprotonation, respectively. The green dot symbolises the amine function of **138** where the red dot is the corresponding ammonium. Reproduced from ref. 89.

Shuttling in a non-degenerate guest **138**, one with heptyl segment and the other with a diethyl amine segment, was also determined. ^{1}H and ^{19}F NMR indicated that **135** resides in a 58/42 proportion at the two stations. Upon titrating complex **133**⊃**138** with an acid, only one set of signals corresponding to **135** residing only on an alkyl station was observed as it is repelled by the ammonium station. Adding a base instantly reverses the process. The time scale of this controlled motion is much faster than the rates of unfolding and refolding of **135** around **140**, implying that motion is mediated by the rapid sliding of **135** along **140**.

1.7 Scope of the Thesis

The present thesis explores the strategies to develop a new transition metal-complexed [2]rotaxane and its use as a stimuli-responsive molecular shuttle. Chapter II describes an investigation of the strategies to control a directional movement of submolecular components that can be utilised in molecular shuttle in particular, the exchange between "3+1" and "2+2" cyclometalated platinum complexes. Chapter III focuses on attempts to synthesis platinum(II) complexed-[2]rotaxanes using the active-metal template CuAAC strategy and transition metal template approach to be function as acid-base responsive molecular shuttles. Finally, Chapter IV is concerned self-assembly of the Pd^{II}-coordination nanotubes to be exploited as self-assembled bistable stimuli-responsive molecular shuttles.

1.8 References

1. S. Silvi, M. Venturi and A. Credi, *J. Mater. Chem.*, **2009**, *19*, 2279-2294.
2. J. E. Walker, *Angew. Chem. Int. Ed.*, **1998**, *37*, 2308-2319.
3. I. Rayment, H. Holden, M. Whittaker, C. Yohn, M. Lorenz, K. Holmes and R. Milligan, *Science*, **1993**, *261*, 58-65.
4. N. Hirokawa, *Science*, **1998**, *279*, 519-526.
5. S. Hahn, *Nat. Struct. Mol. Biol.*, **2004**, *11*, 394-403.
6. V. Balzani, A. Credi and M. Venturi, *Chem. Eur. J.*, **2002**, *8*, 5524-5532.
7. in *Molecular Catenanes, Rotaxanes and Knots*, eds. J.-P. Sauvage and C. Dietrich-Buchecker, Wiley-VCH Verlag GmbH, Chichester, 1999, p. 382.
8. I. T. Harrison and S. Harrison, *J. Am. Chem. Soc.*, **1967**, *89*, 5723-5724.
9. M. C. T. Fyfe and J. F. Stoddart, *Acc. Chem. Res.*, **1997**, *30*, 393-401.
10. (a) S. Anderson, H. L. Anderson and J. K. M. Sanders, *Acc. Chem. Res.*, **1993**, *26*, 469-475; (b) R. Hoss and F. Vögtle, *Angew. Chem. Int. Ed. Engl.*, **1994**, *33*, 375-384.
11. P. R. Ashton, T. T. Goodnow, A. E. Kaifer, M. V. Reddington, A. M. Z. Slawin, N. Spencer, J. F. Stoddart, C. Vicent and D. J. Williams, *Angew. Chem. Int. Ed. Engl.*, **1989**, *28*, 1396-1399.
12. P. L. Anelli, N. Spencer and J. F. Stoddart, *J. Am. Chem. Soc.*, **1991**, *113*, 5131-5133.
13. M. Asakawa, P. R. Ashton, R. Ballardini, V. Balzani, M. Bělohradský, M. T. Gandolfi, O. Kocian, L. Prodi, F. M. Raymo, J. F. Stoddart and M. Venturi, *J. Am. Chem. Soc.*, **1997**, *119*, 302-310.
14. G. Barin, A. Coskun, M. M. G. Fouda and J. F. Stoddart, *ChemPlusChem*, **2012**, *77*, 159-185.
15. For recent examples of functional systems utilised bipyridinium and electron rich motifs (a) A. C. Fahrenbach, S. Sampath, D. J. Late, J. C. Barnes, S. L. Kleinman, N. Valley, K. J. Hartlieb, Z. Liu, V. P. Dravid, G. C. Schatz, R. P. Van Duyne and J. F. Stoddart, *ACS Nano*, **2012**, *6*, 9964-9971; (b) A. C. Fahrenbach, Z. Zhu, D. Cao, W.-G. Liu, H. Li, S. K. Dey, S. Basu, A. Trabolsi, Y. Y. Botros, W. A. Goddard and J. F. Stoddart, *J. Am. Chem. Soc.*, **2012**, *134*, 16275-16288; (c) H. Li, Z. Zhu, A. C. Fahrenbach, B. M. Savoie, C. Ke, J. C. Barnes, J. Lei, Y.-L. Zhao, L. M. Lilley, T. J. Marks, M. A. Ratner and J. F. Stoddart, *J. Am. Chem. Soc.*, **2012**, *135*, 456-467; (d) G. Barin, M. Frasconi, S. M. Dyar, J. Iehl, O. Buyukcakir, A. A. Sarjeant, R. Carmieli, A. Coskun, M. R. Wasielewski and J. F. Stoddart, *J. Am. Chem. Soc.*, **2013**, *135*, 2466-2469; (e) J. C. Barnes, A. C. Fahrenbach, D. Cao, S. M. Dyar, M. Frasconi, M. A. Giesener, D. Benítez, E. Tkatchouk, O. Chernyashevskyy, W. H. Shin, H. Li, S. Sampath, C. L. Stern, A. A. Sarjeant, K. J. Hartlieb, Z. Liu, R. Carmieli, Y. Y. Botros, J. W. Choi, A. M. Z. Slawin, J. B. Ketterson, M. R. Wasielewski, W. A. Goddard and J. F. Stoddart, *Science*, **2013**, *339*, 429-433; (f) A. C. Fahrenbach, S. C. Warren, J. T. Incorvati, A.-J. Avestro, J. C. Barnes, J. F. Stoddart and B. A. Grzybowski, *Adv. Mater.*, **2013**, *25*, 331-348; (g) H. Li, C. Cheng, P. R. McGonigal, A. C. Fahrenbach, M. Frasconi, W.-G. Liu, Z. Zhu, Y. Zhao, C. Ke, J. Lei, R. M. Young, S. M. Dyar, D. T. Co, Y.-W. Yang, Y. Y. Botros, W. A. Goddard, M. R. Wasielewski, R. D. Astumian and

J. F. Stoddart, *J. Am. Chem. Soc.*, **2013**, *135*, 18609-18620; (h) C. J. Bruns, M. Frasconi, J. Iehl, K. J. Hartlieb, S. T. Schneebeli, C. Cheng, S. I. Stupp and J. F. Stoddart, *J. Am. Chem. Soc.*, **2014**, *136*, 4714-4723; (i) L. S. Witus, K. J. Hartlieb, Y. Wang, A. Prokofjevs, M. Frasconi, J. C. Barnes, E. J. Dale, A. C. Fahrenbach and J. F. Stoddart, *Org. Biomol. Chem.*, **2014**, *12*, 6089-6093.

16. M. L. Bender and M. Komiyama, *Cyclodextrin Chemistry*, Springer-Verlag, Berlin, 1987.

17. H. Ogino, *J. Am. Chem. Soc.*, **1981**, *103*, 1303-1304.

18. H. Murakami, A. Kawabuchi, K. Kotoo, M. Kunitake and N. Nakashima, *J. Am. Chem. Soc.*, **1997**, *119*, 7605-7606.

19. D. A. Leigh, A. Murphy, J. P. Smart and A. M. Z. Slawin, *Angew. Chem. Int. Ed. Engl.*, **1997**, *36*, 728-732.

20. A. S. Lane, D. A. Leigh and A. Murphy, *J. Am. Chem. Soc.*, **1997**, *119*, 11092-11093.

21. (a) M. V. Martínez-Díaz, N. Spencer and J. F. Stoddart, *Angew. Chem. Int. Ed. Engl.*, **1997**, *36*, 1904-1907; (b) P. R. Ashton, R. Ballardini, V. Balzani, I. Baxter, A. Credi, M. C. T. Fyfe, M. T. Gandolfi, M. Gómez-López, M. V. Martínez-Díaz, A. Piersanti, N. Spencer, J. F. Stoddart, M. Venturi, A. J. P. White and D. J. Williams, *J. Am. Chem. Soc.*, **1998**, *120*, 11932-11942; (c) S. Garaudée, S. Silvi, M. Venturi, A. Credi, A. H. Flood and J. F. Stoddart, *ChemPhysChem*, **2005**, *6*, 2145-2152.

22. J. E. Beves, B. A. Blight, C. J. Campbell, D. A. Leigh and R. T. McBurney, *Angew. Chem. Int. Ed.*, **2011**, *50*, 9260-9327.

23. C. O. Dietrich-Buchecker, J. P. Sauvage and J. P. Kintzinger, *Tetrahedron Lett.*, **1983**, *24*, 5095-5098.

24. C. O. Dietrich-Buchecker, J. P. Sauvage and J. M. Kern, *J. Am. Chem. Soc.*, **1984**, *106*, 3043-3045.

25. C. Wu, P. R. Lecavalier, Y. X. Shen and H. W. Gibson, *Chem. Mater.*, **1991**, *3*, 569-572.

26. C. J. Campbell, D. A. Leigh, I. J. Vitorica-Yrezabal and S. L. Woltering, *Angew. Chem. Int. Ed.*, **2014**, n/a-n/a.

27. L. Hogg, D. A. Leigh, P. J. Lusby, A. Morelli, S. Parsons and J. K. Y. Wong, *Angew. Chem. Int. Ed.*, **2004**, *43*, 1218-1221.

28. D. A. Leigh, P. J. Lusby, R. T. McBurney, A. Morelli, A. M. Z. Slawin, A. R. Thomson and D. B. Walker, *J. Am. Chem. Soc.*, **2009**, *131*, 3762-3771.

29. D. Pomeranc, D. Jouvenot, J.-C. Chambron, J.-P. Collin, V. Heitz and J.-P. Sauvage, *Chem. Eur. J.*, **2003**, *9*, 4247-4254.

30. C. Hamann, J. M. Kern and J. P. Sauvage, *Dalton Trans.*, **2003**, 3770-3775.

31. A.-M. Fuller, D. A. Leigh, P. J. Lusby, I. D. H. Oswald, S. Parsons and D. B. Walker, *Angew. Chem. Int. Ed.*, **2004**, *43*, 3914-3918.

32. T. Moriuchi, S. Bandoh, M. Miyaishi and T. Hirao, *Eur. J. Inorg. Chem.*, **2001**, *2001*, 651-657.

33. (a) Y. Furusho, T. Matsuyama, T. Takata, T. Moriuchi and T. Hirao, *Tetrahedron Lett.*, **2004**, *45*, 9593-9597; (b) W.-C. Hung, L.-Y. Wang, C.-C. Lai, Y.-H. Liu, S.-M. Peng and S.-H. Chiu, *Tetrahedron Lett.*, **2009**, *50*, 267-270.

34. N. Miyagawa, M. Watanabe, T. Matsuyama, Y. Koyama, T. Moriuchi, T. Hirao, Y. Furusho and T. Takata, *Chem. Commun.*, **2010**, *46*, 1920-1922.

35. A.-M. L. Fuller, D. A. Leigh and P. J. Lusby, *Angew. Chem. Int. Ed.*, **2007**, *46*, 5015-5019.

36. A.-M. L. Fuller, D. A. Leigh and P. J. Lusby, *J. Am. Chem. Soc.*, **2010**, *132*, 4954-4959.

37. C. Browne, T. K. Ronson and J. R. Nitschke, *Angew. Chem. Int. Ed.*, **2014**, *53*, 10701-10705.

38. V. Aucagne, K. D. Hänni, D. A. Leigh, P. J. Lusby and D. B. Walker, *J. Am. Chem. Soc.*, **2006**, *128*, 2186-2187.

39. V. Aucagne, J. Berná, J. D. Crowley, S. M. Goldup, K. D. Hänni, D. A. Leigh, P. J. Lusby, V. E. Ronaldson, A. M. Z. Slawin, A. Viterisi and D. B. Walker, *J. Am. Chem. Soc.*, **2007**, *129*, 11950-11963.

40. H. Lahlali, K. Jobe, M. Watkinson and S. M. Goldup, *Angew. Chem. Int. Ed.*, **2011**, *50*, 4151-4155.

41. J. Winn, A. Pinczewska and S. M. Goldup, *J. Am. Chem. Soc.*, **2013**, *135*, 13318-13321.

42. R. J. Bordoli and S. M. Goldup, *J. Am. Chem. Soc.*, **2014**, *136*, 4817-4820.

43. S. Saito, E. Takahashi and K. Nakazono, *Org. Lett.*, **2006**, *8*, 5133-5136.

44. J. Berná, S. M. Goldup, A.-L. Lee, D. A. Leigh, M. D. Symes, G. Teobaldi and F. Zerbetto, *Angew. Chem. Int. Ed.*, **2008**, *47*, 4392-4396.

45. J. Berná, J. D. Crowley, S. M. Goldup, K. D. Hänni, A.-L. Lee and D. A. Leigh, *Angew. Chem. Int. Ed.*, **2007**, *46*, 5709-5713.

46. J. D. Crowley, K. D. Hänni, A.-L. Lee and D. A. Leigh, *J. Am. Chem. Soc.*, **2007**, *129*, 12092-12093.

47. S. M. Goldup, D. A. Leigh, P. J. Lusby, R. T. McBurney and A. M. Z. Slawin, *Angew. Chem. Int. Ed.*, **2008**, *47*, 3381-3384.

48. B. A. Blight, J. A. Wisner and M. C. Jennings, *Chem. Commun.*, **2006**, 4593-4595.

49. B. A. Blight, X. Wei, J. A. Wisner and M. C. Jennings, *Inorg. Chem.*, **2007**, *46*, 8445-8447.

50. I. Yoon, M. Narita, T. Shimizu and M. Asakawa, *J. Am. Chem. Soc.*, **2004**, *126*, 16740-16741.

51. C.-F. Lee, D. A. Leigh, R. G. Pritchard, D. Schultz, S. J. Teat, G. A. Timco and R. E. P. Winpenny, *Nature*, **2009**, *458*, 314-318.

52. G. H. Clever and M. Shionoya, *Chem. Eur. J.*, **2010**, *16*, 11792-11796.

53. E. R. Kay, D. A. Leigh and F. Zerbetto, *Angew. Chem. Int. Ed.*, **2007**, *46*, 72-191.

54. R. A. Bissell, E. Cordova, A. E. Kaifer and J. F. Stoddart, *Nature*, **1994**, *369*, 133-137.

55. J. D. Badjić, V. Balzani, A. Credi, S. Silvi and J. F. Stoddart, *Science*, **2004**, *303*, 1845-1849.

56. C. M. Keaveney and D. A. Leigh, *Angew. Chem. Int. Ed.*, **2004**, *43*, 1222-1224.

57. J. D. Crowley, D. A. Leigh, P. J. Lusby, R. T. McBurney, L.-E. Perret-Aebi, C. Petzold, A. M. Z. Slawin and M. D. Symes, *J. Am. Chem. Soc.*, **2007**, *129*, 15085-15090.

58. D. A. Leigh, P. J. Lusby, R. T. McBurney and M. D. Symes, *Chem. Commun.*, **2010**, *46*, 2382-2384.

59. H.-R. Tseng, S. A. Vignon and J. F. Stoddart, *Angew. Chem. Int. Ed.*, **2003**, *42*, 1491-1495.

60. A. M. Brouwer, C. Frochot, F. G. Gatti, D. A. Leigh, L. c. Mottier, F. Paolucci, S. Roffia and G. W. H. Wurpel, *Science*, **2001**, *291*, 2124-2128.

61. J.-P. Collin, P. Gavina and J.-P. Sauvage, *New J. Chem.*, **1997**, *21*, 525-528.

62. A. Livoreil, C. O. Dietrich-Buchecker and J.-P. Sauvage, *J. Am. Chem. Soc.*, **1994**, *116*, 9399-9400.

63. (a) F. Durola, J.-P. Sauvage and O. S. Wenger, *Chem. Commun.*, **2006**, 171-173; (b) J.-P. Collin, F. Durola, J. Lux and J.-P. Sauvage, *Angew. Chem. Int. Ed.*, **2009**, *48*, 8532-8535; (c) F. Durola, J. Lux and J.-P. Sauvage, *Chem. Eur. J.*, **2009**, *15*, 4124-4134.

64. H. Murakami, A. Kawabuchi, R. Matsumoto, T. Ido and N. Nakashima, *J. Am. Chem. Soc.*, **2005**, *127*, 15891-15899.

65. D.-H. Qu, Q.-C. Wang, J. Ren and H. Tian, *Org. Lett.*, **2004**, *6*, 2085-2088.

66. Q.-C. Wang, D.-H. Qu, J. Ren, K. Chen and H. Tian, *Angew. Chem. Int. Ed.*, **2004**, *43*, 2661-2665.

67. C. A. Stanier, S. J. Alderman, T. D. W. Claridge and H. L. Anderson, *Angew. Chem. Int. Ed.*, **2002**, *41*, 1769-1772.

68. A. Altieri, G. Bottari, F. Dehez, D. A. Leigh, J. K. Y. Wong and F. Zerbetto, *Angew. Chem. Int. Ed.*, **2003**, *42*, 2296-2300.

69. F. G. Gatti, D. A. Leigh, S. A. Nepogodiev, A. M. Z. Slawin, S. J. Teat and J. K. Y. Wong, *J. Am. Chem. Soc.*, **2001**, *123*, 5983-5989.

70. P. R. Ashton, R. Ballardini, V. Balzani, A. Credi, K. R. Dress, E. Ishow, C. J. Kleverlaan, O. Kocian, J. A. Preece, N. Spencer, J. F. Stoddart, M. Venturi and S. Wenger, *Chem. Eur. J.*, **2000**, *6*, 3558-3574.

71. J.-P. Collin, D. Jouvenot, M. Koizumi and J.-P. Sauvage, *Eur. J. Inorg. Chem.*, **2005**, *2005*, 1850-1855.

72. (a) T. Iijima, S. A. Vignon, H.-R. Tseng, T. Jarrosson, J. K. M. Sanders, F. Marchioni, M. Venturi, E. Apostoli, V. Balzani and J. F. Stoddart, *Chem. Eur. J.*, **2004**, *10*, 6375-6392; (b) S. A. Vignon, T. Jarrosson, T. Iijima, H.-R. Tseng, J. K. M. Sanders and J. F. Stoddart, *J. Am. Chem. Soc.*, **2004**, *126*, 9884-9885.

73. D. S. Marlin, D. González Cabrera, D. A. Leigh and A. M. Z. Slawin, *Angew. Chem. Int. Ed.*, **2006**, *45*, 77-83.

74. D. S. Marlin, D. González Cabrera, D. A. Leigh and A. M. Z. Slawin, *Angew. Chem. Int. Ed.*, **2006**, *45*, 1385-1390.

75. M. C. Jiménez, C. Dietrich-Buchecker and J.-P. Sauvage, *Angew. Chem. Int. Ed.*, **2000**, *39*, 3284-3287.

76. J. Frey, C. Tock, J.-P. Collin, V. Heitz and J.-P. Sauvage, *J. Am. Chem. Soc.*, **2008**, *130*, 4592-4593.

77. M. J. Barrell, D. A. Leigh, P. J. Lusby and A. M. Z. Slawin, *Angew. Chem. Int. Ed.*, **2008**, *47*, 8036-8039.

78. M. N. Chatterjee, E. R. Kay and D. A. Leigh, *J. Am. Chem. Soc.*, **2006**, *128*, 4058-4073.

79. V. Serreli, C.-F. Lee, E. R. Kay and D. A. Leigh, *Nature*, **2007**, *445*, 523-527.

80. A. Carlone, S. M. Goldup, N. Lebrasseur, D. A. Leigh and A. Wilson, *J. Am. Chem. Soc.*, **2012**, *134*, 8321-8323.

81. B. Lewandowski, G. De Bo, J. W. Ward, M. Papmeyer, S. Kuschel, M. J. Aldegunde, P. M. E. Gramlich, D. Heckmann, S. M. Goldup, D. M. D'Souza, A. E. Fernandes and D. A. Leigh, *Science*, **2013**, *339*, 189-193.

82. G. De Bo, S. Kuschel, D. A. Leigh, B. Lewandowski, M. Papmeyer and J. W. Ward, *J. Am. Chem. Soc.*, **2014**, *136*, 5811-5814.

83. J. E. Beves, V. Blanco, B. A. Blight, R. Carrillo, D. M. D'Souza, D. Howgego, D. A. Leigh, A. M. Z. Slawin and M. D. Symes, *J. Am. Chem. Soc.*, **2014**, *136*, 2094-2100.

84. V. Blanco, D. A. Leigh, U. Lewandowska, B. Lewandowski and V. Marcos, *J. Am. Chem. Soc.*, **2014**.

85. (a) J. W. Steed and J. L. Atwood, *Supramolecular Chemistry*, 2 edn., Wiley, Chichester, 2009; (b) M. D. Ward and P. R. Raithby, *Chem. Soc. Rev.*, **2013**, *42*, 1619-1636.

86. M. M. Safont-Sempere, G. Fernández and F. Würthner, *Chem. Rev.*, **2011**, *111*, 5784-5814.

87. P. R. Symmers, M. J. Burke, D. P. August, P. I. T. Thomson, G. S. Nichol, M. R. Warren, C. J. Campbell and P. J. Lusby, *Chem. Sci.*, **2015**.

88. E. Okuno, S. Hiraoka and M. Shionoya, *Dalton Trans.*, **2010**, *39*, 4107-4116.

89. Q. Gan, Y. Ferrand, C. Bao, B. Kauffmann, A. Grélard, H. Jiang and I. Huc, *Science*, **2011**, *331*, 1172-1175.

90. (a) M. Aoyagi, K. Biradha and M. Fujita, *J. Am. Chem. Soc.*, **1999**, *121*, 7457-7458; (b) M. Aoyagi, S. Tashiro, M. Tominaga, K. Biradha and M. Fujita, *Chem. Commun.*, **2002**, 2036-2037.

91. (a) S. Sakamoto, M. Fujita, K. Kim and K. Yamaguchi, *Tetrahedron*, **2000**, *56*, 955-964; (b) K. Yamaguchi, *J. Mass Spectrom.*, **2003**, *38*, 473-490.

92. M. Tominaga, S. Tashiro, M. Aoyagi and M. Fujita, *Chem. Commun.*, **2002**, 2038-2039.

93. M. Tominaga, M. Kato, T. Okano, S. Sakamoto, K. Yamaguchi and M. Fujita, *Chem. Lett.*, **2003**, *32*, 1012-1013.

94. T. Yamaguchi, S. Tashiro, M. Tominaga, M. Kawano, T. Ozeki and M. Fujita, *J. Am. Chem. Soc.*, **2004**, *126*, 10818-10819.

95. T. Yamaguchi, S. Tashiro, M. Tominaga, M. Kawano, T. Ozeki and M. Fujita, *Chem. Asian J.*, **2007**, *2*, 468-476.

96. S. Tashiro, M. Tominaga, T. Kusukawa, M. Kawano, S. Sakamoto, K. Yamaguchi and M. Fujita, *Angew. Chem. Int. Ed.*, **2003**, *42*, 3267-3270.

97. C.-Y. Su, M. D. Smith and H.-C. zur Loye, *Angew. Chem. Int. Ed.*, **2003**, *42*, 4085-4089.

98. X. Wang, J. Huang, S. Xiang, Y. Liu, J. Zhang, A. Eichhofer, D. Fenske, S. Bai and C.-Y. Su, *Chem. Commun.*, **2011**, *47*, 3849-3851.

99. W. Meng, A. B. League, T. K. Ronson, J. K. Clegg, W. C. Isley, D. Semrouni, L. Gagliardi, C. J. Cramer and J. R. Nitschke, *J. Am. Chem. Soc.*, **2014**, *136*, 3972-3980.

Chapter II

Acid-base responsive switching between “3+1” and “2+2” platinum complexes

Published as *Acid-base responsive switching between "3+1" and "2+2" platinum complexes*, D. Sooksawat, S. J. Pike, A. M. Z. Slawin, P. J. Lusby, *Chem. Commun.,* **2013**, *49*, 11077-11079.

Acknowledgements

For their contribution to this chapter, I would like to thank Dr. Sarah Pike for her synthesis and preliminary studies of [**L**^{1}Pt(DMSO)], [H**L**^{1}Pt(dmbipy)]OTs, [**L**^{1}Pt(py)], [**L**^{1}Pt(3,5-lut)] and [**L**^{1}Pt(DMAP)] and Prof. Alexandra Slawin for X-ray crystallography.

Synopsis

The acid-base induced changes to cyclometallated platinum complexes can be used to facilitate the exchange of ligands with different denticities. Acyclic and macrocyclic diphenylpyridine-based cyclometallated platinum complexes were examined using ^{1}H NMR spectroscopy starting with the neutral monodentate ligand complexes. In the absence of acid, a bidentate ligand does not displace the monodentate ligand and remains uncoordinated. A slight excess of acid was needed to switch the coordinating preference to a bidentate complex. The amount of acid used is varied by the strength of each pyridyl monodentate ligands. The binding mode can be simply reversed by adding an excess amount of base. This metallosupramolecular switch shows excellent selectivity in both states and could be used to develop a stimuli-responsive bistable [2]rotaxane as an example of molecular machine.

2.1 Introduction

Bistable rotaxanes and catenanes have played a central role in the development of synthetic molecular machines. The strategies to control the directional movement of submolecular components in synthetic molecular machines in order to perform functions similar to those of biological ones are major challenges for chemists.[1] As exemplified in Chapter I, section 1.3, stimuli-responsive molecular shuttles reported so far mostly employ the manipulation of non-covalent interactions including π-π interactions, hydrogen bonding, hydrophobic interactions or ion-dipole interactions to induce a reversible translational motion. The systems which utilise transition metal-ligand interactions are particularly attractive[2] as their inherent strength have potential to be used in ratchet mechanism.[3] In addition, a large thermodynamic bias between each state is desirable for switchable systems. Sauvage was the first to describe metal-containing rotaxanes and catenanes in which some stimuli that alternates the coordination preference can be used to achieve large-amplitude net motion of submolecular components. In this case the different preferred geometries of Cu(I) and Cu(II) were exploited to bring about motion.[2f] This system set the benchmark for metal-containing rotaxanes and catenanes for nearly twenty years.

Previous work within the Lusby group had reported the pH-switching of heteroleptic cyclometallated platinum complexes monitoring with ^{1}H NMR spectroscopy. [**L**^{1}Pt(DMAP)] (H_2**L**^{1} = 2,6-diphenylpyridine) was reversibly interconverted into [**L**^{1}Pt(DMAP)(OTs)] upon treatment with acid or base (Scheme 2.1). The switching process revealed or masked *cis*-coordinating group of the square-planar platinum complex, and this was used to create acid-base responsive assembly/disassembly of two- and three-dimensional metallosupramolecular architectures.[4]

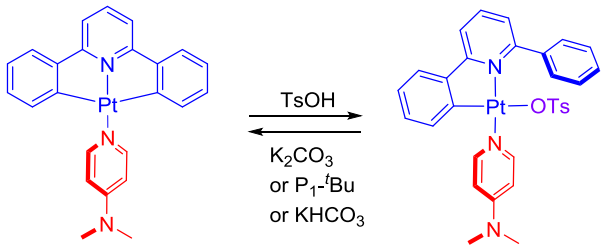

Scheme 2.1 Acid-base switchable revealing/masking *cis*-coordinate platinum centre.

When the mixture of [**L**^{1}Pt(DMAP)] and py or $pyCF_3$ was treated with one equivalent of TsOH, formation of [*trans*-H**L**^{1}Pt(DMAP)(py/$pyCF_3$)]OTs was observed. Adding a second

equivalent of acid to [*trans*-H**L**^{1}Pt(DMAP)(py/pyCF$_3$)]OTs resulted in liberation of py/pyCF$_3$ along with a solvato complex of [H**L**^{1}Pt(DMAP)(S)], (S = DMF-d_7) (Scheme 2.2).[5]

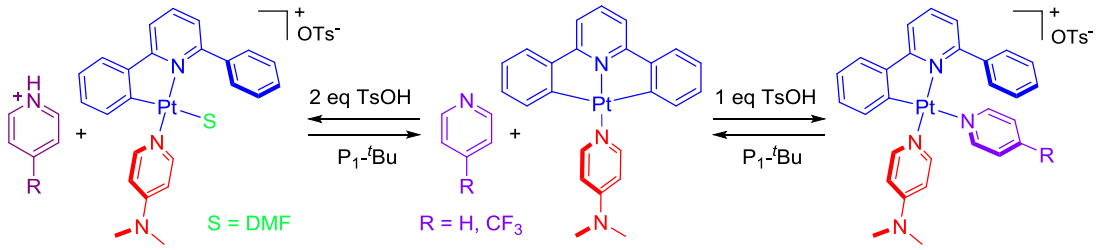

Scheme 2.2 Acid-base responsive exchange between platinum coordinated DMAP and PyR.

As platinum(II) can coordinate with H$_2$**L**^{1} and monodentate ligands in either η^3 C^N^C doubly anionic or η^2 C^N monoanionic fashion, it was envisaged that a H**L**^{1}-Pt(II) complex that coordinate in C^N fashion could accept a bidentate ligand as well as two monodentate ligands to form a square planar complex. This led to an investigation of an acid-base stimuli responsive "3+1" and "2+2" cyclometallated platinum motifs that are able to exchange monodentate and bidentate ligands with excellent selectivity.

2.2 Results and Discussion

2.2.1 Formation of a "2+2" complex with an acyclic cyclometallated Pt complex

To probe whether a bidentate ligand could be accommodated within the primary coordination sphere of H**L**¹Pt, initially [**L**¹Pt(DMSO)] was first treated with *p*-toluenesulfonic acid (TsOH) and then 5,5′-dimethyl-2,2′-bipyridine (dmbipy) in CH_2Cl_2. This bidentate ligand was selected as it was felt this would give a better representation of a station, particularly in terms of steric demands, say in comparison to unfunctionalised 2,2'-bipy. It was also anticipated that the two methyl moieties could be used as a further spectroscopic handle to discriminate between each pyridyl half. We were pleased to see that the compound obtained from the this complexation presented two methyl signal ($H_{J'}$), consistent the formation of an unsymmetrical complex (Figure 2.2b). The two differing halves of the coordinated dmbipy ligand are also clearly seen in the *ortho* protons, which appear at chemical shift 9.28 (H_k) and 7.65 (H_d) ppm. This large difference, as was observed in the methyl groups, is due to shielding effects from the non-coordinating phenyl ring which is positioned almost directly over $H_{d,}$ whereas for H_k these same non-covalent interactions are absent (Figure 2.2).

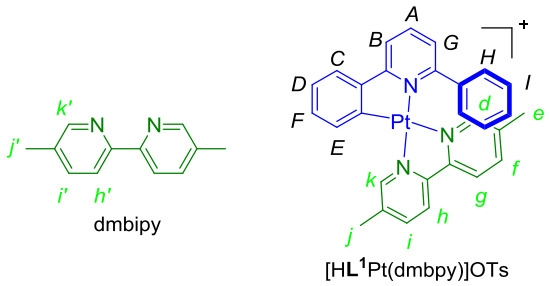

Figure 2.1 Chemical structures of dmbipy and [H**L**¹Pt(dmbipy)]⁺.

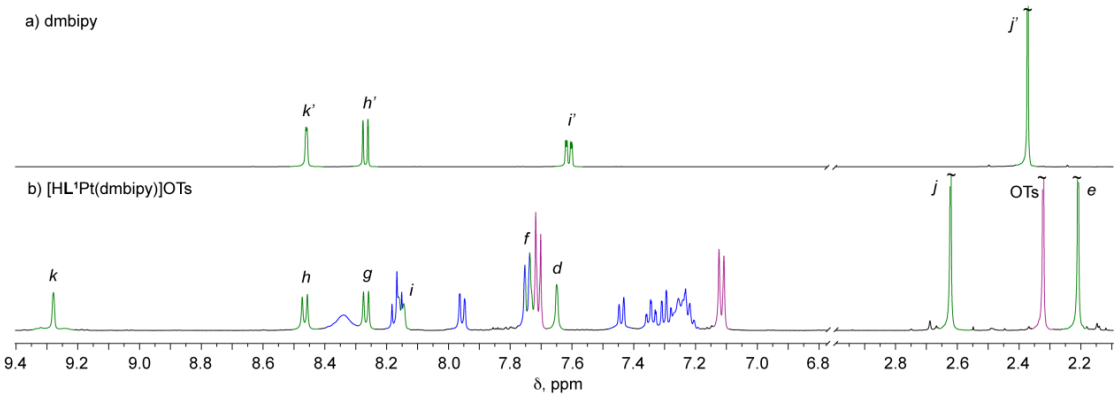

Figure 2.2 Partial ^{1}H NMR spectra (500 MHz, CD_2Cl_2, 298 K) of a) dmbipy; b) [H**L**^{1}Pt(dmbipy)]OTs. The assignments correspond to the lettering shown in Figure 2.1.

The structure of [H**L**^{1}Pt(dmbipy)]OTs was confirmed by X-ray crystallography (Figure 2.3), using single crystals grown from slow diffusion of diisopropyl ether into a saturated chloroform solution.

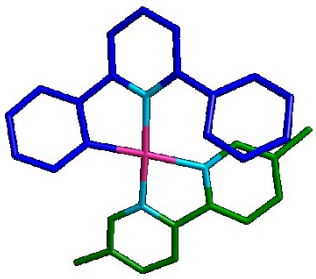

Figure 2.3 Crystal structure of [H**L**^{1}Pt(dmbipy)]OTs.[6]

The sterically congested nature of this complex creates a helical axis of asymmetry, as had previously been described by von Zelewsky.[7] In the solid state, both *P* and *M* enantiomers[8] are observed, in which the non-coordinating phenyl group sits either above or below the plane of the dmbipy ligand making the molecule adopted a helical geometry[9]. To investigate this further, [H**L**^{1}Pt(dmbipy)]CSA (CSA = camphorsulfonate) was generated using CSA to ring open [**L**^{1}Pt(DMSO)] to determine whether this axis of asymmetry could be observed in solution. However, only a single set of ^{1}H NMR resonances in CD_2Cl_2, a solvent in which tight ion pairing could be expected, was observed. Similarly, the addition of TRISPHAT to [H**L**^{1}Pt(dmbipy)]OTs in CD_2Cl_2 did not show any signal splitting, which probably suggests that the interconvesrion between *M* and *P* diastereoisomers is fast on the NMR timescale (Scheme 2.3). This would also suggest that interconversion does not involve decoordination of dmbipy, rather just slippage of the the non-coordinating phenyl group past the bidentate ligand.

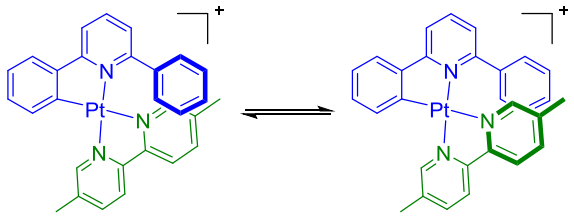

Scheme 2.3 The interconversion between the *M*- and the *P*-enantiomer of [H**L**^{1}Pt(dmbipy)]$^{+}$ was rapid in solution.

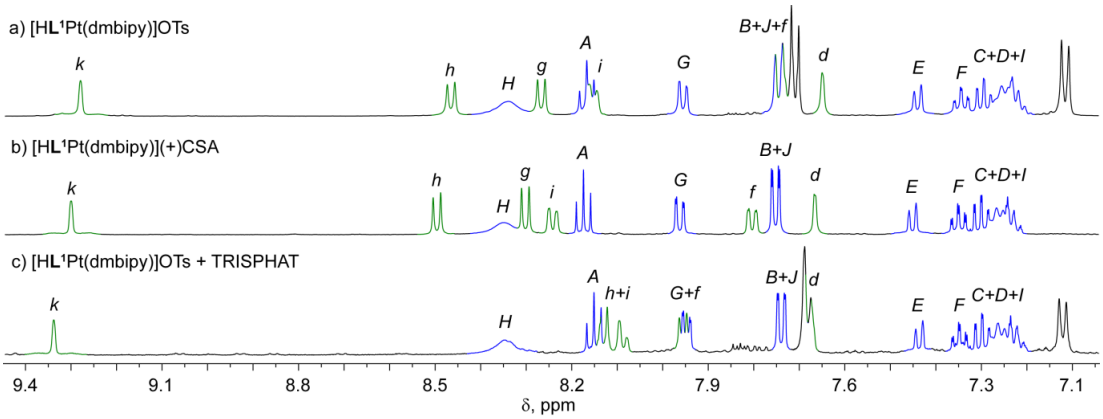

Figure 2.4. Partial ^{1}H NMR spectra (500 MHz, CD_2Cl_2, 298 K) of a) [H**L**^{1}Pt(dmbipy)]OTs, b) *in situ* generated [H**L**^{1}Pt(dmbipy)](+)CSA and c) [H**L**^{1}Pt(dmbipy)]OTs + TRISPHAT. The assignments correspond to the lettering shown in Figure 2.1.

2.2.2 Reversible Ligand Exchange Experiments with Acyclic Pt complexes

To explore whether more strongly coordinating neutral monodentate pyridyl-based ligands could be similarly displaced by the same bidentate ligand upon treatment with acid, the platinum complexes [**L**^{1}Pt(py)], [**L**^{1}Pt(3,5-lut)] and [**L**^{1}Pt(DMAP)] (py = pyridine; 3,5-lut = 3,5-lutidine; DMAP = 4-dimethylaminopyridine) were prepared following established procedures.[9]. The formation of [**L**^{1}Pt(py)], [**L**^{1}Pt(3,5-lut)] and [**L**^{1}Pt(DMAP)] were confirmed by ^{1}H NMR spectroscopy. Additionally, the structure of [**L**^{1}Pt(3,5-lut)][6] (Figure 2.5) and [**L**^{1}Pt(DMAP)][5] were confirmed by X-ray crystallography.

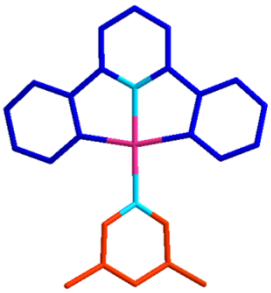

Figure 2.5 Crystal structure of [**L**^{1}Pt(3,5-lut)].[6]

The previously described pH-switching of heteroleptic cyclometallated platinum complexes [**L**^{1}PtL'] that can be coordinated in either η^2 or η^3 fashion upon a treatment with acid or base, respectively was used to reversibly assemble/disassemble metallosupramolecular complexes *via* the available *cis* coordinate. Furthermore, platinum binding preference of [**L**^{1}PtL'] in the presence of another ligand cannot be reversed by adding only one equivalent of TsOH.[4-5] It was anticipated that addition of chelating ligand such as dmbipy to a protonated C^N complex would result in a displacement of monodentated ligand due to chelate effect and introduce a "3+1"-"2+2" switchable system.

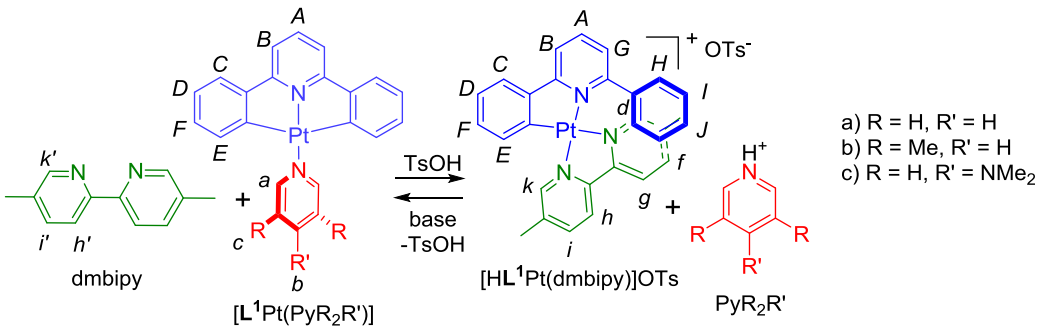

Scheme 2.4 Acid-Base responsive switching between "3+1" and "2+2" cyclometallated Pt complexes.

In the absence of TsOH, ^{1}H NMR spectroscopy showed that, in all cases, dmbipy does not displace the monodentate ligand and remains uncoordinated (Figure 2.6b, 2.7b and 2.8b) as the signals corresponding to [**L**^{1}Pt(PyR$_2$R')] remained unchanged as do those of free dmbipy (Figure 2.2a).

For [**L**^{1}Pt(py)], the addition of a slight excess (1.3 equivalents) of TsOH to the charge neutral complex and dmbipy resulted in the rapid displacement of the monodentate ligand and accompanying generation of [H**L**^{1}Pt(dmbipy)]OTs (Figure 2.6c).

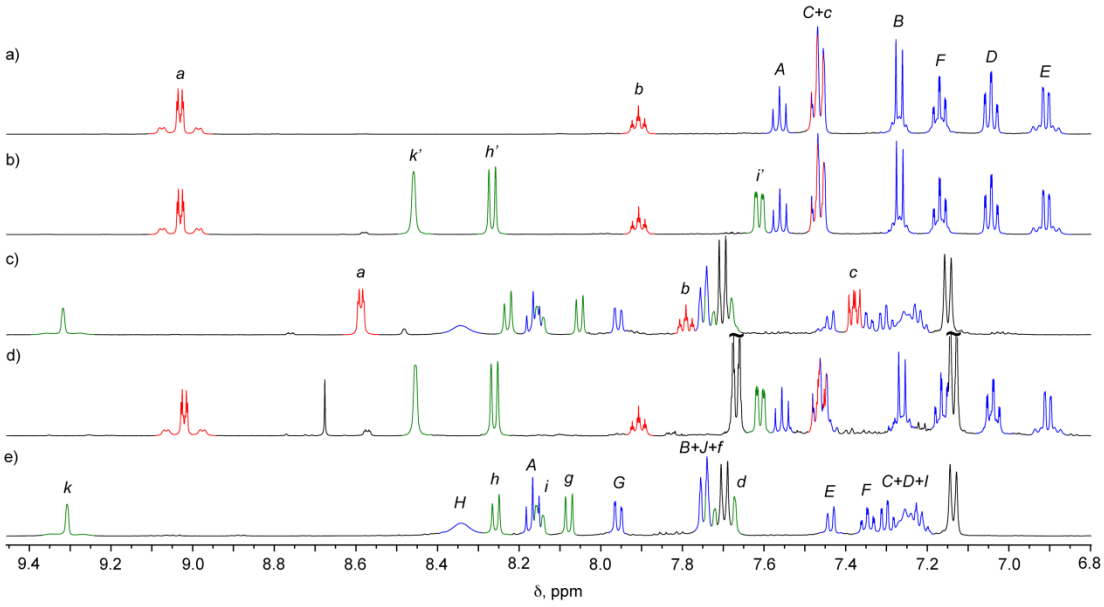

Figure 2.6 Partial ^{1}H NMR spectra (500 MHz, CD_2Cl_2, 298 K) of a) [**L**^{1}Pt(py)]; b) [**L**^{1}Pt(py)] + 5,5'-dimethyl-2,2'-bipyridine; c) [**L**^{1}Pt(py)] + 5,5'-dimethyl-2,2'-bipyridine, 5 minutes after the addition of 1.3 eq TsOH; d) 1.5 h after the subsequent addition of 5 eq P_1-^{t}Bu; e) Authentic [HL^{1}Pt(dmbipy)]OTs (containing 3% CD_3OD).

When similar ligand exchange experiments were carried out with [**L**¹Pt(3,5-lut)] and [**L**¹Pt(DMAP)], it was found that the addition of over 2 equivalents of TsOH were required in order to generate the "2+2" complex (Figure 2.7c, 2.8c). In all the acyclic ligand exchange experiments, the minimum quantity of TsOH required to switch "3+1" to "2+2" complex was determined using titration-type experiments. When the monodentate ligand is pyridine, only a slight excess (1.3 eq) was required, however, for 3,5-lut and DMAP, 2.4 and 2.7 equivalents were needed to induce complete switching, respectively. For example, Figure 2.9 shows a selection of the NMR spectra for the [**L**¹Pt(DMAP)]-dmbipy exchange experiment as a function of TsOH equivalents added. With a slight excess of TsOH (Figure 2.9a) both the "3+1" and "2+2" complexes are present, as well as "free" dmbipy and DMAP (protonated to various degrees), however, additional intermediate species can also be observed. For instance, the signal at 6.05 ppm is indicative of the protonated DMAP complex (the "2+1+1" species) [H**L**¹Pt(DMAP)OTs].[5] As the equivalents of TsOH (Figures 2.9b and c) are increased, a reduction in both the "3+1" complex, [**L**¹Pt(DMAP)], and the intermediate [H**L**¹Pt(DMAP)OTs] and an increase in [H**L**¹Pt(dmbipy)]OTs were observed.

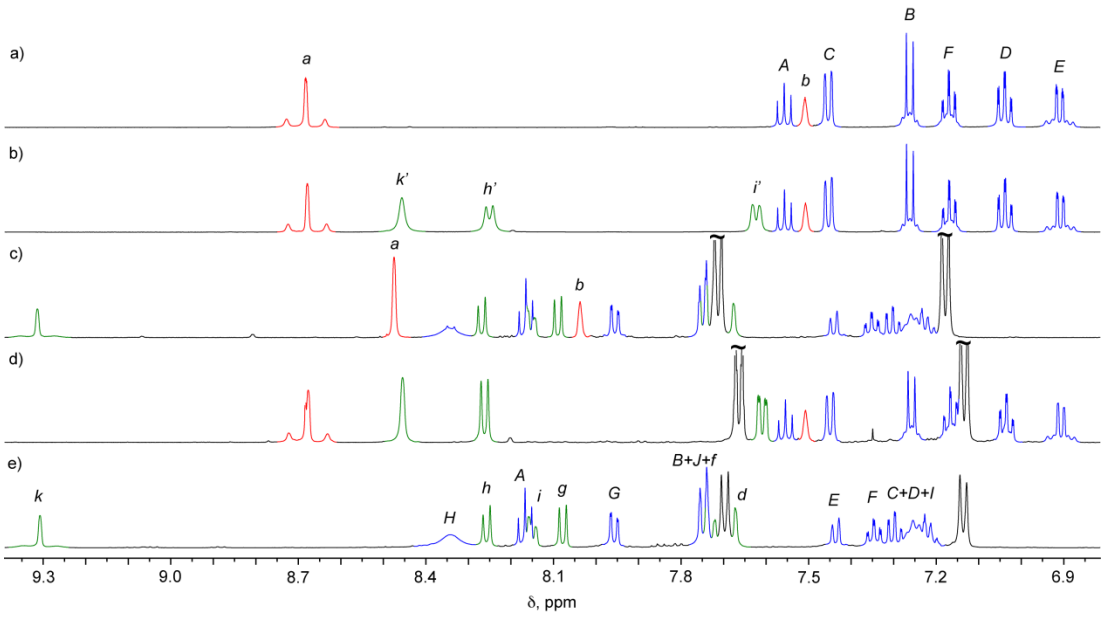

Figure 2.7 Partial ¹H NMR spectra (500 MHz, CD_2Cl_2, 298 K) of a) [**L**¹Pt(3,5-lut)]; b) [**L**¹Pt(3,5-lut)] + 5,5'-dimethyl-2,2'-bipyridine; c) [**L**¹Pt(3,5-lut)] + 5,5'-dimethyl-2,2'-bipyridine, 5 minutes after the addition of 2.4 eq TsOH; d) 2 h after the subsequent addition of 5 eq P_1-^{t}Bu; e) Authentic [H**L**¹Pt(dmbipy)]OTs (containing 3% CD_3OD).

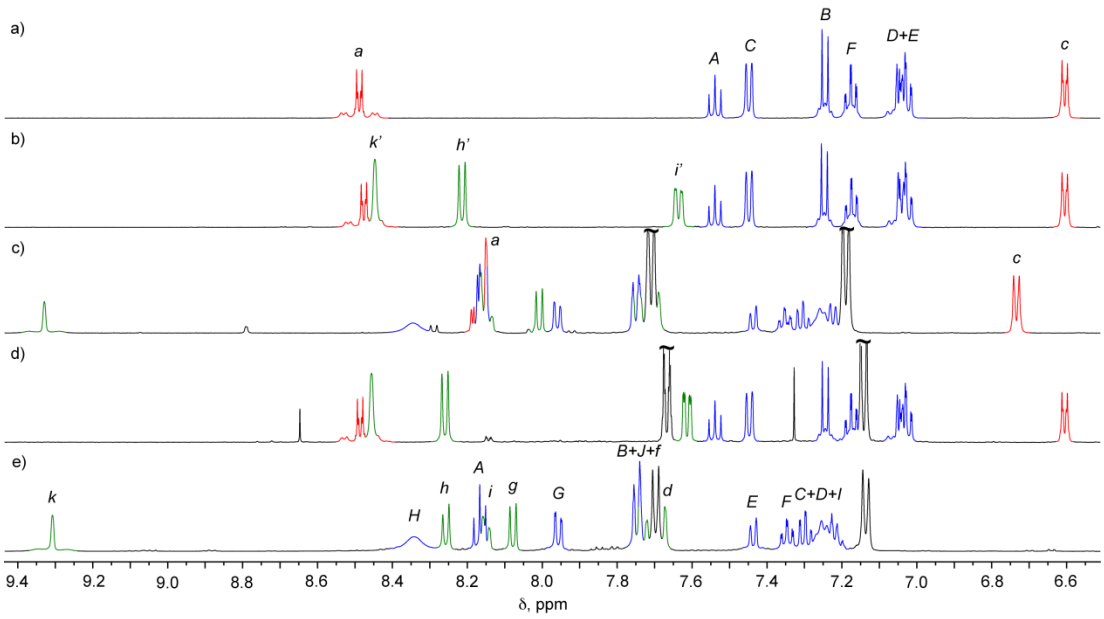

Figure 2.8 Partial ^{1}H NMR spectra (500 MHz, CD_2Cl_2, 298 K) of a) [**L**^{1}Pt(DMAP)]; b) [**L**^{1}Pt(DMAP)] + 5,5'-dimethyl-2,2'-bipyridine; c) [**L**^{1}Pt(DMAP)] + 5,5'-dimethyl-2,2'-bipyridine, 5 minutes after the addition of 2.7 eq TsOH; d) 2 h after the subsequent addition of 5 eq P_1-^{t}Bu; e) Authentic [H**L**^{1}Pt(dmbipy)]OTs (containing 3% CD_3OD).

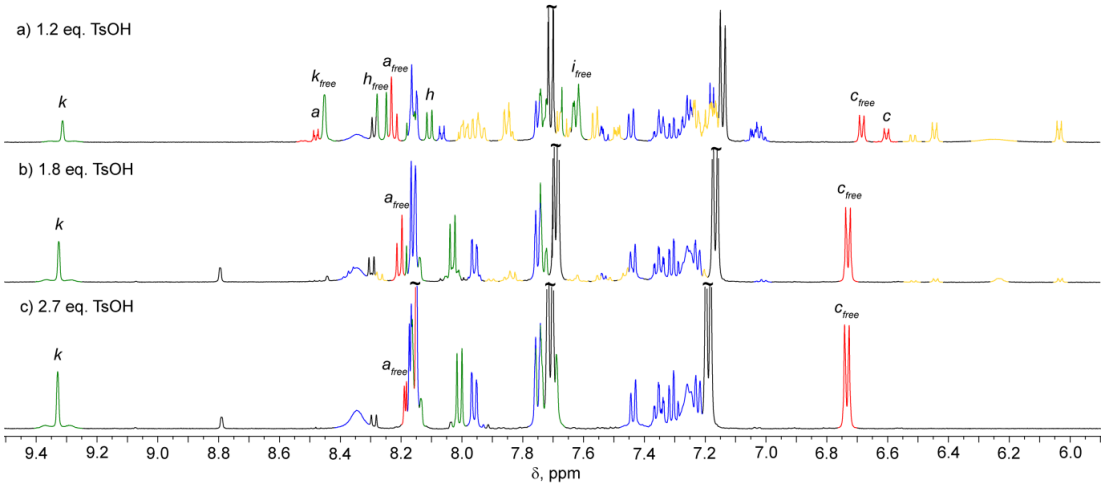

Figure 2.9 Partial ^{1}H NMR spectra (500 MHz, CD_2Cl_2, 298 K) of a) [**L**^{1}Pt(DMAP)] and dmbipy with a) 1.2; b) 1.8 and c) 2.7 eq TsOH.

The difference in the amount of acid required has been attributed to two principle effects. Firstly, liberated DMAP is significantly more basic than py (pK_a of DMAP-H$^+$ = 9.7, py-H$^+$ = 5.2)[10] such that free DMAP can cause the re-cyclometallation to give the "3+1" complex. The second effect is that DMAP is also a better ligand in comparison to py. In particular, the observation of more stable "2+1+1" intermediates *e.g.* [H**L**^{1}Pt(DMAP)OTs], suggests that the chelate effect of dmbipy is not sufficient to fully displace the strongly

coordinating monodenate DMAP. The use of excess acid almost certainly shifts the equilibrium towards the "2+2" complex, [H**L**^{1}Pt(dmbipy)]OTs, through protonation of the liberated DMAP. Similar, but less pronounced, effects were observed for the exchange of [**L**^{1}Pt(3,5-lut)].

As it was observed that monodentate ligands are not displaced by dmbipy in the absence of acid, it was envisaged that simply adding base to a mixture of [H**L**^{1}Pt(dmbipy)]OTs and monodentate moiety (or protonated species in the case where excess acid had been used) would reverse the coordinative bias. Phosphazene base, P_1-^{t}Bu had previously been used to affect (re)cyclometallation of similar complexes,[4] thus when P_1-^{t}Bu was added to the mixture of [H**L**^{1}Pt(dmbipy)]OTs and monodentate pyridyl ligand (py, 3,5-lut or DMAP), the gradual disappearance of signals due to [H**L**^{1}Pt(dmbipy)]OTs and re-appearance of [**L**^{1}Pt(py)], [**L**^{1}Pt(3,5-lut)] and [**L**^{1}Pt(DMAP)] followed 1.5-2 h at room temperature (Scheme 2.2; Figures 2.6d-2.8d).

2.2.3 Macrocyclic cyclometallated Pt complexes

To develop the system further, and with a stimuli-responsive molecular shuttle in mind, the macrocyclic C^N^C Pt complex, [**L**²Pt(DMSO)], has been prepared. The free macrocycle, H_2**L²**, was obtained in an excellent 80% yield from the Williamson-ether reaction of 2,6-di-(4-hydoxyphenyl)pyridine (**1**)[11] and the bisphenol A derived dialkylbromide (**2**)[12] as shown in Scheme 2.5. Compound **1** was synthesised from the commercially available 4-hydroxyphenylboronic acid and 2,6-dibromopyridine *via* Suzuki coupling while compound **2** was obtained in one step by a Williamson-ether reaction between bisphenol A and a large excess 1,4-dibromobutane.

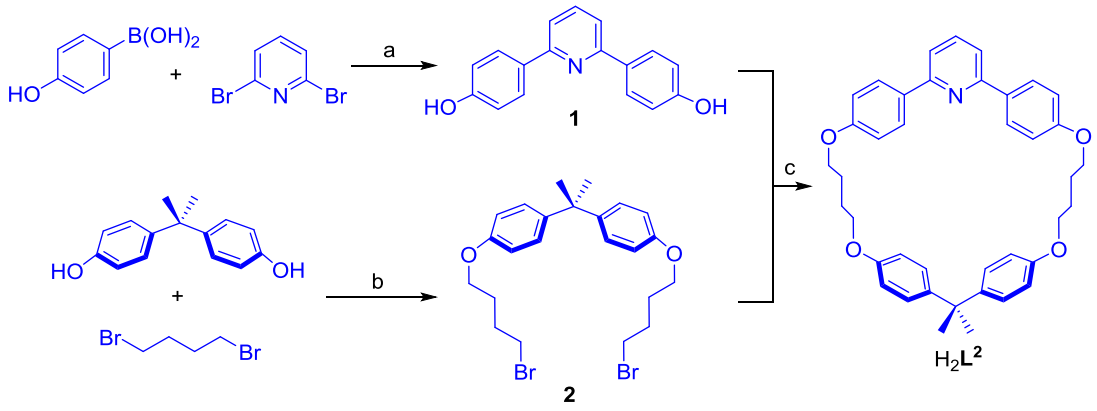

Scheme 2.5 Synthesis of macrocycle H_2**L²**. Reaction conditions: a) KO^{t}Bu, PEPPSI-IPr, ^{i}PrOH, rt, 48 h, 73%; b) Cs_2CO_3, DMF, 60 °C, 16 h, 47%; c) Cs_2CO_3, DMF, 65 °C, 80%.

The insertion of platinum also occurred in a highly respectable 80% yield (Scheme 2.6). This is perhaps surprising, as reaction of potassium tetrachloroplatinate with similar C^N^C chelates in acetic acid usually gives a cyclometallated chloride bridged dimer, and it could have been anticipated that the increased steric bulk of the macrocycle would make this process less facile.[13]

An unsymmetrical bidentate 2-(1-ethylphenyl-1*H*-1,2,3-triazol-4-yl)-5-bromopyridine (**L³**) was prepared by a CuAAC click reaction from terminal alkyne **4** and azide **5** in a good yield as shown in Scheme 2.7. Having a bidentate ligand synthesised from a CuAAC click reaction would be beneficial for expanding the system to a molecular shuttle as the rotaxane can be prepared using the active metal template CuAAC click reaction. This ligand could act as the active components for forming the interlocked structure and as one of the station in a molecular shuttle. The pyridyl alkyne **4** was synthesised from Sonogashira coupling of 5-bromo-2-iodopyridine and (*tert*-butyldimethylsilyl)acetylene

first at 0°C then warmed to rt to prevent either di-coupling or 5-position coupling. The alkyne **3** was then deprotected with tetrabutylammonium fluoride (TBAF) to give terminal alkyne **4**. 2-phenylethylazide, **5**, was prepared according to literature procedure[14].

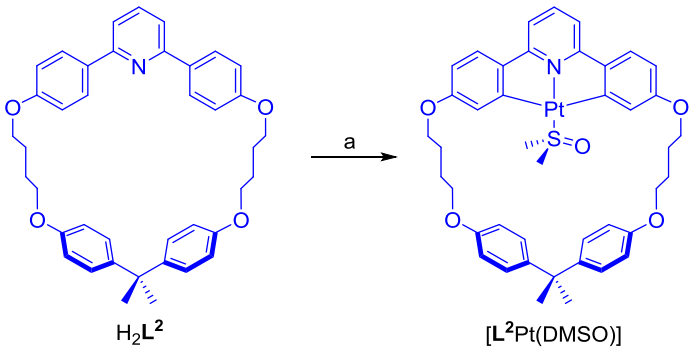

Scheme 2.6 Synthesis of a platinum complexed macrocycle [**L**²Pt(DMSO)]. Reagents and conditions: a) i) $K_2[PtCl_4]$, TBACl, acetic acid, 125 °C, 2d; ii) K_2CO_3, DMSO, H_2O, 90°C, 2 h, 80%.

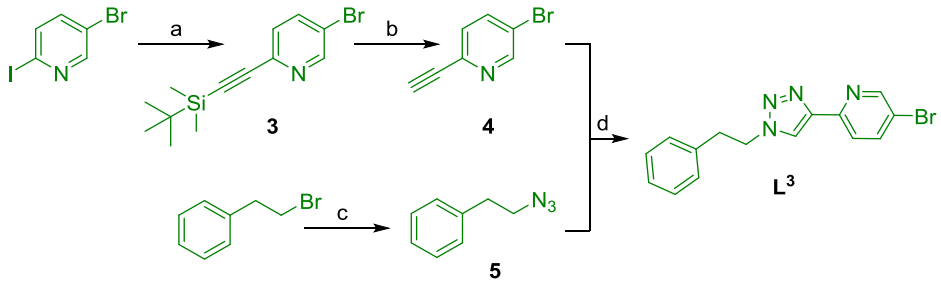

Scheme 2.7 Synthesis of ligand **L**³. Reagents and conditions: a) TBDMS acetylene, CuI, $Pd(PPh_3)_2Cl_2$, Et_3N, THF, 0 °C – rt, 82%; b) TBAF, CH_2Cl_2, rt, 3 h, 78%; c) NaN_3, DMF, 80 °C, 18 h, *quant.*; d) $Cu(CH_3CN)_4PF_6$, DCE, rt – 70 °C, 55%.

[**L**²Pt(3,5-lut)] was prepared from [**L**²Pt(DMSO)] by exchange of the coordinated DMSO for 3,5-lut (Scheme 2.8, step a). In solution, the ^{1}H NMR spectrum of [**L**²Pt(3,5-lut)] (Figure 2.10a) exhibits coordinated *ortho* lutidine signals (H_a) with characteristic ^{195}Pt satellites, while the *para* site (H_b) is significantly upfield shifted with respect to the free heterocycle, most likely due to shielding by the bisphenol A unit. The structure of [**L**²Pt(3,5-lut)] has been confirmed by X-ray crystallography using single crystals grown from slow diffusion of diethyl ether into a saturated dichloromethane solution (Figure 2.12) and from the refined X-ray diffraction data it was observed that [**L**²Pt(3,5-lut)] had crystallized in a P-1 (#2) space group and has a pseudo square planar geometry around the Pt(II) centre.

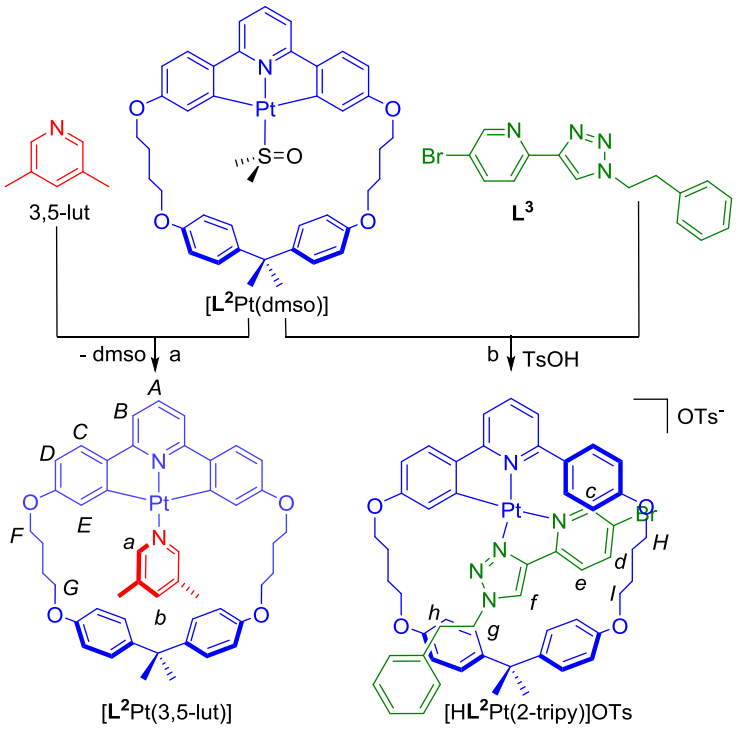

Scheme 2.8 Synthesis of macrocyclic cyclometallated Pt complexes. Conditions: a) CH_2Cl_2, 40 °C, 16 h, 37%; b) CH_2Cl_2, rt, 1 h, 34%.

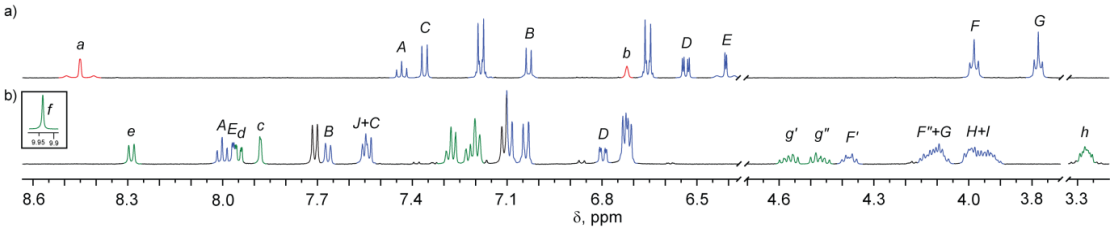

Figure 2.10 Partial ^{1}H NMR spectra (500 MHz, CD_2Cl_2, 298 K) of a) [**L**²Pt(3,5-lut)]; b) [H**L**²Pt(**L**³)]OTs.

The preparation of a "2+2" macrocyclic complex from TsOH induced [**L**²Pt(DMSO)] using **L**³ was also carried out (Scheme 2.8, step b). The ^{1}H NMR spectrum of the product revealed several interesting features (Figure 2.10b). Only one of two possible geometric isomers (Figure 2.11) was produced - *trans*-[H**L**²Pt(**L**³)]OTs. In the *trans*-isomer, the better ligand, pyridyl, is coordinated *cis* to nitrogen of 2,6-diphenylpyridyl as a results of the trans effect of the phenylato unit, could be considered as a kinetic product. As the NMR of this product did not change over time, it would suggest that this product is both the kinetically and thermodynamically favoured isomer, as it has been previously observed that platinum isomers which feature cyclometallated ligands undergo sluggish rearrangement.[5, 15] Another trait of the ^{1}H NMR spectrum of [H**L**²Pt(**L**³)]OTs is the

sterically congested nature of the complex around alkyl chains of the macrocycle, as the four triplets that arise from the H_F, H_G, H_g and H_h environments in the [**L**²Pt(3,5-lut)] and **L**³ precursors have been replaced by a complex diastereotopic pattern of signals.

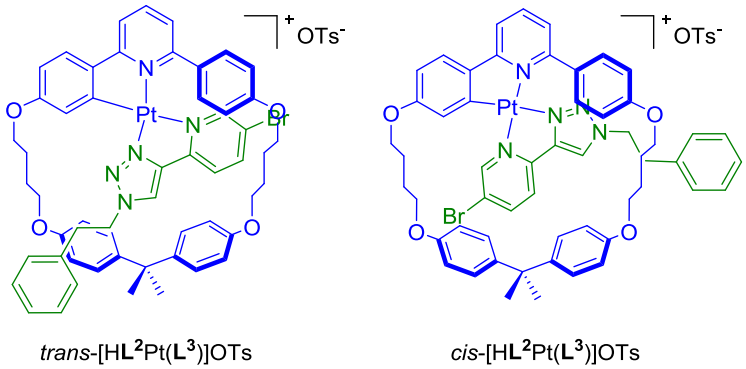

Figure 2.11 Two possible isomers of [H**L**²Pt(**L**³)]OTs.

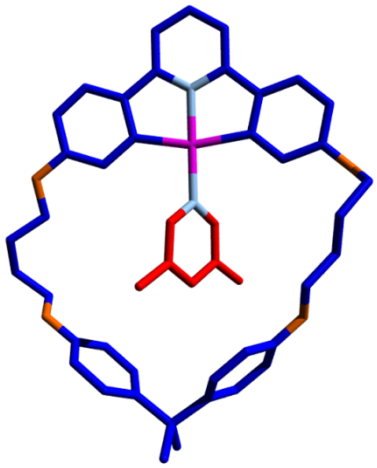

Figure 2.12 X-ray crystal structure of [**L**²Pt(3,5-lut)]. Colour code: C(**L**²), blue; C(3,5-lut), red; N, light blue; O, orange; Pt, magenta. Solvent molecules have been removed for clarity.

The absolute assignment of *trans*-[**L**²Pt(**L**³)]OTs was made on the basis of the following observations:

(i) The presence of a strong NOESY signal between H_E and H_K in the acyclic "2+2" complex, [H**L**¹Pt(dmbipy)]OTs (Figure 2.13) and a clear lack of corresponding cross-peak between the signal at just below 10 ppm with H_E for [H**L**²Pt(**L**³)]OTs (Figure 2.14).

(ii) Clear NOESY cross signals between the peak at just below 10 and signals that can be ascribed to H_e, H_g and H_h of the **L**³ ligand.

(iii) The relative chemical shifts of the H_c and H_f resonances – whereas H_f is deshielded with respect to the same signal for free **L**³ (due to Pt complexation), H_c is upfield shifted by *ca*. 05 ppm, a result of shielding by the non-coordinating phenoxy alkyl group of **L**².

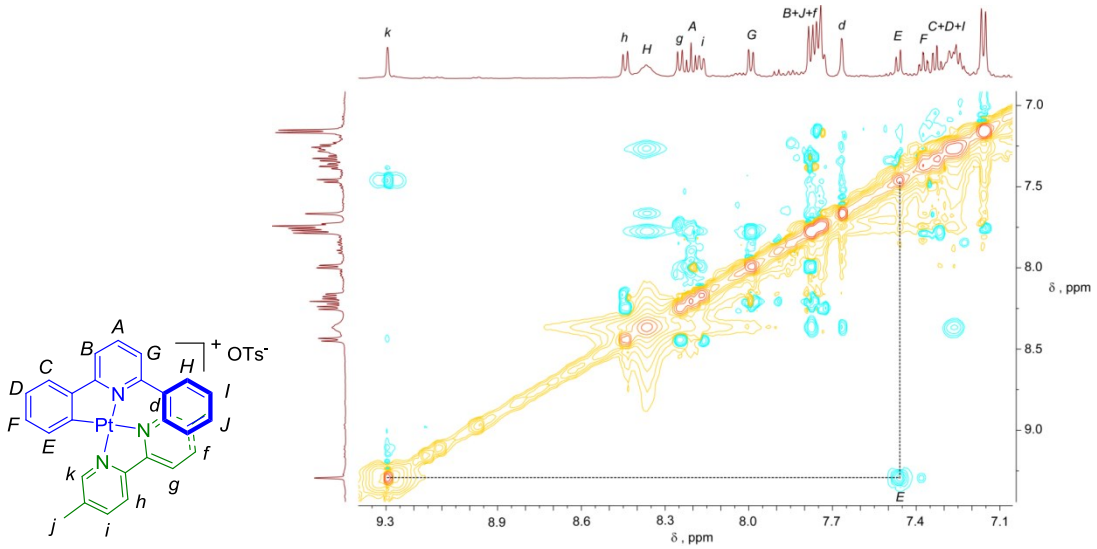

Figure 2.13 ^{1}H-^{1}H NOESY spectrum (500 MHz, CD_2Cl_2, 298 K) of [H**L**¹Pt(dmbipy)]OTs.

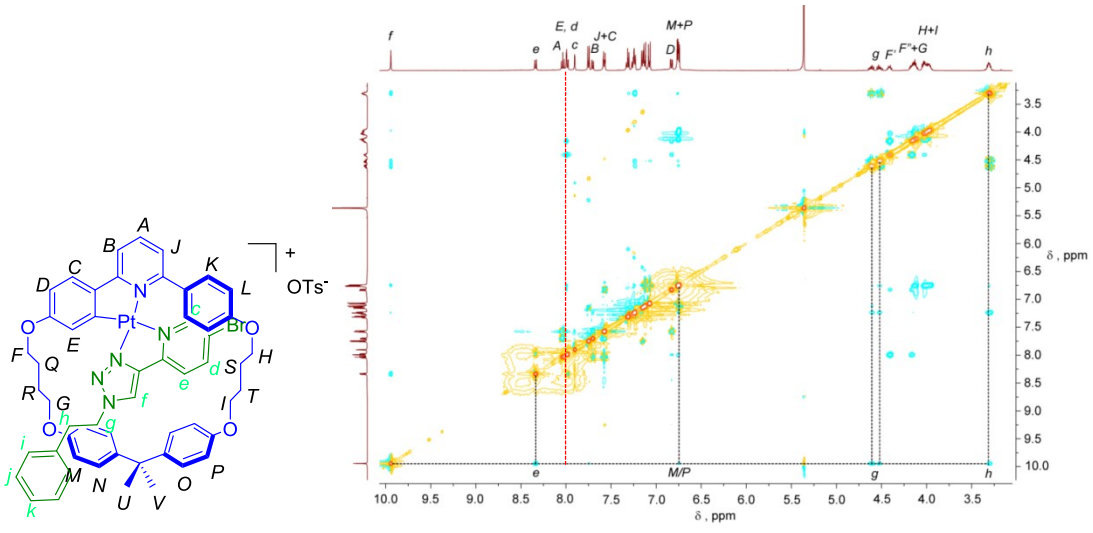

Figure 2.14 ^{1}H-^{1}H NOESY spectrum (500 MHz, CD_2Cl_2, 298 K) of [**L**²Pt(**L**³)]OTs.

2.2.4 Ligand Exchange Experiments for Macrocyclic Pt complexes

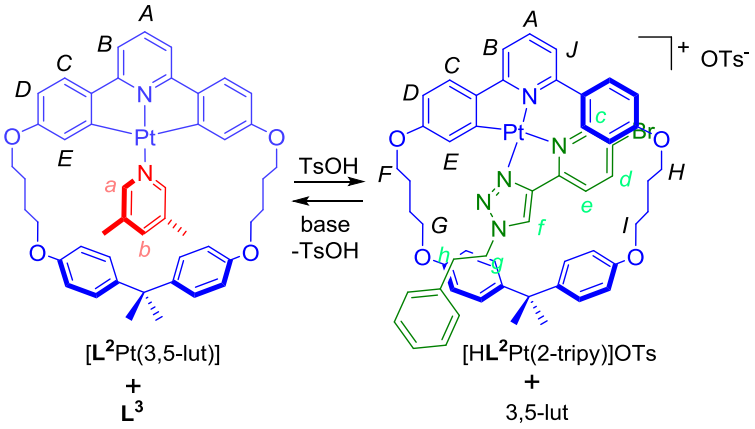

Scheme 2.9 Acid-Base responsive switching between "3+1" and "2+2" macrocyclic cyclometallated Pt complexes.

The "3+1" to "2+2" interconversion between [**L**²Pt(3,5-lut)] and [H**L**²Pt(**L**³)]OTs was examined using ^{1}H NMR spectroscopy (Scheme 2.9 and Figures 2.15b-d). When **L**³ was mixed with [**L**²Pt(3,5-lut)] in CD_2Cl_2, only signals which are correspond to those two species were apparent (Figure 2.15b). Upon the addition of 1.7 eq of TsOH, the NMR spectrum changed to give a set of signals that were indistinguishable from those of *trans*-[H**L**²Pt(**L**³)]OTs (Figure 2.15c). The lesser amount of TsOH used to exchange the coordination of the platinum^{II} centre from monodentate lutidine to bidentate pyridyltriazole **L**³ than that of the acyclic system suggests that **L**³ is a better ligand than dmbipy. As with the acyclic system, this change occurred within the time taken to record a subsequent spectrum. This rapid generation coupled to the lack of observation of another isomer further supports that *trans*-[H**L**²Pt(**L**³)]OTs is the kinetic (and thermodynamic) product, irrespective of the identity of the neutral monodentate ligand in the starting "3+1" complex. When five equivalents of P_1-^{t}Bu was added to the NMR sample containing [H**L**²Pt(**L**³)]OTs and free lutidine, the signals due to the "2+2" complex and monodentate ligand started to disappear, accompanied by the appearance of signals due to [**L**²Pt(3,5-lut)] and free **L**³. After 48 h, only signals due to [**L**²Pt(3,5-lut)] and free **L**³ could be observed (Figure 2.15d). The lethargy of this reaction in comparison to the same process for the acyclic complexes is almost certainly due to an increased steric barrier.

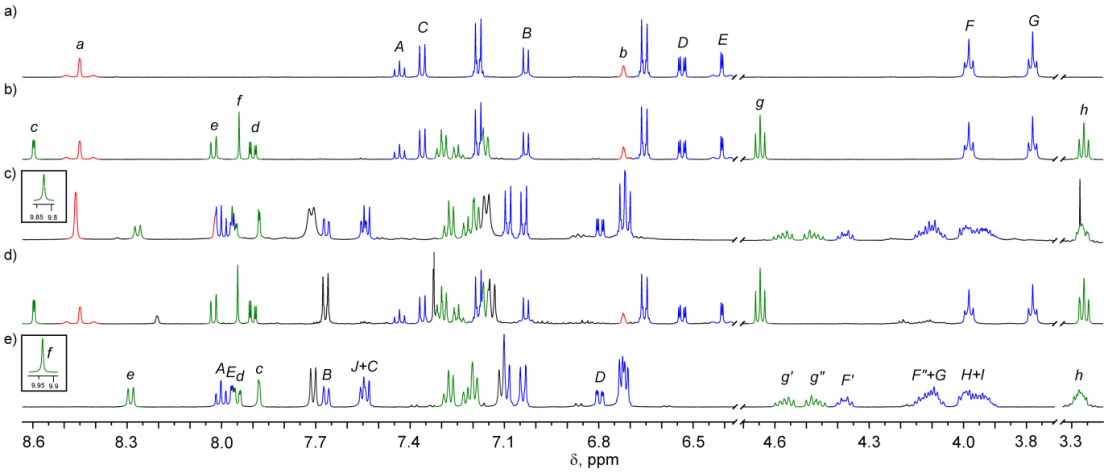

Figure 2.15 Partial ^{1}H NMR spectra (500 MHz, CD_2Cl_2, 298 K) of a) [L^{2}Pt(3,5-lut)]; b) [L^{2}Pt(3,5-lut)] + L^3; c) [L^{2}Pt(3,5-lut)] + L^3, 5 minutes after the addition of 1.7 eq TsOH; d) 48 h after the subsequent addition of 5 eq P_1-^{t}Bu; e) Authentic [HL^{2}Pt(L^3)]OTs. The

2.3 Conclusion

The acid-base responsive switching between "3+1" and "2+2" cyclometallated platinum complexes have been investigated. The acyclic C^N^C platinum motifs with pyridyl monodentate ligands including py, 3,5-lut and DMAP can be displaced with bidentate dmbipy ligand induced by acid addition. Furthermore, the "2+2" complex with the presence of monodentate ligand could be reversed to corresponding "3+1" complex after treated with base. The macrocyclic form of C^N^C platinum complexes gave similar results. These types of externally addressable coordination complexes could be developed to be useful molecular machines.

2.4 Experimental Section

2.4.1 General Experimental Procedure

Unless stated otherwise, all reagents and solvents were purchased from commercial sources and used without further purification. H_2**L^1**,[11] [**L^1**Pt(DMSO)],[13, 16] [**L^1**Pt(DMAP)],[5] [**L^1**Pt(py)],[5] [**L^1**Pt(3,5-lut)],[6] [H**L^1**Pt(dmbipy)]OTs,[6] were synthesised by Dr. Sarah J. Pike according to reported in literature. 1,1'-propane-2,2-diylbis[4-(4-bromobutoxy)benzene] (**2**)[12] and 2-phenylethylazide (**5**)[14] were prepared according to literature procedures.

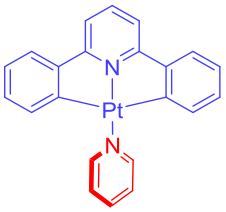

[**L**^{1}Pt(py)]

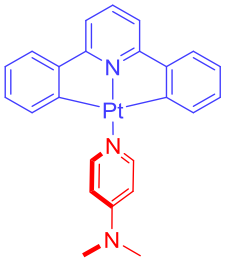

[**L**^{1}Pt(DMAP)]

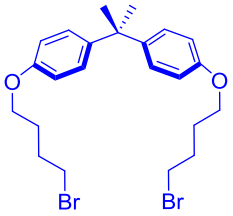

2

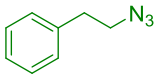

5

2.4.2 Synthesis

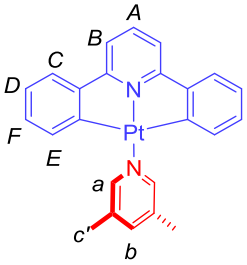

[**L**^{1}Pt(3,5-lut)]

To a yellow solution of [L^{1}Pt(DMSO)] (0.093 g, 0.19 mmol) in CH_2Cl_2 (10 mL) was added 3,5-lutidine (0.040 g, 0.37 mmol), which resulted in a darkening of the solution to orange. The reaction was stirred for 18 h at rt and the excess solvent was removed under reduced pressure. Purification of the crude product using column chromatography (1:1:0.01; CH_2Cl_2:hexane:NEt_3) gave the compound as an orange solid (0.052 g, 53 %). Bright orange crystals suitable for X-ray crystallography were grown *via* slow diffusion of diisopropyl ether into a saturated CH_2Cl_2 solution of the desired complex. m.p. 205-210 °C (dec.); ^{1}H NMR (500 MHz, CD_2Cl_2): 8.68 (s, J (^{195}Pt) = 45.2 Hz, 2H, H_a), 7.56 (t, J = 8.0 Hz, 1H, H_A), 7.51 (s, 1H, H_b), 7.45 (dd, J = 7.6, 0.6 Hz, 2H, H_C), 7.29-7.24 (m, 2H, H_B), 7.20-7.14 (m, 2H, H_F), 7.07-7.01 (m, 2H, H_D), 6.95 – 6.87 (m, 2H, H_E), 2.39 (s, 6H, $H_{c'}$).

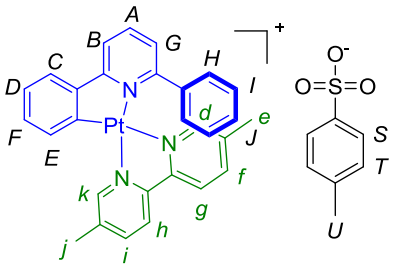

[H**L**^{1}Pt(dmbipy)]OTs

To a solution of [L1Pt(DMSO)] (0.50 g, 10.0 mmol) in CH_2Cl_2 (30 mL) was added 5,5′-dimethyl-2,2′-bipyridyl.TsOH (0.37 g, 10.0 mmol) and the reaction mixture stirred at rt for 5 minutes. After this time, the solution was concentrated to ~ 3 mL under reduced pressure and upon the slow addition of hexane, the desired product precipitated from solution as a bright yellow solid. The crude solid was filtered off and collected. Crystals suitable for X-ray crystallography were grown *via* slow diffusion of diisopropyl ether into a saturated chloroform solution (0.48 g, 78%); ^{1}H NMR (500 MHz, CD_2Cl_2); δ = 9.28 (s, *J* (^{195}Pt) = 35.6 Hz, 1H, H_k), 8.46 (d, *J* = 8.2 Hz, 1H, H_h), 8.34 (br, 2H, H_H), 8.27 (d, *J* =8.2 Hz, 1H, H_g), 8.20-8.13 (m, 2H, H_{A+i}), 7.96 (d, *J* = 8.0 Hz, 1H, H_G), 7.77-7.68 (m, 5H, $H_{B+J+f+S}$), 7.65 (s, 1H, H_d), 7.44 (d, *J* = 7.6 Hz, 1H, H_E), 7.34 (td, *J* = 7.6, 1.5 Hz, 1H, H_F), 7.32-7.19 (m, 4H, H_{C+D+I}), 7.11 (d, *J* = 8.0 Hz, 2H, H_T), 2.62 (s, 3H, H_j), 2.32 (s, 3H, H_U), 2.21 (s, 3H, H_e).

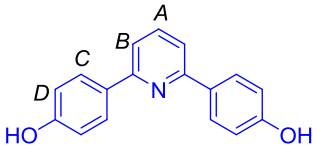

2,6-(bis-4-hydroxyphenyl)pyridine, **1**

Adapted from a procedure by Aucagne *et al.*[11] Isopropanol (50 mL) was purged with nitrogen for 5 minutes then potassium *tert*-butoxide (2.24 g, 20 mmol), PEPPSI-IPr (0.27 g, 0.40 mmol, 5 mol%), 4-hydroxyphenylboronic acid (2.43 g, 17.6 mmol) and 2,6-dibromopyridine (1.89 g, 8 mmol) were added and the reaction flask was resealed and purged with nitrogen. The reaction mixture was stirred at rt for 48 h, then quenched with saturated NH_4Cl solution (100 mL) and extracted with EtOAc (3×100 mL). The combined organic layers were dried over $MgSO_4$, filtered, concentrated under reduced pressure, then purified by column chromatography (0-30% Et_2O in CH_2Cl_2) providing the desired product as a pale yellow solid (1.53 g, 73%). m.p. 222-226 °C; ^{1}H NMR (500 MHz, CD_3OD); 7.97 (d, *J* = 8.8 Hz, 4H, H_C), 7.77 (t, *J* = 7.8 Hz, 1H, H_A), 7.59 (d, *J* = 7.8 Hz, 2H, H_B), 6.90 (d, *J* = 8.8 Hz, 4H, H_D); ^{13}C NMR (125 MHz, CD_3OD); 160.0, 158.1, 138.8, 132.3, 129.4, 118.2,

116.4; LR-FABMS (3-NOBA matrix): *m/z* = 263 $[M]^+$; HR-FABMS (3-NOBA matrix); *m/z* = 263.09510 (calc. for $C_{17}H_{13}O_2N$, 263.09518).

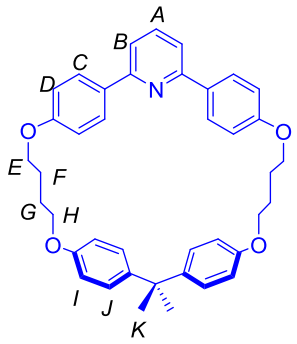

H_2**L²**

Adapted from a procedure by Durola *et al.*[12] To a stirred mixture of Cs_2CO_3 (19.68 g, 60 mmol) and 2,6-(bis-4-hydroxyphenyl)pyridine (0.27 g, 1.0 mmol) in 600 mL of degassed DMF at 65 °C was added dropwise, using a pressure equalising funnel, over a period of 24 h a solution of 1,1′-propane-2,2-diylbis[4-(4-bromobutoxy)benzene] (0.51 g, 1.0 mmol) in 200 mL of degassed DMF. When addition was complete, the reaction was stirred at 65 °C for a further 30 h. After this time, the reaction mixture was cooled to rt, the solvent removed under reduced pressure, and the residue partitioned between CH_2Cl_2 and H_2O. The organic phase was separated, and the aqueous phase extracted twice with CH_2Cl_2. The combined organic phases were washed with brine, H_2O and dried over $MgSO_4$. The solvent was removed under reduced pressure and the residue purified by column chromatography (25-50% CH_2Cl_2:Petroleum ether) to give a colourless solid as the product (0.70 g, 80%) m.p. 203-206 °C; ^{1}H NMR (500 MHz, $CDCl_3$); 8.01 (d, *J* = 8.1 Hz, 4H, H_C), 7.73 (t, *J* = 7.4 Hz, 1H, H_A), 7.54 (d, *J* = 7.4 Hz, 2H, H_B), 7.16 (d, *J* = 8.1 Hz, 4H, H_J), 6.99 (d, *J* = 8.1 Hz, 4H, H_D), 6.82 (d, *J* = 8.1 Hz, 4H, H_I), 4.24 (t, *J* = 6.8 Hz, 4H, H_E), 4.01 (t, *J* = 5.7 Hz, 4H, H_H), 2.05-1.98 (m, 4H, H_F), 1.98-1.92 (m, 4H, H_G), 1.63 (s, 6H, H_K); ^{13}C NMR (125 MHz, $CDCl_3$); 159.5, 156.8, 156.5, 143.1, 137.4, 132.5, 128.4, 127.8, 117.0, 115.2, 113.8, 67.8, 67.3, 41.8, 31.3, 25.8, 25.5; LR-FABMS (3-NOBA matrix) *m/z* = 600 $[MH]^+$; HR-FABMS (3-NOBA matrix) *m/z* = 600.31179 (calc. for $C_{40}H_{42}NO_4$ 600.31084).

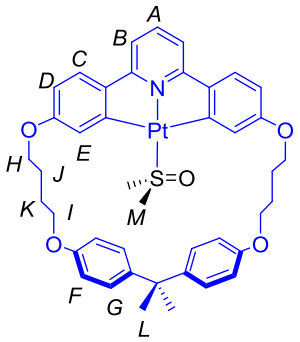

[**L**²Pt(DMSO)]

To a solution of H_2**L²** (0.24 g, 0.40 mmol) in acetic acid (12 mL) was added $K_2[PtCl_4]$ (0.17 g, 0.40 mmol) and tetrabutylammonium chloride (0.13 g, 0.40 mmol). The mixture was heated at 125 °C for 2 days over which time the suspension turned green-yellow with some unconsumed red Pt salt. The entire solids were filtered off and then washed with water (5 mL) to remove the red starting Pt salt. The resultant green-yellow precipitate was washed with acetone (5 mL) and Et_2O (5 mL). The green-yellow solid was then dissolved in hot DMSO (6 mL) and K_2CO_3 (0.57 g, 4.1 mmol) and H_2O (2 mL) were added. The mixture was heated to 90 °C for 2 h. Upon the addition of more water (10 mL) the product precipitated as a bright yellow solid. Flash column chromatography (CH_2Cl_2) and crystallization from Et_2O and CH_2Cl_2 gave the product as a bright yellow solid. (0.28 g, 80%). m.p. >270 °C (dec.); ^{1}H NMR (500 MHz, $CDCl_3$); δ 7.48 (t, *J* = 8.0 Hz, 1H, H_A), 7.36 (d, *J* = 8.5 Hz, 2H, H_C), 7.34 (d, *J* = 2.5 Hz, 2H, H_E), 7.14 (d, *J* = 8.8 Hz, 4H, H_G), 7.05 (d, *J* = 8.0 Hz, 2H, H_B), 6.84 (d, *J* = 8.8 Hz, 4H, H_F), 6.58 (dd, *J* = 8.5, 2.5 Hz, 2H, H_D), 4.17 (t, *J* = 6.4 Hz, 4H, H_H), 4.07 (t, *J* = 6.2 Hz, 4H, H_I), 3.14 (s, 6H, *J*(^{195}Pt) = 25.4 Hz, H_M), 2.02-1.90 (m, 8H, H_{J+K}), 1.62 (s, 6H, H_L); ^{13}C NMR (125 MHz, $CDCl_3$); δ 168.4, 166.5, 160.7, 157.1, 143.3, 142.5, 141.0, 127.8, 126.1, 121.5, 114.2, 113.2, 112.0, 68.01, 67.99, 48.0, 41.7, 31.1, 26.5, 26.0; LR-ESIMS *m/z* = 871 $[MH]^+$; HR-ESIMS *m/z* = 871.27380 (calc. for $C_{42}H_{46}NO_5{}^{195}Pt^{32}S$ 871.27391).

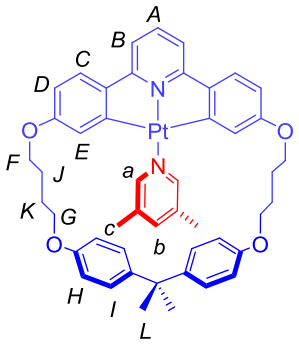

[**L**²Pt(3,5-lut)]

To a yellow solution of [**L**²Pt(DMSO)] (0.032 g, 0.037 mmol) in CH_2Cl_2 (5 mL) was added 3,5-lutidine (0.004 g, 0.037 mmol), which resulted in a darkening of the solution to orange. The reaction was stirred at 40 °C overnight and the excess solvent was removed under reduced pressure. The crude residue was purified by Et_2O diffusion into a saturated CH_2Cl_2 solution, yielding the product as bright orange crystals (0.012 g, 37%). ^{1}H NMR (500 MHz, CD_2Cl_2); δ 8.45 (s, 2H, J(^{195}Pt) = 43.4 Hz, H_a), 7.43 (t, J = 8.0 Hz, 1H, H_A), 7.36 (d, J = 8.4 Hz, 2H, H_C), 7.18 (d, J = 8.7 Hz, 4H, H_I), 7.03 (d, J = 8.0 Hz, 2H, H_B), 6.72 (s, 1H, H_b), 6.65 (d, J = 8.7 Hz, 4H, H_H), 6.54 (dd, J = 8.4, 2.5 Hz, 2H, H_D), 6.41 (d, J = 2.5 Hz, 2H, J(^{195}Pt) = 27.3 Hz, H_E), 3.98 (t, J = 6.5 Hz, 4H, H_F), 3.78 (t, J = 6.5 Hz, 4H, H_G), 1.88-1.78 (m, 14H, $H_{J,K,c}$), 1.67 (s, 6H, H_L); ^{13}C NMR (125 MHz, CD_2Cl_2); δ 175.3, 167.5, 160.8, 157.0, 150.7, 143.2, 141.8, 139.2, 137.9, 135.4, 127.5, 125.4, 117.2, 114.3, 112.4, 111.6, 67.9 ,67.4, 41.2, 29.9, 25.7, 25.4, 17.5; LR-FABMS (3-NOBA matrix) m/z = 900 $[MH]^+$; HR-FABMS (3-NOBA matrix) m/z = 900.33538 (calc. for $C_{47}H_{49}N_2O_4{}^{195}Pt$ 900.33346).

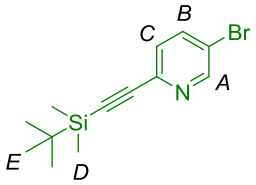

2-*tert*-butyldimethylsilylethynyl-5-bromopyridine, **3**

To a suspension of 5-bromo-2-iodopyridine (0.85 g, 3 mmol), CuI (0.06 g, 0.31 mmol, 10 mol%), $Pd(PPh_3)_2Cl_2$ (0.10 g, 0.14 mmol, 5 mol%) in dry THF (20 mL) and Et_3N (15 mL) at 0 °C was charged *tert*-butyldimethylsilylacetylene (0.58 mL, 3 mmol). The colour changed from yellow to dark brown. The reaction mixture was stirred at 0 °C for 1 h before being warmed to rt and then left stirring overnight. A white precipitate formed and the solution had turned yellow. The mixture was filtered through celite and washed

with Et_2O. The filtrate was concentrated under reduced pressure. The resulting residue was dissolved in CH_2Cl_2, washed with brine and dried over $MgSO_4$. Following filtration and removal of the solvent under reduced pressure, the residue was purified by column chromatography (0-50% CH_2Cl_2/hexane) to give a colourless solid (0.73 g, 82%). m.p. 89-92 °C; ^{1}H NMR (500 MHz, $CDCl_3$); δ 8.63 (d, *J* = 2.0 Hz, 1H, H_A), 7.77 (dd, *J* = 8.3, 2.4 Hz, 1H, H_B), 7.34 (dd, J = 8.3, 0.5 Hz, 1H, H_C), 1.00 (s, 9H, H_E), 0.20 (s, 6H, H_D); ^{13}C NMR (125 MHz, $CDCl_3$); 151.2, 141.6, 138.9, 128.6, 120.4, 103.5, 95.1, 26.3, 16.8, -4.7; LRESI-MS: *m/z* = 296 $[MH]^+$; HRESI-MS: *m/z* = 296.046565 (calc. for $C_{13}H_{19}NSiBr$ 296.04647)

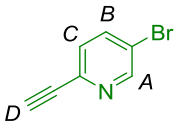

2-ethynyl-5-bromopyridine, **4**

To a solution of 2-*tert*-butyldimethylsilylethynyl-5-bromopyridine (0.15 g, 0.50 mmol) in CH_2Cl_2 (3 mL) was added TBAF (1M in THF, 0.5 mL, 0.50 mmol), which resulted in the colourless solution turning yellow. The solution was stirred at rt for 3 h and then the solvent was removed under reduced pressure. The residue was purified by column chromatography (0-50% CH_2Cl_2/hexane) to get the product as an off white solid (0.07 g, 78%). m.p. 80-83 °C; ^{1}H NMR (500 MHz, $CDCl_3$); δ 8.65 (d, *J* = 2.1 Hz, 1H, H_A), $_C$), 3.22 (s, 1H, H_D); ^{13}C NMR (125 MHz, $CDCl_3$); 151.3, 140.6, 138.9, 128.4, 120.8, 81.8, 78.5; LRESI-MS: *m/z* = 182 $[MH]^+$; HRESI-MS: *m/z* = 181.960374 (calc. for C_7H_5NBr 181.95999)

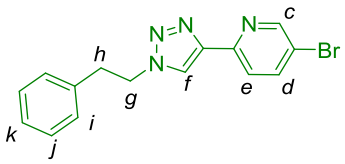

L^3

To a colourless solution of 2-ethynyl-5-bromopyridine (0.018 g, 0.10 mmol) and 2-phenylethylazide (0.025 g, 0.10 mmol) in TCE (10 mL) was added $Cu(CH_3CN)_4PF_6$ (0.042 g, 0.11 mmol). The resultant yellow solution was then stirred at rt for 1 h before being heated at 70 °C for 18 h. After cooling to rt, the mixture was filtered through celite and washed with TCE. The filtrate was concentrated under reduced pressure. The resulting residue was dissolved in CH_2Cl_2, washed with 0.1 M Sodium EDTA, dried over $MgSO_4$. The product was obtained as a colourless solid following purification by from column

chromatography (CH_2Cl_2) (0.018 g, 55%). ^{1}H NMR (500 MHz, $CDCl_3$); δ 8.60 (d, *J* = 2.2 Hz, 1H, H_c), 8.06 (d, *J* = 8.4 Hz, 1H, H_e), 7.92 (s, 1H, H_f), 7.89 (dd, *J* = 8.4, 2.2 Hz, 1H, H_d), 7.33-7.28 (m, 2H, H_j), 7.26-7.24 (m, 1H, H_k), 7.15 (d, *J* = 7.1 Hz, 2H, H_i), 4.65 (t, *J* = 7.4 Hz, 2H, H_g) 3.27 (t, *J* = 7.4 Hz, 2H, H_h); ^{13}C NMR (125 MHz, $CDCl_3$); δ 150.6, 148.8, 147.4, 139.7, 136.9, 129.1, 128.8, 127.4, 122.5, 121.5, 119.6, 52.0, 36.8; LR-FABMS (3-NOBA matrix) *m/z* = 329 $[MH]^+$; HR-FABMS (3-NOBA matrix) *m/z* = 329.03933 (calc. for $C_{15}H_{14}BrN_4$ 329.03964)]

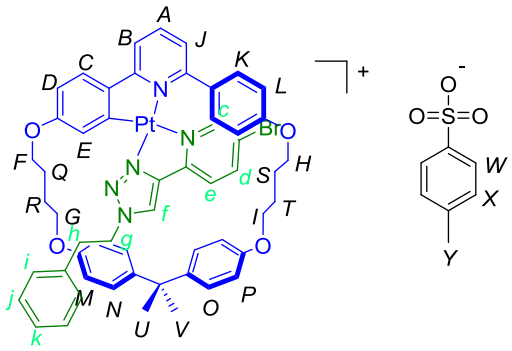

trans-[**L**²Pt(**L**³)]OTs

To a yellow solution of [**L**²Pt(DMSO)] (0.012 g, 0.013 mmol) in CH_2Cl_2 (5 mL) was added **L**³ (0.004 g, 0.013 mmol) and TsOH (0.002 g, 0.013 mmol), which resulted in a changing of the solution to greenish yellow. The solution was stirred at rt for 1 h and the excess solvent was removed under reduced pressure. The yellow solid was recrystallized in CH_2Cl_2 and Et_2O (0.005 g, 34 %). For the ^{1}H-^{1}H NOESY assisted assignment of *trans*-[**L**²Pt(**L**³)]OTs, see pages 11-12.^{1}H NMR (500 MHz, CD_2Cl_2); δ 9.94 (s, 1H, H_f), 8.29 (d, *J* = 8.4 Hz, 1H, H_e), 8.00 (t, *J* = 7. 8 Hz, 1H, H_A), 7.97 (d, *J* = 2.4 Hz, 1H, H_E), 7.95 (ddd, *J* = 8.4, 2.1, 0.9, 1H, H_d), 7.88 (d, *J* = 1.9 Hz, 1H, H_c), 7.71 (d, *J* = 7.9 Hz, 2H, H_W), 7.67 (d, *J* = 8.0 Hz, 1H, H_B), 7.57-7.52 (m, 2H, H_{J+C}), 7.30-7.25 (m, 2H, H_j), 7.24-7.16 (m, 3H, H_{k+i}), 7.14-7.07 (m, 4H, $H_{X+N/O}$), 7.04 (d, *J* = 8.2 Hz, 2H, $H_{O/N}$), 6.80 (dd, *J* = 8.5, 2.4, 1H, H_D), 6.75-6.69 (m, 4H, H_{M+P}), 4.61-4.53 (m, 1H, $H_{g'}$), 4.52-4.43 (m, 1H, $H_{g''}$), 4.42-4.34 (m, 1H, $H_{F'}$), 4.19-4.04 (m, 3H, $H_{F''+G}$), 4.04-3.89 (m, 4H, H_{H+I}), 3.28 (m, 2H, H_h), 2.31 (s, 3H, H_Y), 2.20-1.93 (m, 5H, $H_{Q+R+S'}$), 1.92-1.82 (m, 1H, $H_{S''}$), 1.82-1.70 (m, 2H, H_T), 1.60 (s, 3H, $H_{U/V}$), 1.57 (s, 3H, $H_{V/U}$); ^{13}C NMR (125 MHz, CD_2Cl_2); δ 168.0, 161.2, 159.8, 159.3, 157.4, 157.3, 150.0, 149.9, 146.1, 143.8, 143.5, 142.8, 140.0, 139.6, 139.2, 136.8, 130.4, 129.4, 129.3, 129.0, 128.6, 128.21, 128.19, 127.7, 126.4, 126.1, 123.7, 122.1, 120.6, 119.0, 116.8, 114.4, 114.3, 113.9, 68.3, 68.0, 67.95, 67.9, 53.7, 42.0, 36.2, 31.5, 30.3, 26.2, 26.0, 25.8, 25.5, 21.5; LR-FABMS

(3-NOBA matrix) *m/z* = 1122 $[MH]^+$; HR-FABMS (3-NOBA matrix) *m/z* = 1122.30287 (calc. for $C_{55}H_{54}BrN_5O_4{}^{195}Pt$ 1122.30014).

2.4.3 Ligand exchange experiment

General procedure for acyclic cyclometallated Pt complexes

To a solution of [**L**^{1}Pt(PyR$_2$R')] (4.0 µmol) in CD_2Cl_2 (0.30 mL) at 298 K was added dmbipy (4.0 µmol). The subsequent addition TsOH in 97:3 CD_2Cl_2:CD_3OD (5.2, 9.6 and 10.8 µmol of TsOH for the experiments with [**L**^{1}Pt(py)], [**L**^{1}Pt(3,5-lut)] and [**L**^{1}Pt(DMAP)], respectively), followed by agitation for 1 minute, caused the solution to lighten. A ^{1}H NMR spectrum was then recorded immediately, confirming quantitative conversion to [H**L**^{1}Pt(dmbipy)]OTs. P_1-^{t}Bu in CD_2Cl_2 (20 µmol) was added directly to the NMR tube and the solution agitated for one minute. ^{1}H NMR spectra were recorded at regular intervals until no further change was observed. The backward reaction of "2+2" to "3+1" complex was complete in 1.5 h for [**L**^{1}Pt(py)] and 2 h for [**L**^{1}Pt(3,5-lut)] and [**L**^{1}Pt(DMAP)].

Procedure for macrocyclic cyclometallated Pt complexes

To a solution of [**L**^{2}Pt(3,5-lut)] (1.7 mg, 1.9 µmol) in CD_2Cl_2 (0.30 mL) at 298 K was added **L**^{3} (0.62 mg, 1.9 µmol). The subsequent addition TsOH in 97:3 CD_2Cl_2:CD_3OD (3.2 µmol) followed by agitation for 1 minute, caused the solution to lighten. A ^{1}H NMR spectrum was then recorded immediately, confirming complete conversion to [H**L**^{2}Pt(**L**^{3})]OTs. P_1-^{t}Bu in CD_2Cl_2 (9.5 µmol) was added directly to the NMR tube and the solution agitated for one minute. ^{1}H NMR spectra were recorded at regular intervals until no further change was observed, indicating that at 298 K, the backward reaction of macrocyclic "2+2" to "3+1" complex was complete after 48 h.

2.4.4 Crystal data and structure refinement for [L^{2}Pt(3,5-Lut)]

Structural data was collected using *Rigaku AFC12* goniometer equipped with an enhanced sensitivity (HG) *Saturn724+* detector mounted at the window of an *FR-E+ SuperBright* molybdenum rotating anode generator with VHF *Varimax* optics (70µm focus). Cell determination and data collection employed *CrystalClear-SM Expert 2.0 r11* (Rigaku, 2011). The structures were solved using *SHELXL97* (Sheldrick, G.M. (2008). Acta Cryst. A64, 112-122).

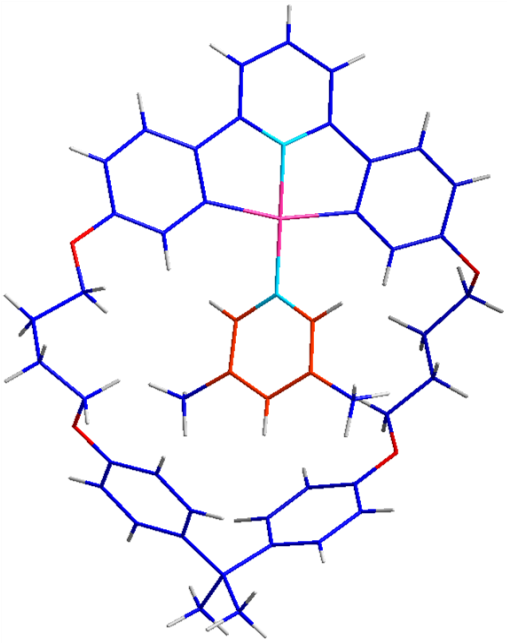

Figure 2.16 X-ray crystal structure of [**L**²Pt(3,5-Lut)]. The carbon atoms of a macrocycle are shown in blue, Lut in orange, platinum in pink, nitrogen in pale blue, and oxygen in red.

Table 2.1 Crystal data and structure refinement for [**L**²Pt(3,5-Lut)].

Identification code	[L2Pt(3,5-lut)]	
Empirical formula	C47 H48 N2 O4 Pt	
Formula weight	900.00	
Temperature	93(2) K	
Wavelength	0.71075 Å	
Crystal system	Triclinic	
Space group	P-1 (#2)	
Unit cell dimensions	a = 10.3265(10) Å	α = 110.841(6)°
	b = 13.6884(13) Å	β = 107.420(5)°
	c = 15.3966(12) Å	γ = 95.035(5)°
Volume	1894.1(3) Å^3	
Z	2	
Density (calculated)	1.578 g/cm^3	
Absorption coefficient	3.7379 mm^{-1}	
F(000)	908.00	
Crystal size	0.10 x 0.03 x 0.03 mm3	

Theta range for data collection	2.38 to 25.35°
Index ranges	-12<=h<=12, -16<=k<=16, -18<=l<=18
Reflections collected	18722
Independent reflections	6861 [R(int) = 0.0261]
Completeness to theta = 25.00°	98.5%
Absorption correction	Multiscan
Max. and min. transmission	0.894 and 0.760
Refinement method	Full-matrix least-squares on F^2
Data / restraints / parameters	6861/ 0 / 487
Goodness-of-fit on F^2	1.199
Final R indices [I>2sigma(I)]	R1 = 0.0234
R indices (all data)	wR2 = 0.0771
Largest diff. peak and hole	1.050 and -1.030 e. $Å^{-3}$

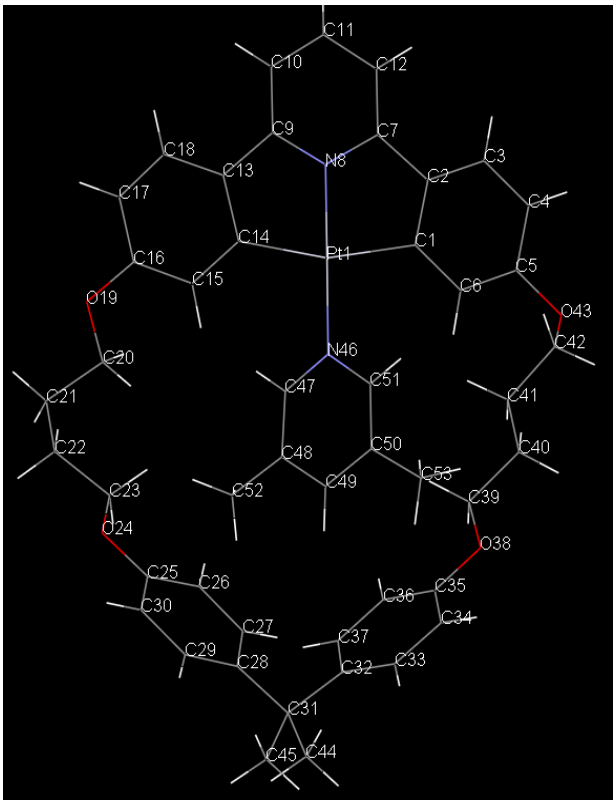

Table 2.2 Selected Bond lengths [Å], angles [°] and torsion angles [°] for [**L²**Pt(3,5-Lut)].

Pt(1)-N(8)	1.956(4)	C(23)-O(24)	1.434(5)
Pt(1)-C(14)	2.046(6)	O(24)-C(25)	1.383(6)
Pt(1)-C(1)	2.063(6)	C(25)-C(26)	1.398(8)
Pt(1)-N(46)	2.010(4)	C(26)-C(27)	1.390(7)
C(1)-C(2)	1.401(8)	C(27)-C(28)	1.389(6)
C(1)-C(6)	1.405(7)	C(28)-C(29)	1.398(8)
C(6)-C(5)	1.39(1)	C(29)-C(30)	1.393(7)
C(5)-C(4)	1.393(8)	C(30)-C(25)	1.373(6)
C(4)-C(3)	1.382(7)	C(28)-C(31)	1.538(7)
C(3)-C(2)	1.39(1)	C(31)-C(32)	1.55(1)
C(2)-C(7)	1.473(7)	C(31)-C(44)	1.544(9)
C(7)-C(12)	1.381(8)	C(31)-C(45)	1.536(6)
C(12)-C(11)	1.385(8)	C(32)-C(33)	1.380(8)
C(11)-C(10)	1.40(1)	C(32)-C(37)	1.389(9)
C(10)-C(9)	1.382(8)	C(37)-C(36)	1.39(1)
N(8)-C(9)	1.359(7)	C(36)-C(35)	1.386(8)
N(8)-C(7)	1.376(9)	C(35)-C(34)	1.387(9)
C(9)-C(13)	1.468(9)	C(34)-C(33)	1.40(1)
C(13)-C(14)	1.417(6)	C(35)-O(38)	1.377(8)
C(13)-C(18)	1.401(8)	O(38)-C(39)	1.438(8)
C(18)-C(17)	1.38(1)	C(39)-C(40)	1.511(9)
C(17)-C(16)	1.392(7)	C(40)-C(41)	1.525(9)
C(16)-C(15)	1.389(8)	C(41)-C(42)	1.514(9)
C(15)-C(14)	1.410(9)	O(43)-C(5)	1.391(6)
N(46)-C(47)	1.354(7)	O(43)-C(42)	1.450(6)
N(46)-C(51)	1.348(7)	C(28)-C(52)	4.105(8)
C(51)-C(50)	1.366(8)	C(52)-C(25)	3.783(9)
C(50)-C(49)	1.404(8)	C(53)-C(32)	4.755(7)
C(49)-C(48)	1.392(8)	C(35)-C(53)	3.600(6)
C(48)-C(47)	1.379(8)	C(48)-C(27)	4.507(9)
H(53B)-C(53)	0.980(5)	C(48)-C(26)	4.39(1)
C(52)-C(48)	1.506(8)	C(48)-C(30)	4.546(9)
C(16)-O(19)	1.378(8)	C(48)-C(29)	4.668(9)
C(21)-C(22)	1.524(9)	C(53)-C(37)	4.893(6)
C(22)-C(23)	1.520(7)	C(36)-C(53)	4.392(6)

C(33)-C(53)	4.054(7)	C(15)-C(16)-O(19)	123.7(5)
C(34)-C(53)	3.402(6)	C(20)-C(21)-C(22)	112.7(5)
C(20)-C(21)	1.499(9)	C(22)-C(23)-O(24)	108.8(5)
C(20)-O(19)	1.437(7)	C(23)-O(24)C(25)	117.7(4)
		O(24)-C(25)C(26)	123.7(5)
N(46)-Pt(1)-C(14)	99.0(2)	O(24)-C(25)C(30)	116.9(5)
N(46)-Pt(1)-C(1)	98.5(2)	C(29)-C(28)-C(31)	123.2(5)
Pt(1)-C(14)-C(13)	111.9(4)	C(37)-C(32)-C(31)	119.8(5)
C(14)-C(13)-C(9)	115.4(5)		
C(9)-N(8)-C(7)	123.1(5)	C(14)-Pt(1)-N(46)-C(47)	-51.7(4)
C(9)-N(8)-Pt(1)	118.9(4)	C(12)-C(7)-C(2)-C(3)	-1(1)
C(7)-N(8)-Pt(1)	118.0(4)	C(10)-C(9)-C(13)-C(18)	-1.0(9)
C(7)-C(2)-C(1)	116.1(5)	C(6)-C(1)-Pt(1)-N(46)	-3.6(6)
C(6)-C(5)-O(43)	120.2(5)	C(15)-C(16)-O(19)-C(20)	-24.7(8)
C(5)-O(43)-C(42)	114.9(4)	C(16)-O(19)-C(20)-H(21B)	147.6(4)
O(43)-C(42)-C(41)	113.8(5)	C(20)-C(21)-C(22)-O(24)	82.3(5)
C(42)-C(41)-C(40)	113.7(5)	Pt(1)-N(46)-C(51)-C(1)	33.1(2)
C(40)-C(39)-O(38)	108.4(5)	C(33)-C(32)-C(31)-C(28)	-105.1(6)
C(39)-O(38)-C(35)	117.6(4)	C(31)-C(28)-C(27)-C(37)	-61.2(4)
C(52)-C(48)-C(47)	120.4(5)	C(26)-C(25)-O(24)-C(23)	-1.6(8)
C(47)-N(46)-C(51)	117.4(5)	C(34)-C(35)-O(38)-C(39)	164.6(5)
C(51)-C(50)-H(39B)	93.3(3)	O(38)-C(39)-C(40)-C(41)	177.1(5)
C(16)-O(19)-C(20)	117.5(4)	C(6)-C(5)C(42)-C(41)	1.0(6)

2.5 References

1. E. R. Kay, D. A. Leigh and F. Zerbetto, *Angew. Chem. Int. Ed.*, **2007**, *46*, 72-191.
2. (a) N. Armaroli, V. Balzani, J.-P. Collin, P. Gaviña, J.-P. Sauvage and B. Ventura, *J. Am. Chem. Soc.*, **1999**, *121*, 4397-4408; (b) D. J. Cárdenas, A. Livoreil and J.-P. Sauvage, *J. Am. Chem. Soc.*, **1996**, *118*, 11980-11981; (c) J.-P. Collin, F. Durola, J. Lux and J.-P. Sauvage, *Angew. Chem. Int. Ed.*, **2009**, *48*, 8532-8535; (d) J. D. Crowley, D. A. Leigh, P. J. Lusby, R. T. McBurney, L.-E. Perret-Aebi, C. Petzold, A. M. Z. Slawin and M. D. Symes, *J. Am. Chem. Soc.*, **2007**, *129*, 15085-15090; (e) D. A. Leigh, P. J. Lusby, R. T. McBurney and M. D. Symes, *Chem. Commun.*, **2010**, *46*, 2382-2384; (f) A. Livoreil, C. O. Dietrich-Buchecker and J.-P. Sauvage, *J. Am. Chem. Soc.*, **1994**, *116*, 9399-9400; (g) A. Livoreil, J.-P. Sauvage, N. Armaroli, V. Balzani, L. Flamigni and B. Ventura, *J. Am. Chem. Soc.*, **1997**, *119*, 12114-12124; (h) M. J. Barrell, D. A. Leigh, P. J. Lusby and A. M. Z. Slawin, *Angew. Chem. Int. Ed.*, **2008**, *47*, 8036-8039.
3. (a) A. Carlone, S. M. Goldup, N. Lebrasseur, D. A. Leigh and A. Wilson, *J. Am. Chem. Soc.*, **2012**, *134*, 8321-8323; (b) M. N. Chatterjee, E. R. Kay and D. A. Leigh, *J. Am. Chem. Soc.*, **2006**, *128*, 4058-4073; (c) V. Serreli, C.-F. Lee, E. R. Kay and D. A. Leigh, *Nature*, **2007**, *445*, 523-527.
4. P. J. Lusby, P. Müller, S. J. Pike and A. M. Z. Slawin, *J. Am. Chem. Soc.*, **2009**, *131*, 16398-16400.
5. S. J. Pike and P. J. Lusby, *Chem. Commun.*, **2010**, *46*, 8338-8340.
6. D. Sooksawat, S. J. Pike, A. M. Z. Slawin and P. J. Lusby, *Chem. Commun.*, **2013**, *49*, 11077-11079.
7. C. Deuschel-Cornioley, H. Stoeckli-Evans and A. von Zelewsky, *J. Chem. Soc., Chem. Commun.*, **1990**, 121-122.
8. A. D. McNaught and A. Wilkinson, *IUPAC. Compendium of Chemical Terminology*, 2nd edn., Blackwell Scientific Publications, Oxford, 1997.
9. S. J. Pike, *Dynamic Platinum(II)-Based Metallosupramolecular Architectures*, The University of Edinburgh, 2011.
10. J. Clayden, N. Greeves, S. Warren and P. Wothers, *Organic Chemistry*, Oxford University Press, Oxford, 2006.
11. V. Aucagne, J. Berná, J. D. Crowley, S. M. Goldup, K. D. Hänni, D. A. Leigh, P. J. Lusby, V. E. Ronaldson, A. M. Z. Slawin, A. Viterisi and D. B. Walker, *J. Am. Chem. Soc.*, **2007**, *129*, 11950-11963.
12. F. Durola, J.-P. Sauvage and O. S. Wenger, *Helv. Chim. Acta*, **2007**, *90*, 1439-1446.
13. G. W. V. Cave, F. P. Fanizzi, R. J. Deeth, W. Errington and J. P. Rourke, *Organometallics*, **2000**, *19*, 1355-1364.
14. G. Colombano, C. Travelli, U. Galli, A. Caldarelli, M. G. Chini, P. L. Canonico, G. Sorba, G. Bifulco, G. C. Tron and A. A. Genazzani, *J. Med. Chem.*, **2009**, *53*, 616-623.
15. O. Chepelin, J. Ujma, P. E. Barran and P. J. Lusby, *Angew. Chem. Int. Ed.*, **2012**, *51*, 4194-4197.
16. J. D. Crowley, I. M. Steele and B. Bosnich, *Inorg. Chem.*, **2005**, *44*, 2989-2991.

Chapter III

Towards a stimuli-responsive platinum complexed [2]rotaxane

Acknowledgements

Dr. Paul Lusby, Dr. Paul Symmers and Michael Burke are gratefully thanked for their proofreading of this chapter.

Synopsis

Having established the occurrence of acid-base activated switching between "3+1" and "2+2" square planar platinum coordination modes in model cyclometalated C^N^C complexes in the previous chapter, the task now became to extend this chemistry for use in a molecular machine system.

The synthesis towards a rotaxane using an active metal template, CuAAC "click" strategy initially showed promised as [2]rotaxane ***R*** ^{2b} *was obtained. However, as the incorporation of the platinum(II) centre into the macrocycle of* ***R*** ^{2b} *to generate [****R*** ^{2b}*Pt]Cl was unsuccessful, a redesign was necessary. A series of 3,5-pyridine functionalized axle molecules (unsaturated/saturated hydrocarbon chain adjacent to pyridine) were developed and submitted to exchange with DMSO in a platinum-complexed macrocycle under various conditions in a threading-followed-by-stoppering methodology. Upon the attachment of stopper units to a pseudorotaxane, the rotaxane product was synthesised but failed to purify from the reaction mixture. The preformed clicked pyridine thread was synthesised and underwent a ligand exchange reaction. Even though the* ^{1}*H NMR spectrum and mass spectrum were encouraging, the appropriate separation conditions remained elusive. The attempt to exchange an unsymmetrical half-thread was undertaken but encountered the same purification problem as with other designs.*

3.1 Introduction

Rotaxanes can be synthesised using various strategies and several effective ways to make complexes have been developed utilising metal template effects. At first, metal ions were used for their coordination chemistry to gather and organize ligands in the proper positions and orientations to encourage the formation of an interlocked assembly. Metal ions with tetrahedral, trigonal bipyramidal or octahedral coordination geometries have all been used for such architectures (as detailed in Chapter I, section 1.2.2).

As the synthesis of rotaxanes has been well-established, useful properties or functions of the interlocked systems are the next goal for further development. After the successful redox-responsive Cu^{I}/Cu^{II} catenane[1] and rotaxane[2] systems first described by Sauvage and co-workers nearly twenty years ago, only the switchable palladium-complexed molecular shuttles developed by Leigh and co-workers[3] stand as examples of stimuli-responsive molecular shuttles based on the manipulation of metal-ligand interactions between components. The acid-base induced changes to cyclometallated platinum complexes described in Chapter II could be used to develop a stimuli-responsive bistable [2]rotaxane as an example of molecular machine.

3.2 Results and Discussion

3.2.1 Basis of the Design

In Chapter II, the "3+1" to "2+2" interconversion of non-interlocked platinum C^N^C macrocyclic compounds was discussed. The results suggested that a platinum-complexed [2]rotaxane featuring a C^N^C macrocycle, 3,5-disubstituted monodentate pyridine† and bidentate pyridyl triazole stations in the thread would act as an acid-base responsive molecular shuttle (Scheme 3.1). Under neutral conditions, the cyclometallated platinum macrocycle would coordinate to the monodentate pyridine site (*py*-**R**^{1}Pt).‡ Upon addition of TsOH, the intermediate "2+1+1" where the Pt-macrocycle coordinated with Py and OTs would be generated, before an excess amount of acid would protonate py to induce a change in the coordination mode at the metal centre, generating the 2+2 rotaxane ([*2-tripy*-**R**^{1}Pt]OTs). When P_1-^{t}Bu is added, recurrence of the 3+1 rotaxane would be expected (Scheme 3.1).

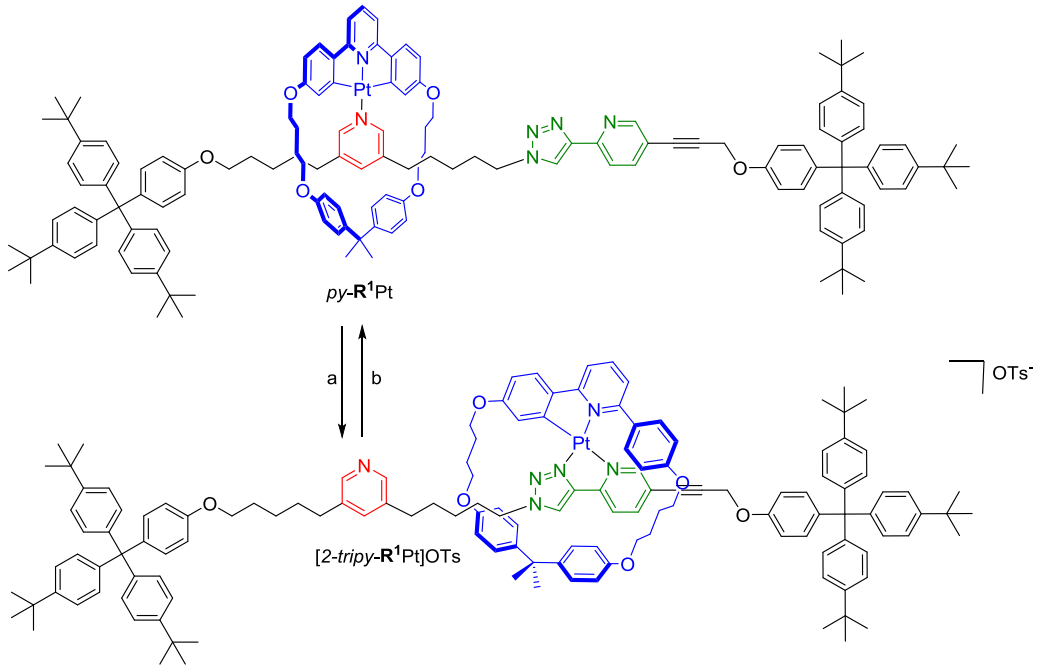

Scheme 3.1 Acid-base interconversion between "3+1" and "2+2" platinum complexed-[2]rotaxanes. Conditions: a) TsOH; b) P_1-^{t}Bu.

†Pt(II) complex of 3,5-disubstituted pyridines are thermodynamically preferred to 2,6-disubstituted analogues.[4]

‡ The italicized prefixes *py*- and *2-tripy*- denote that the Pt-complexed macrocycle is coordinated to the ligand.

3.2.2 Prototype one-station-[2]rotaxane

It has been reported that an active-metal template strategy using copper(I)-catalysed azide-alkyne cycloaddition (CuAAC) "click" reaction is a highly effective procedure for rotaxane synthesis.[5] A [2]rotaxane with a bidentate station generated by the click reaction has not been studied. A prototype [2]rotaxane with one station ([**R**^{2a}Pt]X) was designed to assess the potential for rotaxane formation by CuAAC reaction (Scheme 3.2). A very similar pyridine macrocycle without a bisphenol A unit has been successfully carried out by click reaction to produce a rotaxane.[5b] Pyridyl-azide half-thread **4** was proposed to click with alkyne **2** and macrocycle H_2**L**^{2} to afford the first clicked bidentate rotaxane. Insertion of the platinum(II) centre into the macrocycle after the click reaction would be carried out to furnish the desired rotaxane. There were only few reports on the dual use of a triazole unit as a component to complete the mechanically interlocked structure and also a fundamental element of the system (*i.e.* a station).[5b, 6]

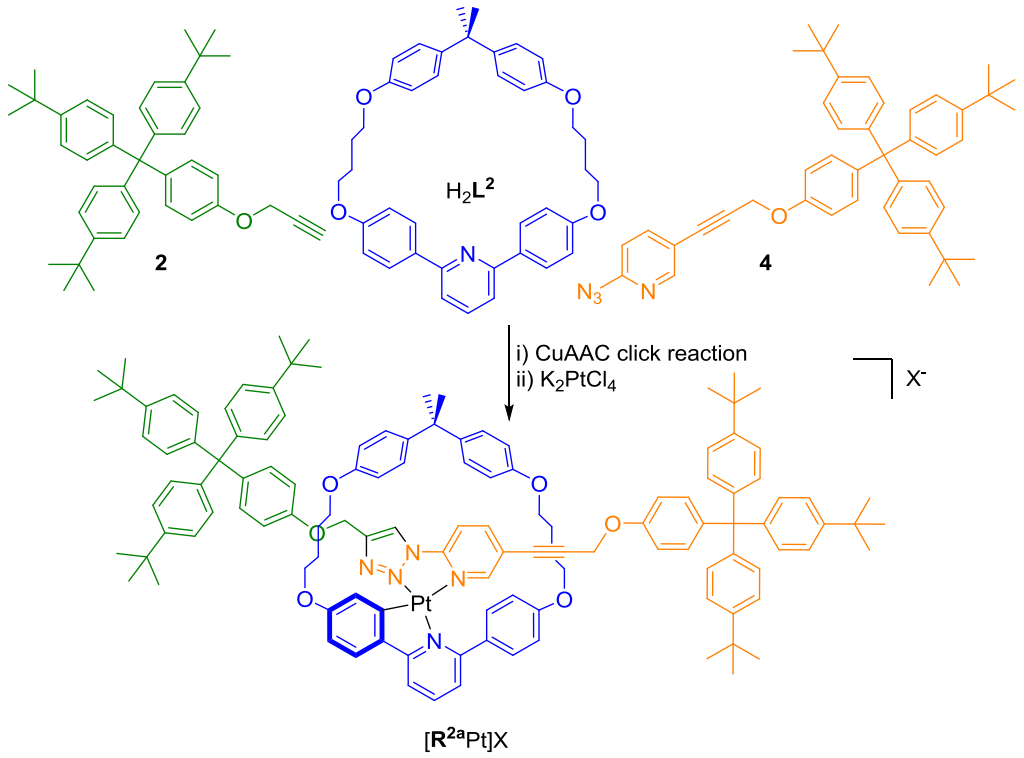

Scheme 3.2 Prototype 1-station-[2]rotaxane, [**R**^{2a}Pt]X.

3.2.2.1 Retrosynthesis of rotaxane [**R**^{2a}Pt]X

The components required for the formation of active-metal template CuAAC click rotaxane include a macrocycle, terminal alkyne and azide unit. Alkyne **2**, 1-(prop-3-ynoxy)-4-(tris-(4-*tert*-butyl-phennyl)-methyl)-benzene, is a known compound that was synthesised as described in the literature.[5a] The synthesis of macrocycle H_2**L**^{2} has been described in previous chapter. Azidopyridine compound **4** could be obtained from Sonogashira coupling of pyridine with alkyne 2 followed by introduction of the azido group. Once the rotaxane is produced, it was anticipated that complexation with platinum(II) would be carried out using a modification of Rouke's procedure.[7]

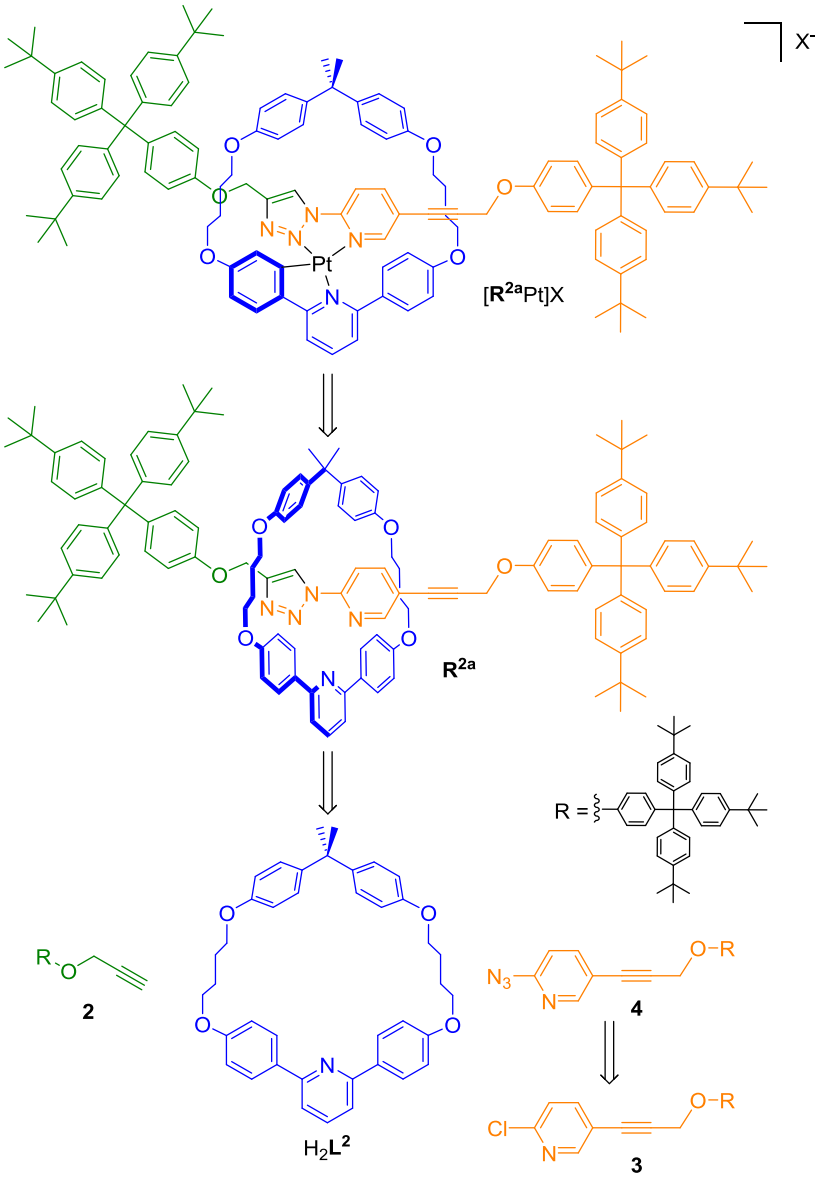

Scheme 3.3 Retrosynthesis of prototype 1-station-[2]rotaxane [**R**^{2a}Pt]X.

3.2.2.2 Synthesis of rotaxane [$\mathbf{R^{2a}}$Pt]X

The first route towards the half-thread precursor **3** was developed by Dr. Sarah Pike starting from the commercially available 2-chloro-5-iodopyridine (Scheme 3.4a-c). Pyridine was treated first with propargyl alcohol under standard Sonogashira conditions before the alcohol moiety was then converted into the alkynylbromide using the Appel reaction followed by Williamson-ether reaction with stopper **1** to afford compound **3**.

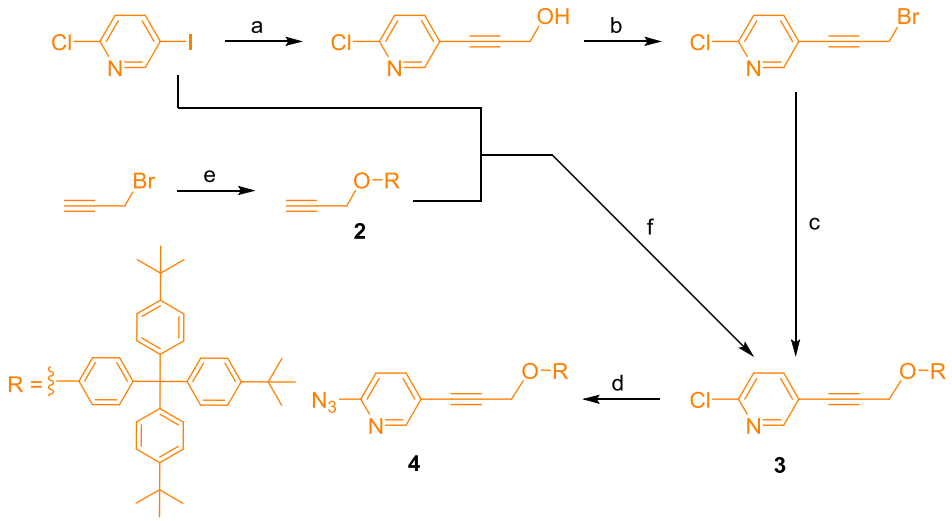

Scheme 3.4 Synthetic route of 2-azidopyridine half-thread **4**. Reagents and conditions: a) propargyl alcohol, $Pd(PPh_3)_4$, CuI, Et_3N, 25 °C, absence of light, 20 h, 91%; b) CBr_4, CH_2Cl_2, PPh_3, 25 °C, 18 h, 23%; c) stopper **1**, K_2CO_3, butanone, reflux, 36 h, 79%; d) NaN_3, DMF, 120 °C, 18 h, 34%; e) stopper **1,** K_2CO_3, butanone, reflux, 92%; f) $Pd(PPh_3)_2Cl_2$, PPh_3, CuI, DEA, THF, rt, 86%.

Another shorter, parallel synthetic pathway was studied to improve the overall yield (Scheme 3.4e-f). A Sonogashira coupling of 2-chloro-5-iodopyridine with preformed alkynyl stopper **2**, from Williamson ether synthesis of propargyl bromide and stopper **1**, under standard conditions gave **3** in 86% yield. Interconversion of the chloride group of **3** for an azide moiety was accomplished in 34% yield.

CuAAC reaction was carried out to construct a rotaxane $\mathbf{R^{2a}}$ using a modified literature procedure.[5b] A solution of macrocycle $H_2\mathbf{L^2}$, azide **4**, alkyne **2** (each one eq), and $[Cu(CH_3CN)_4]PF_6$ (1.1 eq) in dry CH_2Cl_2 was stirred at rt for 24 h then the mixture was demetallated with KCN. The ^{1}H NMR spectrum of the crude product showed no reaction occurred, only peaks corresponding to the starting material were present. Conventional heating to reflux in $ClCH_2CH_2Cl$ (DCE) for 43 h still gave no evidence of product. Further attempts were made to elucidate the conditions needed to produce a non-interlocked

thread. Both conventional heating for 5 d and microwave-assisted synthesis[8] in various conditions failed to yield the desired product however.

It has been reported that 2-azidopyridine exist in an equilibrium between closed form (tetrazole) and open form (azide) in solution (Scheme 3.5).[9] In the solid state, only the tetrazole form was previously obtained.[10] The presence of the tetrazole form of 2-azidopyridine may explain the harsh conditions and reactive Cu^{I} catalyst generally required for formation of the pyridyl-triazole product.[11] Those conditions used might not suitable for the product formation.

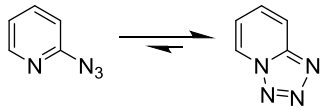

Scheme 3.5 Predominant tetrazolic form of 2-azidopyridine.

There was a report on the click reaction of 2-ethynylpyridine and 2-azidopyridine and their corresponding azide and alkyne reactants.[11b] The ethynylpyridine gave very good yield of triazole product in mild conditions[11c] whereas the azidopyridine needed to be refluxed for five days. These results suggested a potential change in the design of a prototype rotaxane. Therefore, ethynylpyridine half-thread **10** and azidopropyl half-thread **12** became the preferred reactants to alleviate some of the synthetic problem.

3.2.2.3 Retrosynthesis of rotaxane [$\mathbf{R^{2b}}$Pt]X

Similar to the first design of rotaxane [$\mathbf{R^{2a}}$Pt]X, the reactants for CuAAC reaction consist of alkyne, azide and macrocycle as shown in Scheme 3.6. It was envisaged that the ethynylpyridine half-thread **10** could be prepared from a Sonogashira coupling reaction of precursor **3** with commercial silyl-protected acetylene followed by deprotection. Synthesis of azido propyl half-thread **12** could be derived from 1,3-dibromopropane using two Williamson reactions.

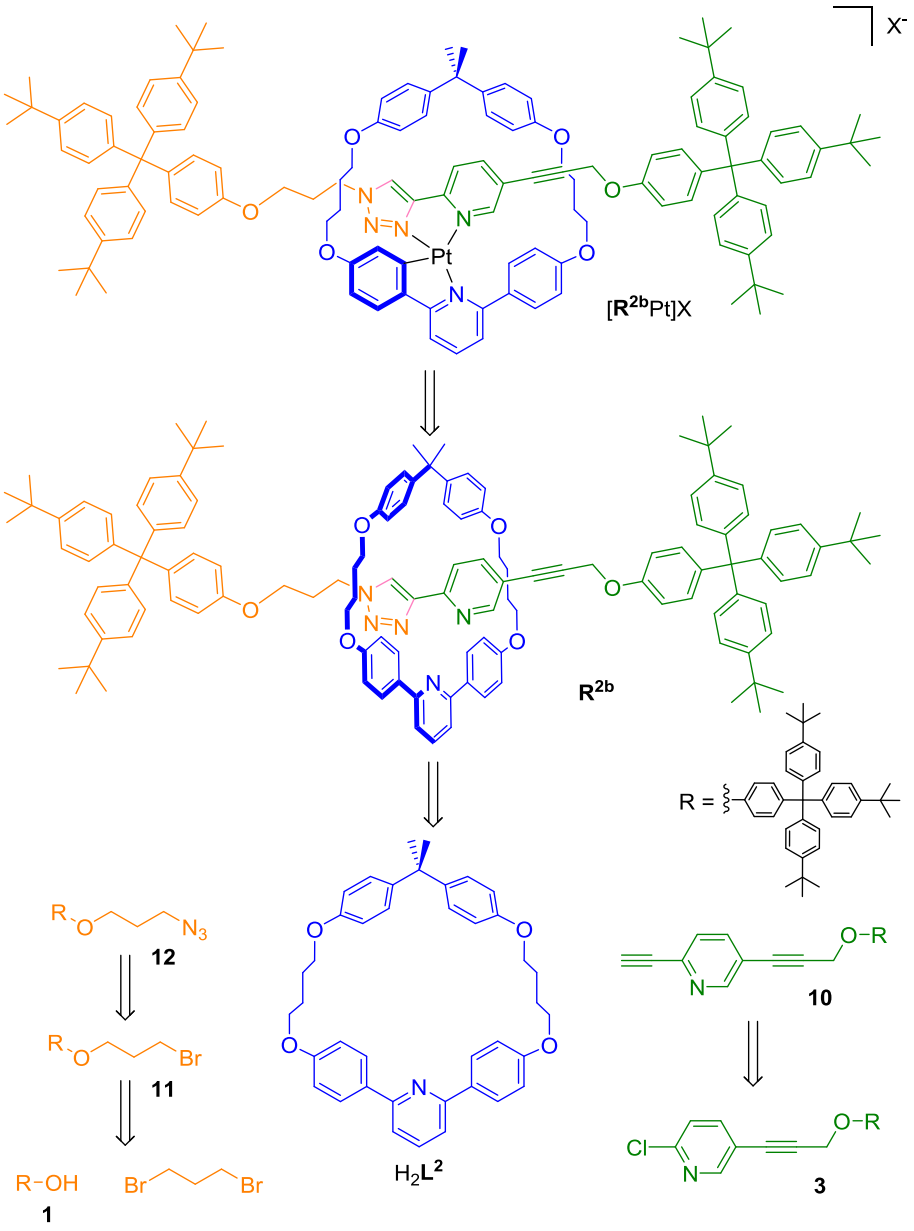

Scheme 3.6 Retrosynthesis of prototype 1-station-[2]rotaxane [**R**^{2b}Pt]X.

3.2.2.4 Synthesis of rotaxane [**R**^{2b}Pt]Cl

Pyridine **3** was coupled with trimethylsilylacetylene under Sonogashira reaction conditions (Scheme 3.7), either by conventional heating or microwave irradiation. Chromatographic purification of the crude product failed to yield the desired product giving uncharacterizable compounds.

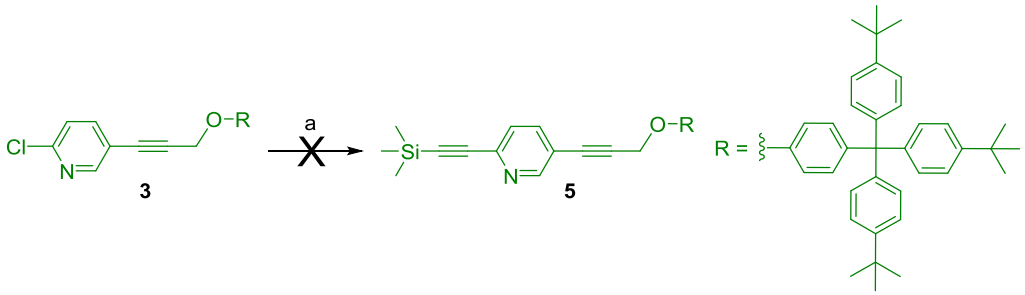

Scheme 3.7 Synthesis of ethynylpyridine half-thread **5**. Reagents and conditions: a) TMSacetylene, $Pd(PPh_3)_2Cl_2$, PPh_3, CuI, DEA, THF (conventional heating)/DMF (microwave).

A revised synthetic pathway was undertaken starting from 5-bromo-2-iodopyridine (Scheme 3.8). A Sonogashira coupling with trimethylsilylacetylene was carried out to afford **6** in 45% yield. A second Sonogashira reaction of the *meta*-bromo position was also undertaken. However following reaction at 70 °C for 3 days, no desired product could be obtained even though TLC showed consumption of starting materials. This unsuccessful reaction was attributed to a low stability of the TMS-acetylene group, which could be cleaved under the reaction conditions resulting in decomposition of the reactants or possibly oligomerization. Changing the silyl protecting group to a TBDMS unit was considered as it has been reported to be *ca*. 10^4 times more stable than TMS.[12] This new substrate **8** was produced in a good yield as described in Chapter II.

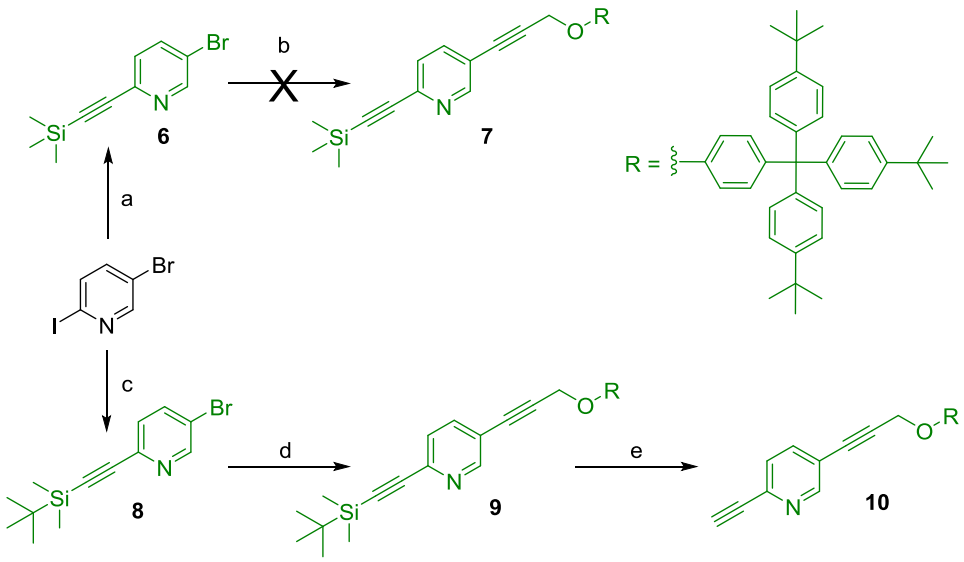

Scheme 3.8 Synthesis of ethynylpyridine half-thread **10**. Reagents and conditions: a) TMSacetylene, $Pd(PPh_3)_2Cl_2$, PPh_3, CuI, Et_3N, THF, rt, 20 h, 45%; b) alkyne **2**, $Pd(PPh_3)Cl_2$, PPh_3, CuI, Et_3N, THF rt-70 °C; c) TBDMS acetylene, CuI, $Pd(PPh_3)_2Cl_2$, Et_3N, THF, 0 °C–rt, 82%; d) alkyne **2**, $Pd(PPh_3)_4$, CuI, Et_3N, THF, 60 °C, 87%; e) TBAF, THF, rt, 18 h, 35%.

A new synthesis of ethynylpyridine half-thread **10** was developed (Scheme 3.8c-e) starting from previously prepared 2-*tert*-butyldimethylsilylethynyl-5-bromopyridine **8** and subjecting it to a Sonogashira coupling conditions with alkyne **2**. This reaction afforded **9** in good yield (87%). The alkyne **9** was then deprotected with tetrabutylammonium fluoride (TBAF) to give terminal alkyne **10.**

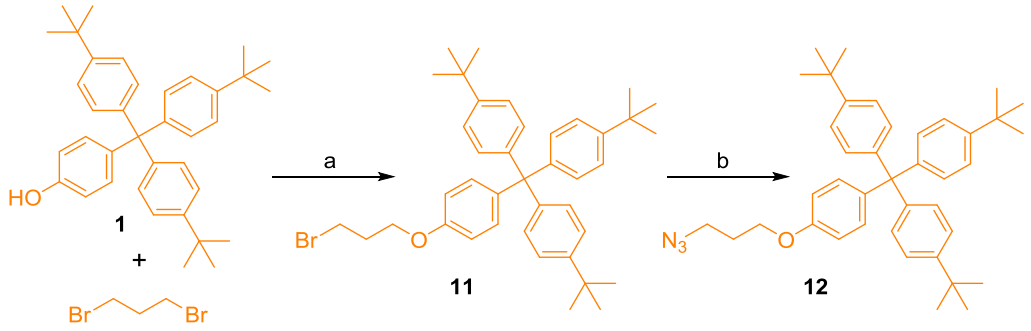

Scheme 3.9 Synthesis of alkyl azide half-thread **12**. Reagents and conditions: a) K_2CO_3, NaI, butanone, reflux, 18 h, 92%; b)NaN_3, DMF, 100 °C, 18 h, 84%.

Azide functionalised stopper **12** was derived from a Williamson-ether reaction starting from 1,3-dibromopropane following by azidation reaction with a high 84% final yield (Scheme 3.9).

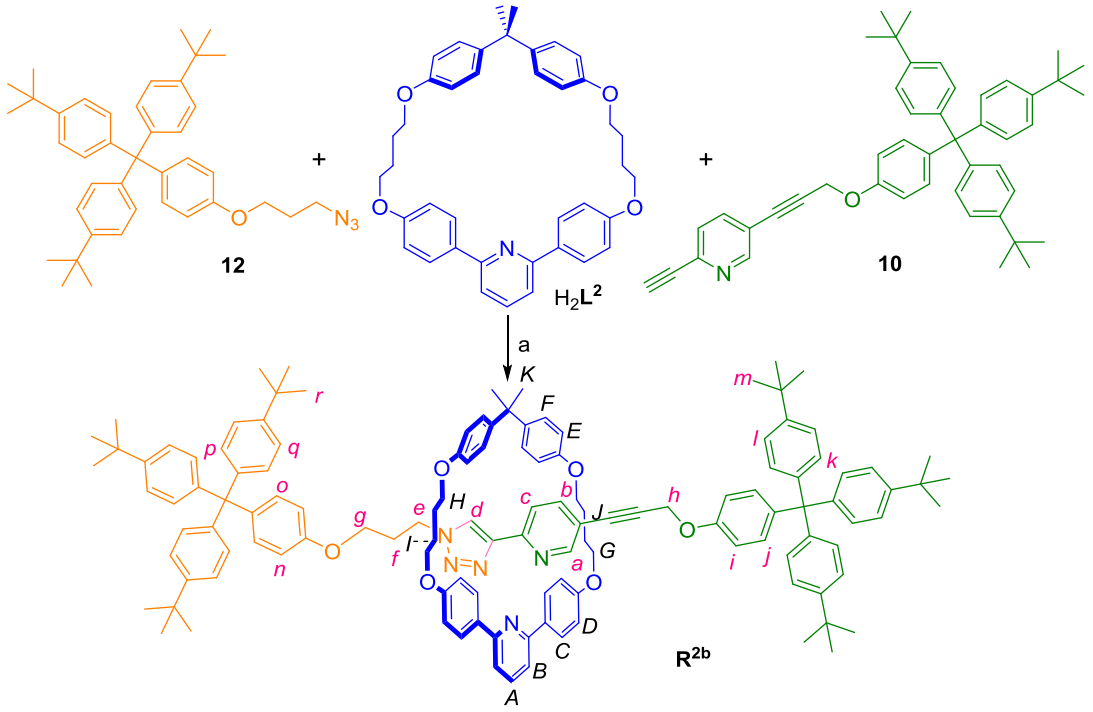

Scheme 3.10 Synthesis of rotaxane $\mathbf{R^{2b}}$. Reagents and conditions: a) i)$Cu(CH_3CN)_4PF_6$, DCE, 70 °C; II) 0.1 M Na_4EDTA, 16%.

Synthesis of rotaxane **R^{2b}** was adapted from a procedure by Leigh *et al* (Scheme 3.10).[5b] Azide **12** (1 eq), alkyne **10** (1 eq), macrocycle H_2**L^2** (1 eq) and $[Cu(CH_3CN)_4]PF_6$ (1.1 eq) were added to a flask under N_2 atmosphere. 1,2-Dichloroethane (DCE) was injected as a solvent. The mixture was purged with N_2 and left stirring at rt for 24 h then the reaction flask was heated at 70 °C for 3 d. The rotaxane formed was demetallated using 0.1 M Sodium EDTA. The product was obtained as a white solid following purification from column chromatography. Along with rotaxane **R^{2b}**, noninterlocked thread **13** was generated during click reactions as well as unreacted macrocycle.

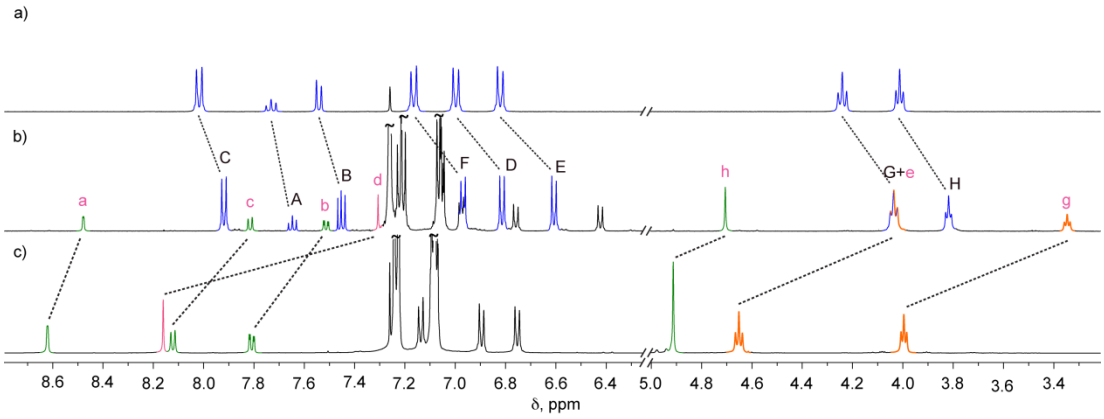

Figure 3.1 Partial ^{1}H NMR spectra (500 MHz, $CDCl_3$, 298 K) of a) macrocycle H_2**L^2**; b) rotaxane **R^{2b}**; c) noninterlocked thread **13**. The assignments correspond to the lettering shown in Scheme 3.10.

The ^{1}H NMR spectrum of rotaxane **R^{2b}** shows the upfield shifts of several signals with respect to the signals of the noninterlocked components (thread, Figure 3.1c and macrocycle, Figure 3.1a). Such shielding is typical of interlocked structures in which the aromatic rings of the macrocycle are positioned face on with the thread. The shielding is observed for resonances of the axle from one edge of the stopper to the other indicating that the macrocycle can access the full length of the thread. This is as expected as there should be no strong interaction between the thread and the macrocycle in the metal-free rotaxane.

Complexation of platinum(II) with the C^N^C unit and the pyridyl triazole moiety was carried out using a modified Rourke's procedure (Scheme 3.11).[7] Rotaxane **R^{2b}**, $K_2[PtCl_4]$ and TBACl were added to a flask under nitrogen flow, glacial acetic acid was then added and the mixture was purged with N_2 for 15 min. The reaction mixture was heated to reflux at 125 °C for 50 h. However, the ^{1}H NMR of the crude compound showed decomposition of the rotaxane (Figure 3.2). There was no signal corresponding to a

pyridyl triazole of the thread (signal *a*-*d*) nor the multiplet due to sterically congested nature of the complex around alkyl chains of the macrocycle (signal *G*, *H*) as seen in [H**L**²Pt(**L**³)]OTs (Chapter II). Therefore, a new strategy for constructing a platinum-complexed rotaxane was sought.

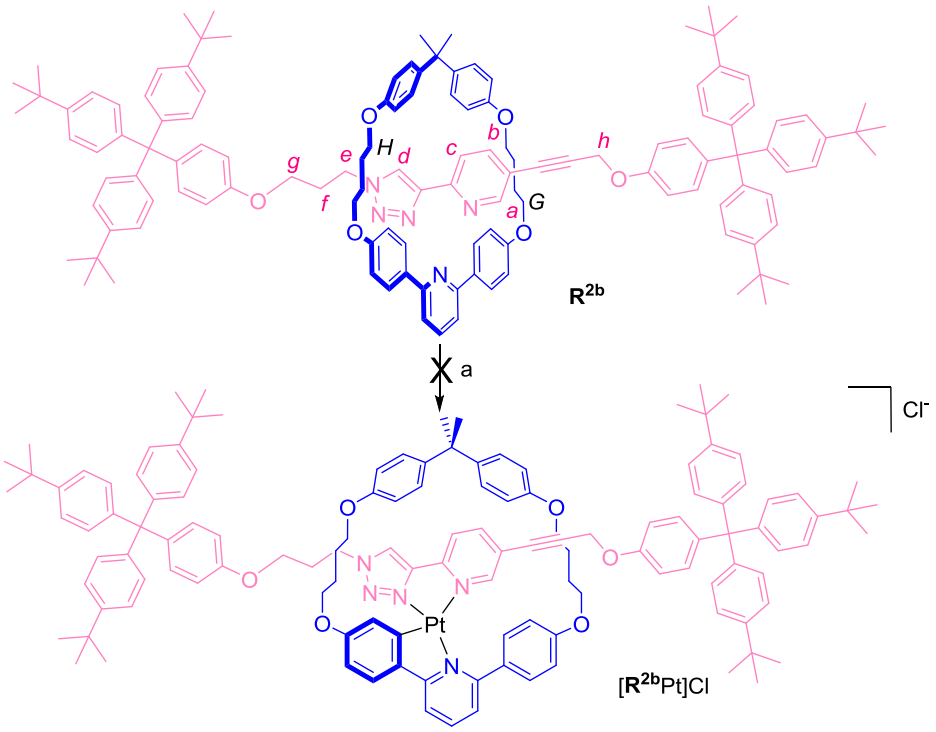

Scheme 3.11 Complexation of platinum(II) with rotaxane **R²ᵇ**. Reagents and conditions: a) $K_2[PtCl_4]$, TBACl, CH_3COOH, 125 °C, 50h.

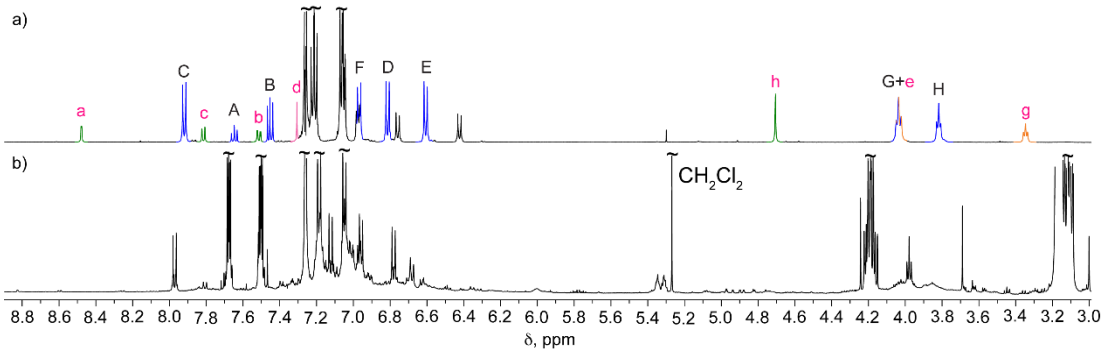

Figure 3.2 Partial ^1H NMR spectra (500 MHz, $CDCl_3$, 298 K) of a) rotaxane **R²ᵇ**; b) crude product of the complexation of platinum(II) with rotaxane **R²ᵇ**. The assignments correspond to the lettering shown in Scheme 3.10.

This result indicated that introducing platinum(II) to a final complicated rotaxane structure might not be straightforward as would be expected for a non-rotaxane. Usually,

metallation of 2,6-diphenylpyridine and similar derivatives by potassium tetrachloroplatinate in acetic acid gives monocyclometallated chloride-bridged dimers[7, 13] which can be further reacted to form dicycloplatinated C^N^C complexes *via* an electrophilic attack by platinum on the adjacent aromatic ring.[7] In the case of rotaxane **R^{2b}** however, a first cyclometallation might not occur due to steric crowding of the rotaxane structure or the conditions for the second cyclometallation by pyridyl triazole were not appropriate, given unsuccessful formation of [**R^{2b}**Pt]Cl. Other side reactions such as a C-coordination of a triazole ring due to rotation of the pyridyl triazole bond, a complexation of platinum to the acetylene moiety or a cleavage of a stopper unit adjacent to the alkyne could also result in a failure of a product formation.

3.2.3 Rotaxane synthesis *via* threading-followed-by-stoppering strategy

An alternative approach was proposed that involved a threading-followed-by-stoppering strategy. In this strategy, the platinum-complexed macrocycle would undergo a ligand exchange reaction with a functionalised pyridine to generate a threaded pseudorotaxane before being capped with stopper molecules to interlock the macrocycle and furnish a [2]rotaxane. It was envisaged that a 3,5-functionalised pyridine would replace DMSO in [**L^2**Pt(DMSO)] and thread through a macrocycle as the two methyl groups (C52, C53) of 3,5-lutidine in [**L^2**Pt(3,5-lut)] point nearly perpendicular to the C^N^C plane according to the crystal structure (Figure 3.3).

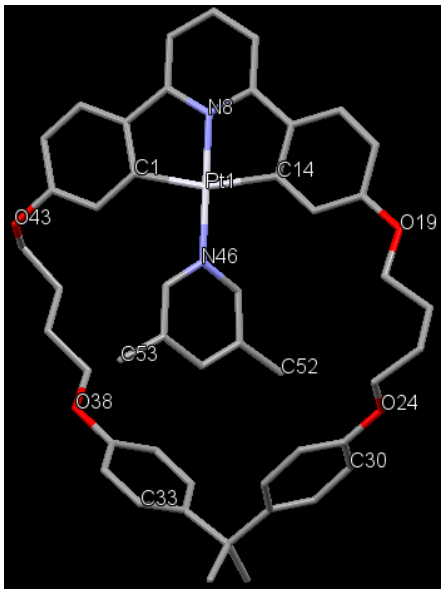

Figure 3.3 X-ray crystal structure of [**L^2**Pt(3,5-lut)]. Colour code: C, grey; N, blue; O, red; Pt, white. Solvent molecules and hydrogen atoms have been removed for clarity.

3.2.3.1 Design of platinum-complexed [2]rotaxane

An alternative design for a suitable [2]rotaxane is shown in Figure 3.4. This consists of a three-station thread, two of which are the same pyridyl tirazole bidentate ligand site and the other is a 3,5-pyridine monodentate station and a C^N^C Pt macrocycle that can bind to those stations. The CuAAC or click reaction of 2-ethynyl pyridine and terminal azide has proved to be successful to generate rotaxane **R^{2b}**. Therefore, a double "click" capping of two azide ends of the threaded pseudo-rotaxane complex with ethynyl pyridine stoppered was envisaged.

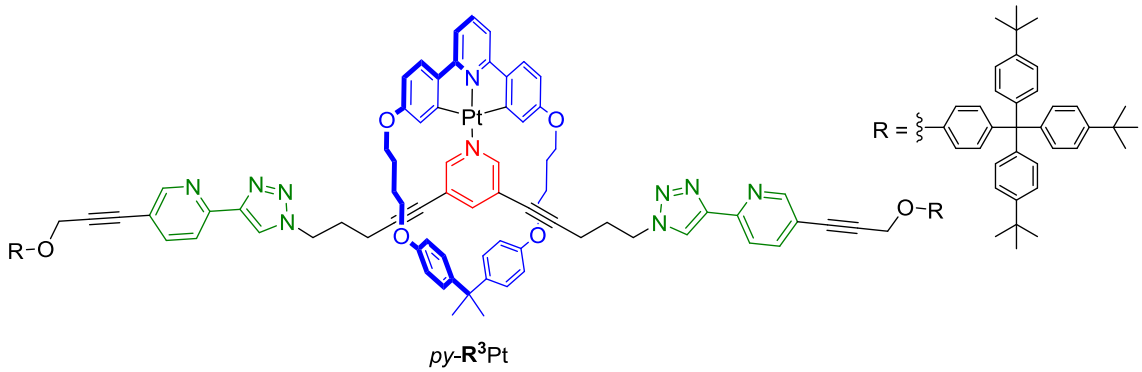

py-**R^3**Pt

Figure 3.4 Structure of platinum(II)-complexed [2]rotaxane *py*-**R^3**Pt.

3.2.3.2 Retrosynthesis of rotaxane *py*-**R^3**Pt

The proposed retrosynthesis of the molecular shuttle *py*-**R^3**Pt is shown in Scheme 3.12. Here a double click reaction of the threaded pseudo-rotaxane platinum complex and two complementary stoppers should afford [2]rotaxane. The monodentate macrocycle complex **17** can be obtained *via* a ligand exchange reaction of the premetallated [**L^2**Pt(DMSO)] with the 3,5-disubstituted pyridine monodentate ligand. Sonogashira coupling reaction of 3,5-dihalopyridine and pentynol following tosylation and azidation would achieve 3,5-bisazidopyridine **16**.

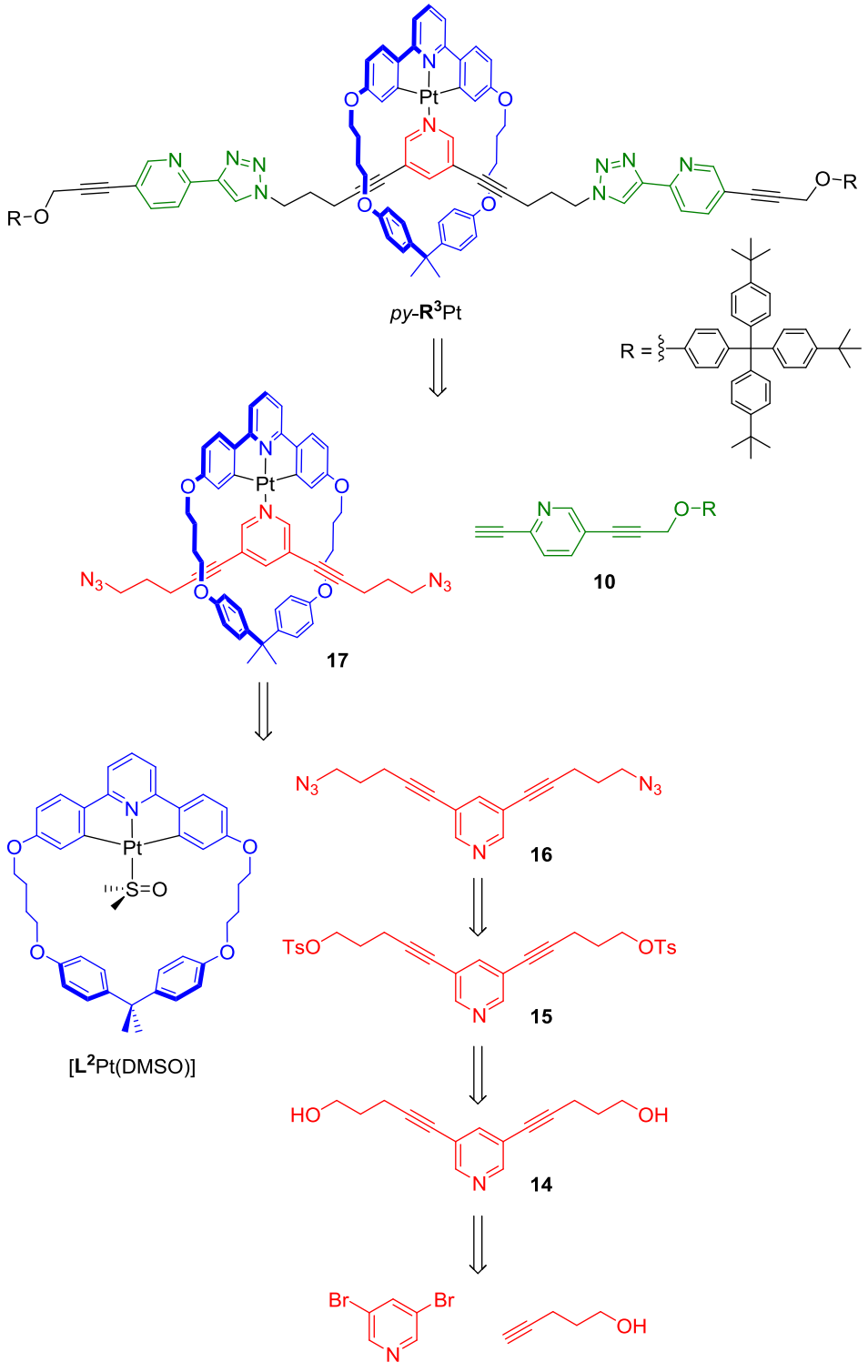

Scheme 3.12 Retrosynthesis of platinum-complexed rotaxane *py*-**R**^{3}Pt.

3.2.3.3 Synthesis of rotaxane *py*-**R**^{3}Pt

The route towards the monodentate ligand **16** starts from the commercially available 3,5-dibromopyridine and 4-pentyn-1-ol (Scheme 3.13). 3,5-Dibromopyridine was treated with an excess amount of 4-pentyn-1-ol under a standard Sonogashira coupling reaction, forming alkynylpyridine diol **14** in excellent yield. Subsequent conversion of the alcohol groups into tosylates using *p*-toluenesulfonyl chloride and Et_3N in CH_2Cl_2 affords bistosylate **15**, which was then further reacted with NaN_3 to form the bisazido compound **16** in good yield.

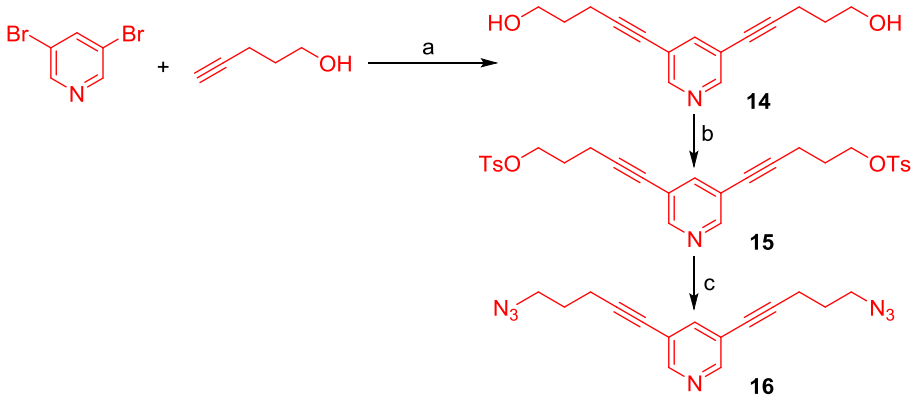

Scheme 3.13 Synthesis of bisazido compound **16**. Reagents and conditions: a) CuI, $Pd(PPh_3)_2Cl_2$, PPh_3, Et_3N, DMF, 80 °C, 16 h, 94%; b) TsCl, Et_3N, CH_2Cl_2, 0 °C-rt, 16 h, 82%; c) NaN_3, DMF, 80 °C, 16 h, 62%.

The premetallated macrocycle was subjected to a ligand exchange reaction, where the labile dimethylsulfoxide was expected to be displaced by monodentate ligand **16** to afford the desired product **17**. The reaction was carried out in THF-d_8 and $CDCl_3$ at 55 °C for five days. The ^{1}H NMR spectrum showed no reaction had occurred as the peaks corresponding to both starting materials remained (Figure 3.5). There were some new peaks possibly from the product (Figure 3.5b, pink labelled) but the amount was low. In addition, the signal corresponding to coordinated DMSO at 3.19 ppm, remained unchanged with no observation of free DMSO signal at around 2.45 ppm.

According to the crystal structure of [**L**^{2}Pt(3,5-lut)] (Figure 3.3), the distance from the lutidine methyl carbon atom to the closest carbons of bisphenol A moiety in the macrocycle, C52-C30 and C53-C33, are 3.53 and 3.40 Å respectively. It was therefore concluded that the steric hindrance and rigidity of the monodentate ligand, in particular

the 3,5-dialkyne groups, hampers the ligand exchange reaction. It was therefore decided that a new version of the ligand featuring saturated alkyl linkages should be explored.

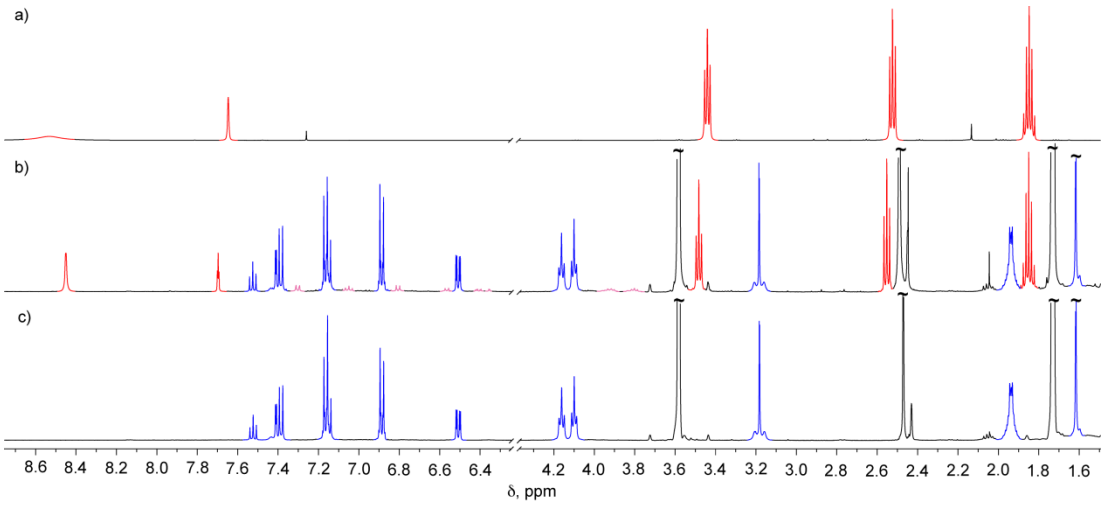

Figure 3.5 Partial ^{1}H NMR spectra (500 MHz, THF-d_8, 298 K) of a) bisazido ligand **16** (in $CDCl_3$); b) reaction solution after heated at 55 °C for 5 d; c) [**L**^{2}Pt(DMSO).

3.2.3.4 Saturated 3,5-substituted pyridine ligand for rotaxane formation

The structure of the revised rotaxane is shown in Figure 3.6 featuring a saturated ligand. The monodentate ligand **16** and **20** differ only in two triple bonds close to pyridine ring. Synthetic routes of ligand **20** are proposed in Scheme 3.14.

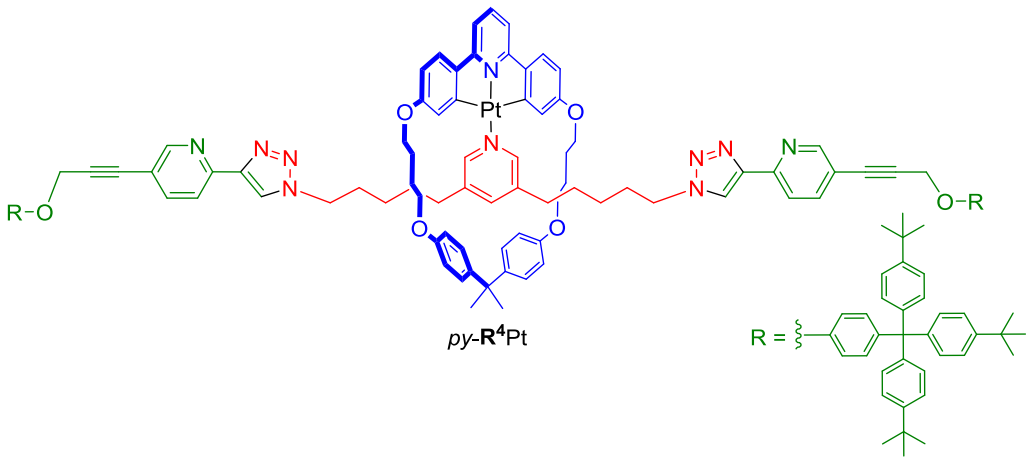

Figure 3.6 Structure of platinum(II)-complexed [2]rotaxane *py*-**R**^{4}Pt.

Direct hydrogenation of ligand **16** would also reduce the azide group to amines, hence this step needed to be done prior to the introduction of azide moieties. The hydrogenation reaction, which utilises palladium on carbon (Pd/C) to catalyse the addition of hydrogen to C–C multiple bonds could be employed with diol **14** or

bistosylate **15** (Scheme 3.14a, c). The reactions were near quantitative and clean enough that the saturated diol **18** and bistosylate **19** could be used without further purification. Diol **14** was hydrogenated and gave diol **18** in almost quantitative yield (97%). Subsequent transformation of the alcohol to tosyl using standard reagents and condition for tosylation produced the desired product **19** in moderate 33%, whereas direct hydrogen addition to bistosylate **15** afforded **19** in a relatively high yield (93%). Finally, NaN_3 was reacted with **19** to finish the saturated bisazido compound **20** in good yield.

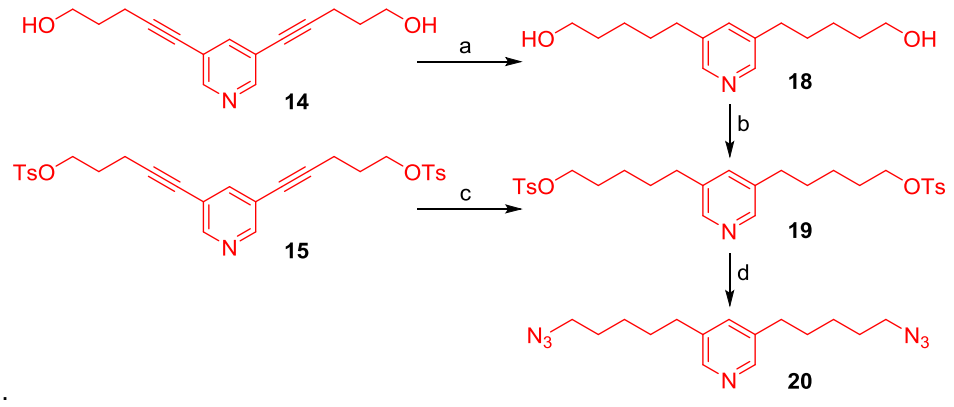

Scheme 3.14 Synthesis of bisazido **20**. Reagents and conditions: a) H_2, Pd/C, CH_2Cl_2, MeOH, rt, 48 h, 97%; b) TsCl, Et_3N, CH_2Cl_2, 0 °C-rt, 16 h, 33%; c) H_2, Pd/C, CH_2Cl_2, MeOH, rt, 16 h, 93%; d) NaN_3, DMF, 80 °C, 16 h, 78%.

As had been observed in the previous chapter, and is common for Pd^{2+} and Pt^{2+} ligand substitution,[14] an increase in steric bulk often results in a significant retardation in the rate. Therefore it was expected that even harsher conditions would be necessary for the exchange of ligand **20** for DMSO to afford **21**, Scheme 3.15, in comparison to the similar reactions reported in Chapter II. The reaction was first set up in chloroform (rather the dichloromethane) to allow higher temperature. Refluxing the reaction mixture at 70 °C for 16 h revealed 50% product conversion according to ^{1}H NMR spectroscopy (Figure 3.7). Prolonged heating for 22 h and 40 h resulted in formation of other species and a decrease of the desired product (Figure 3.7d-e). Slower conversion rates were found using DCE and TCE at 85 °C. Furthermore, by-products from these solvents at higher temperature were more pronounced than those obtained in $CHCl_3$. It should be noted that ligand **20** was prepared in a $CHCl_3$ stock solution and was used in every experiment and NMR samples of the reactions performed in DCE and TCE were prepared in $CDCl_3$.

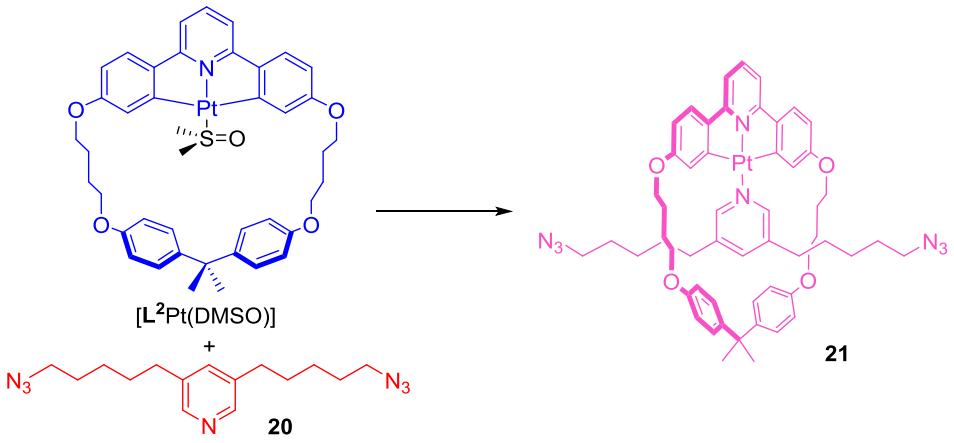

Scheme 3.15 Ligand exchange reaction of [**L²**Pt(DMSO)] and **20**.

The ^{1}H NMR signals of intermediate species (green peaks) were observed at similar chemical shifts to the "2+1+1" species.[15] The formation of the extra species was attributed to the acidity of $CHCl_3$/$CDCl_3$ that can cleave a Pt-C bond.

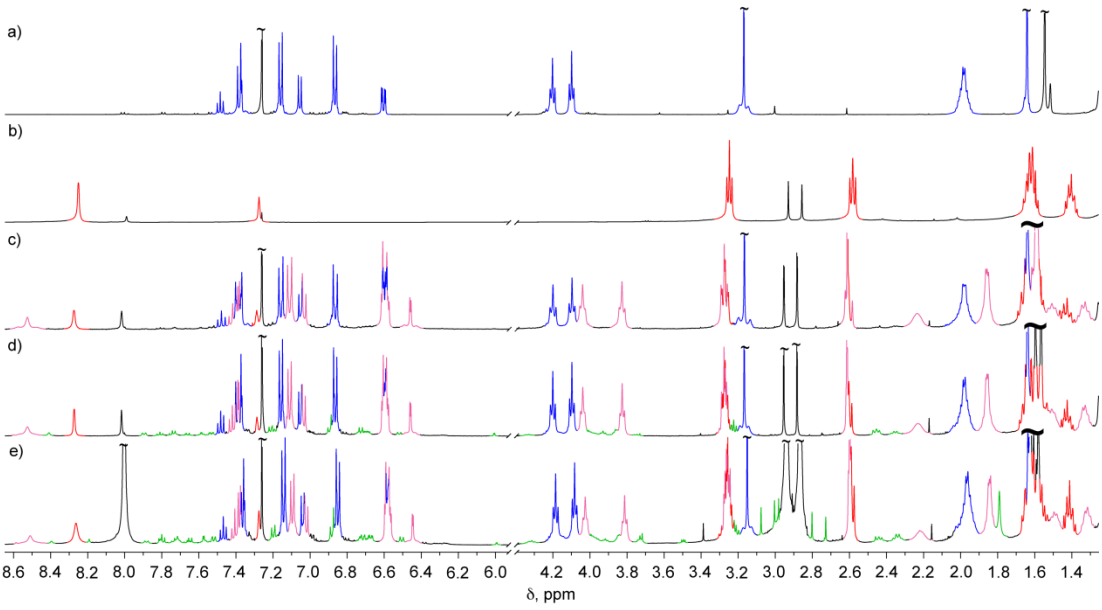

Figure 3.7 Partial ^{1}H NMR spectra (500 MHz, $CDCl_3$, 298 K) of a) [**L²**Pt(DMSO)]; b) bisazido ligand **20**; c) a mixture of [**L²**Pt(DMSO)] and **20** at 70 °C for 16 h; d) a mixture of [**L²**Pt(DMSO)] and **20** at 70 °C for 22 h; e) a mixture of [**L²**Pt(DMSO)] and **20** at 70 °C for 40 h.

The reactions were also carried out in CD_2Cl_2, THF-d_8 and DMF-d_7 at 50 °C to screen for a suitable solvent. The progress was monitored by ^{1}H NMR spectroscopy. The desired product started to form in all three solvents upon heating for 1 h. In THF-d_8, the amount of the exchanged product was decreased as the reaction continued heating for 16 h, 40 h

and 72 h. The equilibrium was shifted to the left where coordinated DMSO was the major species. In contrast, the reactions in CD_2Cl_2 and DMF-d_7 were gradually moved to the right side of the equilibrium. No significant change was observed after heating longer than 72 h in DMF where the reaction did not go to completion. The reaction in CD_2Cl_2 also did not reach a point where only the product remained in the solution, however, it gave the highest conversion of all studied solvents. The ^{1}H NMR spectra in Figure 3.8 shows the set of signals of the product (pink labelled) increasing over time for the reaction in CD_2Cl_2. In addition, the coordinated DMSO peak at chemical shift 3.15 ppm is decreasing to be replaced as free DMSO at 2.55 ppm (orange labelled) as the reaction progress. Increasing the amount of the ligand **20** to 1.3-2 eq, did not drive the reaction to completion either.

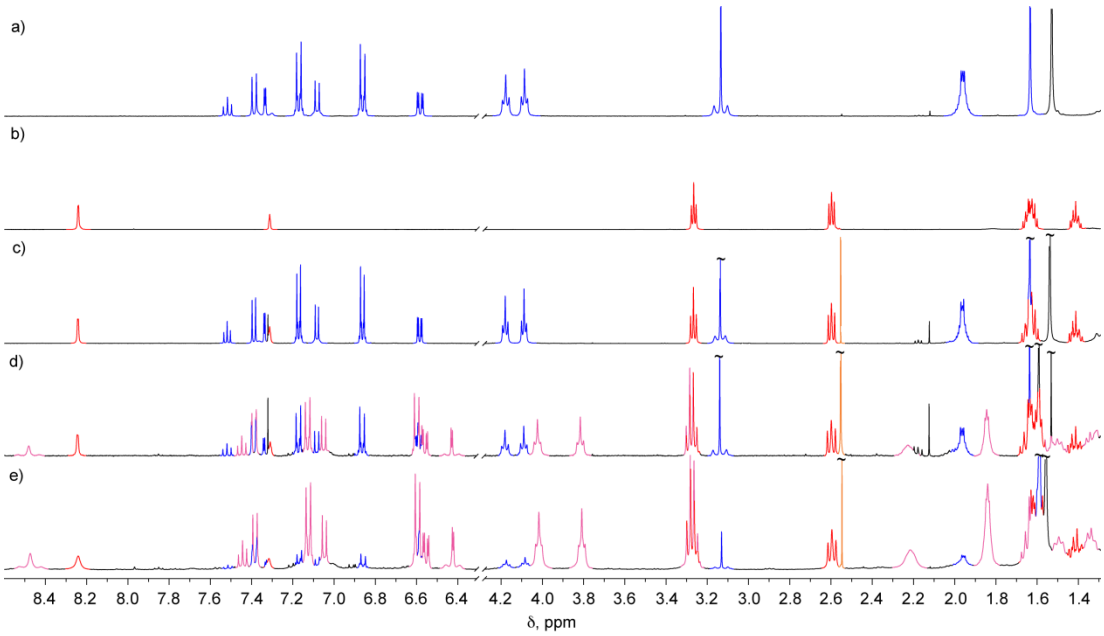

Figure 3.8 Partial ^{1}H NMR spectra (500 MHz, CD_2Cl_2, 298 K) of a) [**L²**Pt(DMSO)]; b) saturated bisazido ligand **20**; c) a mixture of [**L²**Pt(DMSO)] and **20** at rt for 1 h; d) a mixture of [**L²**Pt(DMSO)] and **20** at 50 °C for 40 h; e) a mixture of [**L²**Pt(DMSO)] and **20** at 50 °C for 6 d.

While it was thought that the desired product was present in solution, several attempts to separate the product using silica gel chromatography (with and without Et_3N deactivation), preparative alumina TLC or size exclusion chromatography over Sephadex LH-20 all failed to purify the reaction mixture and the product also decomposed on the columns. Only a stopper unit was obtained from the columns.

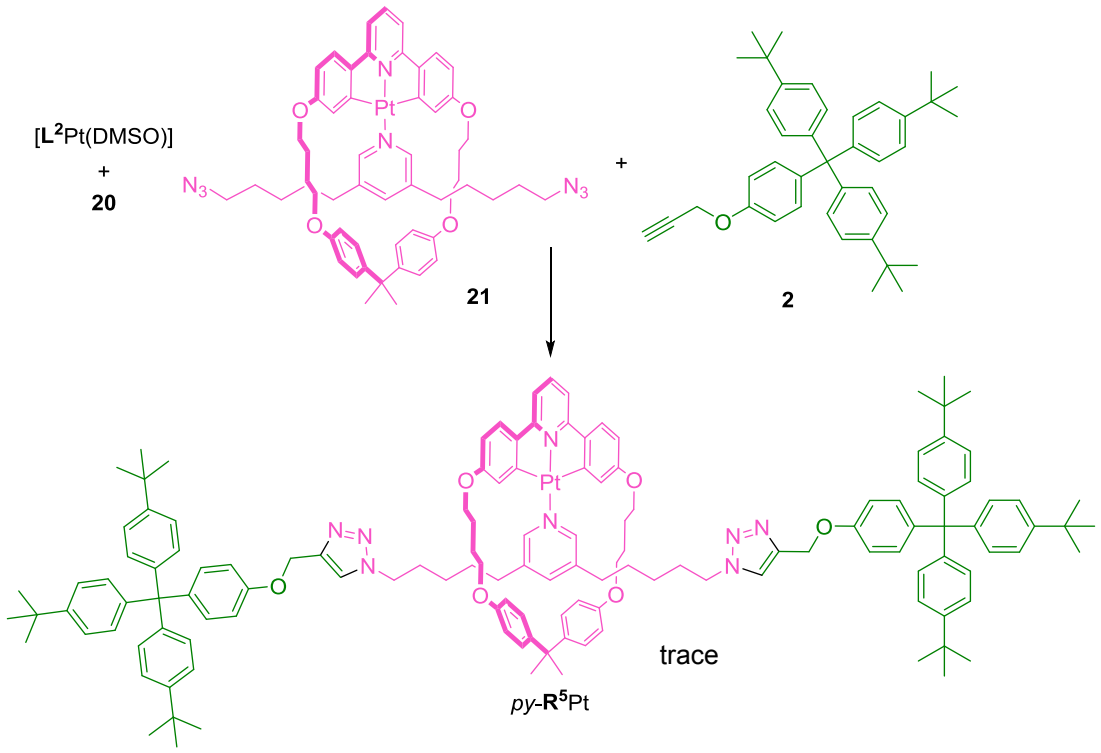

Scheme 3.16 Click reaction of complex **21** with alkyne stopper **2**. Reagents and conditions: DIPEA, TBTA, $[Cu(CH_3CN)_4]PF_6$, CH_2Cl_2

As bisazido complex **21** would not tolerate chromatographic purification methods, it was carried on to the last step click reaction without further purification. A reaction of a mixture of **21** and unreacted [**L**²Pt(DMSO)] and **20** with alkyne stopper **2** by a Cu^I-catalysed azide-alkyne 1,3-cycloaddition (CuAAC)[16] in the presence of tris(benzyltriazolylmethyl)amine (TBTA)[6, 17] and diisopropylamine (DIPEA) was carried out as shown in Scheme 3.16 in an attempt to generate rotaxane *py*-**R**⁵Pt which, it was hoped, would be more stable, in particular to purification by a chromatographic procedure. The reaction mixture was stirred at rt using $[Cu(CH_3CN)_4]PF_6$ as a Cu^I source. However, no target rotaxane could be determined by ^1H NMR of the crude product and all fractions from column chromatography. Exactly the same procedure was employed using ligand **20** in place of platinum complex **21** to obtain a thread molecule for the purpose of comparison by NMR spectroscopy (Scheme 3.17). The thread was obtained as an off-white solid in 59% yield following purification by column chromatography. Longer chain alkyne stopper **29** was used as a replacement for alkyne **2** to ensure steric congestion was not retarding the reaction (Scheme 3.18). The resonance of

pseudorotaxane **21** was noticeably diminished when the alkyne stopper was introduced. Column chromatography of the crude product recovered only the stopper.

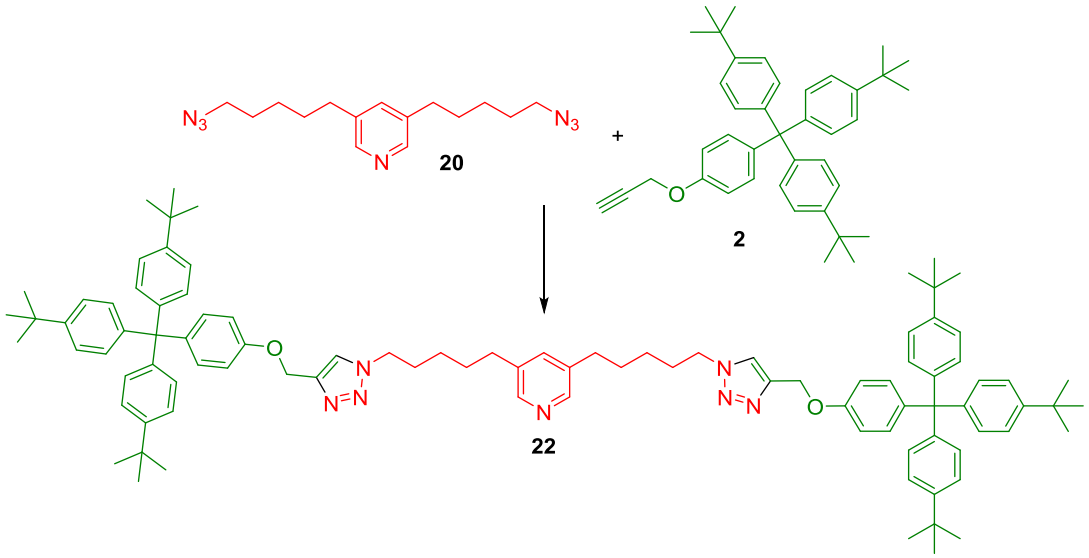

Scheme 3.17 Synthesis of thread **22**. Reagents and condition: DIPEA, TBTA, $[Cu(CH_3CN)_4]PF_6$, CH_2Cl_2, rt, 24 h, 59%.

Adding a catalytic amount of acetic acid to the reaction has been known to increase the product yield and decrease reaction time significantly[18], as it protonates the C-Cu bond in the intermediate which then accelerates product formation.[19] This reaction conditions gave the desired rotaxane when it was adopted for compound **21** and longer alkyne **29** as evidenced from ESI(+)-MS of rotaxane *py*-**R**^{6}Pt showing $[M+H]^+$ (*m/z* 2235.87) and noninterlocked thread **22** $[M+H]^+$ (*m/z* 1442.95) along with mono-clicked pseudorotaxane ($[M+H^+]$, *m/z* 1665.65). Column chromatography failed to give any of the products.

Heterogeneous copper-on-charcoal has been utilised to catalyse click cycloaddition of various types of alkyne and azides.[20] The reaction between 2-ethynylpyridine and phenylethylazide at 60 °C using 5 mol% Cu/C and one equivalent Et_3N gave corresponding triazole product as high as 98% yield after filtration of the catalyst and removal of the volatiles. Similar conditions were employed for the reaction of complex **21** and pyridylalkyne **10**. The crude NMR spectrum showed only the signals of compound **10** and other impurities. The same result was obtained when longer chain alkyne **29** was used.

Another common catalytic system for the CuAAC rather than the combination of Cu^{I}/NR_3 is the combination of $CuSO_4$/NaAsc.[16a] This condition was used to successfully generate the thread molecule **23** (Scheme 3.19a). A mixture of bisazido compound **20**, ethynylpyridine stopper **10** and $CuSO_4$ in 1:1 *t*-butanol/water was stirred at rt followed by adding of (+)-Sodium *L*-ascorbate. The reaction mixture was stirred at 60 °C overnight. After working up and silica gel column purification, the thread was obtained as a pale yellow solid in 69% yield. When the same conditions were applied to form the rotaxane, there was no evidence of its formation by ^{1}H NMR spectroscopy. Column chromatography of the crude product only gave the thread molecule **23**. However, the ESI(+)-MS of the reaction mixture showed evidence for the formation of the rotaxane with a peak at *m/z* 2382.28 which corresponds to $[M+H]^+$ for *py*-**R**^{7}Pt (Scheme 3.19b) and non-interlocked thread **23** $[M+H+Cu]^{2+}$ (*m/z* 1651.93). Despite this evidence for its formation, it was concluded that this was generated on a very small scale and no product could be isolated following column chromatography.

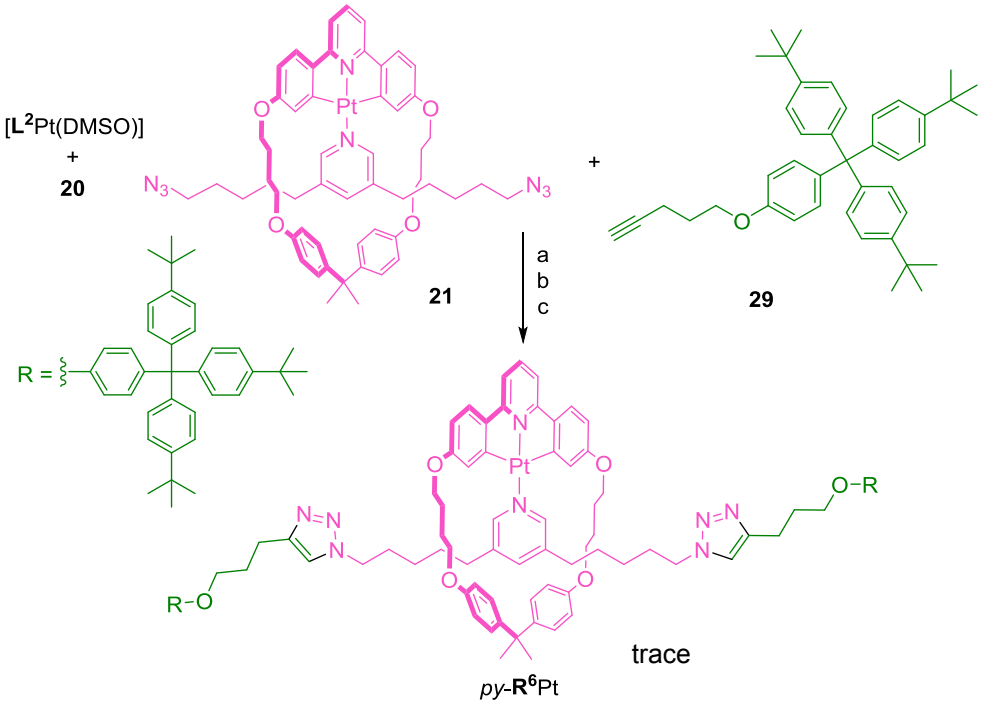

Scheme 3.18 Click reaction of complex **21** with alkyne stopper **29**. Reagents and conditions: a) DIPEA, TBTA, $[Cu(CH_3CN)_4]PF_6$, CH_2Cl_2, rt, 16 h; b) DIPEA, HOAc, TBTA, $[Cu(CH_3CN)_4]PF_6$, DCE, rt, 16 h; c) Cu/C, Et_3N, DEC, 60 °C, 16 h.

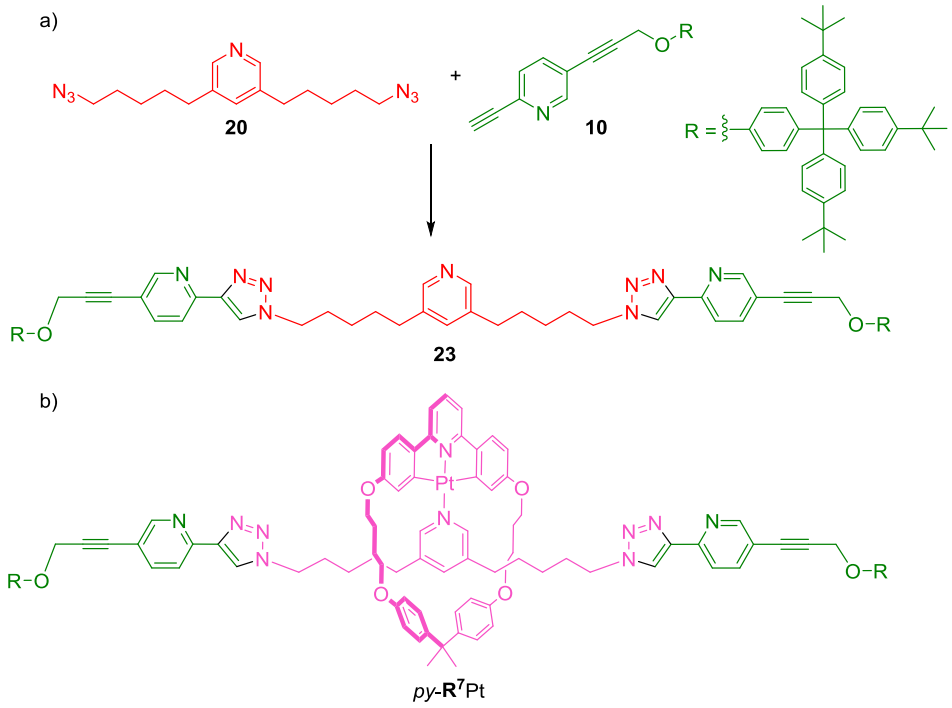

Scheme 3.19 a) Synthesis of thread **23**. Reagents and condition: 30 mol% $CuSO_4$, 40 mol%, NaAsc, 1:1 *t*-butanol/H_2O, 60 °C, 18 h, 69%; b) structure of rotaxane *py*-**R**^{7}Pt.

Another approach towards rotaxane formation was proposed. The click reaction of bisazido compound and ethynylpyridine stopper was not successful in all conditions of rotaxane fabrication but the corresponding threads were achieved in good yield. This indicated that the conditions for click reaction were suitable. What presumably hampered the formation of a rotaxane was the instability of its starting azide complex which most likely led to its decomposition. A new design of thread was suggested in which the click reaction would be done prior to threading to the platinum macrocycle. Once the axle molecule was threaded, stoppering with a bulky component was to be performed to furnish the [2]rotaxane.

3.2.3.5 Retrosynthesis of rotaxane *py*-**R**^{8}Pt

The main features of the rotaxane remained unchanged, the thread molecule consisting of three binding sites: one monodentate and two degenerate bidentate sites. The retrosynthetic analysis (Scheme 3.20) showed the first disconnections are at the stopper that could be achieved from reaction of the diol thread and isocyanate stopper as it has been described in the literature using the same type of stopper to achieve the corresponding rotaxane as high as 96% yield after chromatographic purification. [6a, 23] The ligand exchange reaction of the three-station-thread and [**L**^{2}Pt(DMSO)] would yield

pseudorotaxane **31**. The full thread **26** would be obtained from the click reaction used to achieve thread **23**. Compound **25** would be obtained in the same manner of synthesis as **10**; by two Sonogashira couplings starting from **8**.

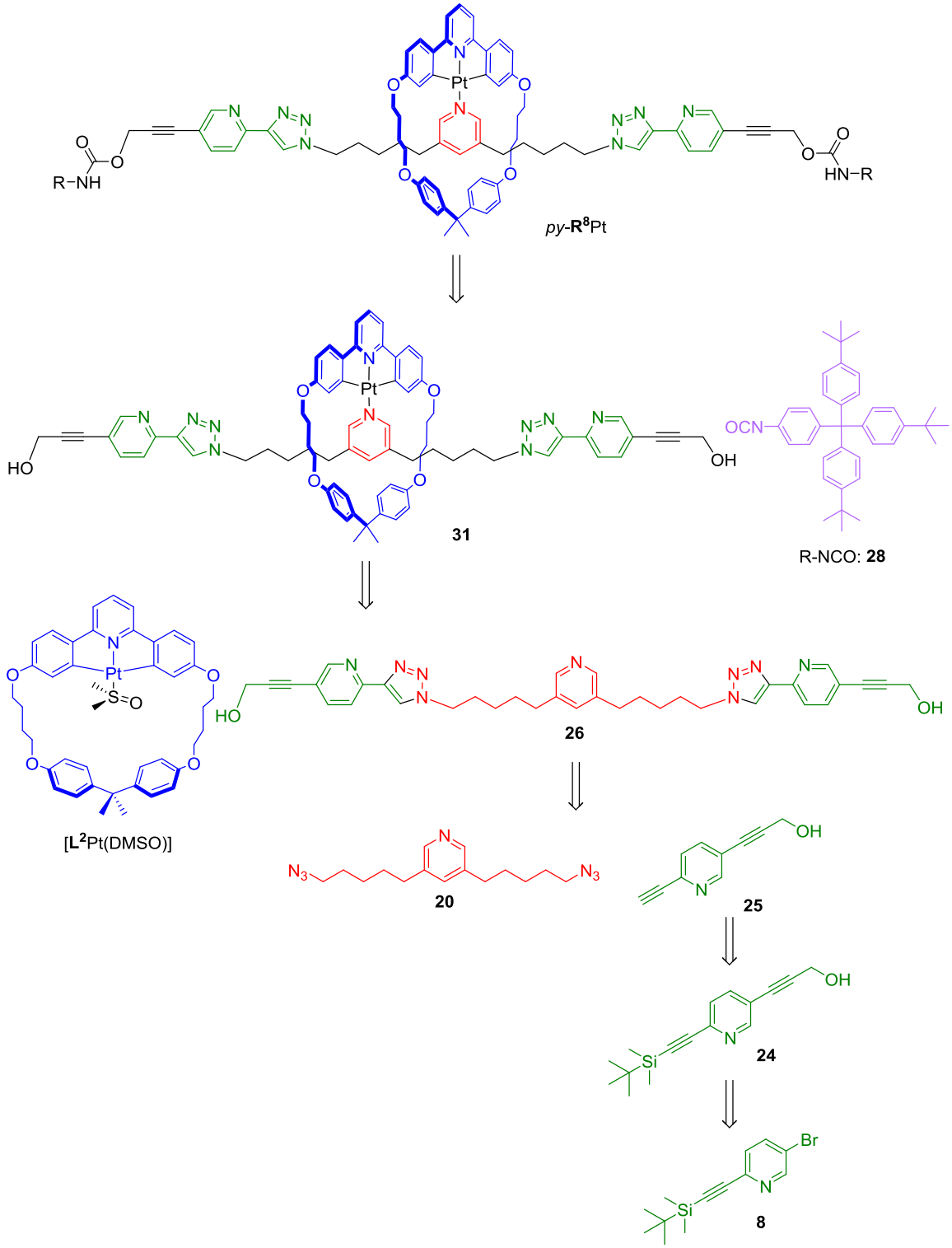

Scheme 3.20 Retrosynthesis of platinum-complexed rotaxane *py*-**R**[8]Pt.

3.2.3.6 Synthesis of rotaxane *py*-**R**^{8}Pt

The synthesis of ethynyl pyridine **25** started with a Sonogashira coupling of TBDMS-protected pyridine compound **8** with propargyl alcohol to yield **24** in 82%. The silyl group was cleaved with TBAF to give **25**.

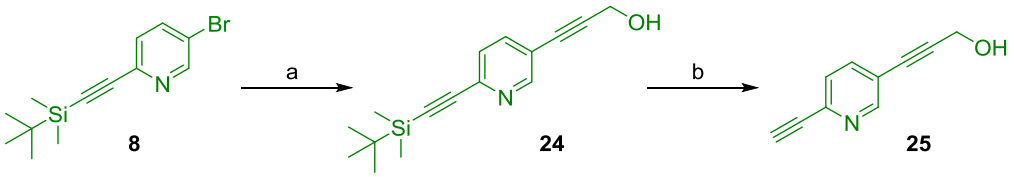

Scheme 3.21 Synthesis of pyridyl alkyne **25**. Reagents and conditions: a) CuI, $Pd(PPh_3)_4$, Et_3N, THF, 60 °C, 5 d, 82%; b) TBAF, THF, rt, 16 h, 63%.

Thread compound **26** was obtained from a double click reaction of the bisazido pyridine **20** and pyridyl alkyne **25** using $CuSO_4$/NaAsc (Scheme 3.22).

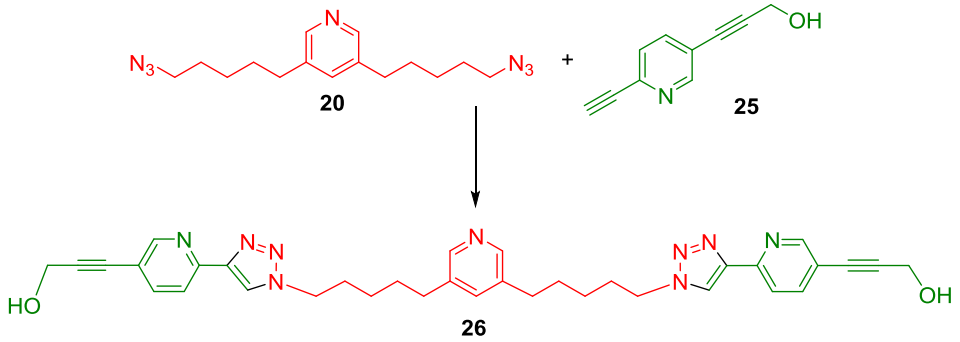

Scheme 3.22 Synthesis of axle molecule **26**. Reagents and condition: 30 mol% $CuSO_4$, 40 mol% NaAsc, 1:1 *t*-butanol/water, 60 °C, 16 h, 42%.

The Ligand exchange reaction to produce pseudorotaxane **31** was investigated in CD_2Cl_2 and TCE-d_2. It took 7 h of heating at 80 °C to displace DMSO (Scheme 3.23a). However, the ^{1}H NMR spectrum of this reaction showed multiple species. (Figure 3.9). The reaction was continued at high temperature for 15 d with no significant signal change. A DOSY spectrum (Figure 3.10) confirmed more than one species was in solution. It was complicated to assign all the peaks since many of the resonances overlapped.

Adding a slight excess of TsOH to the mixture of macrocycle and thread (Scheme 3.23b) should shift the coordination site to a bidentate ligand and that made the system more complicated as it was no longer symmetric. Although the thread was present in the same ratio as the macrocycle and the coordinated DMSO peak disappeared after acid was

introduced, the resulting complexes were not the only expected species. The ^{1}H NMR spectra was taken regularly for a week until no change was observed (Figure 3.11). The spectra showed overlapping signals in many regions however a DOSY spectrum suggested two main species in the solution (Figure 3.12). TLC of the reaction solution did not show good separation between each species (in a range of eluents).

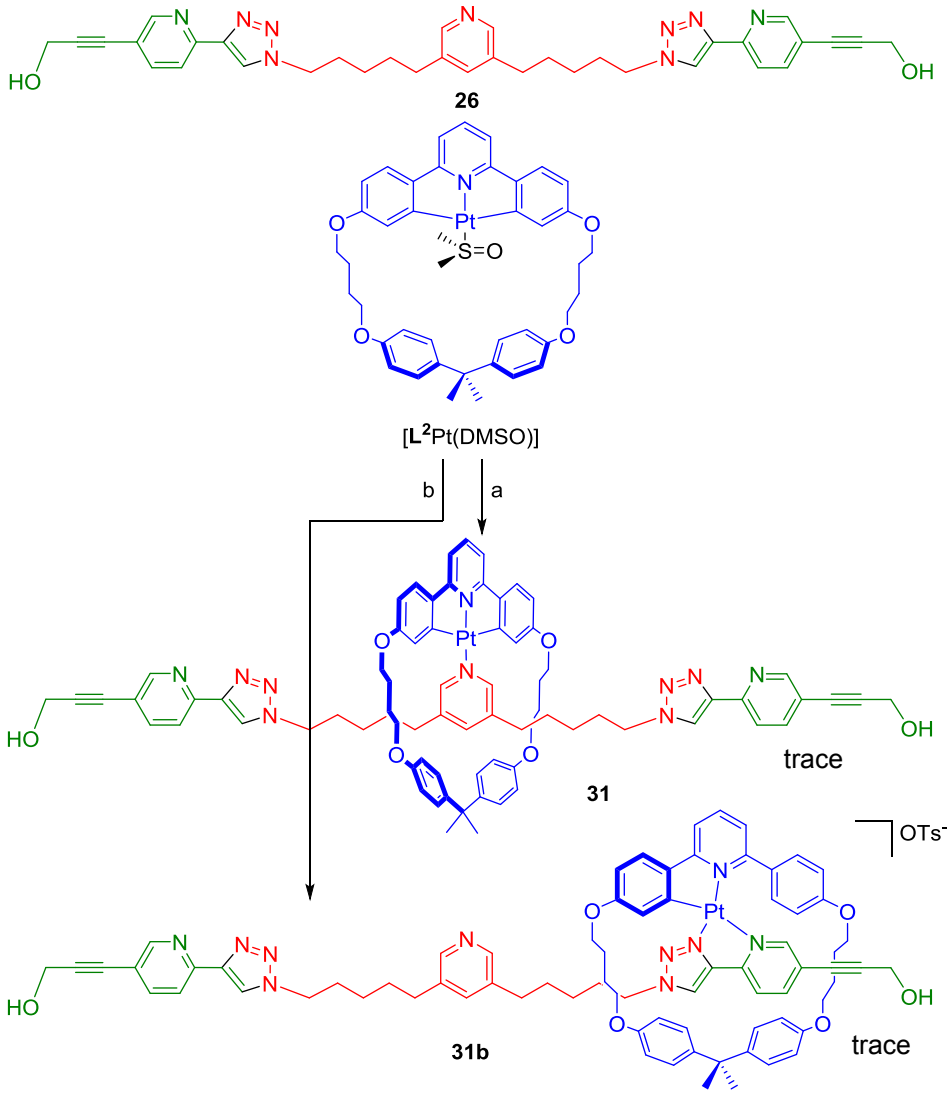

Scheme 3.23 Ligand exchange reaction of thread **26** and [**L**²Pt(DMSO)] to form pseudorotaxane **31**. Reagents and conditions: a) TCE-d_2, 80 °C, 4 d; b) 2 eq TsOH, CD_2Cl_2, rt, 30 h.

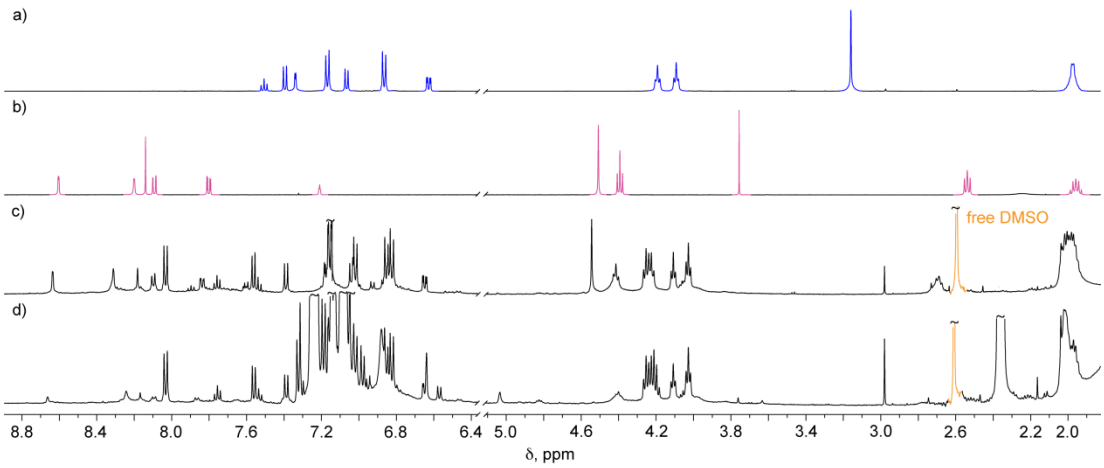

Figure 3.9 Partial ^{1}H NMR spectra (500 MHz, $C_2D_2Cl_4$, 298 K) of: a) [**L²**Pt(DMSO)]; b) thread molecule **26** in CD_2Cl_2; c) The reaction mixture after 15 d at 80 °C; d) The reaction mixture c) after adding isocyanate stopper **28** and dibutyltin dilaurate (DBTDL) 24 h at rt.

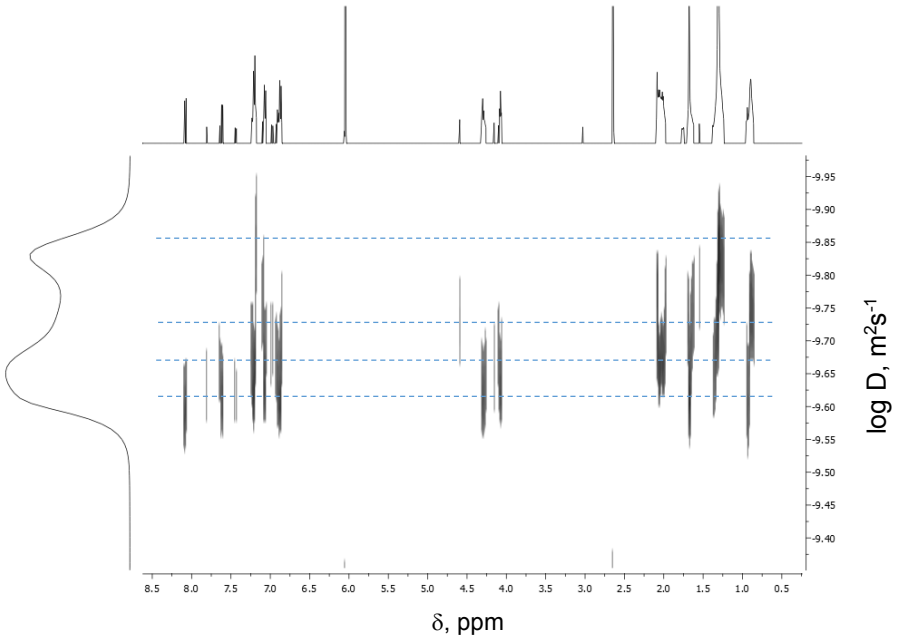

Figure 3.10 ^{1}H DOSY spectrum of the reaction mixture of [**L²**Pt(DMSO)] and **26** after 15 d at 80°C.

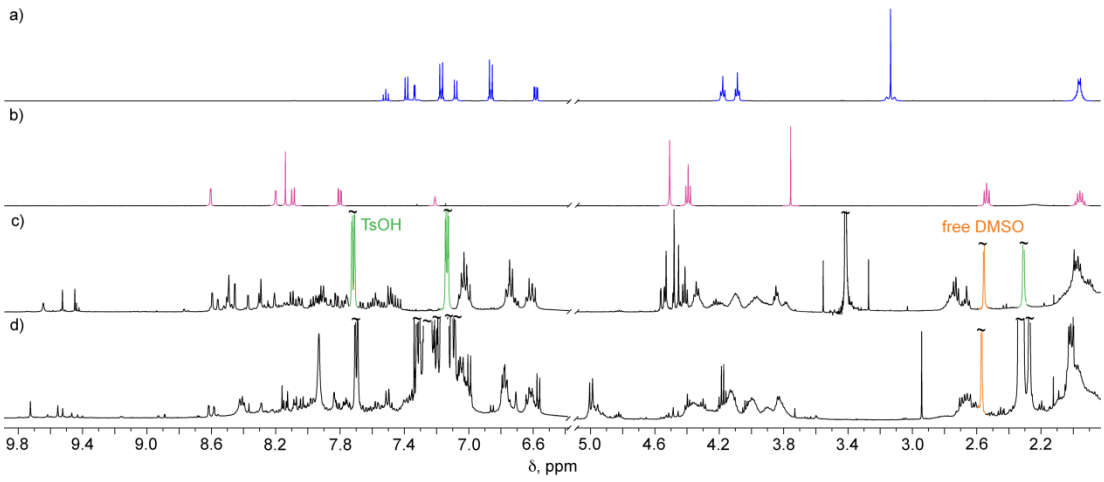

Figure 3.11 Partial ^{1}H NMR spectra (500 MHz, CD_2Cl_2, 298 K) of: a) [**L**^{2}Pt(DMSO)]; b) thread molecule **26**; c) The reaction mixture after added excess TsOH at 40 °C for 8 d; d) The reaction mixture c) after adding **28** and DBTDL 24 h at rt.

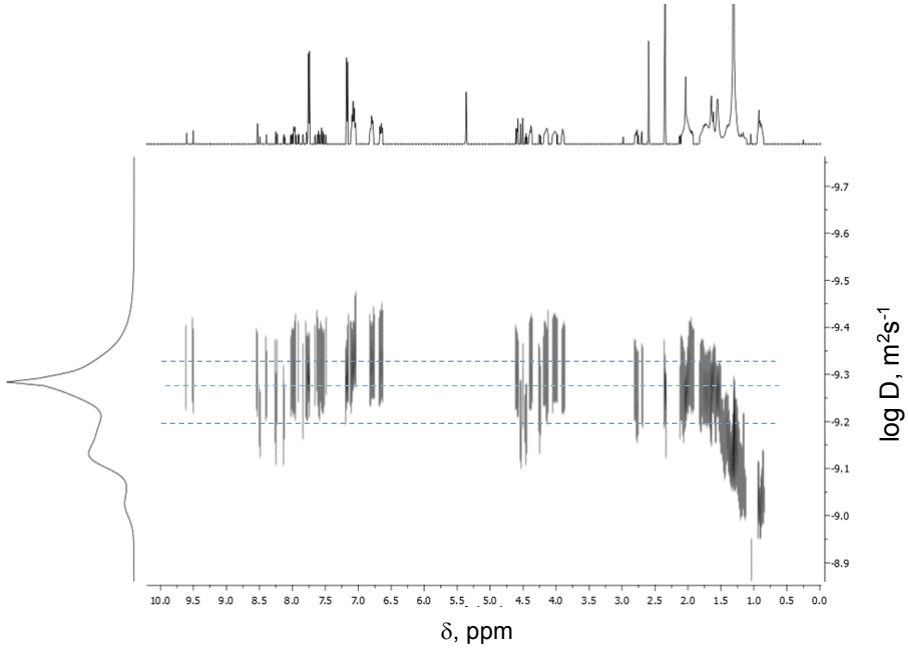

Figure 3.12 ^{1}H DOSY spectrum of the reaction mixture after added excess TsOH at 40 °C for 8 d

The reaction mixtures, both of with acid and without acid, were further reacted with stoppers to attempt to furnish rotaxane *py*-**R**^{8}Pt. The precursor pseudorotaxane was stoppered by reaction of bulky isocyanate units **28** with the terminal hydroxyl groups of the thread in the presence of di-*n*-butyltin dilaurate (DBTDL) in dichloromethane at room temperature for 24 h.[21] The reaction with TsOH was promising as the DOSY spectrum of the reaction with the stopper indicated a large hydrodynamic radius than the one with only macrocycle, thread and acid present (Figure 3.13). The appropriate conditions for separation of the potential product could not be found. In the case of

reaction of macrocycle and thread and stoppers, the NMR was less conclusive and the mixture was stuck to the baseline of TLC even in a highly polar eluent system *i.e.* 5% MeOH/CH_2Cl_2. The crude products of both reaction with/without acid were determined by ESI(+)-MS. The mass spectrum showed $[M+H]^+$ (*m/z* 2468.30) corresponded to a rotaxane *2-tripy*-**R^8**Pt for the reaction that added TsOH and $[M+3H]^{3+}$ (m/z 2469.24) for a rotaxane *py*-**R^8**Pt for the reaction in the absence of acid.

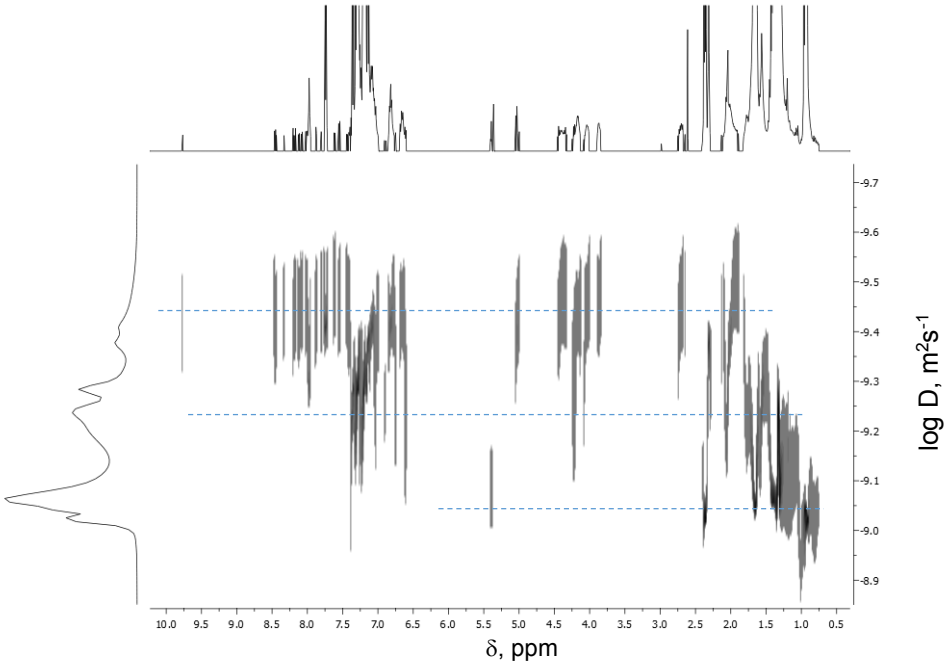

Figure 3.13 ^{1}H DOSY spectrum of the reaction mixture with acid after adding **28** and DBTDL 24 h at rt.

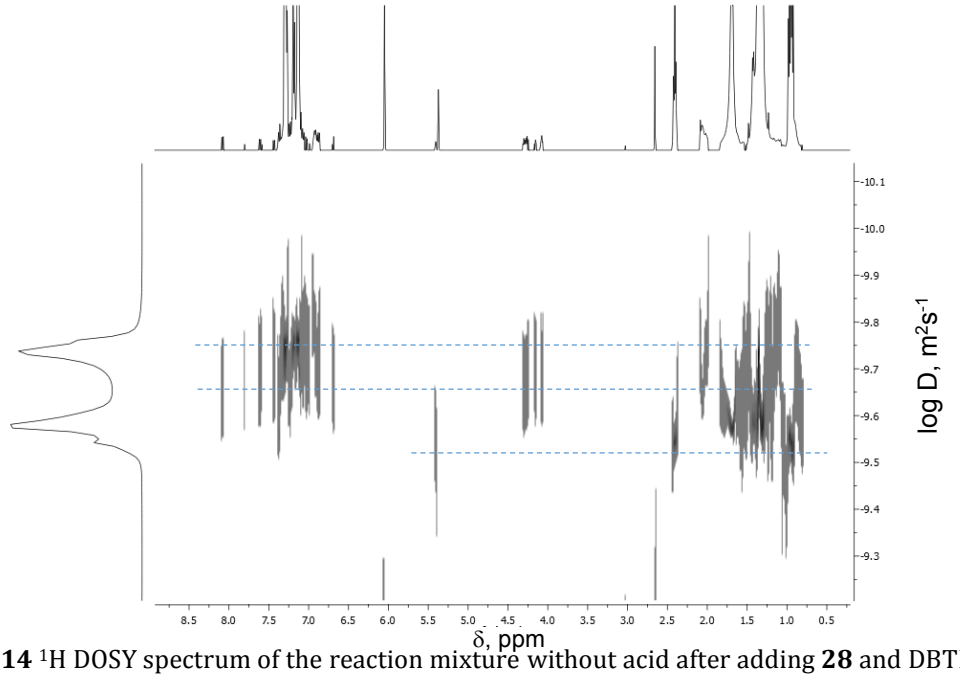

Figure 3.14 ^{1}H DOSY spectrum of the reaction mixture without acid after adding **28** and DBTDL 24 h at rt.

3.2.3.7 Non-symmetric half-thread in rotaxane *py*-**R**^{9}Pt

Another attempt at rotaxane formation was undertaken. The new design of rotaxane, *py*-**R**^{9}Pt, incorporates only two different binding sites. This non symmetric rotaxane would be achieved from a click reaction of an alkyne half-thread **10** with pseudorotaxane featuring terminal azide **35**. Similar rotaxane construction has been successfully achieved in a palladium complexed-[2]rotaxane.[3a] Palladium containing macrocycle was complexed with one of the stations before the thread was capped with a stopper molecule. The synthetic pathway of asymmetric half-thread **34** did not differ from the earlier symmetric ones.

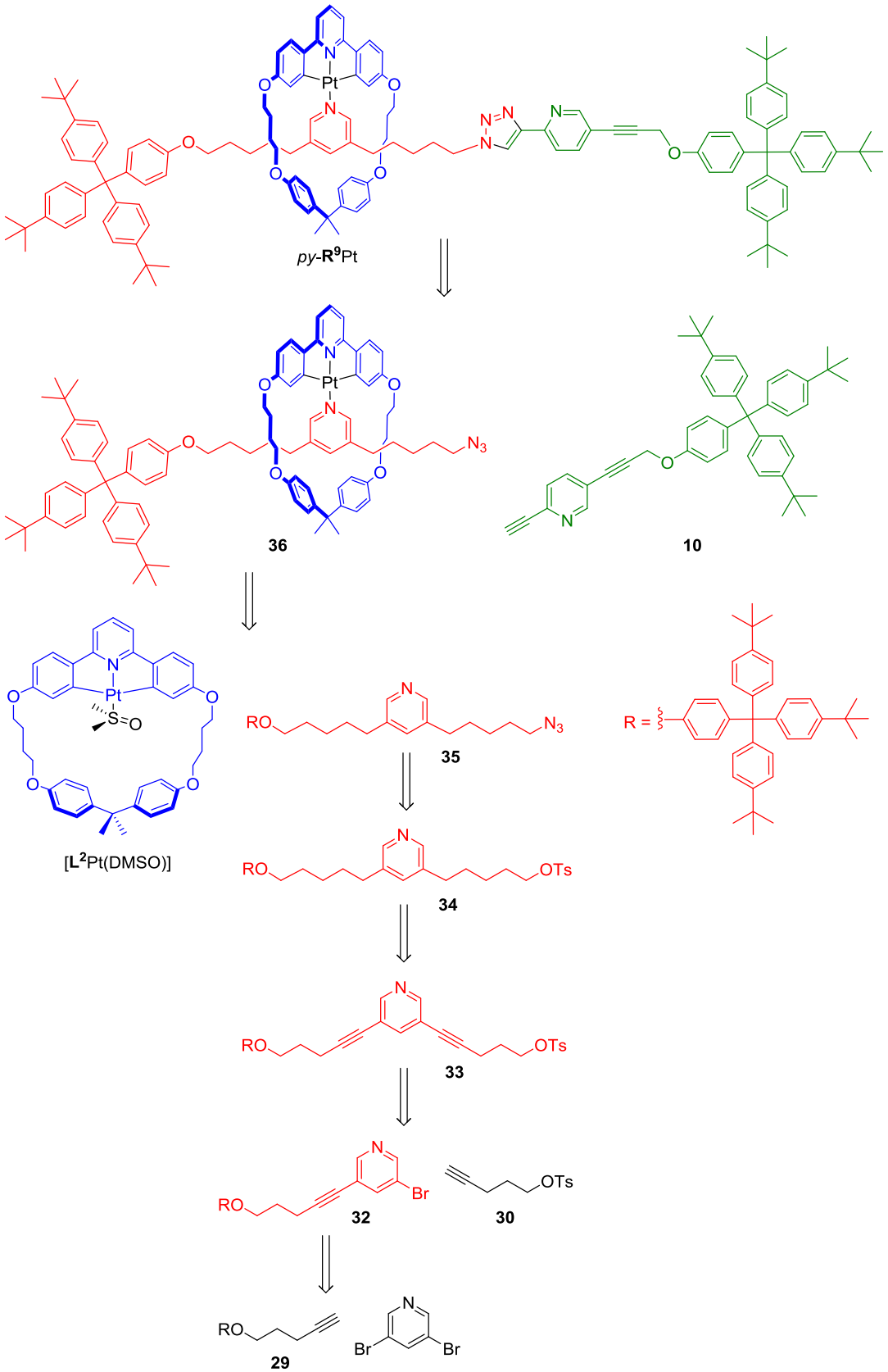

Scheme 3.24 Retrosynthesis of rotaxane *py*-**R**^{9}Pt

3.2.3.8 Synthesis of non-symmetric pseudorotaxane

The Synthesis towards a non-symmetric half-thread **35** (Scheme 3.25) started with desymmetrising Sonogashira coupling reaction of 3,5-dibromopyridine and the known pentynyl stopper **29** under standard conditions. Another Sonogashira coupling was done under the same conditions with ethynyltosylate **30** to afford **33** in a moderate 44% yield. Hydrogenation using Pd/C as catalyst afforded **34** in quantitative yield. Azidation was carried out to give **35** in 45%.

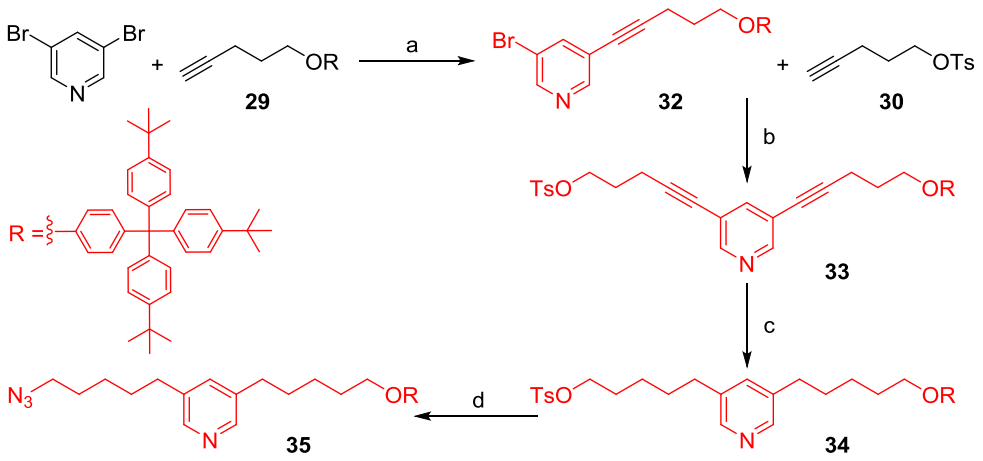

Scheme 3.25 Synthesis of asymmetric thread **35**. Reagents and conditions: a) CuI, $Pd(PPh_3)_2Cl_2$, DIPEA, THF, 60 °C, 67%; b) CuI, $Pd(PPh_3)_2Cl_2$, DIPEA, THF, 60 °C, 44%; c) H_2, Pd/C, CH_2Cl_2, MeOH, rt, quantitative; d) NaN_3, DMF, 80 °C, 16 h, 45%.

The ligand exchange reaction of **35** was subjected to displacement of DMSO in [**L**²Pt(DMSO)] in TCE-d_2 (Scheme3.26). Consistent with other ligand exchange experiments of the platinum macrocycle with 3,5-disubstituted pyridine thread, the reaction proceeded slowly and remained incomplete after heating for several days. The ^{1}H NMR spectrum became broad as the reaction was heated. The reaction was worked up when the coordinating DMSO peak had disappeared. The ^{1}H NMR of the crude product was inconclusive thus it was also examined by ESI(+)-MS which revealed the existence of the product showing $[M+2H]^{2+}$ (*m/z* 1556.80). Again column chromatography failed to purify the desired pseudorotaxane **36**.

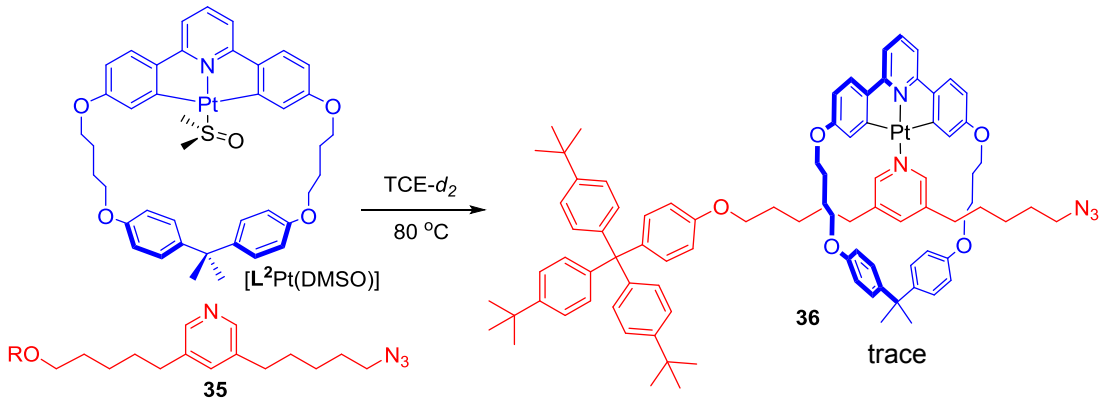

Scheme 3.26 Synthesis of asymmetric pseudorotaxane **36**.

3.3 Conclusion and Outlook

Attempts to synthesise a platinum complexed-[2]rotaxane have been investigated. Rotaxane formation using an active metal template copper(I)-catalysed azide-alkyne cycloaddition (CuAAC) "click" reaction was successful. Insertion of platinum(II) into the rotaxane using the modified known procedure did not afford the desired product which led to redesigns of the rotaxanes. Utilisation of a platinum complexed-macrocycle to undergo ligand exchange reactions with series of 3,5-disubstituted pyridine based-thread were studied. The instability of the rotaxane precursor with azide moiety discouraged the final click reaction step and purification process. Once the full threads with all binding stations were determined to avoid stability problems, a difficulty in separation was encountered.

It is hoped that conditions that overcome the reactivity problems without disturbing the macrocycle-thread interactions may be found. If such conditions are not found, a redesign will be required to finish the rotaxane.

The preliminary results from this chapter are encouraging, however. It is hoped that either the design presented here or one very similar may soon be made to overcome the purification problems and realise the desired rotaxanes. Once the rotaxane is realised, studies of acid-base stimuli-responsive bistable platinum-complexed [2]rotaxane will be explored, as suggested from the positive results of the "3+1" to "2+2" interconversion of non-interlocked platinum C^N^C macrocyclic compounds in Chapter II.

3.4 Experimental Section

3.4.1 General Experimental Procedure

Unless stated otherwise, all reagents and solvents were purchased from commercial sources and used without further purification. tris-(*p*-*tert*-butylphenyl)(4-hydroxyphenyl)methane (**1**)[22], 1-(prop-3-ynoxy)-4-(tris-(4-tert-butyl-phenyl)-methyl)-benzene (**2**)[5a], compound **27**[22], **28**[21a], **29**[5b] and **30**[5b] were prepared according to literature procedures.

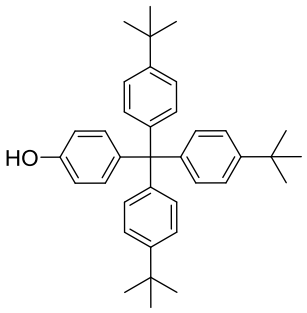

1

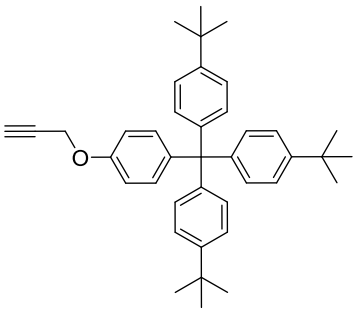

2

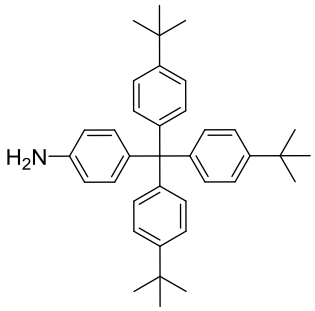

27

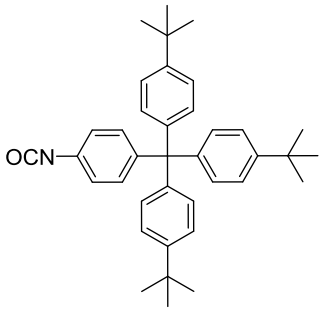

28

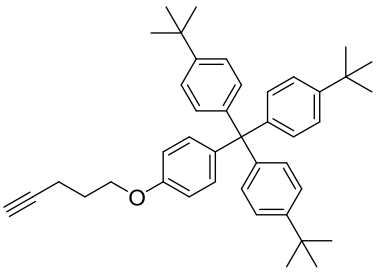

29

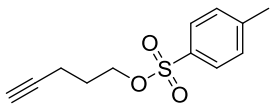

30

3.4.2 Synthesis

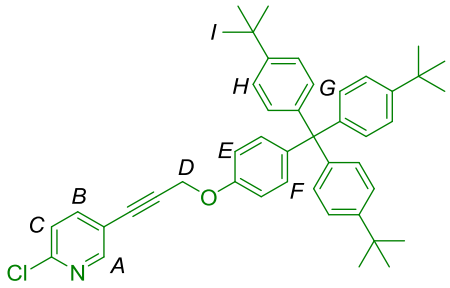

3

A two-necked flask was charged with $[Pd(PPh_3)_2]Cl_2$ (35 mg, 0.05 mmol, 5 mol%) and PPh_3 (26 mg, 0.10 mmol, 10 mol%) and was purged with nitrogen. Contents were suspended in Et_3N (3 mL) and the solution was allowed to stir under N_2 for 10 min. 2-Chloro-5-iodopyridine (0.24 g, 1 mmol) and CuI (19 mg, 0.10 mmol, 10 mol%) were added as solids. After an additional 10 min, **2** (0.54 g, 1 mmol) and degassed THF (8 mL) were added and the mixture was allowed to stir overnight. All the volatile organic substances were removed under vacuum, dissolved with CH_2Cl_2 and filtered through celite. The residue was washed with H_2O (3×20 mL) and the aqueous phase was extracted with CH_2Cl_2 (3×20 mL). The combined organic phases were dried over Na_2SO_4. The white solid product was obtained after purification by column chromatography (20-40% CH_2Cl_2/hexane), (0.56 g, 86%). m.p. 216-219°C; ^{1}H NMR (400 MHz, $CDCl_3$); 8.45 (d, J = 2.2 Hz, 1H, H_A), 7.67 (dd, J = 8.3, 2.2 Hz, 1H, H_B), 7.29 (d, J = 8.3 Hz, 1H, H_C), 7.23 (d, J = 8.6 Hz, 6H, H_G), 7.13 (d, J = 8.9 Hz, 2H, H_F), 7.07 (d, J = 8.6 Hz, 6H, H_H), 6.87 (d, J = 8.9 Hz, 2H, H_E), 4.89 (s, 2H, H_D), 1.30 (s, 27H, H_I); ^{13}C NMR (100 MHz, $CDCl_3$); 155.5, 152.3, 151.0, 148.4, 144.0, 141.2, 140.7, 132.4, 130.7, 124.1, 123.9, 118.4, 113.4, 88.8, 82.5, 63.1, 56.4, 34.3, 31.4; HR-ESIMS m/z = 653.34222 $[M-H]^-$ (calc. for $C_{45}H_{48}NOCl$, 653.34189).

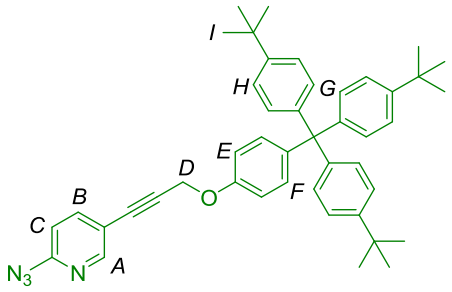

4

To a solution of **3** (0.22 g, 0.34 mmol) in dry DMF (5 mL) was added NaN_3 (65 mg, 1 mmol) and the reaction mixture was stirred at 120°C for 18 h. The solution was cooled down to rt and H_2O (15 mL) was added to the reaction mixture and the aqueous phase was extracted with CH_2Cl_2 (3×20 mL). The organic phases were combined, dried over $MgSO_4$ and then filtered off. The excess solvent was removed under reduced pressure and the resulting residue was purified by flash column chromatography (0-2% MeOH in CH_2Cl_2) to give desired product as a white solid (0.08 g, 34%). ^{1}H NMR (400 MHz, $CDCl_3$); 8.88 (d, J = 2.3 Hz, 1H, H_A), 8.14 (dd, J = 8.3, 2.3 Hz, 1H, H_B), 7.42 (d, J = 8.3 Hz, 1H, H_C), 7.24 (d, J = 8.6 Hz, 6H, H_G), 7.12 (d, J = 8.9 Hz, 2H, H_F), 7.08 (d, J = 8.6 Hz, 6H, H_H), 6.88 (d, J = 8.9 Hz, 2H, H_E), 5.23 (s, 2H, H_D), 1.30 (s, 27H, H_I); ^{13}C NMR (100 MHz, $CDCl_3$); 171.2, 155.6, 151.6, 148.5, 143.9, 140.8, 137.7, 134.9, 130.7, 126.9, 124.1, 112.5, 110.0, 95.9, 85.7, 63.1, 55.8, 34.3, 31.4; HR-ESIMS m/z = 697.33342 $[M+K]^+$ (calc. for $C_{45}H_{46}ON_4K$, 697.33142).

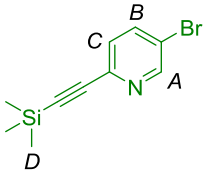

6

To a round bottom flask with a septum under nitrogen, 5-bromo-2-iodopyridine (0.28 g, 1 mmol) in degassed THF (15 mL) were successively added ethynyltrimethylsilane (0.295 g, 0.43 mL, 3 mmol), $Pd(PPh_3)_2Cl_2$ (0.035 g, 0.05 mmol, 5 mol%), PPh_3 (0.026 g, 0.10 mmol, 10 mol%), CuI (0.019 g, 0.10 mmol, 10 mol%) and finally Et_3N (8 mL). The solution was stirred at rt. The colour of the solution turned black with the formation of white solid. After the starting materials were consumed (TLC, NMR, ~48 h), the mixture was treated with activated carbon (*ca.* 200 mg) and filtered through celite. The solvent was evaporated and the product was obtained by column chromatography (0-20%

CH_2Cl_2/hexane) as a white solid (0.12 g, 45.2%). ^{1}H NMR (500 MHZ, $CDCl_3$); 8.55 (d, *J* = 2.2 Hz, 1H, H_A), 7.70 (dd, *J* = 8.3, 2.2 Hz, 1H, H_B), 7.27 (d, *J* = 8.3, 1H, H_C), 0.20 (s, 9H, H_D); ^{13}C NMR (125 MHz, $CDCl_3$); 151.0, 141.3, 138.7, 128.2, 120.3, 102.6, 96.4, -0.4.

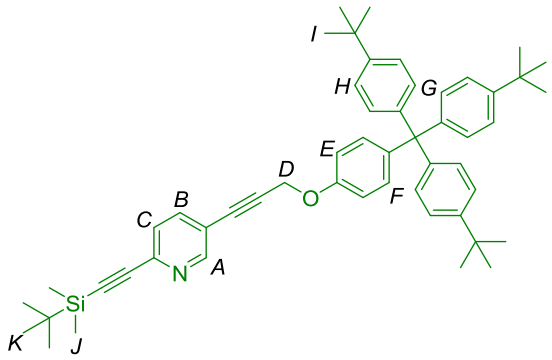

9

A Schlenk tube was evacuated and backfilled with N_2 (3x) before 2-*tert*-butyldimethylsilylethynyl-5-bromopyridine, **8** (Chapter II) (0.40 g, 1.35 mmol, 1 eq), CuI (0.016 g, 0.084 mmol, 6 mol%) and $Pd(PPh_3)_4$ (0.047 g, 0.041 mmol, 3 mol%) were added under positive flow of nitrogen. A solution of 1-(prop-3-ynoxy)-4-(tris-(4-tert-butyl-phenyl)-methyl)-benzene, **2** (0.88 g, 1.62 mmol, 1.2 eq) in 1:1 dry THF/ Et_3N (12 mL) was injected. The solution was heated at 60°C for 24 h. The reaction was quenched with saturated aqueous ammonium chloride and then filtered through celite and washed with THF. The crude product was extracted with CH_2Cl_2, dried over $MgSO_4$, filtered, concentrated in vacuo and purified by flash column chromatography (SiO_2, 0-40% CH_2Cl_2/hexane) to get an off-white solid (0.90 g, 87%). ^{1}H NMR (500 MHz, $CDCl_3$); δ 8.70 (d, *J* = 1.4 Hz, 1H, H_A), 7.70 (dd, *J* = 8.1, 2.1 Hz, 1H, H_B), 7.45 (dd, *J* = 8.1, 0.6 Hz, 1H, H_C), 7.34 – 7.28 (m, 6H, H_H), 7.24 – 7.21 (m, 2H, H_F), 7.21 – 7.15 (m, 6H, H_G), 6.97 – 6.90 (m, 2H, H_E), 4.93 (s, 2H, H_D), 1.38 (s, 27H, H_I), 1.11 (s, 9H, H_K), 0.31 (s, 6H, H_J); ^{13}C NMR (125 MHz, $CDCl_3$); δ 155.6, 152.6, 148.4, 144.1, 142.2, 140.7, 138. 8, 132.4, 130.8, 126.7, 124.2, 118.8, 113. 6, 104.2, 95.7, 89.4, 83.6, 63.2, 56.5, 34.4, 31.5, 26.2, 16.8, -4.7; HR-ESIMS *m/z* = 758.47230 $[M+H]^+$ (calc. for $C_{53}H_{64}NOSi$ 758.47517).

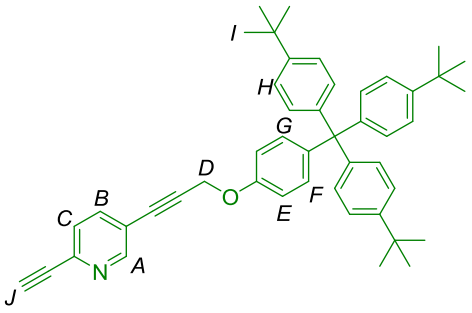

10

To a solution of **9** (0.96 g, 1.27 mmol) in dry THF (12 mL) was added TBAF (1 M in THF, 2.5 mL, 2.50 mmol) which resulted in the pale yellow solution turning brown. The stirring was continued for 18 h at room temperature until TLC indicated that no starting materials remained. The solvent was removed under reduced pressure. The residue was purified by flash column chromatography (SiO_2, 0-50% CH_2Cl_2/hexane) to get **4** as an off white solid (0.19 g, 35%) m.p. 188 °C (dec.); ^{1}H NMR (500 MHz, $CDCl_3$); δ 8.64 (s, 1H, H_A), 7.69 (dd, J = 8.1, 2.1 Hz, 1H, H_B), 7.42 (dd, J = 8.1, 0.7 Hz, 1H, H_C), 7.24 (d, J = 8.7 Hz, 6H, H_H), 7.13 (d, J = 9.0 Hz, 2H, H_F), 7.08 (d, J = 8.7 Hz, 6H, H_G), 6.88 (d, J = 9.0 Hz, 2H, H_E), 4.90 (s, 2H, H_D), 3.24 (s, 1H, H_J), 1.30 (s, 27H, H_I); ^{13}C NMR (125 MHz, $CDCl_3$); δ 155.7, 152.8, 148.6, 144.2, 141.5, 140.9, 139.0, 132.5, 130.9, 126.8, 124.2, 119.4, 113.6, 89.7, 83.5, 82.5, 79.2, 63.2, 56.6, 34.4, 31.5; HR-ESIMS *m/z* = 644.38620 $[M+H]^+$ (calc. for $C_{47}H_{50}NO$ 644.38869).

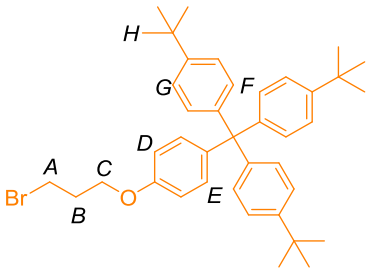

11

To a flame-dried round bottom flask with K_2CO_3 (2.77 g, 20 mmol) and NaI (0.03 g, 0.2 mmol) in it, was added 1,3-dibromopropane (4.05 g, 20 mmol) and tris-(*p-tert*-butylphenyl)(4-hydroxyphenyl)methane, **1** (1.01 g, 2 mmol). Degassed butanone (100 mL) was added and the resulting mixture was stirred at reflux temperature overnight. The solvent was removed and the residue was partitioned in CH_2Cl_2/H_2O. The aqueous phase was extracted with CH_2Cl_2 (3×20 mL), the organic phases were washed with H_2O,

dried over $MgSO_4$. The solvent was evaporated and the residue was purified by flash column chromatography (10% CH_2Cl_2/hexane) to give a white solid as a product (1.15 g, 92%). m.p. 249-250 °C; ^{1}H NMR (400 MHz, $CDCl_3$); 7.23 (d, J = 8.7 Hz, 6H, H_F), 7.09 (d, J = 8.9 Hz, 2H, H_E), 7.08 (d, J = 8.7 Hz, 6H, H_G), 6.77 (d, J = 8.9 Hz, 2H, H_D), 4.08 (t, J = 5.8 Hz, 2H, H_C), 3.60 (t, J = 6.5 Hz, 2H, H_A), 2.36-2.25 (m, 2H, H_B), 1.30 (s, 27H, H_H); ^{13}C NMR (100 MHz, $CDCl_3$); 155.5, 148.4, 144.0, 140.5, 132.3, 130.7, 124.1, 113.0, 64.2, 63.1, 48.3, 34.3, 31.4, 28.9; HR-ESIMS m/z = 647.28560 $[M+Na]^+$ (calc. for $C_{40}H_{49}O^{79}BrNa$ 647.28590).

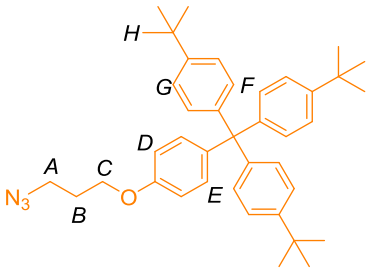

12

To a solution of **11** (0.62 g, 1 mmol) in dry DMF (25 mL) was added NaN_3 (0.20 g, 3 mmol) and the reaction mixture was stirred at 100°C overnight. The mixture was cooled to rt and H_2O (25 mL) was added and the aqueous phase was extracted with CH_2Cl_2 (3×40 mL). The organic phases were combined, dried over $MgSO_4$ and filtered off. The solvent was removed and the residue was purified by flash column chromatography (2-20% CH_2Cl_2/hexane). The product was a white solid (0.49 g, 84%). m.p. 220-222 °C; ^{1}H NMR (400 MHz, $CDCl_3$); 7.23 (d, J = 8.7 Hz, 6H, H_F), 7.11-7.05 (m, 8H, H_{E+G}), 6.76 (d, J = 9.0 Hz, 2H, H_D), 4.02 (t, J = 5.9 Hz, 2H, H_C), 3.51 (t, J = 6.7 Hz, 2H, H_A), 2.09-1.98 (m, 2H, H_B), 1.30 (s, 27H, H_H); ^{13}C NMR (100 MHz, $CDCl_3$); 155.5, 148.3, 144.1, 140.5, 132.3, 130.7, 124.1, 113.0, 64.3, 63.1, 48.3, 34.3, 31.4, 28; HR-ESIMS m/z = 610.37590 $[M+Na]^+$ (calc. for $C_{40}H_{49}N_3ONa$ 610.37678).

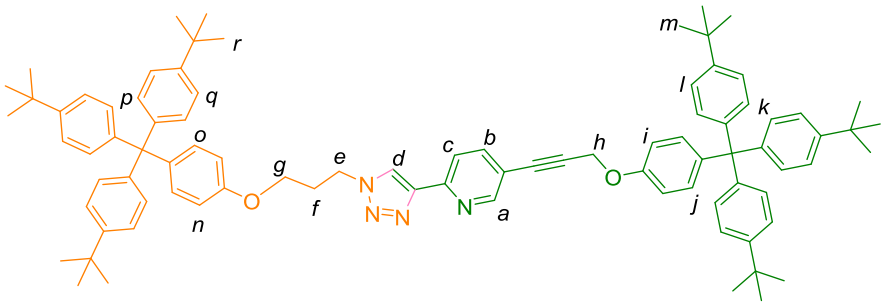

13

Azide **12** (0.018 g, 31 µmol, 1 eq), alkyne **10** (0.02 g, 31 µmol, 1 eq) and $[Cu(CH_3CN)_4]PF_6$ (0.014 g, 37 µmol, 1.1 eq) were added to a flask under N_2. Degassed 1,2-dichloroethane (6 mL) was injected. The mixture was purged with N_2 and left stirring at rt for 24 h. The reaction flask was heated at 70 °C for 3 d. The mixture was cooled to rt and diluted with CH_2Cl_2 (10 mL), filtered through celite. The filtrate was evaporated under vacuum. The residue was dissolved in CH_2Cl_2, washed with 0.1 M Sodium EDTA and brine, dried over Na_2SO_4 The product was obtained as a white solid following purification from column chromatography (CH_2Cl_2) (0.01 g, 28%). m.p. 190-192 °C; ^{1}H NMR (600 MHz, $CDCl_3$); δ 8.64 (d, *J* = 1.1 Hz, 1H, H_a), 8.18 (s, 1H, H_d), 8.13 (d, *J* = 8.2 Hz, 1H, H_c), 7.81 (dd, *J* = 8.2, 2.0 Hz, 1H, H_b), 7.27 – 7.22 (m, 12H, H_{l+q}), 7.15 (d, *J* = 8.9 Hz, 2H, H_j), 7.13 – 7.08 (m, 16H, H_{k+o+p}), 6.90 (d, *J* = 8.9 Hz, 2H, H_i), 6.76 (d, *J* = 8.9 Hz, 2H, H_n), 4.91 (s, 2H, H_h), 4.66 (t, *J* = 6.9 Hz, 2H, H_g), 4.00 (t, *J* = 5.6 Hz, 2H, H_e), 2.50 – 2.38 (m, 2H, H_f), 1.32 (s, 54H, H_{m+r}); ^{13}C NMR (150 MHz, $CDCl_3$); δ 156.3, 155.8, 152.3, 151.4, 149.5, 148.5×2, 147.8, 144.2×2, 140.8 140.3, 139.9, 132.5×2, 130.9×2, 124.2, 123.0, 119.6, 118.6, 113.6, 113.1, 88.2, 84.0, 63.9, 63.2×2, 56.7, 34.4, 31.5, 30.1; HR-ESIMS *m/z* = 1253.75370 $[M+Na]^+$ (calc. for $C_{87}H_{98}N_4O_2Na$ 1253.75820).

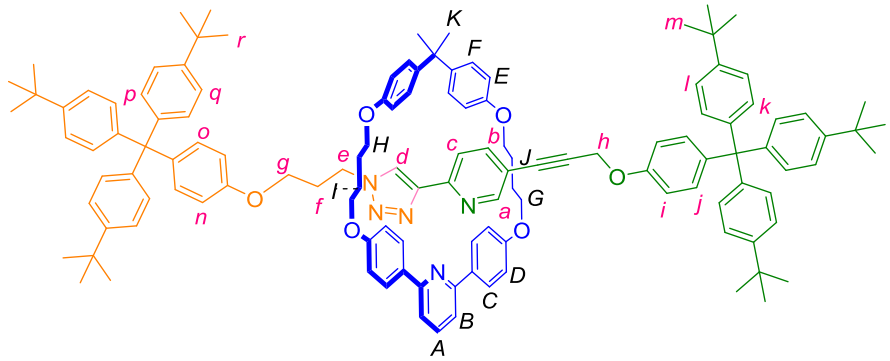

R^{2b}

Adapted from a procedure by Leigh and co-workers.[5b] Azide **6** (41.1 mg, 70 μmol), alkyne **4** (45.1 mg, 70μmol), macrocycle H_2**L²** (Chapter II) (42.0 mg, 70 μmol) and $[Cu(CH_3CN)_4]PF_6$ (28.7 mg, 77μmol) were added to a flask under N_2 atmosphere. Degassed 1,2-dichloroethane (12 mL) was injected. The mixture was purged with N_2 and left stirring at rt for 24 h. The reaction flask was heated at 70 °C for 3 d. The mixture was cooled to rt and diluted with CH_2Cl_2 (10 mL), filtered through celite. The filtrate was evaporated under vacuum. The residue was dissolved in CH_2Cl_2, washed with 0.1 M Sodium EDTA and brine, dried over Na_2SO_4 The product was obtained as a white solid following purification from column chromatography (1% MeOH/CH_2Cl_2) (21.2 mg, 16%). Along with rotaxane, non-interlocked thread **13** (50.6 mg) was generated during click reactions as well as unreacted macrocycle (8.9 mg). ^{1}H NMR (500 MHz, $CDCl_3$); δ 8.48 (d, *J* = 1.4 Hz, 1H, H_a), 7.92 (d, *J* = 8.8 Hz, 4H, H_C), 7.82 (d, *J* = 8.2 Hz, 1H, H_c), 7.65 (t, *J* = 7.8 Hz, 1H, H_A), 7.51 (dd, *J* = 8.2, 2.1 Hz, 1H, H_b), 7.48 – 7.42 (m, 2H, H_B), 7.31 (s, 1H, H_d), 7.24 – 7.18 (m, 12H, H_{l+q}), 7.09 – 7.02 (m, 14H, H_{j+k+p}), 6.97 (dd, *J* = 8.8, 3.7 Hz, 6H, H_{o+F}), 6.81 (d, *J* = 8.8 Hz, 4H, H_D), 6.76 (d, *J* = 9.0 Hz, 2H, H_i), 6.61 (d, *J* = 8.8 Hz, 4H, H_E), 6.42 (d, *J* = 8.9 Hz, 2H, H_n), 4.71 (s, 2H, H_h), 4.04 (t, *J* = 6.7 Hz, 6H, H_{G+e}), 3.82 (t, *J* = 5.6 Hz, 4H, H_H), 3.35 (t, *J* = 5.6 Hz, 2H, H_g), 1.92 – 1.78 (m, 10H, H_{J+I+f}), 1.56 (s, 6H, H_K), 1.30 (s, 27H, $H_{m/r}$), 1.29 (s, 27H, $H_{m/r}$); ^{13}C NMR (125 MHz, $CDCl_3$); δ 159.4, 156.8, 156.5×2, 155.9, 152.1, 149.5, 148.5×2, 147.5, 144.2×2, 143.2, 140.5, 139.8, 139.6, 137.3, 132.5, 132.4, 132.4, 130.9×2, 128.8, 127.7, 124.2, 122.9, 119.2, 118.2, 116.9, 115.1, 114.0, 113.4, 112.9, 88.0, 84.0, 67.5, 67.3, 64.0, 63.2×2, 56.6, 47.4, 41.4, 34.4, 31.5, 31.2, 29.8×2, 25.3, 22.8, 14.3; HR-ESIMS *m/z* = 1831.07940 $[M+H]^+$ (calc. for $C_{127}H_{140}N_5O_6$ 1831.07981).

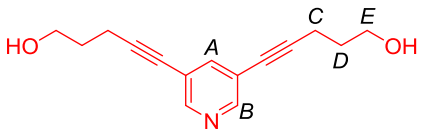

14

To a mixture of 3,5-dibromopyridine (0.71 g, 3 mmol), CuI (60.9 mg, 0.32 mmol, 10 mol%), $Pd(PPh_3)_2Cl_2$ (0.10 g, 0.14 mmol, 5 mol%) and PPh_3 (79.1 mg, 0.30 mmol, 10 mol%) in dry DMF (10 mL) under N_2 flow were injected 4-pentyn-1-ol (2.80 mL, 30 mmol) and Et_3N (6 mL). The solution was stirred at rt for 30 min and then heated to 80 °C overnight. The reaction mixture was cooled down, white precipitate was filtered off through celite. The filtrate was concentrated under reduced pressure. The residue was dissolved in CH_2Cl_2, washed with saturated NH_4Cl, brine. Combined organic phases were dried over $MgSO_4$, filtered, evaporated off the solvent. The pale yellow oil that solidified after several days (0.69 g, 94%) was obtained by flash column chromatography (SiO_2, 0-5% MeOH/CH_2Cl_2). ^{1}H NMR (400 MHz, MeOD-d_4); δ 8.36 (s, 2H, H_B), 7.65 (t, J = 1.9 Hz, 1H, H_A), 3.67 (t, J = 6.2 Hz, 4H, H_E), 2.51 (t, J = 7.1 Hz, 4H, H_C), 1.83 – 1.74 (m, 4H, H_D); ^{13}C NMR (100 MHz, MeOD-d_4); δ 150.7, 142.1, 122.2, 95.4, 77.4, 61.4, 32.3, 16.6; HR-ESIMS m/z = 244.13470 $[M+H]^+$ (calc. for $C_{15}H_{18}NO_2$ 244.13321).

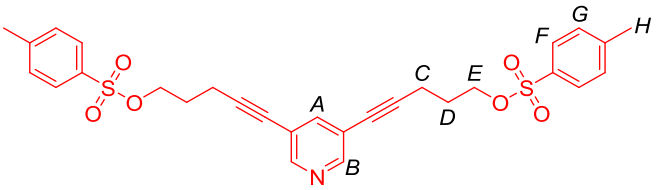

15

The solution of diol **14** (0.40 g, 1.6 mmol) in dry CH_2Cl_2 (5 mL) was cooled in an ice bath at 0 °C. A cold solution of *p*-toluenesulfonyl chloride, TsCl (1.30 g, 6.8 mmol) in dry CH_2Cl_2 (5 mL) was added and the solution mixture was stirred for 10 min followed by adding of Et_3N (10 mL). The reaction was stirred at 0 °C for 1 h then warmed to rt and kept stirring overnight. The mixture was filtered through celite. The filtrate was washed with saturated $NaHCO_3$. Combined organic layers were dried over $MgSO_4$, filtered and concentrated. The crude was purified by flash column chromatography (SiO_2, 50-100% CH_2Cl_2/hexane) to obtain a pale yellow oil (0.74 g, 82%). ^{1}H NMR (500 MHz, $CDCl_3$); δ 8.37 (d, J = 1.4 Hz, 2H, H_B), 7.80 (d, J = 8.2 Hz, 4H, H_F), 7.49 (t, J = 1.9 Hz, 1H, H_A), 7.31 (d, J = 8.2 Hz, 4H, H_G), 4.18 (t, J = 6.0 Hz, 4H, H_E), 2.51 (t, J = 6.8 Hz, 4H, H_C), 2.39 (s, 6H, H_H),

1.94 (tt, appearing as apparent pentet, J = 6.5 Hz, 4H, H_D); ^{13}C NMR (125 MHz, $CDCl_3$); δ 150.5, 145.0, 140.7, 132.8, 129. 9, 128.0, 120.0, 92.0, 77.8, 68.6, 27.7, 21.6, 15.7; HR-ESIMS m/z = 574.13410 $[M+Na]^+$ (calc. for $C_{29}H_{29}NO_6Na^{32}S_2$ 574.13285).

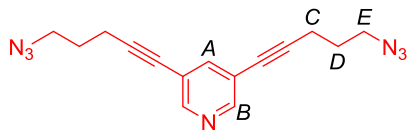

16

To a solution of bistosylate **15** (0.22 g, 0.4 mmol) in DMF (8 mL) under N_2 atmosphere was added an aqueous solution of NaN_3 (0.12 g in 1 mL, 1.8 mmol). The reaction was heated at 80 °C overnight. After the reaction was cooled down, water (8 mL) and Et_2O (15 mL) were added. Organic phase was collected and washed with water (3×10 mL). The combined Et_2O layers were dried over $MgSO_4$ and concentrated under reduced pressure to yield a brown residue. Purification by flash column chromatography (SiO_2, 0 – 3% MeOH/CH_2Cl_2) gave **16** (73 mg, 62%) as a yellow oil. ^{1}H NMR (500 MHz, $CDCl_3$); δ 8.53 (s, 2H, H_B), 7.65 (s, 1H, H_A), 3.44 (t, J = 6.6 Hz, 4H, H_E), 2.52 (t, J = 6.9 Hz, 4H, H_C), 1.85 (tt, appearing as apparent pentet, J = 6.8 Hz, 4H, H_D). ^{13}C NMR (125 MHz, $CDCl_3$); δ 150.5, 140.8, 120.5, 92.5, 50.2, 27.7, 16.8; HR-ESIMS m/z = 294.14640 $[M+H]^+$ (calc. for $C_{15}H_{16}N_7$ 294.14617).

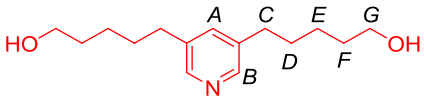

18

A Schlenk tube was evacuated and backfilled with N_2 (3×). Pd on activated carbon (10% Pd, 0.47 g, excess) was added under an inert atmosphere. A small amount of CH_2Cl_2 was injected to wash down any Pd/C stuck to the walls. A solution of unsaturated diol **14** (0.58 g, 2.4 mmol) in a mixture of CH_2Cl_2 and MeOH (6 mL) was charged carefully. The reaction mixture was stirred and the flask was evacuated just until the solvent begins to bubble, then carefully backfilled with nitrogen (3×). A balloon of H_2 was attached with a valve closed. The flask was evacuated (3×) and then the valve was opened. The reaction mixture was stirred at rt for 2 d when TLC showed no starting material remained. The balloon was taken off and the flask was refilled with nitrogen. The catalyst was filtered

off through celite, washed with CH_2Cl_2. The solvent was removed under vacuum to afford a pale yellow oil (0.57 g, 97%). ^{1}H NMR (500 MHz, $CDCl_3$); δ 8.26 (s, 2H, H_B), 7.31 (s, 1H, H_A), 3.64 (t, J = 6.5 Hz, 4H, H_G), 2.60 (m, 4H, H_C), 1.69-1.62 (m, 4H, H_F), 1.62 – 1.56 (m, 4H, H_D), 1.47 – 1.33 (m, 4H, H_E); ^{13}C NMR (100 MHz, $CDCl_3$); δ 145.0, 136.5, 120.9, 62.9, 33.0, 32.6, 31.0, 25.4.

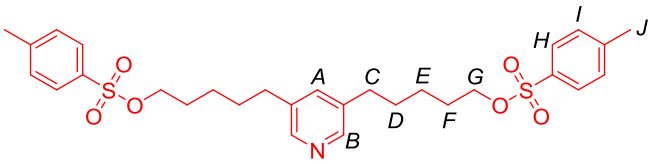

19

The title compound **19** could be obtained either from tosylation of diol **18** or hydrogenation of bistosylate **15**.

a) To a solution of diol **18** (0.40 g, 1.6 mmol) in dry CH_2Cl_2 (5 mL) was charged a solution of TsCl in dry CH_2Cl_2 (5 mL) at 0 °C. The solution was stirred for 10 min then Et_3N was charged. The reaction was stirred at 0 °C for 1 h, warmed to rt and kept stirring overnight. A saturated $NaHCO_3$ was added. The organic layer was collected and washed with water. The combined organic phases were dried ($MgSO_4$), filtered. The solvent was removed under reduced pressure. Flash column chromatography (SiO_2, 0 – 2% MeOH/CH_2Cl_2) gave pale yellow oil (0.30 g, 33%) as a product.

b) Saturated bistosylate **19** was synthesised following the same procedure as for diol **18** starting from **15** (0.74 g, 1.3 mmol). The reaction was stirred overnight, using Pd/C (10% Pd, 0.14 g). A pale yellow oil (0.70 g, 93%) was obtained. ^{1}H NMR (400 MHz, $CDCl_3$); δ 8.22 (d, J = 1.8 Hz, 2H, H_B), 7.77 (d, J = 8.3 Hz, 4H, H_H), 7.35 (d, J = 8.0 Hz, 4H, H_I), 7.26 (s, 1H, H_A), 4.02 (t, J = 6.4 Hz, 4H, H_G), 2.54 (t, J = 7.7 Hz, 4H, H_C), 2.44 (s, 6H, H_J), 1.72 – 1.61 (m, 4H, H_F), 1.61 - 1.51 (m, 4H, H_D), 1.42 – 1.30 (m, 4H, H_E); ^{13}C NMR (100 MHz, $CDCl_3$); δ 147.2, 144.6, 136.8, 135.5, 132.9, 129.7, 127.6, 70.3, 32.4, 30.2, 28.4, 24.8, 21.4; HR-ESIMS m/z = 560.2140 $[M+H]^+$ (calc. for $C_{29}H_{38}NO_6{}^{32}S_2$ 560.21351).

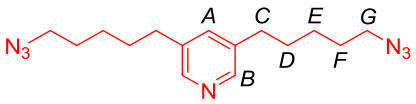

20

The title compound **20** was synthesised following the same procedure as for **16** starting from **19** (0.30 g, 0.5 mmol). Using NaN_3 (0.11 g, 1.7 mmol), brown oil (0.12 g, 78%) was obtained following flash column chromatography (SiO_2, 0–3% MeOH/CH_2Cl_2). ^{1}H NMR (600 MHz, $CDCl_3$); δ 8.27 (d, *J* = 2.1 Hz, 2H, H_B), 7.31-7.29 (m, 1H, H_A), 3.27 (t, *J* = 6.9 Hz, 4H, H_G), 2.63 – 2.59 (m, 4H, H_C), 1.69 – 1.60 (m, 8H, H_{D+F}), 1.47 – 1.39 (m, 4H, H_E); ^{13}C NMR (150 MHz, $CDCl_3$); δ 147.5, 137.0, 135.7, 51.4, 32.8, 30.7, 28.7, 26.3; HR-ESIMS *m/z* = 302.20890 $[M+H]^+$ (calc. for $C_{15}H_{24}N_7$ 302.20877).

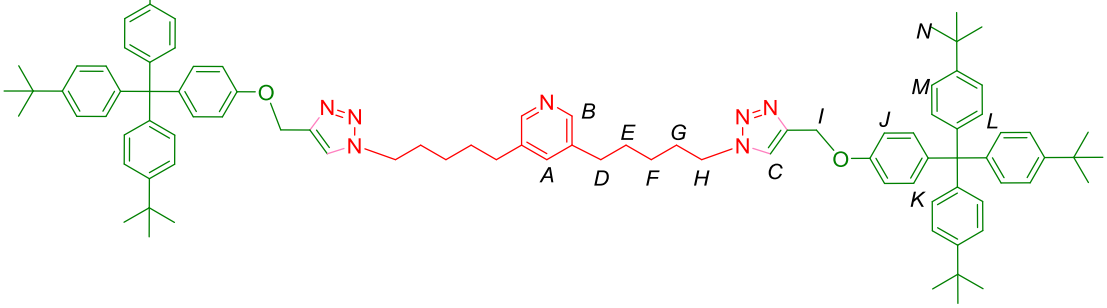

22

To a solution of 1-(prop-3-ynoxy)-4-(tris-(4-*tert*-butyl-phenyl)-methyl)-benzene, **2** (0.19 g, 0.3 mmol, 4 eq) in CH_2Cl_2 (3 mL) was added a solution of **20** (25.8 mg, 0.08 mmol, 1 eq) in CH_2Cl_2 (3 mL) and the solution was stirred for 10 min. DIPEA (15 µL, 0.08 mmol, 1 eq), TBTA (67.9 mg, 0.1 mmol, 1.5 eq) and tetrakis(acetonitrile)copper(I) hexafluorophosphate (32.1 mg, 0.08 mmol, 1 eq) were charged. The reaction mixture was stirred at rt for 24 h. The reaction was washed with 0.1 M Sodium EDTA (3×12 mL). The organic layer was dried over $MgSO_4$ and filtered. The solvent was removed under reduced pressure. The product was purified using flash column chromatography (SiO_2, 0–3% MeOH/CH_2Cl_2) to yield an off white solid. m.p. 219 °C; ^{1}H NMR (500 MHz, $CDCl_3$) δ 7.57 (s, 2H, H_C), 7.32 (bs, 2H, H_B), 7.25 – 7.19 (m, 12H, H_M), 7.13 – 7.09 (m, 5H, H_{K+A}), 7.08 (d, *J* = 8.6 Hz, 12H, H_L), 6.85 (d, *J* = 8.9 Hz, 4H, H_J), 5.17 (s, 4H, H_I), 4.35 (t, *J* = 7.1 Hz, 4H, H_H), 2.68 – 2.51 (m, 4H, H_D), 2.01 – 1.89 (m, 4H, H_G), 1.72 – 1.59 (m, 4H, H_E), 1.42 – 1.34

(m, 4H, H_F), 1.30 (s, 54H, H_N); ^{13}C NMR (125 MHz, $CDCl_3$); δ 156.2, 148.4, 144.5, 144.2, 140.3, 132.4, 130.8, 129.2, 128.2, 124.2, 122.6, 114.2, 113.3, 63.2, 62.2, 53.5, 50.3, 34.4, 31.5, 30.6, 30.2, 26.2; HR-ESIMS *m/z* = 1386.92020 $[M+H]^+$ (calc. for $C_{95}H_{116}N_7O_2$ 1386.91850).

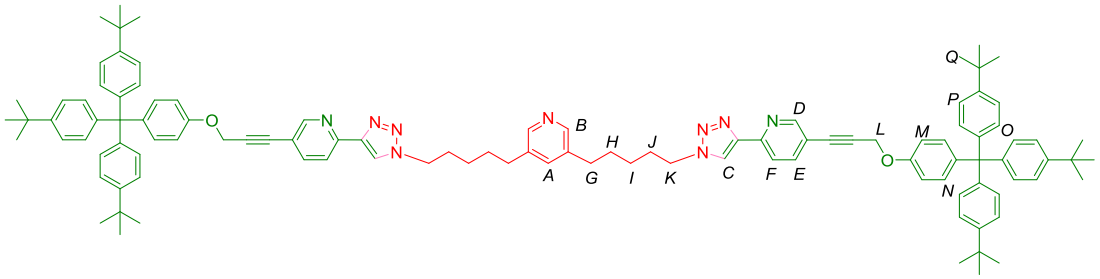

23

A mixture of **20** (18 mg, 0.06 mmol), **10** (76.9 mg, 0.1 mmol) and $CuSO_4$ (2.8 mg, 0.018 mmol, 30 mol%) in 1:1 *t*-butanol/water (5 mL) was stirred at rt. (+)-Sodium *L*-ascorbate (6.5 mg, 0.033 mmol, 40 mol%) was then charged as solid. The reaction mixture was stirred at 60 °C overnight. The mixture was partition by adding CH_2Cl_2. The organic layer was washed with 0.1 M Sodium EDTA (3×20 mL). The combined organic phases were dried ($MgSO_4$), filtered, concentrated and purified by flash column chromatography (SiO_2, 0–2% MeOH/CH_2Cl_2) to obtained a pale yellow solid (65.8 mg, 69 %). ^{1}H NMR (600 MHz, $CDCl_3$); δ 8.62 (dd, *J* = 2.1, 0.9 Hz, 2H, H_D), 8.25 (s, 2H, H_B), 8.14 (s, 2H, H_C), 8.12 (d, *J* = 0.9 Hz, 2H, H_F), 7.80 (dd, *J* = 8.2, 2.1 Hz, 2H, H_E), 7.25 – 7.21 (m, 13H, H_{P+A}), 7.14 (d, *J* = 9.0 Hz, 4H, H_N), 7.09 (d, *J* = 8.7 Hz, 12H, H_O), 6.89 (d, *J* = 9.0 Hz, 4H, H_M), 4.90 (s, 4H, H_L), 4.42 (t, *J* = 7.1 Hz, 4H, H_K), 2.57 (t, *J* = 7.7 Hz, 4H, H_G), 2.03 – 1.94 (m, 4H, H_J), 1.71 – 1.62 (m, 4H, H_H), 1.45 – 1.37 (m, 4H, H_I), 1.30 (s, *J* = 2.2 Hz, 54H, H_Q); ^{13}C NMR (150 MHz, $CDCl_3$); δ 155.7, 152.2, 149.6, 148.5, 147.9, 147.5, 144.2, 140.7, 139.8, 137.0, 135.8, 132.4, 130.8, 124.2, 122.4, 119.5, 118.5, 113. 6, 88.1, 84.0, 63.2, 56.7, 53.5, 50.4, 34.4, 32.7, 31.5, 30.6, 30.1, 26.1; HR-ESIMS *m/z* = 1588.97520 $[M+H]^+$ (calc. for $C_{109}H_{122}O_2N_9$ 1588.97160)

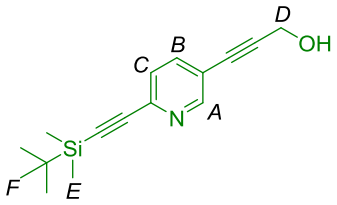

24

A Schlenk tube was evacuated and backfilled with N_2 (3x) before 2-*tert*-butyldimethylsilylethynyl-5-bromopyridine **8** (0.80 g, 2.7 mmol, 1 eq), CuI (31.1 mg, 0.16 mmol, 6 mol%) and $Pd(PPh_3)_4$ (93.4 mg, 0.08 mmol, 3 mol%) were added under nitrogen flow. A solution of propargyl alcohol (0.2 mL, 3.4 mmol, 1.2 eq) in dry 2:1 THF/ Et_3N (15 mL) was added. The solution was heated at 60°C for 5 d. The reaction was quenched with saturated NH_4Cl, filtered through celite and washed with THF. The crude product was extracted with CH_2Cl_2, dried over $MgSO_4$, filtered, concentrated in vacuo and purified by flash column chromatography (SiO_2, 0-100% CH_2Cl_2/hexane) to obtain an off-white solid (0.60 g, 82%). ^{1}H NMR (600 MHz, $CDCl_3$); δ 8.61 (dd, *J* = 2.2, 0.9 Hz, 1H, H_A), 7.62 (dd, *J* = 8.1, 2.2 Hz, 1H, H_B), 7.37 (dd, *J* = 8.1, 0.9 Hz, 1H, H_C), 4.49 (s, 2H, H_D), 0.97 (s, 9H, H_F), 0.18 (s, *J* = 3.4 Hz, 6H, H_E); ^{13}C NMR (125 MHz, $CDCl_3$); δ 152.3, 141.6, 138.9, 126.9, 119.4, 103.8, 96.2, 93.6, 81.5, 51.1, 26.2, 16.7, -4.8; HR-ESIMS *m/z* = 272.14720 $[M+H]^+$ (calc. for $C_{16}H_{22}NOSi$ 272.14652).

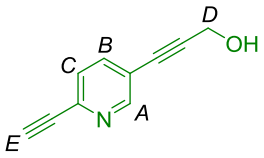

25

To a solution of **24** (0.23 g, 0.8 mmol, 1 eq) in dry THF (5 mL) was added TBAF (1 M in THF, 1.2 mL, 1.50 eq). The reaction was stirred overnight at room temperature until TLC indicated that no starting material remained. The solvent was removed under reduced pressure. The residue was purified by flash column chromatography (SiO_2, 50 - 100% CH_2Cl_2/hexane) to get brown solid (80.4 mg, 63%). m.p. 173 °C; ^{1}H NMR (500 MHz, $CDCl_3$); δ 8.65 (dd, *J* = 2.2, 0.9 Hz, 1H, H_A), 7.69 (dd, *J* = 8.1, 2.2 Hz, 1H, H_B), 7.44 (dd, *J* = 8.1, 0.9 Hz, 1H, H_C), 4.53 (s, 2H, H_D), 3.25 (s, 1H, H_E); ^{13}C NMR (125 MHz, $CDCl_3$); δ 152.6, 141.3, 138.9, 126.9, 119.7, 92.8, 82.4, 82.1, 79.3, 51.6; HR-ESIMS *m/z* = 158.05860 $[M+H]^+$ (calc. for $C_{10}H_8NO$ 158.06004).

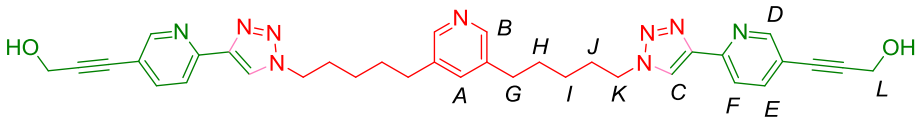

26

A mixture of **25** (31.1 mg, 0.2 mmol), **20** (29.8 mg, 0.1 mmol) and $CuSO_4$ (5.5 mg, 0.03 mmol, 30 mol%) in 1:1 *t*-butanol/water (6 mL) was stirred at rt under nitrogen atmosphere. A solution of (+)-sodium *L*-ascorbate (1 M, 40 µL, 0.04 mmol, 40 mol%) was then charged. The reaction mixture was stirred at 60 °C overnight. The mixture was partition by adding CH_2Cl_2. The organic layer was washed with 0.1 M Sodium EDTA (3×15 mL). The combined organic phases were dried ($MgSO_4$), filtered, concentrated. The residue was recrystallised in a mixture of MeOH/CH_2Cl_2 to obtain yellow solid (25.7 g, 42%). ^{1}H NMR (500 MHz, CD_2Cl_2); δ 8.60 (dd, *J* = 2.2, 0.9 Hz, 2H, H_D), 8.20 (d, *J* = 2.1 Hz, 2H, H_B), 8.14 (s, 2H, H_C), 8.09 (dd, *J* = 8.2, 0.9 Hz, 2H, H_F), 7.80 (dd, *J* = 8.2, 2.2 Hz, 2H, H_E), 7.21 (t, *J* = 2.1 Hz, 1H, H_A), 4.51 (s, 4H, H_L), 4.39 (t, *J* = 7.1 Hz, 4H, H_K), 3.76 (s, 2H, H_M), 2.57 – 2.50 (m, 4H, H_G), 2.00 – 1.91 (m, 4H, H_J), 1.66 – 1.58 (m, 4H, H_H), 1.40 - 1.31 (m, 4H, H_I); ^{13}C NMR (125 MHz, $CDCl_3$); δ 152.1, 149.4, 147.9, 145.2 (br), 139.8, 138.2, 122.5, 119.7, 118.9, 91.6, 82.5, 51.5, 50.5, 32.6, 30.3, 30.0, 26.0; HR-ESIMS *m/z* = 616.31520 $[M+H]^+$ (calc. for $C_{35}H_{37}N_9O_2$ 616.31430).

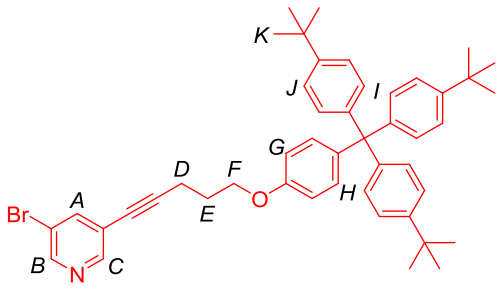

32

To a suspension of 3,5-dibromopyridine (0.22 g, 0.9 mmol, 1 eq), CuI (27.3 mg, 0.14 mmol, 10 mol%) and $Pd(PPh_3)_2Cl_2$ (32.3 mg, 0.046 mmol, 5 mol%) in dry THF (10 mL) was added a solution of **29** (0.57 g, 1 mmol, 1.1 eq) in THF followed by diisopropylamine (0.3 mL, 2 mmol, 2 eq). The reaction mixture was heated at 60 °C and left stirring overnight. The mixture was cooled down. The solvent was taken off in vacuo. The residue was dissolved in CH_2Cl_2, washed with saturated NH_4Cl and brine. Combined organic layers were dried over $MgSO_4$, filtered. The off white solid product (0.44 g, 67%) was

obtained by flash column chromatography (SiO_2, 0–3% $MeOH/CH_2Cl_2$). off white solid. m.p. 195-197 °C; ^1H NMR (500 MHz, $CDCl_3$); δ 8.60 (d, J = 2.2 Hz, 1H, $H_{B/C}$), 8.57 (d, J = 1.7 Hz, 1H, $H_{B/C}$), 7.85 (dd, appearing as apparent triplet, 1H, H_A), 7.28 (d, J = 8.7 Hz, 6H, H_I), 7.18 – 7.11 (m, 8H, H_{H+J}), 6.82 (d, J = 8.9 Hz, 2H, H_G), 4.11 (t, J = 6.0 Hz, 2H, H_F), 2.69 (t, J = 7.0 Hz, 2H, H_D), 2.15 - 2.07 (m, appearing as apparent pentet, 2H, H_E), 1.35 (s, 27H, H_K); ^{13}C NMR (125 MHz, $CDCl_3$); δ 156.8, 150.5, 148.4, 144.3, 141.1, 139.9, 132.4, 130.9, 124.2, 120.7, 113.1, 93.7, 77.3, 66.2, 63.2, 34.4, 31.5, 28.6, 16.5; HR-ESIMS m/z = 726.32920 $[M+H]^+$ (calc. for $C_{47}H_{53}NO^{79}Br$ 726.33050).

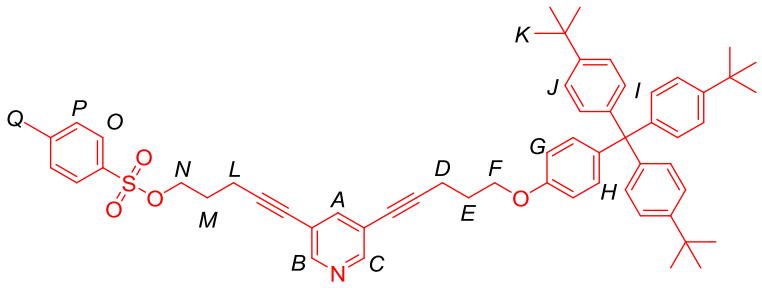

33

To a suspension of **32** (0.45 g, 0.6 mmol, 1 eq), CuI (17.1 mg, 0.09 mmol, 10 mol%) and $Pd(PPh_3)_2Cl_2$ (21.6 mg, 0.03 mmol, 5 mol%) in dry THF (10 mL) was added a solution of **30** (0.19 g, 0.8 mmol, 1.1 eq) in THF followed by diisopropylamine (0.2 mL, 1.4 mmol, 2 eq). The reaction mixture was heated at 60 °C and left stirring overnight. The mixture was cooled down. The solvent was taken off in vacuo. The residue was dissolved in CH_2Cl_2, washed with saturated NH_4Cl and brine. Combined organic layers were dried over $MgSO_4$, filtered. The pale brown solid product (0.24 g, 44%) was obtained by flash column chromatography (SiO_2, 0–3% $MeOH/CH_2Cl_2$). ^1H NMR (500 MHz, $CDCl_3$); δ 8.49 (bs, 1H, $H_{B/C}$), 8.37 (bs, 1H, $H_{B/C}$), 7.80 (d, J = 8.2 Hz, 2H, H_O), 7.55 (dd, appearing as apparent triplet, 1H, H_A), 7.30 (d, J = 8.2 Hz, 2H, H_P), 7.23 (d, J = 8.6 Hz, 6H, H_I), 7.11 - 7.05 (m, 8H, H_{H+J}), 6.78 (d, J = 8.9 Hz, 2H, H_G), 4.18 (t, J = 6.0 Hz, 2H, H_N), 4.07 (t, J = 6.0 Hz, 2H, H_F), 2.64 (t, J = 7.0 Hz, 2H, H_D), 2.50 (t, J = 6.8 Hz, 2H, H_L), 2.38 (s, 3H, H_Q), 2.11 – 2.04 (m, 2H, H_E), 1.97 – 1.90 (m, 2H,H_M), 1.30 (s, 27H, H_K); ^{13}C NMR (125 MHz, $CDCl_3$); δ 156.8, 150.8, 150.5, 148.5, 145.0, 144.3, 140.9, 139.9, 133.0, 132.4, 130.9, 130.0, 128.1, 128.0, 124.2, 113.1, 93.8, 91.9, 78.0, 77.3, 68.7, 66.2, 63.2, 34.4, 31.5, 28.6, 27.8, 21.7, 16.5, 15.8; HR-ESIMS m/z = 884.46670 $[M+H]^+$ (calc. for $C_{59}H_{66}NO_4{}^{32}S$ 884.47071).

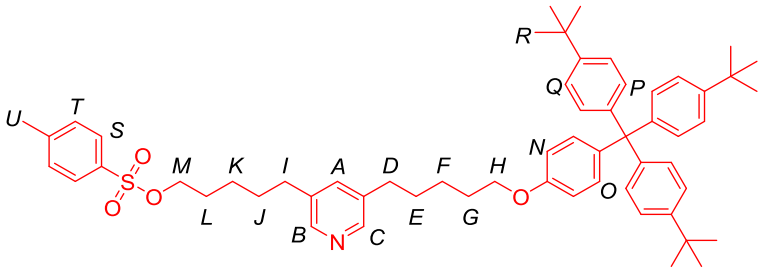

34

The title compound **34** was synthesised as described for hydrogenation reaction to get **19**. Using **33** (0.24 g, 0.27 mmol), Pd/C (10% Pd, 52.5 mg) to afford **34** as pale brown solid (0.24 g, 100%). ^{1}H NMR (500 MHz, $CDCl_3$) δ 8.32 (bs, 1H, $H_{B/C}$), 8.27 (bs, 1H, $H_{B/C}$), 7.77 (d, *J* = 8.3 Hz, 2H, H_S), 7.48 (bs, 1H, H_A), 7.34 (d, *J* = 7.9 Hz, 2H, H_T), 7.22 (d, *J* = 8.7 Hz, 6H, H_P), 7.08 (d, *J* = 8.7 Hz, 8H, H_{Q+O}), 6.74 (d, *J* = 9.0 Hz, 2H, H_N), 4.05 – 3.97 (m, 2H, H_M), 3.93 (t, *J* = 6.3 Hz, 2H, H_H), 2.71 – 2.65 (m, 2H, H_D), 2.60 (m, 2H, H_I), 2.44 (s, 6H, H_U), 1.85 – 1.76 (m, 2H, H_G), 1.75 – 1.46 (m, 8H, $H_{E+K+J+L}$), 1.44 – 1.32 (m, 2H, H_F), 1.30 (s, 27H, H_R); HR-ESIMS *m/z* = 892.53170 $[M+H]^+$ (calc. for $C_{59}H_{74}NO_4{}^{32}S$ 892.53331).

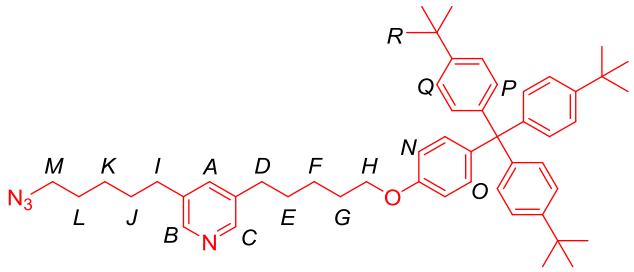

35

To a solution of **33** (0.24 g, 0.27 mmol) in DMF (5 mL) was added an aqueous solution of NaN_3 (30.2 mg, 0.46 mmol). The reaction mixture was stirred at 80 °C overnight. The reaction was cooled to rt, water was added. The crude product was extracted with Et_2O (3×10 mL), dried ($MgSO_4$), and filtered. The light brown solid (95.1 mg, 45%) was obtained from flash column chromatography (SiO_2, 1% $MeOH/CH_2Cl_2$). m.p. 174 – 176 °C; ^{1}H NMR (500 MHz, $CDCl_3$); δ 8.28 (d, *J* = 6.7 Hz, 2H, H_{B+C}), 7.31 (bs, 1H, H_A), 7.23 (d, *J* = 8.7 Hz, 6H, H_P), 7.12 – 7.04 (m, 8H, H_{Q+O}), 6.75 (d, *J* = 8.9 Hz, 2H, H_N), 3.93 (t, *J* = 6.4 Hz, 2H, H_H), 3.26 (t, *J* = 6.9 Hz, 2H, H_M), 2.67 – 2.54 (m, 4H, H_{I+D}), 1.85 – 1.75 (m, 2H, H_G), 1.74 – 1.58 (m, 6H, H_{L+E+G}), 1.57 – 1.45 (m, 2H, H_F), 1.47 – 1.37 (m, 2H, H_K), 1.30 (s, 27H, H_R); ^{13}C NMR (125 MHz, $CDCl_3$); δ 157.0, 148.4, 147.6, 147.5, 144.3, 139.6, 137.5, 137.2, 136.0,

132.4, 130.9, 124.2, 113.1, 67.7, 63.2, 51.5, 34.4, 32.9, 32.5, 31.5, 30.8, 30.6, 29.3, 28.8, 26.6, 26.4; HR-ESIMS *m/z* = 763.530283 $[M+H]^+$ (calc. for $C_{52}H_{67}N_4O$ 763.530939).

3.5 References

1. (a) A. Livoreil, C. O. Dietrich-Buchecker and J.-P. Sauvage, *J. Am. Chem. Soc.*, **1994**, *116*, 9399-9400; (b) D. J. Cárdenas, A. Livoreil and J.-P. Sauvage, *J. Am. Chem. Soc.*, **1996**, *118*, 11980-11981; (c) A. Livoreil, J.-P. Sauvage, N. Armaroli, V. Balzani, L. Flamigni and B. Ventura, *J. Am. Chem. Soc.*, **1997**, *119*, 12114-12124.
2. (a) P. Gaviña and J.-P. Sauvage, *Tetrahedron Lett.*, **1997**, *38*, 3521-3524; (b) N. Armaroli, V. Balzani, J.-P. Collin, P. Gaviña, J.-P. Sauvage and B. Ventura, *J. Am. Chem. Soc.*, **1999**, *121*, 4397-4408; (c) N. Weber, C. Hamann, J.-M. Kern and J.-P. Sauvage, *Inorg. Chem.*, **2003**, *42*, 6780-6792; (d) I. Poleschak, J.-M. Kern and J.-P. Sauvage, *Chem. Commun.*, **2004**, 474-476; (e) U. Létinois-Halbes, D. Hanss, J. M. Beierle, J.-P. Collin and J.-P. Sauvage, *Org. Lett.*, **2005**, *7*, 5753-5756; (f) S. Bonnet, J. P. Collin, M. Koizumi, P. Mobian and J. P. Sauvage, *Adv. Mater.*, **2006**, *18*, 1239-1250; (g) F. Durola and J.-P. Sauvage, *Angew. Chem. Int. Ed.*, **2007**, *46*, 3537-3540.
3. (a) J. D. Crowley, D. A. Leigh, P. J. Lusby, R. T. McBurney, L.-E. Perret-Aebi, C. Petzold, A. M. Z. Slawin and M. D. Symes, *J. Am. Chem. Soc.*, **2007**, *129*, 15085-15090; (b) D. A. Leigh, P. J. Lusby, R. T. McBurney and M. D. Symes, *Chem. Commun.*, **2010**, *46*, 2382-2384.
4. J. E. Beves, V. Blanco, B. A. Blight, R. Carrillo, D. M. D'Souza, D. Howgego, D. A. Leigh, A. M. Z. Slawin and M. D. Symes, *J. Am. Chem. Soc.*, **2014**, *136*, 2094-2100.
5. (a) V. Aucagne, K. D. Hänni, D. A. Leigh, P. J. Lusby and D. B. Walker, *J. Am. Chem. Soc.*, **2006**, *128*, 2186-2187; (b) V. Aucagne, J. Berná, J. D. Crowley, S. M. Goldup, K. D. Hänni, D. A. Leigh, P. J. Lusby, V. E. Ronaldson, A. M. Z. Slawin, A. Viterisi and D. B. Walker, *J. Am. Chem. Soc.*, **2007**, *129*, 11950-11963; (c) S. M. Goldup, D. A. Leigh, P. R. McGonigal, V. E. Ronaldson and A. M. Z. Slawin, *J. Am. Chem. Soc.*, **2010**, *132*, 315-320.
6. M. J. Barrell, D. A. Leigh, P. J. Lusby and A. M. Z. Slawin, *Angew. Chem. Int. Ed.*, **2008**, *47*, 8036-8039.
7. G. W. V. Cave, F. P. Fanizzi, R. J. Deeth, W. Errington and J. P. Rourke, *Organometallics*, **2000**, *19*, 1355-1364.
8. (a) F. Pérez-Balderas, M. Ortega-Muñoz, J. Morales-Sanfrutos, F. Hernández-Mateo, F. G. Calvo-Flores, J. A. Calvo-Asín, J. Isac-García and F. Santoyo-González, *Org. Lett.*, **2003**, *5*, 1951-1954; (b) K. Savin, M. Robertson, D. Gernert, S. Green, E. Hembre and J. Bishop, *Molec. Divers.*, **2003**, *7*, 171-174; (c) P. Appukkuttan, W. Dehaen, V. V. Fokin and E. Van der Eycken, *Org. Lett.*, **2004**, *6*, 4223-4225.
9. (a) J. H. Boyer and E. J. Miller, *J. Am. Chem. Soc.*, **1959**, *81*, 4671-4673; (b) M. Pizzotti, S. Cenini, F. Porta, W. Beck and J. Erbe, *J. Chem. Soc., Dalton Trans.*, **1978**, 1155-1160.

10. S. Jindabot, K. Teerachanan, P. Thongkam, S. Kiatisevi, T. Khamnaen, P. Phiriyawirut, S. Charoenchaidet, T. Sooksimuang, P. Kongsaeree and P. Sangtrirutnugul, *J. Organomet. Chem.*, **2014**, *750*, 35-40.

11. (a) B. Chattopadhyay, C. I. R. Vera, S. Chuprakov and V. Gevorgyan, *Org. Lett.*, **2010**, *12*, 2166-2169; (b) I. Stengel, A. Mishra, N. Pootrakulchote, S.-J. Moon, S. M. Zakeeruddin, M. Gratzel and P. Bauerle, *J. Mater. Chem.*, **2011**, *21*, 3726-3734; (c) G. Colombano, C. Travelli, U. Galli, A. Caldarelli, M. G. Chini, P. L. Canonico, G. Sorba, G. Bifulco, G. C. Tron and A. A. Genazzani, *J. Med. Chem.*, **2010**, *53*, 616-623.

12. E. J. Corey and A. Venkateswarlu, *J. Am. Chem. Soc.*, **1972**, *94*, 6190-6191.

13. (a) G. W. V. Cave, A. J. Hallett, W. Errington and J. P. Rourke, *Angew. Chem. Int. Ed.*, **1998**, *37*, 3270-3272; (b) G. W. V. Cave, N. W. Alcock and J. P. Rourke, *Organometallics*, **1999**, *18*, 1801-1803; (c) C. P. Newman, G. W. V. Cave, M. Wong, W. Errington, N. W. Alcock and J. P. Rourke, *J. Chem. Soc., Dalton Trans.*, **2001**, 2678-2682.

14. (a) F. Basolo and R. G. Pearson, *Mechanisms of Inorganic Reactions: : a study of metal complexes in solution*, 2nd edn., Wiley, New York, 1967; (b) R. J. Cross, *Chem. Soc. Rev.*, **1985**, *14*, 197-223; (c) M. Martinez and G. Muller, *J. Chem. Soc., Dalton Trans.*, **1989**, 1669-1673.

15. S. J. Pike and P. J. Lusby, *Chem. Commun.*, **2010**, *46*, 8338-8340.

16. (a) V. V. Rostovtsev, L. G. Green, V. V. Fokin and K. B. Sharpless, *Angew. Chem. Int. Ed.*, **2002**, *41*, 2596-2599; (b) C. W. Tornøe, C. Christensen and M. Meldal, *J. Org. Chem.*, **2002**, *67*, 3057-3064.

17. T. R. Chan, R. Hilgraf, K. B. Sharpless and V. V. Fokin, *Org. Lett.*, **2004**, *6*, 2853-2855.

18. C. Shao, X. Wang, Q. Zhang, S. Luo, J. Zhao and Y. Hu, *J. Org. Chem.*, **2011**, *76*, 6832-6836.

19. C. Nolte, P. Mayer and B. F. Straub, *Angew. Chem. Int. Ed.*, **2007**, *46*, 2101-2103.

20. B. H. Lipshutz and B. R. Taft, *Angew. Chem. Int. Ed.*, **2006**, *45*, 8235-8238.

21. (a) Y. Furusho, T. Matsuyama, T. Takata, T. Moriuchi and T. Hirao, *Tetrahedron Lett.*, **2004**, *45*, 9593-9597; (b) N. Miyagawa, M. Watanabe, T. Matsuyama, Y. Koyama, T. Moriuchi, T. Hirao, Y. Furusho and T. Takata, *Chem. Commun.*, **2010**, *46*, 1920-1922.

22. H. W. Gibson, S. H. Lee, P. T. Engen, P. Lecavalier, J. Sze, Y. X. Shen and M. Bheda, *J. Org. Chem.*, **1993**, *58*, 3748-3756.

Chapter IV

Self-assembled rotaxanes

Acknowledgements

David August is gratefully thanked for his help with nESI-MS.

Synopsis

Herein, the metal-directed self-assembly of tubular complexes were studied in order to develop self-assembled rotaxanes. The partially-protected palladium complex, [(en)Pd(NO$_3$)$_2$], was employed as a building block to successfully assemble with tris and pentakis(3,5-pyridine) ligands in the presence of biphenyl with different length of ethyleneoxide side chain template ***18*** *(or* ***31****) and produce tubular complexes* ***23***, ***24***, ***36*** *and* ***37****. Some other rod-like molecules and other biphenyl derivatives showed poorer templating abilities than* ***18*** *and* ***31****. The self-assembly of the tube components around stoppered templates* ***22***, ***28*** *and* ***35*** *was not successful. The attempts to synthesise benzidine derivatives to use as a station in rotaxanes failed under various reaction conditions. To extend the scope for a tube self-assembly, a more kinetically inert Pt^{II} analogue was used as an alternative building block. In addition, an assembly-followed-by oxidation protocol[1] with a Co^{III} system was explored.*

4.1 Introduction

Self-assembly relies on the simultaneous organisation of components using supramolecular interactions (ionic, hydrophobic, van der Waals, hydrogen and coordination bonds)[2] producing patterns or structures. Self-assembly strategies have been used to overcome limitations arose by the multistep covalent synthesis.[2-3] The formation of discrete metal-organic structures such as coordination cages, helicates, knots has rapidly increased in recent years. As knowledge of construction of wide range self-assemblies has been well established, the challenge is moving on to how to make a complex functional or useful systems. Applications of the assemblies are a major goal in the field of supramolecular chemistry.

Metal-directed self-assembly of discrete two- and three-dimensional structures using *cis*-protected Pd^{II} building block has been extensively studied by Fujita, Stang and others.[4] Fujita's group first demonstrated formation of a molecular square by the complexation of $[(en)Pd(NO_3)_2]$ (en = ethylenediamine) (**1**) with 4,4'-bipyridine.[5] In 1995, the first synthesis of a three-dimensional octahedral cage using two-dimensional triangular tris(4-pyridyl)triazine "panels" was realised.[4b] Fujita and co-workers have shown the exploitation of two-dimensional organic component as molecular panelling[6] is an efficient method for fabrication of three-dimensional molecules.[6-7] Rectangular tris, tetrakis and pentakis(3,5-pyridine) ligands, **2**, **3** and **4** were linked together with **1** which provides 90° angle to construct corresponding coordination nanotubes from four molecules of pyridine ligands and complimentary numbers of **1** (Figure 4.1, 4.2).[8] Oligo(3,5-pyridine) panels **2**, **3** and **4** contain three, four and five binding sites, respectively. Coordination nanotubes, however, were formed only in the presence of a rod-like template molecule such as 4,4'-biphenylenedicarboxylate (**5**), biphenyl (**6**), *p*-terphenyl (**7**) and were characterised by NMR, cold-spray-ionisation mass spectrometry (CSI-MS)[9] and X-ray crystallography. It was found that the tube dissociated into its components upon removal of template molecule and reassemble by the addition of the guest molecule. There are two isomers of tubes **9** in a ca. 1:1 ratio but only got single crystal for one isomer.

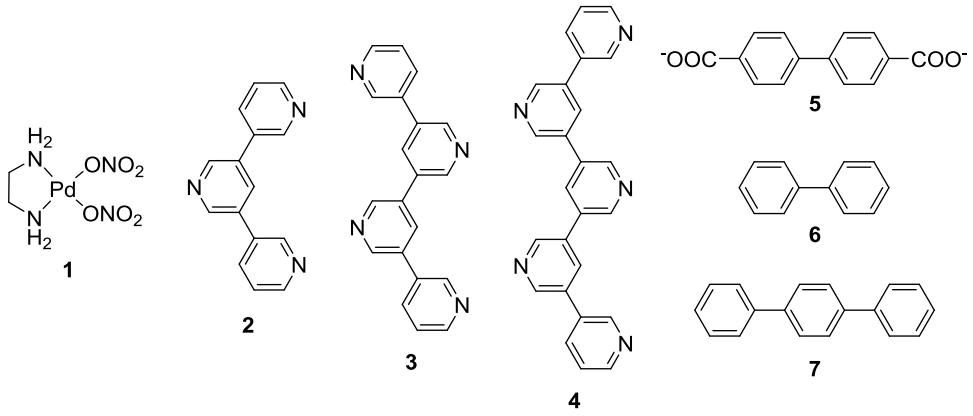

Figure 4.1 *cis*-protected Pd^{II} unit **1**, rectangular ligands **2**, **3**, **4** and template molecule **5**, **6**, **7**.

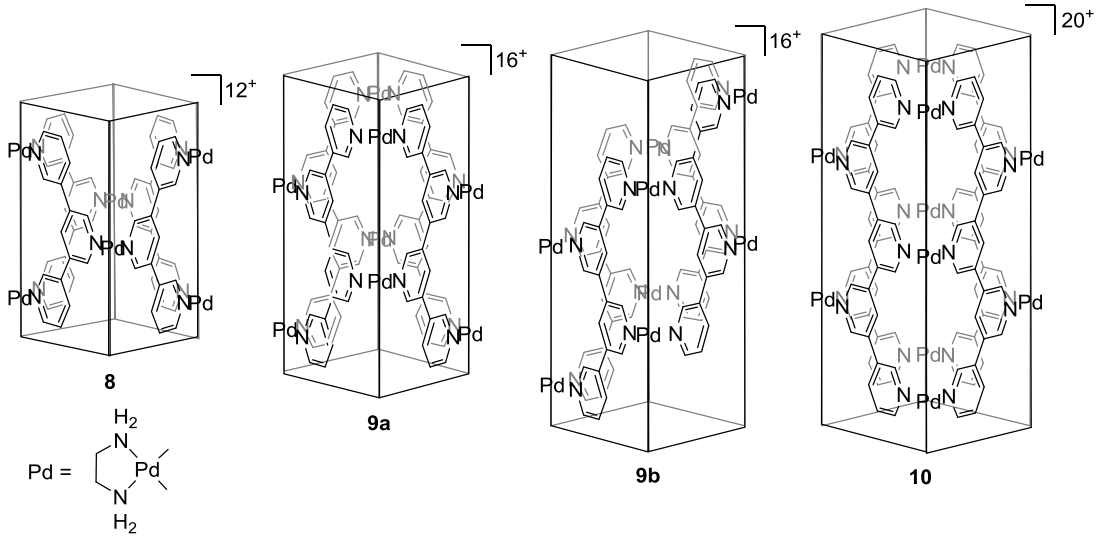

Figure 4.2 Schematic representation of nanotubes **8**, **9a**, **9b** and **10** reported by Fujita *et al.*[8]

The tubular frameworks hosting template molecule in their cavities for tube **8**, **9b** and **10** were confirmed by X-ray crystallographic analysis (Figure 4.3). The crystal structure shows π-π and CH-π interactions between the framework and the template which is a distorted square in such way that two ligands are stacked on the π-face of phenyl rings of the template and two other ligands are orthogonally interacting *via* CH-π interactions.

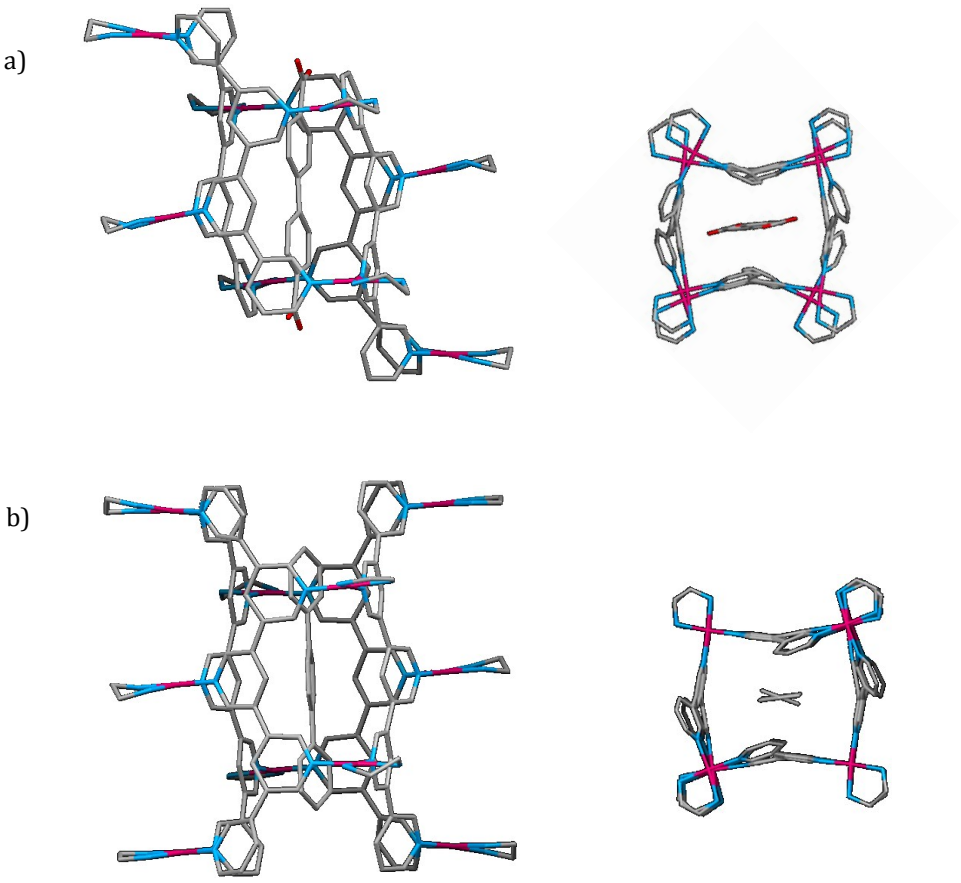

Figure 4.3 Crystal structure of a) **9b** and b) **10**. Left: side view, Right: top view. Colour code: C, grey; N, blue; O, red; Pt, magenta. Solvent, NO_3^- counter anion and hydrogen atoms have been removed for clarity.[8b]

All of the tubular complexes included a template molecule in their cavity, which themselves resemble the structures of pseudo-rotaxanes. This inspired the studies to exploit a discrete nanotube as a self-assembled [2]rotaxane, which could be further developed into a self-assembled stimuli-responsive molecular shuttle.

4.2 Results and Discussion

4.2.1 Design

As the nanotubes studied by Fujita's group can be considered pseudo-rotaxanes, it could be clearly envisaged that modifying the template molecule by lengthening and installing appropriate stoppers would make a novel functional self-assembly rotaxane. Fujita's group has shown that range of neutral/anionic charged symmetric/asymmetric biphenyl derivatives, anthracene derivatives and *p*-terphenyl can be used as templates for tubes fabrication.[8, 10] As well as targeting a simple one-station rotaxane, however, we envisaged that the incorporation of a second station and a suitable means by which to externally address one of these stations, would produce a bistable stimuli-responsive molecular shuttle. Such devices (or mechanical switches) can be considered central to the development of more complicated molecular machines. The design in question, combines Fujita's tube with ideas from Stoddart's laboratory. Thus, the proposed rotaxane features a thread molecule containing both dialkoxy biphenyl (*O*-station) and diamine biphenyl (*N*-station) units linked together by an alkyl chain or oligo(ethyleneoxide) spacer and capped with two bulky, fluorescent naphthalimide-type stoppers, at both ends. It was envisaged that the tubular Pd component would initially prefer the amine station, as this would be a much stronger π-donor and thus interact much more strongly with highly electron π-deficient panels (caused by coordination to the Pd ions) of the tube. Crucially, it was also anticipated that tris and pentakis(3,5-pyridine) tubes are strong enough not to disassemble when the systems are set in motion by the cooperativity of twelve and twenty Pd-N bonds, respectively. With twelve and twenty-cationic charge, tubular rotaxanes would be expected to be capable of binding neutral and anionic guests strongly, but not cationic guests. Therefore, shuttling of the tube to the *O*-station was envisaged upon addition of acid, as this would be repelled by the ammonium functionality of the *N*-station. It was also expected therefore, that the addition of a base should instantly reverse the process (Scheme 4.1).

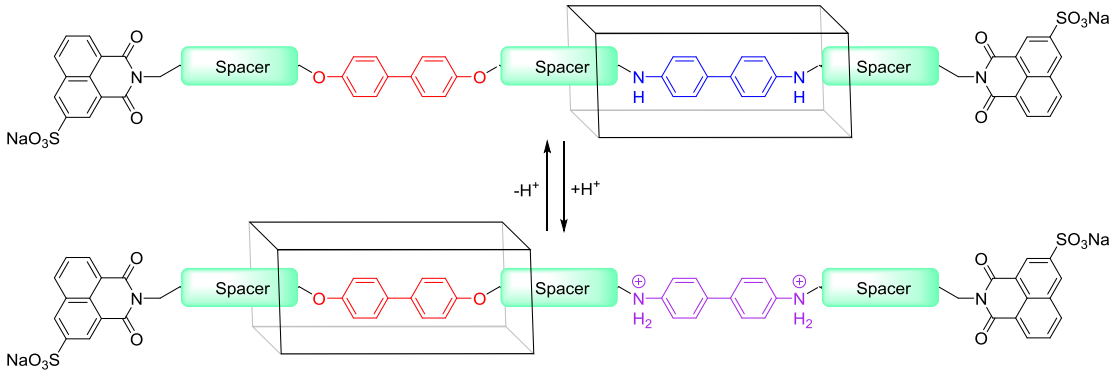

Scheme 4.1 Acid-base shuttling between *O*- and *N*-station self-assembled [2]rotaxanes.

As part of a preliminary study, the discrete self-assembly of the tubular rotaxane with one template station was pursued as an intermediary goal.

4.2.2 Synthesis

4.2.2.1 Synthesis of oligo(3,5-pyridine) ligands

Preparation of tris and pentakis(3,5-pyridine) was documented by Fujita and co-workers[8a] using tributyltin compounds, which can be highly toxic. As a less-toxic alternative, we have pursued standard Suzuki coupling reactions, as shown in Scheme 4.2.

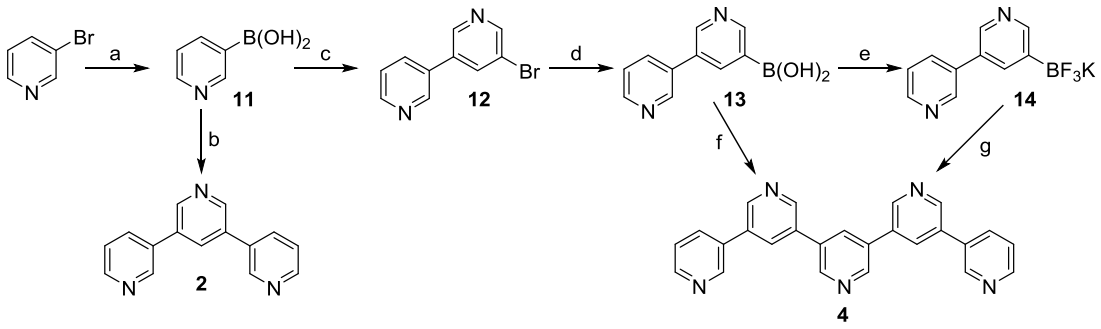

Scheme 4.2 Synthesis of tris and pentakis(3,5-pyridine) ligands. Reagents and conditions: a) i) *n*-BuLi, $B(O^iPr)_3$, toluene, THF, -60 °C, ii) HCl, -15 °C, 90%; b) 3,5-dibromopyridine, $Pd(PPh_3)_2Cl_2$, Na_2CO_3, 1,4-dioxane, reflux, 16 h, 68%; c) 3,5-dibromopyridine, $Pd(PPh_3)_2Cl_2$, PPh_3, K_3PO_4, 1,4-dioxane, reflux, 2 h, 71%; d) i) *n*-BuLi, $B(O^iPr)_3$, , toluene, THF, -60 °C, ii) HCl, -15 °C, 57%; e) KHF_2, MeOH, water, rt, 2 h, 80%; f) $Pd(PPh_3)_2Cl_2$, Na_2CO_3, 1,4-dioxane, reflux, 16 h, 19%; g) $Pd(PPh_3)_2Cl_2$, Na_2CO_3, 1,4-dioxane, reflux, 16 h, 23%.

The synthesis of tris(3,5-pyridine) ligand **2** commenced from a boronic acid prepared from the commercially available 3-bromopyridine following a literature procedure.[11] The 3-pyridylboronic acid **11** was then reacted with 3,5-dibromopyridine under standard Suzuki reaction conditions to afford **2** in good yield (68%). To fabricate a reagent for pentakis(3,5-pyridine) ligand, boronic acid **11** was coupled with only one equivalent of 3,5-dibromopyridine to achieve bromobipyridine **12,** which was subsequently used to afford boronic acid **13**.[12] Bipyridyl boronic acid **13** could be subjected to a Suzuki coupling with 3,5-dibromopyridine right away or further reacted with KHF_2 to produce more the stable potassium trifluoroborate salt **14** and then used as a Suzuki reagent. Trifluoroborate **14** is a versatile coupling partner and gives higher product yield for Suzuki coupling with 3,5-dibromopyridine, giving pentakis(3,5-pyridine) **4** in 23%. This reaction condition is less time consuming and more efficient compared to the procedure proposed by Fujita and co-workers. However, the Suzuki coupling reaction also gave a lot of byproducts *i.e.* tris, tetrakis(3,5-pyridine), 3,3':5',3''-terpyridine-5-bromo- which lowered the yield of the desired product.

4.2.2.2 Synthesis of biphenyl template molecules

The first design of an *O*-station thread molecule featured a biphenyl connected to naphthalimide sulfonate stoppers through ethylenenoxide linkages. Retrosynthetic analysis of thread **22** is shown in Scheme 4.3. A nucleophilic substitution reaction between 4,4′-bis(2-bromoethoxy)-1,1′-biphenyl **19** and naphthalimide stopper **21** would afford a target thread molecule. Bromination of diol **18** would yield **19** and condensation of naphthalic anhydride **20** with ammonia solution would furnish **21**.

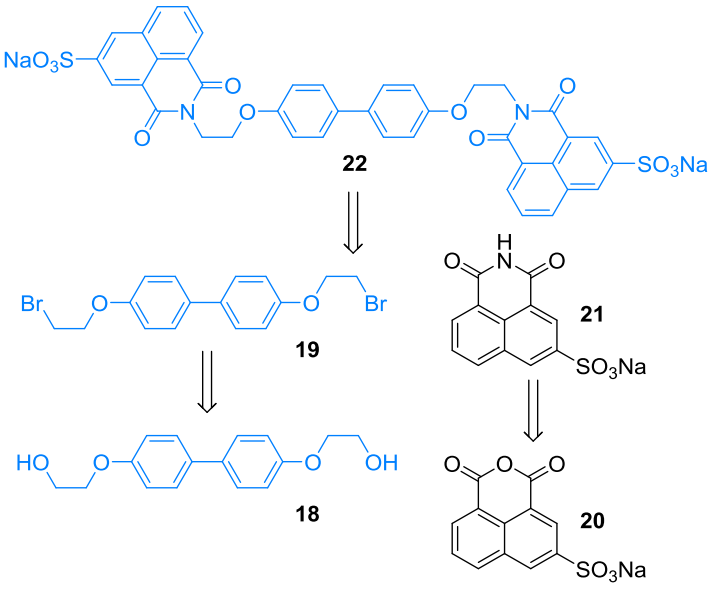

Scheme 4.3 Retrosynthesis of template **22**.

Attempts towards the synthesis of diol **18** were examined. Firstly, a Buchwald-Hartwig homocoupling reaction of 2-(4-bromophenoxy)ethanol **17** was carried out but failed to generate the desired compound. A nucleophilic substitution of 4,4′-dihydroxybiphenyl and bromoethanol gave poor yield after purification. The last attempt, 4,4′-dihydroxybiphenyl were coupled to ethylene carbonate in the presence of K_2CO_3 to give rise to the diol derivatives **18** in 98% yield[13] (Scheme 4.4).

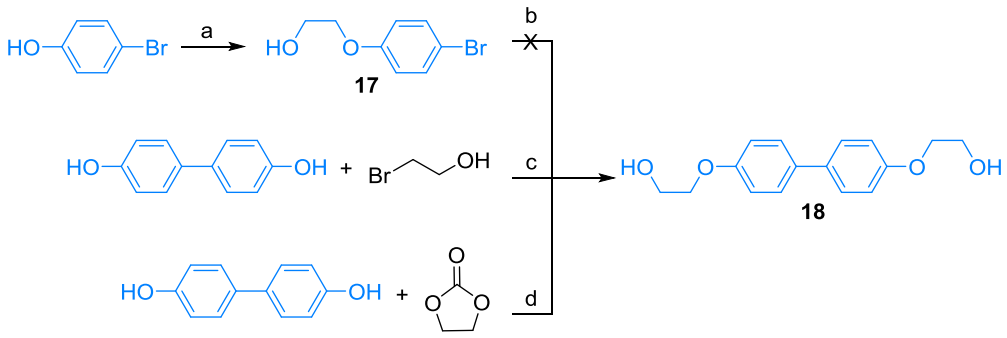

Scheme 4.4 Synthesis of **18**. Reagents and conditions: a) K_2CO_3, DMF, 80 °C, 5 d, 74%; b) $Pd(OAc)_2$, PPh_3, TBAB, NaOMe, H_2O, EtOH, 80 °C, 16 h; $Pd(PPh_3)_4$, In, DMF, 100 °C, 16 h; c) K_2CO_3, Acetone, reflux, 16 h, 15%; d) K_2CO_3, DMF, 80 °C, 16 h, 98%.

Compound **18** was brominated, using bromine and triphenylphosphine, which gave rise to **19** in 60% yield.[14] Salt **20** was prepared according to literature procedure using fuming sulphuric acid and 1,8-napthalic anhydride.[15] Compound **21** was then refluxed with ammonia solution in ethanol to afford the corresponding naphthalimide salt.[15]

Reacting compound **21** with **19** at 120 °C in the presence of K_2CO_3 and NaI for 2 d afforded the product **22** following recrystallisation in poor yield (Scheme 4.5).

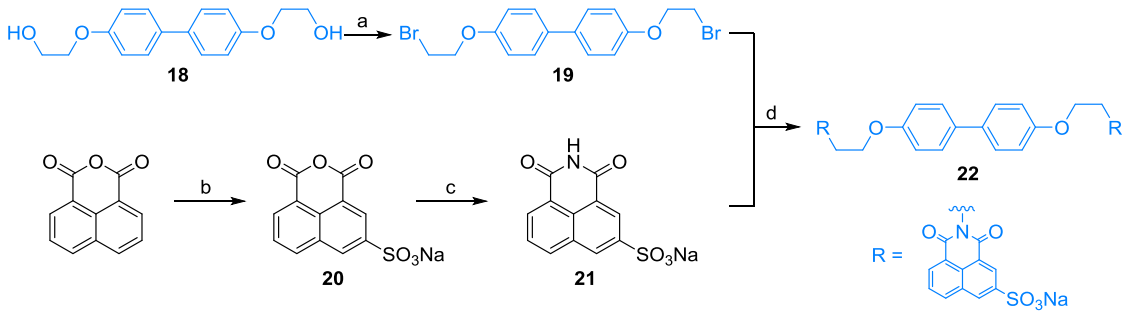

Scheme 4.5 Synthesis of thread **22**. Reagents and conditions: a) Br_2, PPh_3, CH_2Cl_2, 0°C-rt, 16 h, 60%; b) i)fuming H_2SO_4 65%, 90 °C, 1 h ii) ice-water, NaCl, 100%; c) 16% NH_4OH, EtOH, 100 °C, 3 h, 66%; d) K_2CO_3, NaI, DMF, 120 °C, 2%.

4.2.2.3 Self-assembly of tubular rotaxanes

Before the self-assembly reaction with fully stoppered thread (*e.g.* **22**) was undertaken, the thread precursor **18** and **19** were subjected to tube-formation conditions by suspending one equivalent of these templates with four equivalents of ligand **2** or **4** and six or ten equivalents of "Pd^{II}" **1** in D_2O at 70°C for 1 h (Scheme 4.6). As Fujita had previously observed, the reaction of oligopyridine and Pd^{II} complex in D_2O first results in the formation of a complex mixture (Figure 4.4c, 4.5c). Addition of template molecules **18** to the reaction mixture induced the assembly of a single product after the solution was heated at 70 °C for 1 h (Figure 4.4d, 4.5d). The ^1H NMR spectra were in accordance with the quantitative formation of complex **23** and **24**, where the tube accommodated guest **18** in the cavity. The signals of guest **18** are shifted upfield as a result of shielding from face-to-face contact with two panels of the tube and six or nine proton signals which arose from half the framework **2** or **4** confirmed the high symmetry of the tubular structure. The integral ratio indicated a 1:1 host-guest complexation in the same fashion as found by Fujita. NOE correlation between the host and the guest in a NOESY spectrum supported the planar conformation of the ligand framework. The diffusion-ordered spectroscopy (DOSY) NMR spectrum also indicated the formation of a single product with a diffusion coefficient of -9.63 and -9.70 m^2s^{-1} for tube **23** and **24** respectively. Unfortunately, no intact species could be detected using nESI-MS. The template **19** did not successfully form a tubular architecture after a similar treatment. The NMR spectra were complicated.

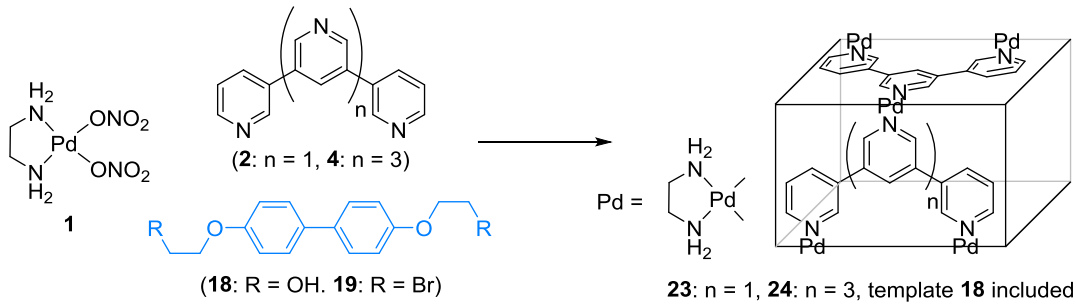

Scheme 4.6 Self-assembly of **1**, **2** or **4** in the presence of template molecule forming tube **23** and **24**.

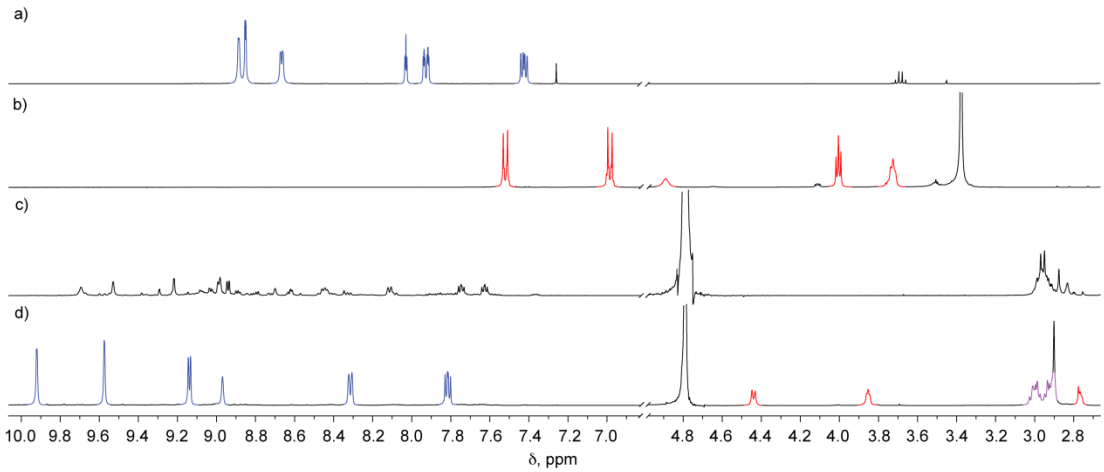

Figure 4.4 Partial ^{1}H NMR spectra (500 mHz, 298 K) of a) tris(3,5-pyridine), **2** in $CDCl_3$; b) template **18** in DMSO-d_6; c) a mixture of **2** and Pd^{II} **1** in D_2O at rt; d) a mixture in c) after addition of **18** and heating at 70 °C for 1h.

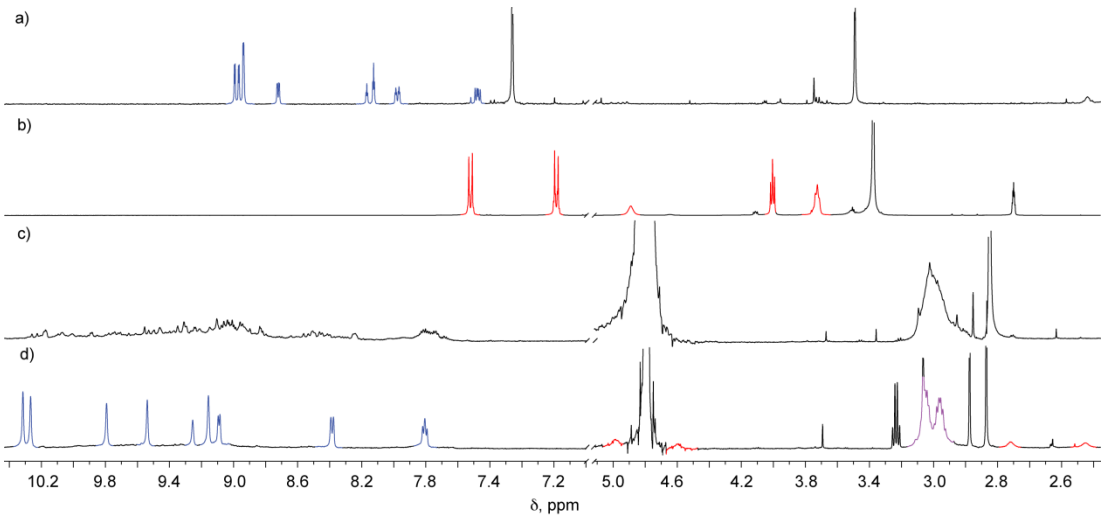

Figure 4.5 Partial ^{1}H NMR spectra (500 mHz, 298 K) of a) pentakis(3,5-pyridine), **4** in $CDCl_3$; b) template **18** in DMSO-d_6; c) a mixture of **4** and Pd^{II} **1** in D_2O at rt; d) a mixture in c) after addition of **18** and heating at 70 °C for 1h.

An assembly of the tube with the stoppered thread **22** was not successful as the NMR was broad and messy due to an oligomeric mixture for both tris and pentakis(3,5-pyridine) despite prolonged heating for several days. This was attributed to the thread structure not being suitable for stabilising the formation of the tube.

4.2.2.4 Other template molecules

Some other rod-like molecules apart from biphenyl derivatives were also examined as templates for the tube assembly including azobenzene, stilbene, *in situ* formation of imine from benzaldehyade and phenylethylamine, anthracene, 4,4'-bipyridine and 1,4-bis(6-((*tert*-butyldimethylsilyl)ethynyl)pyridin-3-yl)benzene† (Figure 4.6). All of the above compounds except anthracene did not show any template effect although 4,4'-bipyridine and 1,4-bispyridyl benzene resembled biphenyl and terphenyl. The host-guest interactions for this assembly required further study to rationalise the stability of the tubes. The complexation of polypyridine with an end-capped Pd^{II} **1** in the presence of anthracene showed somewhat encapsulation of anthracene in both tris and pentakispyridine tubes (Figure 4.7b, d). The signals correspond to anthracene were upfield shifted (pink labelled). The NMR spectra clearly showed the assembly of more than one product compared to the sole product spectrum where diol **18** was a template (Figure 4.7a, c). This suggested the efficient template ability of biphenyl derivatives. Therefore, new designs of template axles based on biphenyl core with longer linker unit were proposed.

†1,4-bis(6-((tert-butyldimethylsilyl)ethynyl)pyridin-3-yl)benzene was synthesised by Paul Symmers.

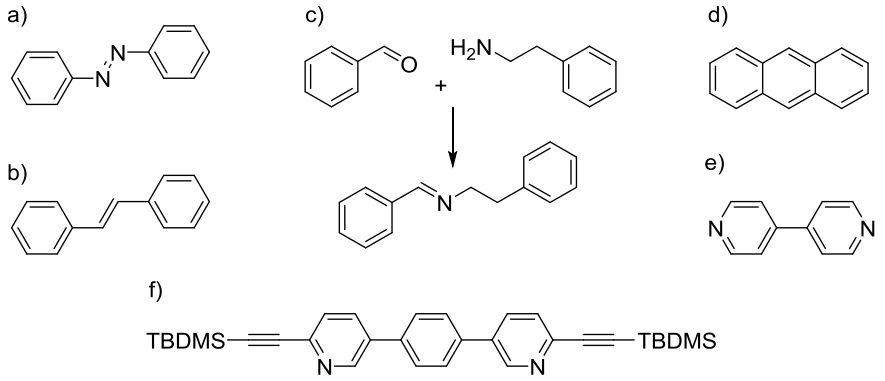

Figure 4.6 Other template molecules considered for tube assembly. a) azobenzene; b) stilbene; c) *in situ* made imine from benzaldehyde and phenylethylamine; d) anthracene and e) 4,4'-bipyridine; f) 1,4-bis(6-((tert-butyldimethylsilyl)ethynyl)pyridin-3-yl)benzene. Only anthracene, d) acted as a template for self-assembly.

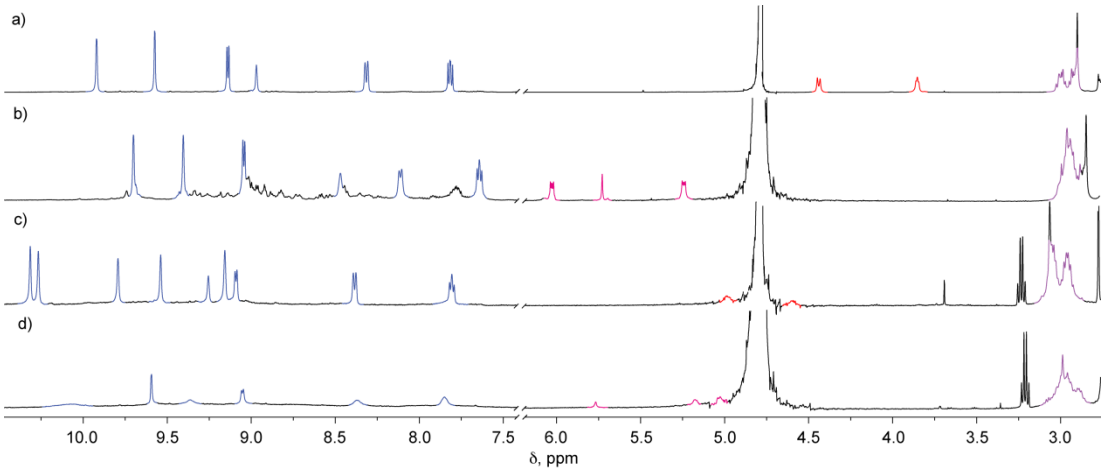

Figure 4.7 Partial ^{1}H NMR spectra (500 mHz, D_2O, 298 K) of a) tris(3,5-pyridine) tube **23**; b) a mixture of tris(3,5-pyridine), **1** and anthracene after heating at 70 °C for 1h; c) pentakis(3,5-pyridine) tube **24**; d) a mixture of pentakis(3,5-pyridine), **1** and anthracene after heating at 70 °C for 1h.

The first set of compounds contains an alkyl chain with an alkyne moiety adjacent to the biphenyl (Scheme 4.7). The π-electron in the triple bond is expected to increase host-guest π-π interactions. The synthesis of **28** started with a double Sonogashira coupling of 4,4'-diiodobiphenyl with 5-chloro-1-pentyne to afford compound **25**. Dichloro compound **25** subsequently underwent an azidation reaction to give bisazido **26**, followed by a reduction of the azide moiety using Zn powder and NH_4Cl to furnish **27**. The reaction of naphthalic anhydride with primary amines was well known from the convenient synthesis of dyes.[16] To bring about the naphthalimide group as a stopper, the

condensation of naphthalic anhydride salt **20** with terminal amine compound was undertaken. Diamine **27** and stopper **20** were refluxed in ethanol to afford **28** in 31%.

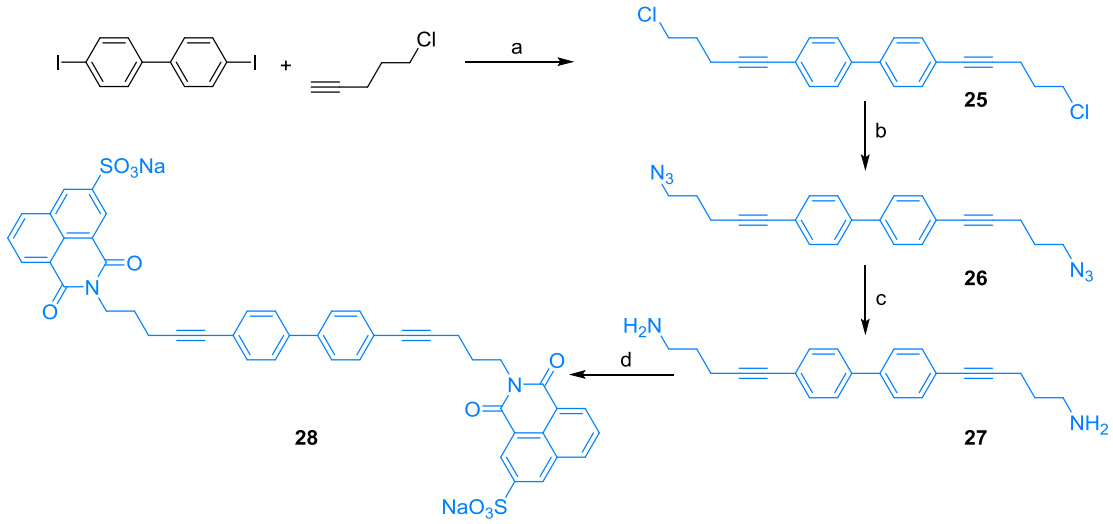

Scheme 4.7 Synthesis of thread **28**. Reagents and conditions: a) $Pd(PPh_3)_2Cl_2$, PPh_3, Et_3N, THF, 65 °C, 16 h, 57%; b) NaN_3, DMF, 80 °C, 4 h, 80%; c) Zn powder, NH_4Cl, EtOH, water, reflux, 30 min, 13%; d) **20**, EtOH, reflux, 2 d, 31%.

Another variety of the template thread derived from biphenol structure featured an alkyl chain connected to oxygen atom adjacent to biphenyl. The ligand-assisted Ullmann coupling reaction[17] of 4,4'-diiodobiphenyl and 5-amino-1-pentanol gave **29** in 31% yield. Unfortunately, coupling two stopper molecules with diamine **29** failed. The reaction gave only monocoupled product **30** regardless of the amount of stopper added and the reaction time (Scheme 4.8).

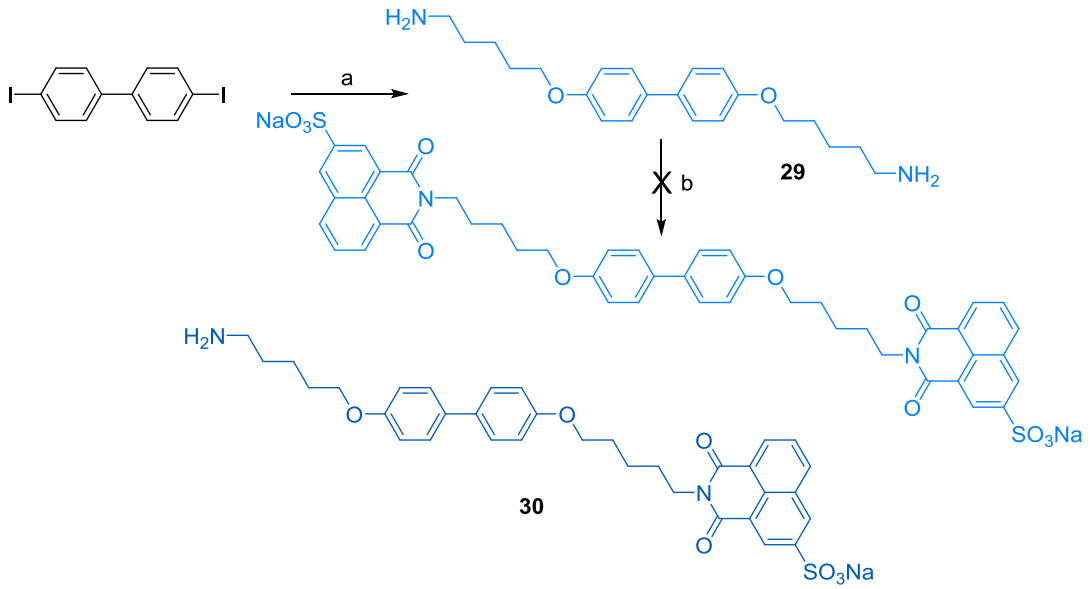

Scheme 4.8 Synthetic pathway of *O*-arylation thread molecule. Reagents and conditions: a)5-amino-1-pentanol, CuI, 3,4,7,8-tetramethyl-1-10-phenanthroline, Cs_2CO_3, toluene, 90 °C, 20 h, 31%; b) **20**, EtOH, reflux, 2 d. The product obtained was **30**.

The thread without/with stopper units from two variants; compounds **27**, **29, 28** and **30** (NMR spectra are shown in Figure 4.8a-d respectively) were investigated as templates for guest-induced assembly of coordination nanotubes using both tris and pentakis(3,5-pyridine) ligands **2** and **4**, and coordination building block **1**. The results for tris and pentakis(3,5-pyridine) ligands were similar. It was found that **27** and **29** showed a templating effect to some extent as the peaks correlate with pyridine signals exhibit a similar chemical shift range as the tubular complex **23** (Figure 4.8e, f). Moreover, the resonances of the biphenyl unit of **29** have shifted upfield to 4.98 and 4.41 ppm. The spectra of the reaction with stoppered thread showed uncharacterised oligomer complexes and none of the naphthalimide resonances were observed (Figure 4.8g, h). The intensity of the reagent peaks decreased as the reaction was reacted. From this result, it can be inferred that oxygen atoms in the template molecule might play some important role in templating the tubular structure.

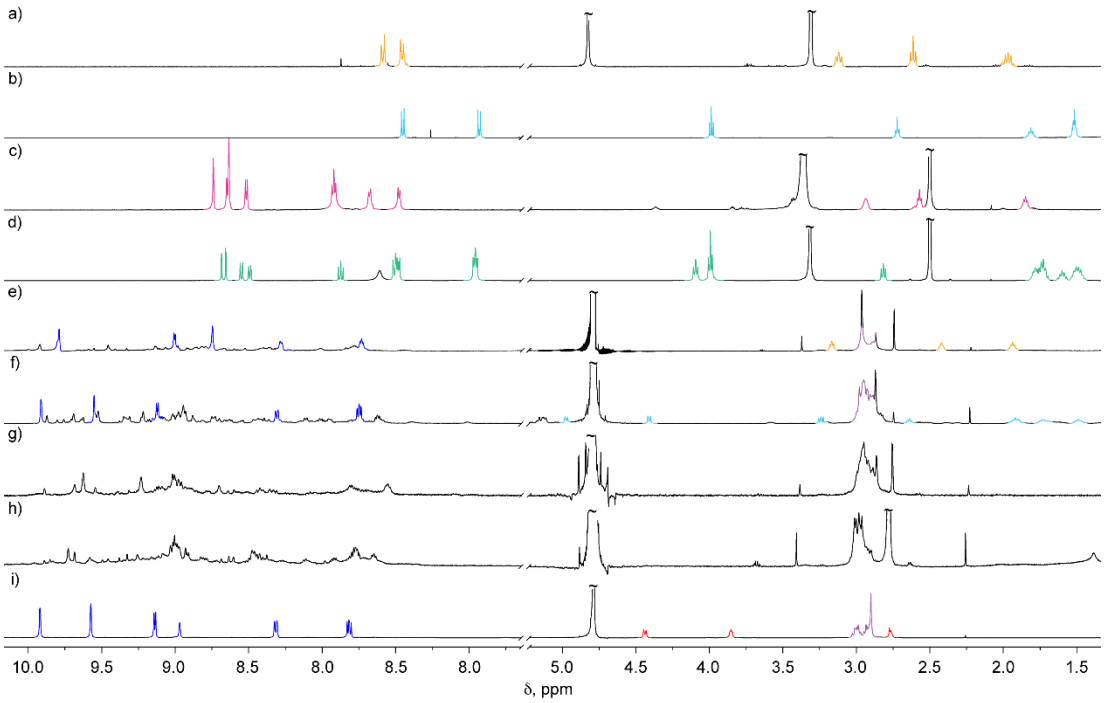

Figure 4.8 Partial ^{1}H NMR spectra (500 MHz, 298 K) of a) **27** in MeOD-*d*$_4$; b) **29** in $CDCl_3$; c) **28** in DMSO-*d*$_6$; d) **30** in DMSO-*d*$_6$; e) the mixture of **2**, [(en)Pd(NO_3)$_2$] **1** and **27** in D_2O for 1 h at 70 °C; f) the mixture of **2**, **1** and **29** in D_2O for 1 h at 70 °C; g) the mixture of **2**, **1** and **28** in D_2O for 1 h at 70 °C; h) the mixture of **2**, **1** and **30** in D_2O for 1 h at 70 °C; i) complex **24** assembled from treating ligand **2** with **1** in the presence of **18** in D_2O for 1 h at 70°C.

4.2.2.5 Longer ethyleneoxide chain *O*-biphenyl based template

A new thread design included an oligo(ethyleneoxide) chain next to biphenyl structure. The synthesis of thread **35** (Scheme 4.9) started from the commercially available 4,4'-dihydroxybiphenyl, which underwent a double Williamson ether reaction with (2-chloroethoxy)ethanol in the presence of K_2CO_3 and LiBr in MeCN to give **31** in 86% yield. **31** was then converted into the dibromo compound **32** using the Appel reaction with CBr_4 and PPh_3. The subsequent azidation was achieved by reacting with NaN_3 in DMF and produced the desired product **33** after recrystallisation in excellent yield. The bisazido ligand was then treated with $LiAlH_4$ to obtain the reduced amine species **33** in 91%. To obtain the thread **35**, amine **34** was reacted with stopper **20** under reflux conditions in mixed solvent. The product was precipitated out of the solution in quantitative yield.

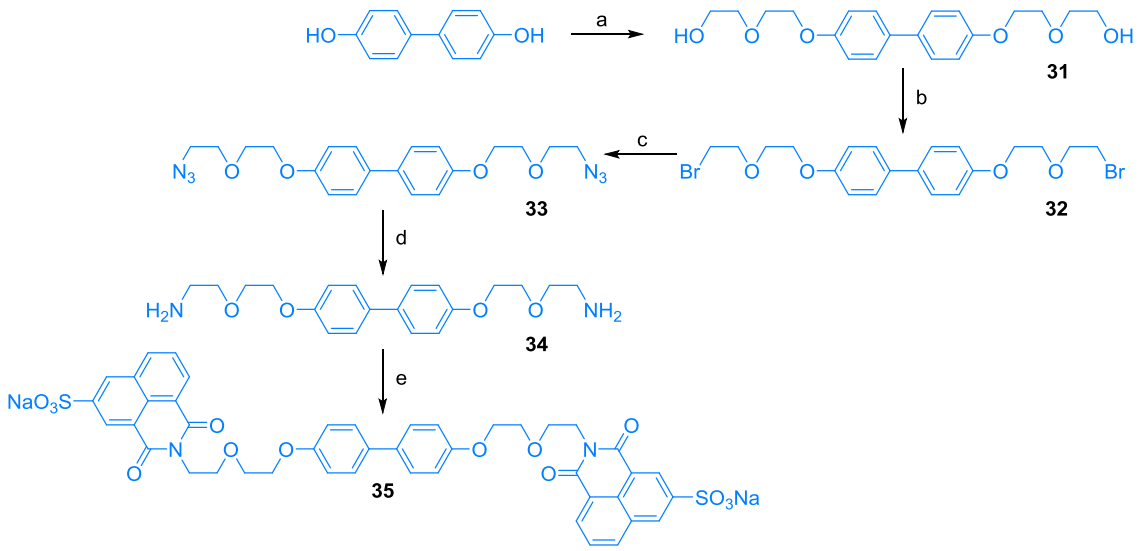

Scheme 4.9 Synthesis of thread template **35**. Reagents and conditions: a) (2-chloroethoxy)ethanol, K_2CO_3, LiBr, 80 °C, 16 h, 86%; b) CBr_4, PPh_3, CH_2Cl_2, rt, 5 h, 78%; c) NaN_3, DMF, 80 °C, 2 d, 93%; d) $LiAlH_4$, THF, reflux, 1 h, 91%; e) **20**, EtOH, MeOH, CH_2Cl_2, DMF, reflux, 16 h, *quant*.

The complexation of ligand **2** and **4** with Pd^{II} **1** in D_2O in the presence of **31** resulted in the quantitative self-assembly of **2** and **4** into coordination tube **36** and **37**, respectively (Figure 4.9). **31** showed a similar template effect as described earlier for **18**. The mixture of oligopyridine and [(en)Pd(NO_3)$_2$] first resulted in a complex mixture. Upon addition of **31**, the conversion of the mixture into a single product was accomplished after 1 h at 70 °C. The NMR spectra were consistent with the formation of tube **36** and **37** (Figure 4.10). Six and nine proton signals that resulted from half of the framework were clearly observed. Template **31** was observed symmetrically with a marked upfield shift that indicates the accommodation of **31** within the tubes. The DOSY NMR spectrum gave a diffusion coefficient of -9.64 and -9.71 m^2s^{-1} for tube **36** and **37** respectively, which are comparable to those of the tube complexes with the shorter template. These two assemblies could not be detected by nESI-MS.

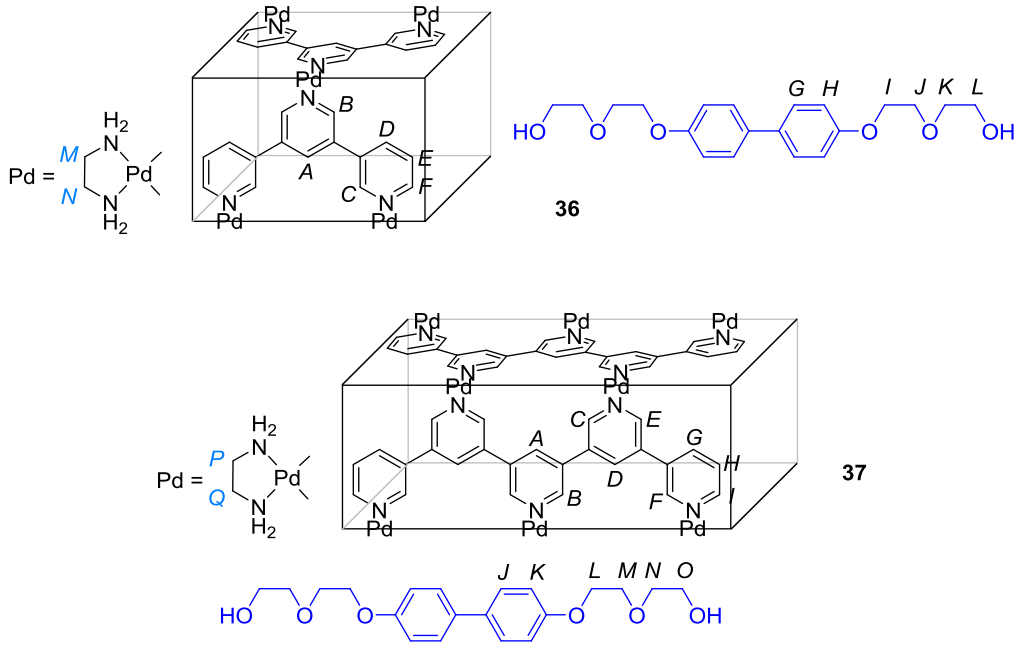

Figure 4.9 Schematic representations of nanotubes **36** and **37**. The template included in the tube was showed to clarify the assignment.

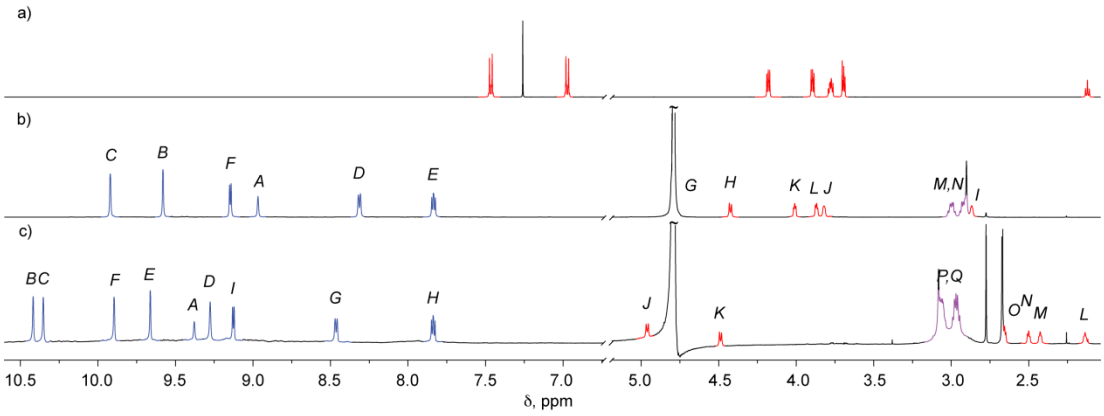

Figure 4.10 Partial ^{1}H NMR spectra (500 MHz, D_2O, 298 K) of a) template **31** in $CDCl_3$; b) complex **36** assembled from treating ligand **2** with **1** in the presence of **31** in D_2O for 1 h at 70°C; c) complex **37** assembled from treating ligand **4** with **1** in the presence of **31** in D_2O for 1 h at 70°C. The assignments correspond to the lettering shown in Figure 4.9.

The thread containing stopper units **35** was used as a template for self-assembly of coordination nanotubes. The reaction mixture for tris(3,5-pyridine) tube remained complex after 72 h at 70 °C while the pentakis(3,5-pyridine) reaction started to show some tube assembly within 18 h (Figure 4.11b). A strong H-bond donor solvent, 2,2,2-trifluoroethanol (TFE) has been used to labilise kinetically inert Pt(II)-pyridine coordination bonds, allowing the formation of $Pt(II)_{12}L_{24}$ spheres.[18] The formation of

tris(3,5-pyridine) tube was also explored in a mixture of 6:4 TFE/D_2O as TFE might help labilise Pd-pyridine bonds in the presence of the thread with bulky ends. After reacting at 70 °C for 6 d, the resonance of the tube was revealed (Figure 4.11c). The spectra of the reaction mixture for both tris- and pentakis-tubes appeared further downfield for pyridine frameworks compared those formed with the template without stopper molecules. Furthermore, the intensities of the spectra were very low and did not reveal any resonance for the stopper unit. The extra naphthalimide unit in the thread molecule has presumably obstructed an assembly and has somehow been cleaved from the biphenyl core. Despite a DOSY spectrum of the rotaxane formation reaction with ligand **4** giving a diffusion coefficient of -9.79 m^2s^{-1}, which was slightly higher than pseudorotaxane complex **37** (-9.71 m^2s^{-1}), this was not sufficient evidence for successful rotaxane formation.

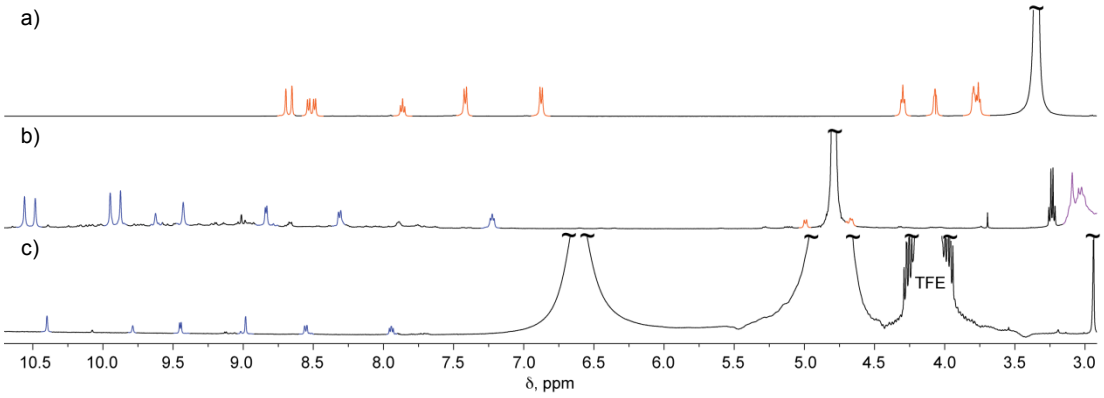

Figure 4.11 Partial ^{1}H NMR spectra (500 MHz, 298 K) of a) thread **35** in DMSO-d_6; b) the mixture of **4**, [(en)Pd(NO_3)$_2$] **1** and **35** in D_2O for 18 h at 70 °C; c) the mixture of **2**, [(en)Pd(NO_3)$_2$] **1** and **35** in 6:4 TFE/D_2O for 6 d at 70 °C.

4.2.2.6 *N*-station template

In the proposed self-assembled stimuli-responsive molecular shuttle, there were two different template stations. The *O*-station has been synthesised and discussed above. For the *N*-station, the first template to be explored was benzidine, 4,4'-diaminobiphenyl **38**, which was prepared according to a literature procedure using a rearrangement reaction of 1,2-diphenylhydrazine with concentrated HCl.[19] The ^{1}H NMR spectrum of the complexation of ligand **2** (or **4**) with **1** using benzidine **38** as a template is shown in Figure 4.12b, d. Under similar conditions as that used for previous tube assembly, the mixture was stirred at 70 °C for at least 1 h to observe the formation of the tubular structure. The peaks corresponding to the tube were observed along with many other

uncharacterisable peaks including benzidine. It was concluded that **38** was too soluble in water (the signals of free **38** were readily observable in D_2O), which would reduce the hydrophobic effect associated with its inclusion, therefore making it a poorer template.

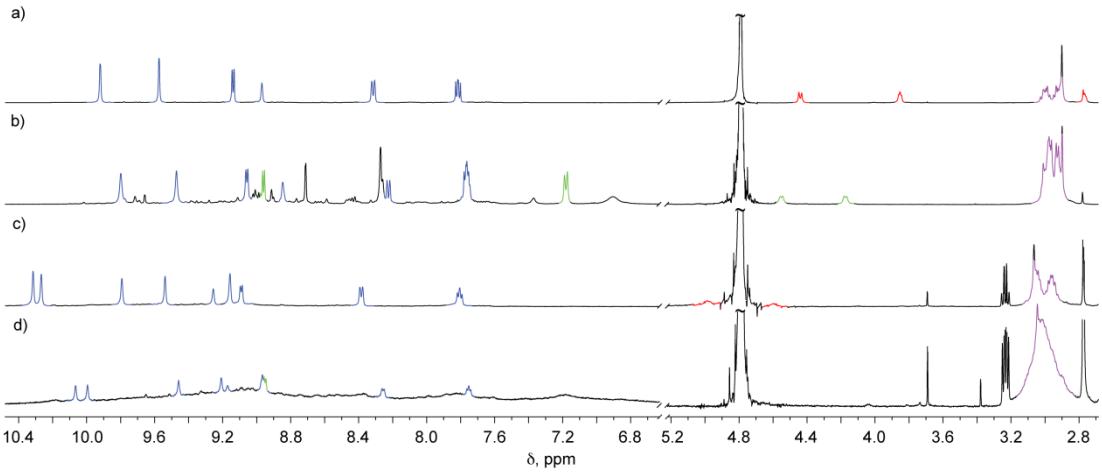

Figure 4.12 Partial ^{1}H NMR spectra (500 MHz, D_2O, 298 K) of a) tube complex **22**; b) the mixture of **2**, **1** and benzidine in for 1 h at 70 °C; c) tube complex **23**; d) the mixture of **4**, **1** and benzidine in for 1 h at 70 °C.

The attempts to synthesise other benzidine-derived threads failed using both Ullmann-type coupling and Buchwald–Hartwig amination of 4,4'-diiodobiphenyl and alkylamine (Scheme 4.10a). No desired product was found from crude ^{1}H and DOSY NMR spectra of the reactions. Oligomerisation of amine starting materials presumably occurred as preferred side reactions. Attaching bis(ethyleneoxide) sidearms to both benzidine nitrogen atoms using an alkylation reaction of benzidine with (2-chloroethoxy)ethanol and K_2CO_3 did not progress as with the oxygen analogue (Scheme 4.10b). The two starting materials were recovered after purification of the crude product by column chromatography.

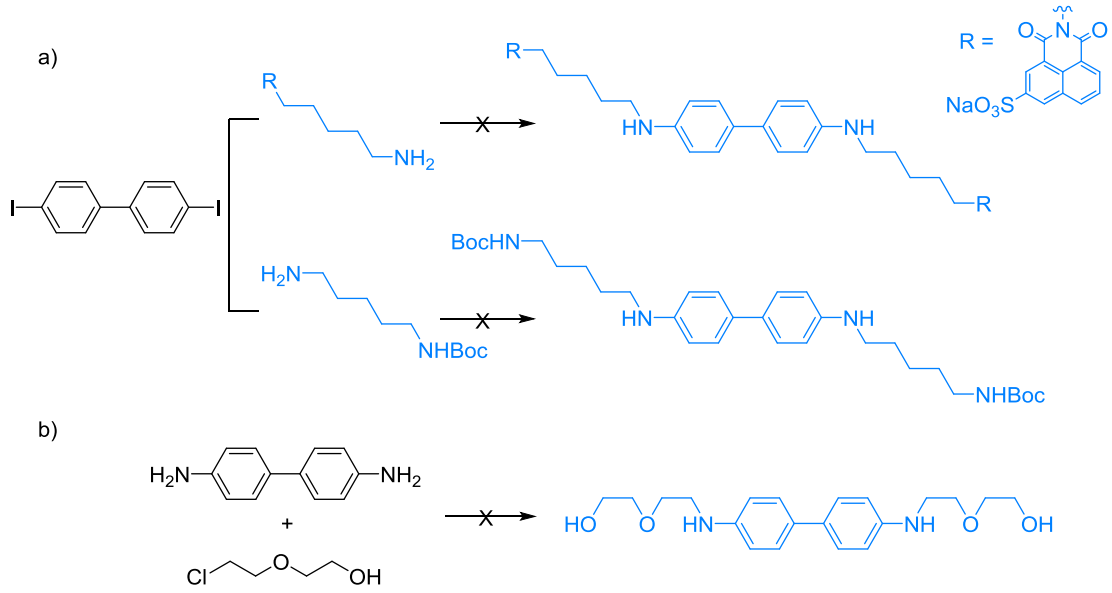

Scheme 4.10 Synthetic scheme for elongated benzidine. Reagents and conditions: a) Ullmann-type: copper source: CuI, CuBr; base: K_3PO_4, Cs_2CO_3, solvent: DMF, ^{i}PrOH, 100-120 °C; Buchwald-Hartwig: Pd_2dba_3, ^{t}BuOK, BINAP, Toluene, reflux.; b) NEt_3, benzene, reflux, 2 weeks[20]; K_2CO_3, NaI, THF, reflux, 48 h.

4.2.2.7 Other metal building blocks

To extend the scope of coordination tube assembly, other metal building blocks were utilised instead of Pd^{II} **1**. The first metal building block employed was a Pt^{II} analogue of $[(en)Pd(NO_3)_2]$ which provided 90 degree coordination with a square planar geometry similar to Pd^{II} **1**. As Pt(II) is more inert than Pd(II), it would need more energy to push the equilibrium forward for an assembly process compared to Pd(II). Self-assembly of ligand **2** with $[(en)Pt(NO_3)_2]$ (**41**)[21] and **31** was done at 100 °C for 7 d (Figure 4.13) while the reaction of ligand **4** did not progress after 40 d at 100 °C.

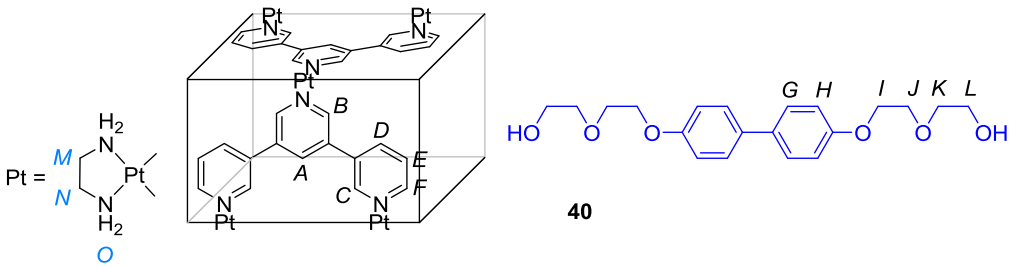

Figure 4.13 Schematic representation of nanotube **40**. The template included in the tube is shown to assist with NMR assignment.

The ^{1}H NMR spectrum of tube **40** is shown in Figure 4.14 with similar a pattern as observed in the former systems. The DOSY spectrum was also comparable with the other two palladium tubes **23** and **36** with a diffusion coefficient of -9.63 m^2s^{-1}.

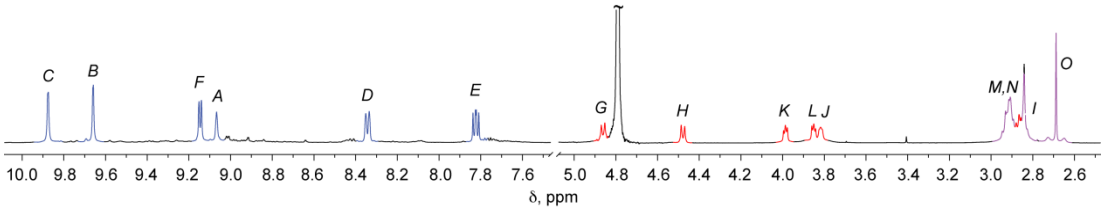

Figure 4.14 Partial ^{1}H spectrum of tube complex **40** (500 mHz, D_2O, 298 K). The assignments correspond to the lettering shown in Figure 4.13.

The results from an assembly of Stang's platinum dodecahedron cage indicated that the preparation requires the gradual addition of the pyridine-containing donor to the Pt acceptor which ensures that the Pt precursor is always present in excess, prohibiting the nucleophilic attack of a free strongly coordinating ligand on the Pt complex.[22] The gradual addition of the pyridine ligand **4** to the solution of Pt^{II} **41** and template was undertaken. However, the ^{1}H NMR spectrum only revealed an oligomer mixture. It was anticipated that the Pt(II)-pyridine coordination bond could be labilised in TFE.[18] Thus, ligand **4** was treated with **41** in a mixed solvent of 1:1 TFE/D_2O. The ^{1}H NMR spectrum of this also revealed a complex mixture after heating at 100 °C for 4 d, moreover the template was dissolved in the mixed solvent. This was the case for an assembly using the stoppered template **35**. No tube rotaxane formation was observed in all of the above conditions.

Recently, cobalt(II) has been used to assemble tetrahedral capsules in an M_4L_6 structure and the capsules were then oxidised to obtain inert Co(III) architectures which are not in equilibrium with their disassembled state.[1] It was envisaged that a partially protected Co(II) centre would assemble with oligopyridine panels and produce a tubular complex in the same manner as with the *cis*-protected square planar Pd^{II} and Pt^{II} complex, and undergo oxidation give a tube which would still exhibit the required kinetic robustness to make it useful for a stimuli-molecular shuttle system. 1,4,7,10-tetrathiacyclododecane (12ane[S_4]) was chosen to protect the four other coordination sites and leave two vacant positions to interact with the oligopyridine ligands. Cobalt(II) complexes were prepared by mixing the same equivalents of $Co(ClO_4)_2.6H_2O$ and 12ane[S_4] in water. The red

solution of $Co(ClO_4)_2$ turned fuchsia pink once thiacrown ether was introduced and the solution was stirred at 50 °C for 1 h then the solvent was evaporated, resulting in a solid complex product which was used without further purification. The complexation of Co^{II} building block, oligopyridine ligand (**2** or **4**) and template **31** was done in D_2O at 70 °C for 2 h then a slight excess cerium ammonium nitrate (CAN) was added to the reaction mixture. The ^1H NMR spectra of Co^{II} reaction were broad as a result of paramagnetism of Co^{II}. After oxidation with CAN, the spectra did not correspond to anything that could be assigned as a tube structures.

4.3 Conclusion and Outlook

The self-assembly of tris and pentakis(3,5-pyridine) with $[(en)Pd(NO_3)_2]$ in the presence of **18** and longer ethyleneoxide side chain **31** to form tubular structures **23**, **24**, **36** and **37** were successful by heating the reaction mixture at 70 °C for 1 h. All the compounds were characterised by ^1H, COSY, NOESY and DOSY NMR to confirm the formation of products. The initially developed naphthalimide template **22** for a self-assembled rotaxane showed no templating effect, resulting in uncharacterised spectra of an oligomeric mixture. Anthracene, some biphenyl derivatives **27**, **29** and benzidine **38** were poorer templates, in each case the tubes were not formed quantitatively. The attempts to derivertise benzidine were not successful. Unfortunately, the longer version of a stoppered template **35** did not provide any evidence for rotaxane formation, presumably due to side reactions with the naphthalimide sulfonate units. Different metal building blocks such as $[(en)Pt(NO_3)_2]$, $[Co(12ane[S_4])(ClO_4)_2]$ were used to determine the self-assembly. Pt^{II} analogue tube was only formed with tris(3,5-pyridine) and **31** template after a week at 100 °C. Cobalt-thiacrown ether complexes did not form any discrete tube.

The non-covalent interactions between template molecule and host framework need to be studied in more detail to improve the system design. Another obvious area for investigation would be the use of alternative stoppers, in particular non-anionic motifs to prevent the interactions with cationic metal building blocks.

4.4 Experimental Section

4.4.1 General experimental procedure

Unless stated otherwise, all reagents and solvents were purchased from commercial sources and used without further purification. [(en)Pd(NO_3)$_2$] (**1**)[23], 3-pyridinylboronic acid (**11**)[11], 5-bromo-3,3'-bipyridine (**12**)[12], [3,3'-bipyridin]-5-yl-boronic acid (**13**)[12], 2-(4-bromophenoxy)ethanol (**17**)[24], 4,4'-bis(hydroxyethyl)biphenyl (**18**)[13], 4,4'-bis(2-bromoethoxy)biphenyl (**19**)[14], benzo[de]isochromene-1,3-dione-5-sulfonic acid sodium salt (**20**)[15], benzo[de]isoquinoline-1,3-dione-5-sulfonic acid sodium salt (**21**)[15],benzidine (**38**)[19] and [(en)Pt(NO_3)$_2$] (**41**)[21] were prepared according to literature procedures.

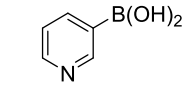

11

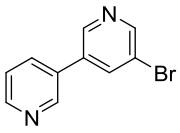

12

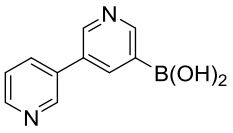

13

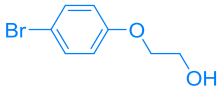

17

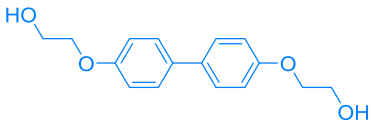

18

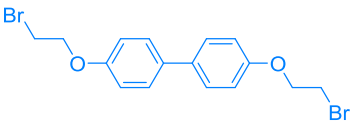

19

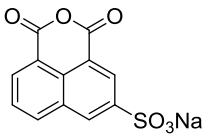

20

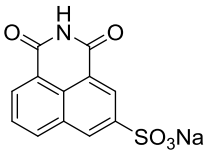

21

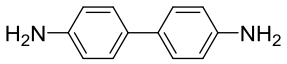

38

4.4.2 General procedure for tube assembly

a) For tris(3,5-pyridine) framework, tris(3,5-pyridine) ligand (**2**) (0.01 mmol. 2.3 mg) and **1** (0.015 mmol, 4.4 mg) were combined in D_2O (0.5 mL) and stirred for 5 min at 70 °C. To this solution, a template molecule (0.0025 mmol) was added, and the texture was stirred at 70 °C for 1 h or longer until no change of resonance was observed.

b) For pentakis(3,5-pyridine) framework, pentakis(3,5-pyridine) ligand (**4**) (0.005 mmol, 1.9 mg) and **1** (0.0075 mmol, 3.6 mg) were combined in D_2O (0.5 mL) and stirred for 5 min at 70 °C. To this solution, a template molecule (0.00125 mmol) was added, and

the texture was stirred at 70 °C for 1 h or longer until no change of resonance was observed.

4.4.3 Synthesis

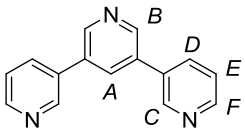

2

Adapted from a procedure by Bryce *et al.*[25] 3-Pyridinylboronic acid (0.15 g, 1.2 mmol, 2.4 equiv.), 3,5-dibromopyridine (0.12 g, 0.5 mmol, 1 equiv.) and $Pd(PPh_3)_2Cl_2$ (0.016 g, 0.023 mmol, 5 mol%) were sequentially added to degassed 1,4-dioxane (10 mL), and the mixture was stirred at 25 °C for 30 min. Degassed solution of Na_2CO_3 (1 M, 5 mL, 3 equiv.) was added. The reaction mixture was heated at reflux overnight. After cooling down, solvent was removed *in vacuo*, EtOAc was added, and the organic layer was washed with brine, separated, and dried over $MgSO_4$. An off white solid (80.1 mg, 68%) was obtained following purification by flash column chromatography (SiO_2, 0 – 5% MeOH/CH_2Cl_2). m.p. 157-159 °C, ^{1}H NMR (500 MHz, $CDCl_3$); δ 8.91 (d, *J* = 2.0 Hz, 2H, H_C), 8.88 (d, *J* = 2.1 Hz, 2H, H_B), 8.70 (dd, *J* = 4.8, 1.3 Hz, 2H, H_F), 8.05 (t, *J* = 2.0 Hz, 1H, H_A), 7.98 – 7.91 (dt, *J* = 7.9, 2.0 Hz, 2H, H_D), 7.45 (dd, *J* = 7.9, 4.9 Hz, 2H, H_E); ^{13}C NMR (125 MHz, $CDCl_3$); δ 149.9, 148.4, 147.9, 134.7, 134.0, 133.2, 133.1, 124.0; HR-ESIMS *m/z* = 234.10350 $[M+H]^+$ (calc. for $C_{15}H_{12}N_3$ 234.10257).

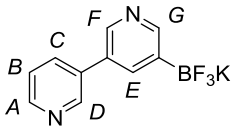

14

A solution of KHF_2 (0.47 g, 6 mmol, 4 equiv.) in water (4 mL) was added to a stirring solution of [3,3'-bipyridin]-5-yl-boronic acid (0.30 g, 1.5 mmol, 1 equiv.) in MeOH (4 mL) resulting in white precipitate. The mixture was stirred for 2 h at room temperature and then concentrated under reduced pressure to reveal white solid. The product was extracted with 20% MeOH/acetone solution (3×10 mL). The extracts were combined and concentrate until a small amount of precipitate was observed. Et_2O was added to encourage precipitation. The precipitate was filtered, washed with Et_2O and dried in air

to afford a white solid (0.31 g, 80%).^{1}H NMR (500 MHz, DMSO-d_6); δ 8.84 (dd, J = 2.3, 0.8 Hz, 1H, H_D), 8.61 (d, J = 2.5 Hz, 1H, H_F), 8.57 (dd, J = 4.8, 1.7 Hz, 1H, H_A), 8.50 (d, J = 0.8 Hz, 1H, H_G), 8.05 (ddd, J = 7.9, 2.3, 1.7 Hz, 1H, H_C), 7.87 (dd, appearing as apparent t, J = 2.5, 1.6 Hz, 1H, H_E), 7.49 (ddd, J = 7.9, 4.8, 0.8 Hz, 1H, H_B); ^{13}C NMR (125 MHz, DMSO-d_6); δ 152.4, 152.4, 148.4, 147.5, 144.8, 136.9, 134.4, 134.2, 131.1, 124.0; ^{19}F NMR (375 MHz, DMSO-d_6); δ -139.2.

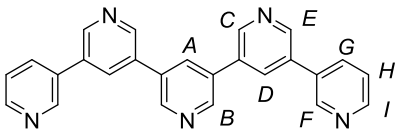

4

To a degassed 1,4-dioxane (7 mL) was charged **14** (0.31 g, 1.2 mmol, 2.4 equiv.), 3,5-dibromopyridine (0.12 g, 0.5 mmol, 1 equiv.) and $Pd(PPh_3)_2Cl_2$ (0.017 g, 0.024 mmol, 5 mol%) sequentially. The mixture was stirred at rt for 30 min then a degassed Na_2CO_3 solution (1 M, 5 mL, 3 equiv.) was added. The reaction mixture was heated to reflux overnight. The mixture was concentrated under reduced pressure. The residue was extracted with $CHCl_3$ (6×20 mL). The combined extracts were dried over $MgSO_4$, filtered, concentrated and purified by flash column chromatography (SiO_2, 0-7% MeOH/CH_2Cl_2) to give an off white solid (44.1 mg, 23%) as a product. m.p. >300 °C, ^{1}H NMR (400 MHz, $CDCl_3$); δ 8.99 (d, J = 2.1 Hz, 2H, H_B), 8.97 (d, J = 2.1 Hz, 2H, H_C), 8.94 (d, J = 2.1 Hz, 4H, H_{F+E}), 8.72 (dd, J = 4.8, 1.5 Hz, 2H, H_I), 8.17 (t, J = 2.1 Hz, 1H, H_A), 8.13 (t, J = 2.2 Hz, 2H, H_D), 7.98 (ddd , appearing as apparent dt, J = 7.8, 2.1, 1.6 Hz, 2H, H_G), 7.48 (ddd, J = 7.9, 4.9, 0.5 Hz, 2H, H_H); ^{13}C NMR (125 MHz, $CDCl_3$) δ 149.9, 148.40, 148.3, 148.2, 147.9, 134.8, 133.5, 133.3, 133.1, 132.2, 125.5, 124.1, 123.3; HR-ESIMS m/z = 388.15560 $[M+H]^+$ (calc. for $C_{25}H_{18}N_5$ 388.15567).

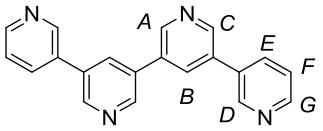

15

Isolated as a byproduct of the pentapyridine-forming reaction. ^{1}H NMR (500 MHz, $CDCl_3$); δ 8.95 (d, J = 2.1 Hz, 2H, H_D), 8.93 (m, 4H, H_{A+C}), 8.72 (dd, J = 4.8, 1.4 Hz, 2H, H_G), 8.11 (t, J = 2.1 Hz, 2H, H_B), 7.97 (ddd, appearing as apparent dt, J = 7.9, 2.4, 1.6 Hz, 2H, H_E),

7.47 (ddd, appearing as apparent dd, J = 7.9, 4.8, 0.9 Hz, 2H, H_F); ^{13}C NMR (125 MHz, $CDCl_3$); δ 149.9, 148.4, 148.2, 147.9, 134.8, 134.1, 133.6, 133.2, 133.2, 124.1; HR-ESIMS m/z = 311.12940 $[M+H]^+$ (calc. for $C_{20}H_{15}N_4$ 311.12912).

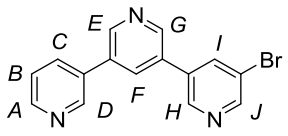

16

Isolated as a byproduct of the pentapyridine-forming reaction. ^{1}H NMR (500 MHz, $CDCl_3$); δ 8.91 (d, J = 2.2 Hz, 2H, H_{D+E}), 8.87 (d, J = 2.2 Hz, 1H, H_G), 8.82 (d, J = 2.0 Hz, 1H, H_H), 8.77 (d, J = 2.0 Hz, 1H, H_J), 8.72 (dd, J = 4.7, 1.7 Hz, 1H, H_A), 8.10 (t, J = 2.0 Hz, 1H, H_I), 8.03 (t, J = 2.1 Hz, 1H, H_F), 7.98 (dt, J = 8.0, 2.1 Hz, 1H, H_C), 7.47 (dd, J = 8.0, 4.8 Hz, 1H, H_B); ^{13}C NMR (125 MHz, $CDCl_3$); δ 150.8, 150.0, 148.4, 148.4, 147.8, 146.5, 137.2, 134.8, 134.8, 134.2, 133.1, 133.0, 132.6, 124.1, 121.4; HR-ESIMS m/z = 312.01230 $[M+H]^+$ (calc. for $C_{15}H_{11}N_3{}^{79}Br$ 312.01309).

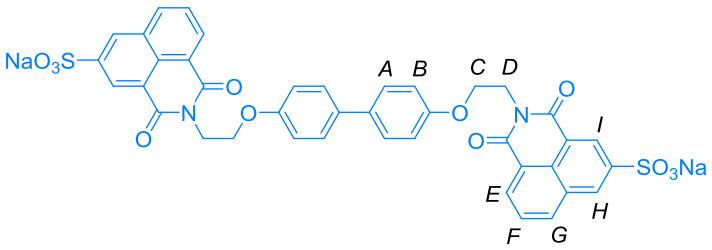

22

To a mixture of benzo[de]isoquinoline-1,3-dione-5-sulfonic acid sodium salt, **21** (0.11 g, 0.4 mmol), K_2CO_3 (0.25 g, 1.8 mmol) and NaI (5.1 mg, 0.034 mmol, 5 mol%) in anhydrous DMF (5 mL) stirring at room temperature for 30 min, was added a solution of **19** (67.3 mg, 0.17 mmol) in DMF (2 mL) and the reaction mixture was heated to 120 °C for 2 d. The reaction mixture was cooled down, filtered through celite. The filtrate was charged acetone (3 mL) and water (3 mL) and placed in a freezer overnight. The precipitate was separated, washed with acetone, dried in air to get a brown solid (2.4 mg, 2%). m.p. >350 °C dec., ^{1}H NMR (500 MHz, DMSO-d_6); δ 8.70 (d, J = 1.3 Hz, 2H, H_I), 8.66 (s, 2H, H_H), 8.56 (d, J = 8.1 Hz, 2H, H_G), 8.52 (d, J = 7.2 Hz, 2H, H_E), 7.89 (t, J = 7.7 Hz, 2H, H_F), 7.49 (d, J = 8.7 Hz, 4H, H_A), 7.00 (d, J = 8.7 Hz, 4H, H_B), 4.47 (t, J = 6.5 Hz, 4H, H_C), 4.27 (t, J = 6.5 Hz, 4H, H_D); ^{13}C NMR (125 MHz, DMSO-d_6); δ 164.0, 163.9, 157. 8, 147.6, 135.6, 133.0, 131.53,

131.49, 130.5, 129.1, 128.1, 127.8, 127.7, 122.5, 122.4, 115.3, 64.7, 39.1; HR-ESIMS *m/z* = 813.08670 $[M-Na]^-$ (calc. for $C_{40}H_{26}O_{12}N_2NaS_2$ 813.08304).

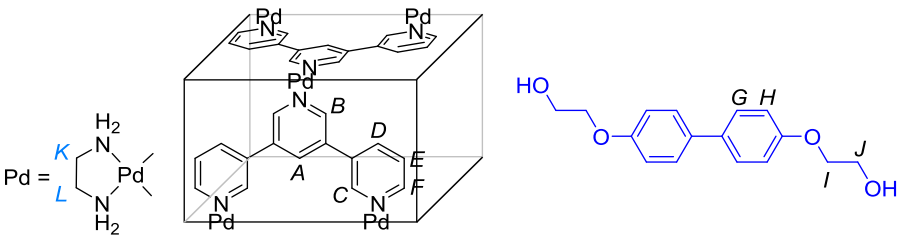

23

^{1}H NMR (500 MHz, D_2O); δ 9.92 (d, appearing as apparent s, *J* = 1.8 Hz, 8H, H_C), 9.58 (d, appearing as apparent s, *J* = 1.7 Hz, 8H, H_B), 9.14 (dd, appearing as apparent d, *J* = 5.7, 1.2 Hz, 8H, H_F), 8.97 (t, appearing as apparent s, *J* = 1.8 Hz, 4H, H_A), 8.31 (dt, appearing as apparent d, *J* = 8.0, 1.6 Hz, 8H, H_D), 7.82 (dd, *J* = 8.1, 5.8 Hz, 8H, H_E), 4.79 (s, appearing under a solvent peak, 4H, H_G), 4.44 (d, *J* = 8.2 Hz, 4H, H_H), 3.85 (t, *J* = 4.6 Hz, 4H, H_J), 3.08 – 2.96 (m, 12H, H_K), 2.97 – 2.85 (m, 12H, H_L), 2.82 – 2.70 (m, 4H, H_I); ^{13}C NMR (125 MHz, D_2O); δ 156.3, 152.4, 149.5, 149.0, 137.6, 134.5, 133.7, 132.2, 127.8, 127.4, 122.0, 113.0, 67.8, 59.5, 46.9, 46.8.

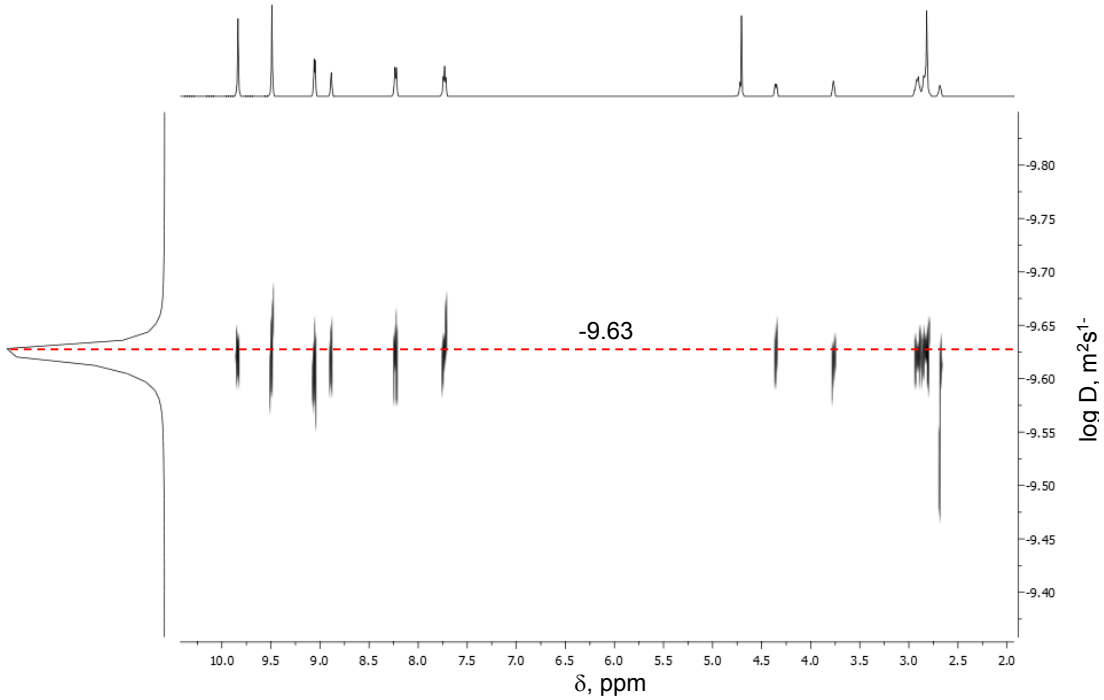

Figure 4.15 ^{1}H DOSY NMR (500 MHz, D_2O, 298 K) spectrum for tube complex **23** with corresponding log D, m^2s^{-1}= -9.63.

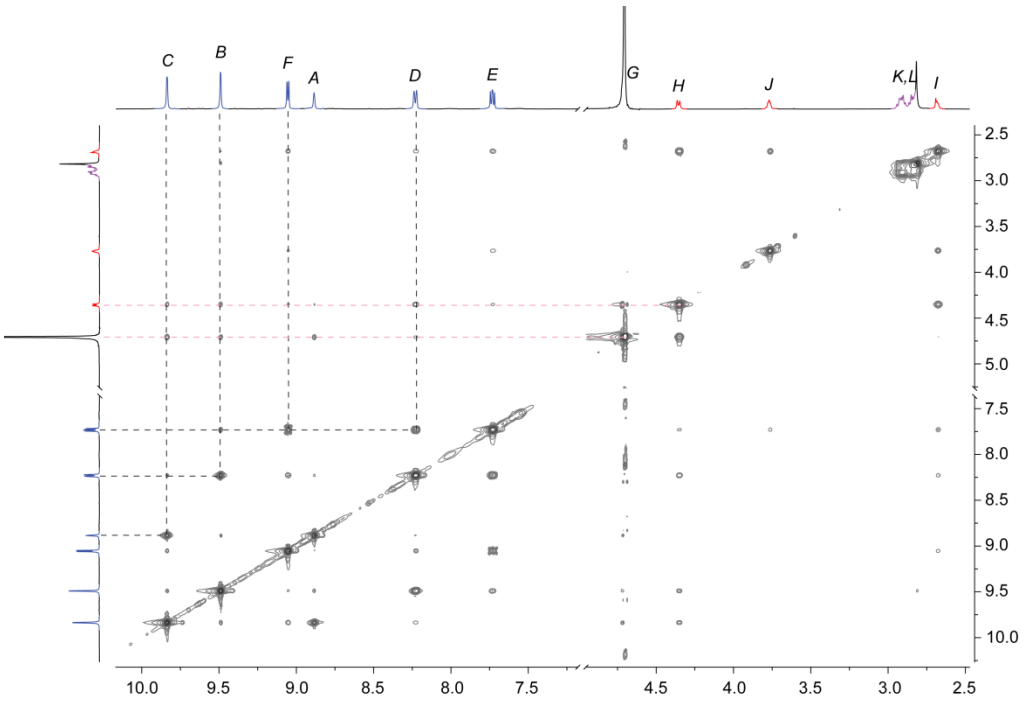

Figure 4.16 ^{1}H,^{1}H-NOESY (500 MHz, D_2O, 298 K) of **23**.

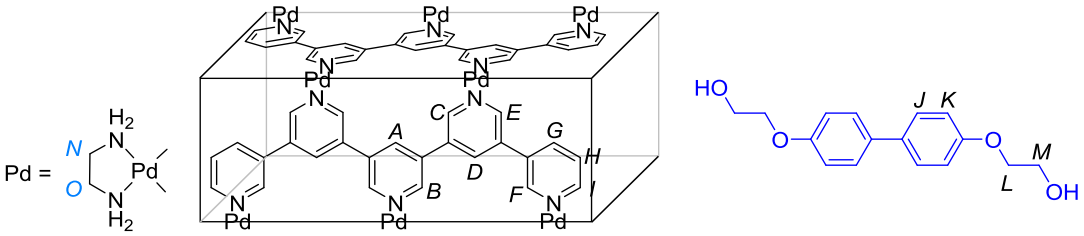

24

^{1}H NMR (500 MHz, D_2O); δ 10.32 (s, 8H, H_B), 10.27 (s, 8H, H_C), 9.79 (s, 8H, H_F), 9.54 (s, 8H, H_E), 9.25 (s, 4H, H_A), 9.16 (s, 8H, H_D), 9.09 (d, J = 5.7 Hz, 8H, H_I), 8.38 (d, J = 7.6 Hz, 8H, H_G), 7.81 (t, J = 7.0 Hz, 8H, H_H), 4.98 (br, 4H, H_J), 4.59 (br, 4H, H_K), 3.05 (m, 20H, H_N), 3.01 – 2.86 (m, 20H, H_O), 2.52 (br, 4H, H_M), 2.05 (br, 4H, H_L); ^{13}C NMR (125 MHz, D_2O); δ 152.21, 152.18, 150.5, 150.3, 149.4, 141.0, 139.7, 138.2, 138.1, 134.6, 134.5, 134.3, 133.1, 132.6, 132.5, 132.3, 127.2, 47.0, 46.9, 46.7, 45.8.

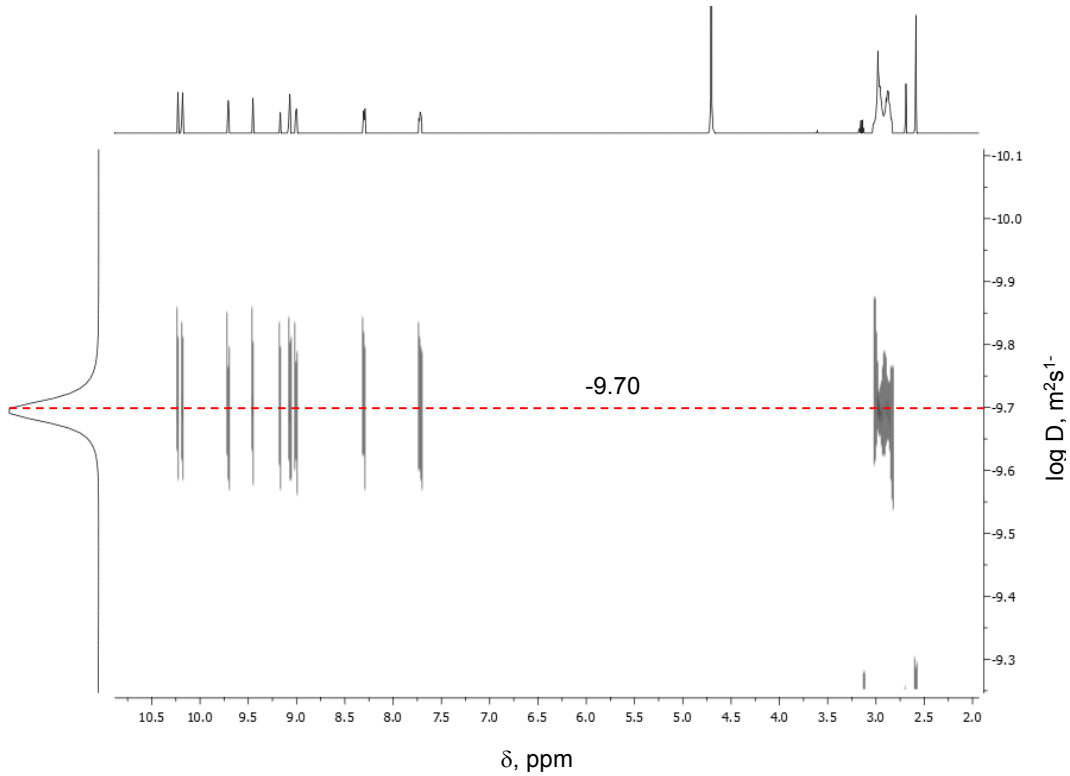

Figure 4.17 ^{1}H DOSY NMR (500 MHz, D_2O, 298 K) spectrum for tube complex **24** with corresponding log D, m^2s^{-1}= -9.70.

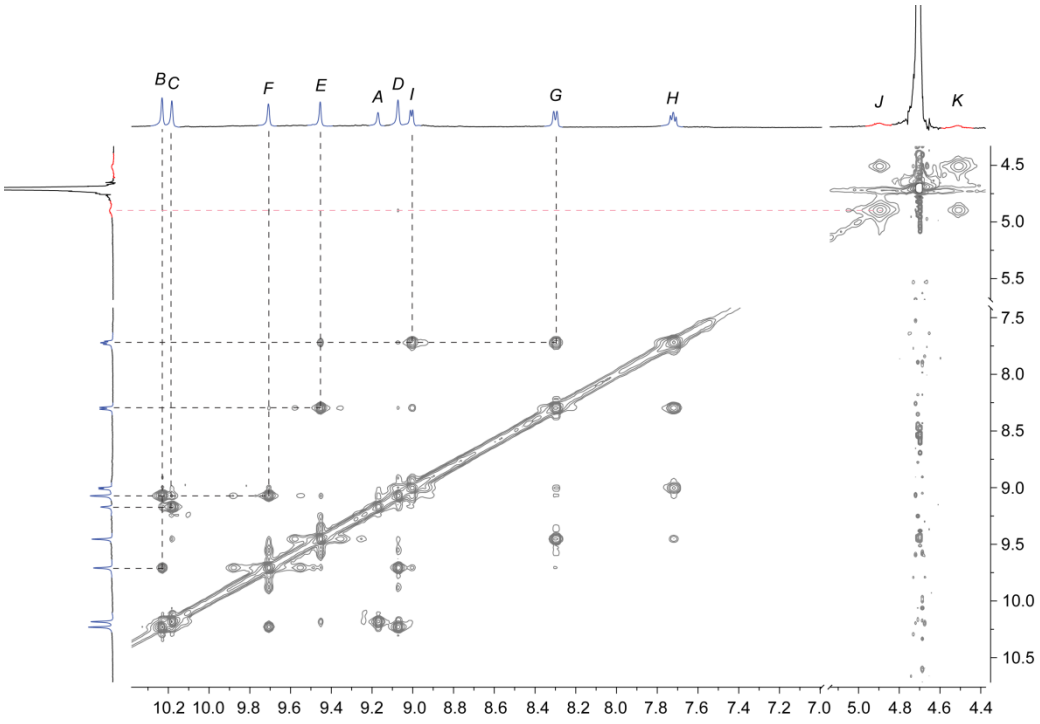

Figure 4.18 ^{1}H,^{1}H-NOESY (500 MHz, D_2O, 298 K) of **24**.

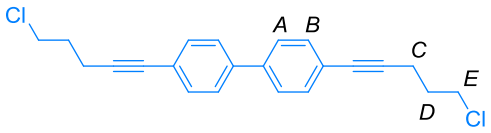

25

To a suspension of 1,4-diiodobiphenyl (0.81 g, 2 mmol), CuI (38.9 mg, 0.20 mmol, 10 mol%), PPh_3 (52.9, 0.20 mmol, 10 mol%) and $Pd(PPh_3)_2Cl_2$ (70.2 mg, 0.10 mmol 5 mol%) in dry THF (12 mL) was charged 5-chloro-1-pentyne (0.63 mL, 6 mmol) and Et_3N (6 mL). The reaction mixture was stirred at rt for 30 min and heated to 65 °C overnight. The reaction was cooled, filtered through celite. The filtrate was washed with saturated NH_4Cl, water. Organic layers were dried over $MgSO_4$, filtered, concentrated. The residue was purified by flash column chromatography (SiO_2, 5% CH_2Cl_2/hexane) to obtain a pale yellow solid (0.40 g, 57%).^{1}H NMR (600 MHz, $CDCl_3$) δ 7.52 (d, *J* = 8.4 Hz, 4H, H_A), 7.46 (d, *J* = 8.4 Hz, 4H, H_B), 3.73 (t, *J* = 6.4 Hz, 4H, H_E), 2.64 (t, *J* = 6.8 Hz, 4H, H_C), 2.08 (p, *J* = 6.6 Hz, 4H, H_D); ^{13}C NMR (150MHz, $CDCl_3$); δ 139.9, 132.2, 126.9, 123.0, 89.2, 81.5, 43.9, 31.6, 17.1.

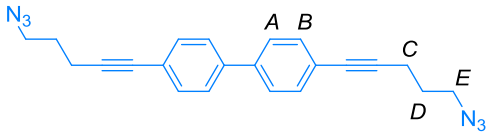

26

To a solution of **25** (0.40 g, 1 mmol) in DMF (9 mL) was added a solution of NaN_3 (0.22 g, 3 mmol) in water (1 mL). The solution was heated at 80 °C for 4 h (TLC indicated that no starting materials remained). The reaction was cooled down, quenched by water (6 mL) resulting in precipitation. The desired product was extracted with Et_2O (3×10 mL). Combined organic layers were dried over $MgSO_4$, filtered and concentrated to afford an off white solid (0.33 g, 80%). ^{1}H NMR (600 MHz, $CDCl_3$) δ 7.51 (d, *J* = 8.4 Hz, 4H, H_A), 7.46 (d, *J* = 8.4 Hz, 4H, H_B), 3.49 (t, *J* = 6.9 Hz, 4H, H_E), 2.56 (t, *J* = 6.9 Hz, 4H, H_C), 1.89 (p, *J* = 6.8 Hz, 4H, H_D); ^{13}C NMR (125 MHz, $CDCl_3$) δ 139.9, 132.2, 126.9, 122.9, 89.3, 81.6, 50.5, 28.1, 17.0; HR-ESIMS *m/z* = 369.18160 $[M+H]^+$ (calc. for $C_{22}H_{21}N_6$ 369.18222).

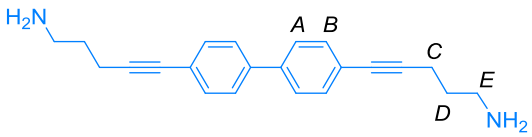

27

Adapted from a procedure by Mi and co-workers[26] To a mixture of **26** (0.18 g, 0.5 mmol) and NH_4Cl (0.14 g, 2 mmol) in EtOH (4 mL) and water (1 mL) was added Zn powder (90.2 mg, 1 mmol) and the mixture was stirred vigorously at refluxing temperature for 30 min. When the reaction was complete (monitored by TLC), EtOAc (6 mL) was added, followed by NH_3 solution (1 mL). The mixture was filtered. The filtrate was washed with brine, dried, solvent was evaporated to obtain a brown solid (25.5 mg, 13%).^{1}H NMR (400 MHz, MeOD-d_4); δ 7.59 (d, J = 8.4 Hz, 4H, H_A), 7.46 (d, J = 8.5 Hz, 4H, H_B), 3.12 (t, J = 7.3 Hz 4H, H_E), 2.61 (t, J = 6.9 Hz, 4H, H_C), 2.01 – 1.91 (m, 4H, H_D); ^{13}C NMR (125 MHz, MeOD-d_4); δ 141.0, 133.1, 127.8, 124.1, 89.4, 82.6, 39.9, 27. 7, 17.3; HR-ESIMS m/z = 317.20080 $[M+H]^+$ (calc. for $C_{22}H_{25}N_2$ 317.20123).

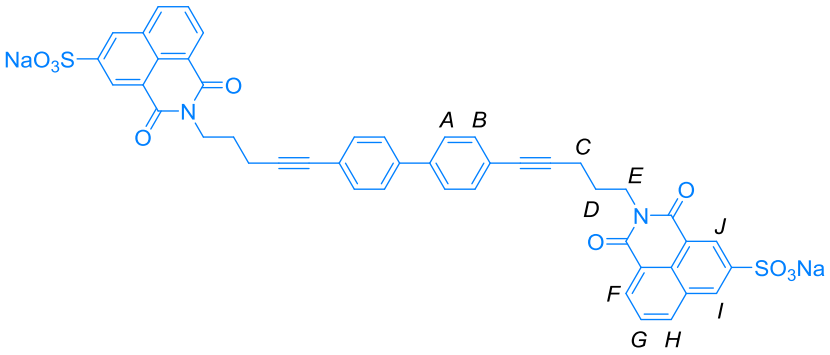

28

The mixture of **27** (0.07 g, 0.18 mmol) and **20** (79.9 mg, 0.27 mmol) in EtOH (10 mL) was heated to reflux for 2 d. After the mixture was cooled, the solid was collected, washed with cold EtOH to get an off white solid (51.7 mg, 31%). m.p. >350, ^{1}H NMR (600 MHz, DMSO-d_6); δ 8.74 (d, J = 1.4 Hz, 2H, H_J), 8.64 (d, J = 8.3 Hz, 2H, H_H), 8.63 (d, J = 1.4 Hz, 2H, H_I), 8.51 (d, J = 7.2 Hz, 2H, H_F), 7.94 – 7.90 (m, 2H, H_G), 7.68 (d, J = 8.3 Hz, 4H, H_A), 7.48 (d, J = 8.3 Hz, 4H, H_B), 2.94 (br, 4H, H_E), 2.57 (t, J = 7.0 Hz, 4H, H_C), 1.83 (dt, J = 14.5, 7.1 Hz, 4H, H_D); ^{13}C NMR (125 MHz, DMSO-d_6); δ 161.2, 161.0, 147.8, 139.1, 136.5, 133.0, 132.4, 131.6, 131.4, 130.3, 130.0, 128.4, 127.2, 122.8, 119.6, 110.0, 90.7, 81.4, 38.6, 26.7, 16.5; HR-ESIMS m/z = 853.29770 $[M-Na+2H]^+$ (calc. for $C_{46}H_{30}N_2O_{10}S_2Na_2$ 859.13906).

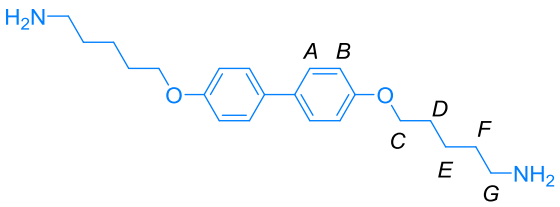

29

Adapted from a procedure by Buchwald and co-workers[17] An oven-dried Schlenk tube was charged with CuI (14.1 mg, 0.075 mmol, 5 mol%), 3,4,7,8-tetramethyl-1-10-phenanthroline (36.3 mg, 0.15 mmol, 10 mol%), 4,4'diiodobiphenyl (0.61 g, 1.5 mmol), Cs_2CO_3 (1.97 g, 6 mmol) and activated 3 Å molecular sieves (200 mg). The tube was evacuated and refilled with N_2. Under a counterflow of N_2, 5-amino-1-pentanol (0.62 g, 6 mmol) was added, followed by 0.75 mL of toluene. The tube was sealed and the mixture was allowed to stir at 90 °C, for 20 h. At the end of the reaction, the mixture was diluted with CH_2Cl_2 and filtered to remove inorganic salts. The solvent was removed by rotary evaporation and the residue was purified by flash column chromatography (SiO_2, 0–5% MeOH/CH_2Cl_2, NH_3 saturated) to afford a pale yellow solid (0.17 g, 31%). m.p. 163-165 °C, ^{1}H NMR (500 MHz, $CDCl_3$); δ 7.45 (d, J = 8.8 Hz, 4H, H_A), 6.93 (d, J = 8.8 Hz, 4H, H_B), 3.99 (t, J = 6.5 Hz, 4H, H_C), 2.76 – 2.65 (m, 4H, H_G), 1.90 – 1.74 (m, 4H, H_D), 1.61 – 1.45 (m, 8H, H_{E+F}); ^{13}C NMR (125 MHz, $CDCl_3$); δ 133.6, 127.8, 114. 9, 110.1, 68.1, 42.3, 33.7, 29.3, 23.6; HR-ESIMS m/z = 357.253452 $[M+H]^+$ (calc. for $C_{22}H_{33}N_2O_2$ 357.253655).

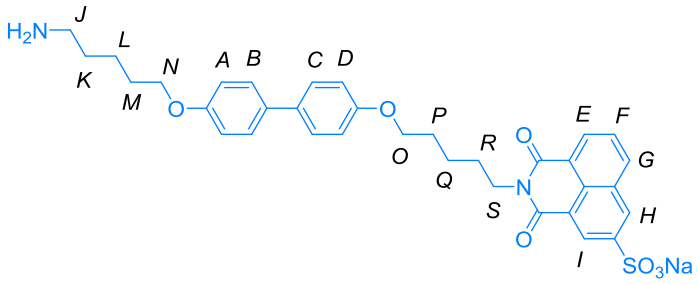

30

A flask was charged with **29** (0.05 g, 0.14 mmol) and **20** (0.08 g, 0.28 mmol) and EtOH (10 mL). The suspension was refluxed for 2 d. The resulting solid was filtered, washed with cold EtOH and dried in air to get an off white solid (0.09 g, quantitative). m.p. >300 °C dec. ^{1}H NMR (500 MHz, DMSO-d_6); δ 8.68 (d, J = 1.2 Hz, 1H, H_I), 8.66 (d, J = 1.6 Hz, 1H, H_H), 8.55 (dd, J = 8.3, 1.1 Hz, 1H, H_G), 8.49 (dt, J = 7.3, 1.5 Hz, 1H, H_E), 7.87 (dd, appearing

as apparent t, J = 8.2, 7.3 Hz, 1H, H_F), 7.49 (m, 4H, H_{B+D}), 6.96 (m, 4H, H_{A+C}), 4.09 (t, J = 7.3 Hz, 2H, H_S), 3.99 (t, J = 6.4 Hz, 4H, H_{N+O}), 2.85 – 2.77 (m, 2H, H_J), 1.75 (m, 6H, H_{M+P+R}), 1.60 (ddd, J = 15.0, 8.6, 6.8 Hz, 2H, H_K), 1.55 – 1.42 (m, 4H, H_{L+Q}); ^{13}C NMR (125 MHz, DMSO-d_6); δ 163.4, 163.3, 157.7, 157.6, 147.0, 134.9, 132.3, 132.2, 132.1, 131.0, 130.9, 129.9, 128.5, 127. 6, 127.2, 127.1, 122.05, 121.97, 114.8, 114.8, 67.2, 67.2, 28.5, 28.4, 28.1, 27.3, 27.2, 26.7, 23.05, 22.98; HR-ESIMS m/z 617.229574 $[M+2H-Na]^+$ (calc. for $C_{34}H_{37}N_2O_7S$ 617.231599).

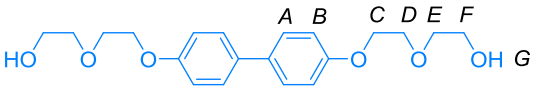

31

A flame-dried flask with K_2CO_3 (2.80 g, 20 mmol) and LiBr (0.08 g, 0.5 mmol) was evacuated and refilled with N_2 (3×) then 4,4'-dihydroxybiphenyl (0.93 g, 5 mmol) was introduced under a positive flow of N_2. Dry MeCN (10 mL) was added followed with 2-(2-chloroethoxy)ethanol (6.26 g, 50 mmol). The reaction mixture was heated to dissolve all the solid and left stirring at 75 – 80 °C overnight. The solution was cooled to rt, clear precipitate formed, water was added to quenched the reaction. The product was extracted with hot CH_2Cl_2 and recrystallised to obtain a colourless solid (1.56 g, 86%). m.p. 152-153 °C, ^{1}H NMR (500 MHz, $CDCl_3$); δ 7.47 (d, J = 8.8 Hz, 4H, H_A), 6.97 (d, J = 8.8 Hz, 4H, H_B), 4.18 (dd, J = 5.4, 4.1 Hz, 4H, H_C), 3.90 (dd, J = 5.4, 4.1 Hz, 4H, H_D), 3.82 – 3.74 (m, 4H, H_F), 3.71 – 3.67 (m, 4H, H_E), 2.12 (t, J = 6.2 Hz, 2H, H_G); ^{13}C NMR (125 MHz, $CDCl_3$); δ 158.0, 133.9, 127.9, 115.1, 72.7, 69. 9, 67.7, 62.0; HR-ESIMS m/z 363.17950 $[M+H]^+$ (calc. for $C_{20}H_{27}O_6$ 363.18131)

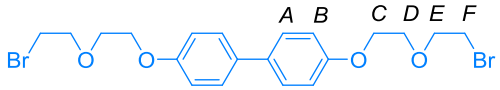

32

To a mixture of diol **31** (1.0 g, 2.8 mmol) and CBr_4 (2.57 g, 7.7 mmol) in dry CH_2Cl_2 (20 mL) was added a solution of PPh_3 (2.02 g, 7.7 mmol) in CH_2Cl_2 (7 mL) and the reaction mixture was stirred at rt for 5 h. Water was added and the aqueous layer was extracted with CH_2Cl_2 (3×). After drying of the organic layer and removal of the solvent under reduced pressure, the crude product was purified by flash column chromatography

(SiO_2, 50% CH_2Cl_2/hexane) to achieve a white solid (1.07 g, 78%). m.p. 116-118 °C, ^{1}H NMR (500 MHz, $CDCl_3$); δ 7.47 (d, *J* = 8.8 Hz, 4H, H_A), 6.97 (d, *J* = 8.8 Hz, 4H, H_B), 4.22 – 4.12 (m, 4H, H_C), 3.95 – 3.83 (m, 8H, H_{D+E}), 3.51 (t, *J* = 6.3 Hz, 4H. H_F); ^{13}C NMR (125 MHz, $CDCl_3$); δ 157.9, 133.8, 127.8, 115.0, 71.5, 69.8, 67.6, 30.4; HR-ESIMS m/z 508.99160 $[M+Na]^+$ (calc. for $C_{20}H_{24}O_4{}^{79}Br_2Na$ 508.99335).

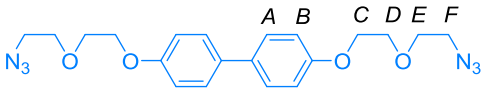

33

To a solution of dibromo **32** (0.71 g, 1.4 mmol) in DMF (9 mL) was added a solution of NaN_3 (0.29 g, 4.4 mmol) in water (1 mL). The reaction mixture was heated at 80 °C for 2 d. The reaction was cooled down, quenched by water (10 mL) resulting in precipitation. An off white solid (0.56 g, 93%) was filtered, washed with water and dried in air. m.p. 112-113 °C, ^{1}H NMR (500 MHz, $CDCl_3$); δ 7.46 (d, *J* = 8.8 Hz, 4H, H_A), 6.97 (d, *J* = 8.8 Hz, 4H, H_B), 4.18 (dd, *J* = 5.4, 4.2 Hz, 4H, H_C), 3.89 (dd, *J* = 5.4, 4.2 Hz, 4H, H_D), 3.77 (dd, *J* = 5.5, 4.6 Hz, 4H, H_E), 3.43 (t, *J* = 5.1 Hz, 4H, H_F); ^{13}C NMR (125 MHz, $CDCl_3$); δ 158.0, 133.9, 127.9, 115.1, 70.4, 70.0, 67.7, 50. 9; HR-ESIMS m/z 435.17360 $[M+Na]^+$ (calc. for $C_{20}H_{24}O_4N_6Na$ 435.17512).

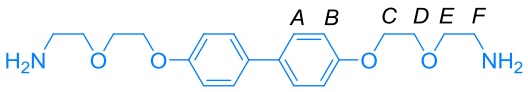

34

$LiAlH_4$ (27 mg, 0.7 mmol, excess) was introduce into a flask and any residues was rinsed in with dry THF (10 mL). The suspension was heated to a gentle reflux. A solution of **33** (0.10 g, 0.24 mmol) in dry THF (10 ml) was added *via* syringe pump at a rate that the THF in the flask maintains the gentle reflux. The reaction mixture was refluxed for an hour, cooled in ice, and treated with a mixture of H_2O and THF to decompose excess $LiAlH_4$. The solution was acidified with 1 M HCl and placed in the fridge overnight to encourage precipitation. A white solid was filtered and wash with cold water, dried in air (0.08 g, 91%). ^{1}H NMR (600 MHz, MeOD-d_4); δ 7.52 (d, *J* = 8.8 Hz, 4H, H_A), 7.03 (d, *J* = 8.8 Hz, 4H, H_B), 4.24-4.21 (m, 4H, H_C), 3.92-3.89 (m, 4H, H_D), 3.71 (t, *J* = 5.2 Hz, 4H, H_E), 2.99

(t, J = 5.2 Hz, 4H, H_F); ^{13}C NMR (125 MHz, MeOD-d_4); δ 159.3, 135.0, 128.6, 115.9, 71.5, 70.8, 68.7, 41.6; HR-ESIMS m/z 361.21480 $[M+H]^+$ (calc. for $C_{20}H_{29}O_4N_2$ 361.21218).

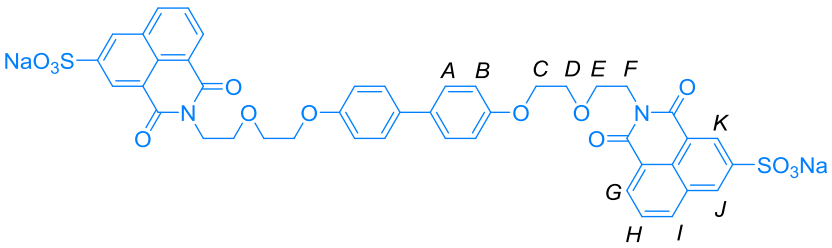

35

To a solution of diamine **34** (72.9 mg, 0.2 mmol, 1 equiv.) in mixed solvent, EtOH, MeOH, CH_2Cl_2 and DMF (~10 mL) was added a solution of **20** (0.31 g, 1 mmol, 5 eq.) in DMF (7 mL). The reaction mixture was refluxed overnight. The mixture was cooled down, put in a freezer overnight and the solid was filtered. An off white solid was obtained (0.19 g, quantitative). m.p. >320 °C dec., ^{1}H NMR (600 MHz, DMSO-d_6); δ 8.70 (d, J = 1.6 Hz, 2H, H_K), 8.66 (d, J = 1.6 Hz, 2H, H_J), 8.54 (dd, J = 8.1, 1.1 Hz, 2H, H_I), 8.49 (dd, J = 7.3, 1.1 Hz, 2H, H_G), 7.87 (t, J = 7.7 Hz, 2H, H_H), 7.42 (d, J = 8.7 Hz, 4H, H_A), 6.88 (d, J = 8.7 Hz, 4H, H_B), 4.30 (t, J = 6.4 Hz, 4H, H_C), 4.08 – 4.06 (m, 4H, H_E), 3.81 – 3.78 (m, 4H, H_F), 3.76 (t, J = 6.4 Hz, 4H, H_D); ^{13}C NMR (125 MHz, DMSO-d_6); δ 163.5, 163.3, 157.5, 147.0, 135.0, 132.3, 131.04, 130.99, 129.99, 128.6, 127.6, 127.2, 127.1, 122.0, 121.9, 114.8, 68.8, 67.11, 67.07, 38.9; HR-ESIMS m/z 947.11470 $[M+Na]^+$ (calc. for $C_{44}H_{34}O_{14}N_2Na_3S_2$ 947.11391).

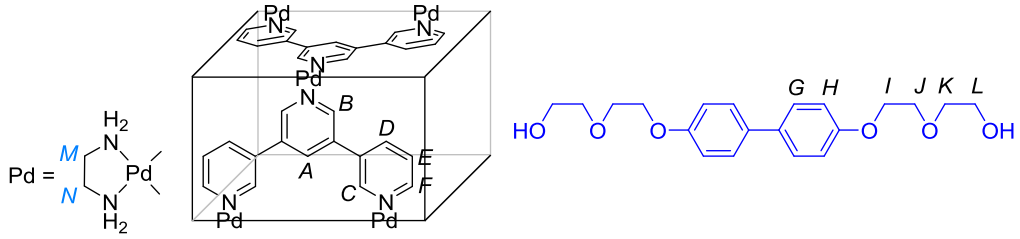

36

^{1}H NMR (600 MHz, D_2O); δ 9.92 (d, J = 2.2 Hz, 8H, H_C), 9.58 (d, J = 1.9 Hz, 8H, H_B), 9.15 (dd, J = 5.8, 1.2 Hz, 8H, H_F), 8.97 (d, J = 2.2 Hz, 4H, H_A), 8.31 (dt, J = 8.1, 1.7 Hz, 8H, H_D), 7.84 (dd, J = 8.0, 5.8 Hz, 8H, H_E), 4.79 (s, appearing under a solvent peak, 4H, H_G), 4.42

(d, J = 8.0 Hz, 4H, H_H), 4.01 (t, J = 4.6 Hz, 4H, H_K), 3.87 (t, J = 4.6 Hz, 4H, H_L), 3.85 – 3.80 (m, 4H, H_J), 3.04 – 2.96 (m, 12H, H_M), 2.96 – 2.89 (m, 12H, H_N), 2.89 – 2.85 (m, 4H, H_I); ^{13}C NMR (125 MHz, D_2O); δ 156.1, 152.4, 149.5, 149.0, 137.6, 134.5, 133.7, 132.2, 127.9, 127.4, 122.1, 112.8, 72.4, 68.4, 66.1, 60.8, 46.9, 46.8.

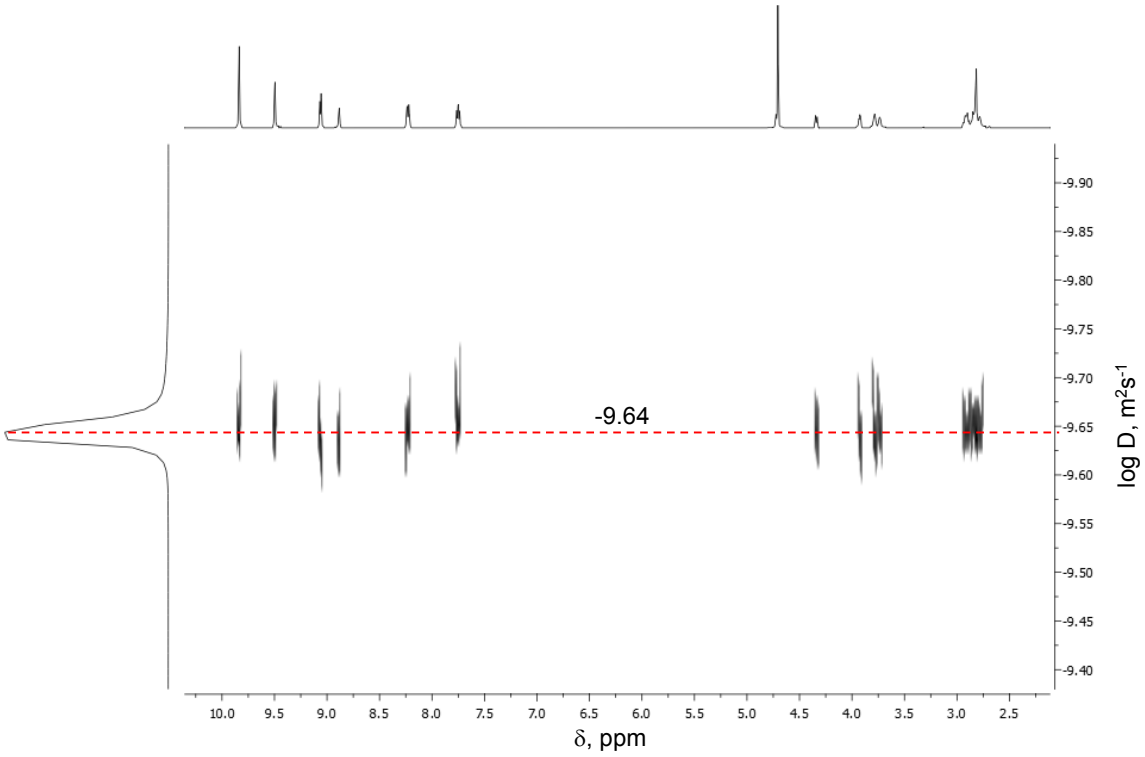

Figure 4.19 ^{1}H DOSY NMR (500 MHz, D_2O, 298 K) spectrum for tube complex **36** with corresponding log D, m^2s^{-1}= -9.64.

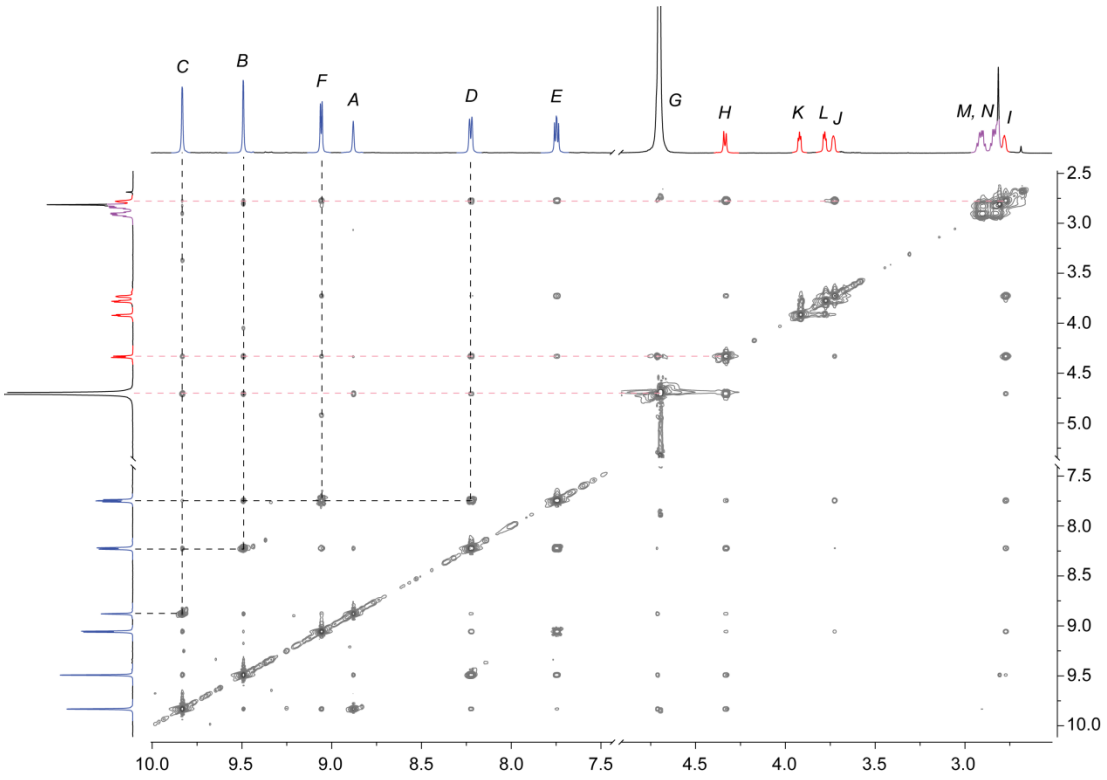

Figure 4.20 ^{1}H,^{1}H-NOESY (500 MHz, D_2O, 298 K) of **36**.

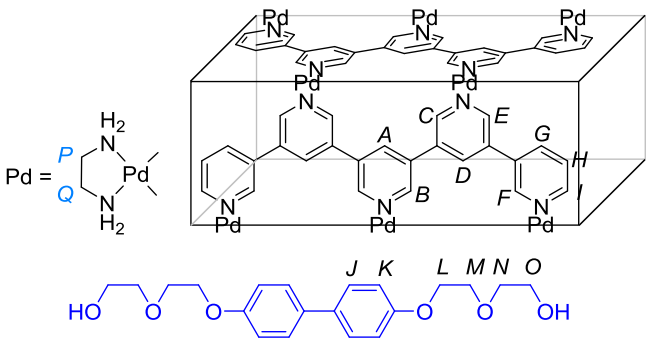

37

^{1}H NMR (600 MHz, D_2O); δ 10.42 (d, J = 1.7 Hz, 8H, H_B), 10.35 (d, J = 1.9 Hz, 8H, H_C), 9.90 (d, J = 2.0 Hz, 8H, H_F), 9.66 (d, J = 1.7 Hz, 8H, H_E), 9.38 (s, 4H, H_A), 9.28 (s, 8H, H_D), 9.13 (dd, J = 5.8, 1.2 Hz, 8H, H_I), 8.46 (d, J = 8.0 Hz, 8H, H_G), 7.84 (dd, J = 7.9, 6.0 Hz, 8H, H_H), 4.96 (d, J = 8.1 Hz, 4H, H_J), 4.49 (d, J = 7.7 Hz, 4H, H_K), 3.11 – 3.03 (m, 20H, H_P), 3.01 – 2.91 (m, 20H, H_Q), 2.69 – 2.64 (m, 4H, H_O), 2.53 – 2.47 (m, 4H, H_N), 2.43 (t, J = 4.5 Hz, 4H, H_M), 2.14 (t, J = 4.5 Hz, 4H, H_L); ^{13}C NMR (125 MHz, D_2O); δ 152.6, 152.5, 150.8, 150.7, 150.5, 150.04, 149.98, 149.4, 149.3, 147.9, 138.1, 134.3, 134.2, 132.8, 132.4, 132.2, 127.3, 71.8, 59.5, 47.2, 47.0, 46. 9, 45.8.

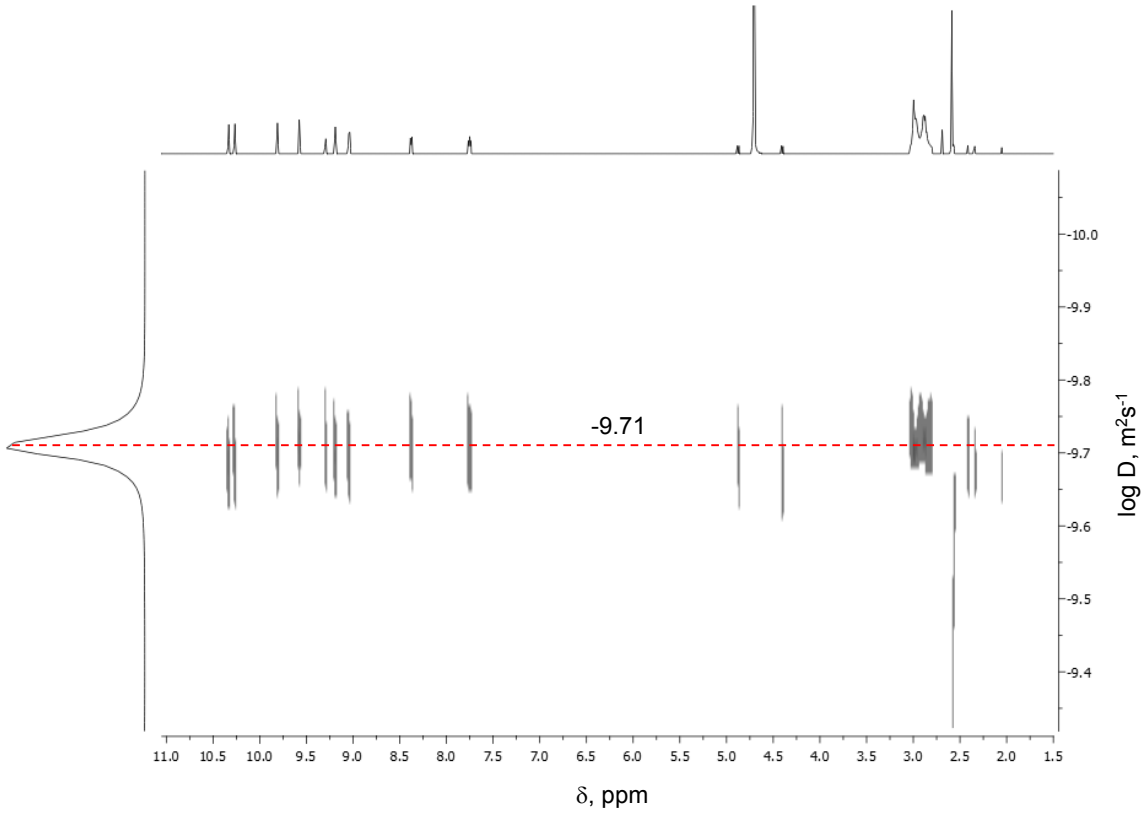

Figure 4.21 ^{1}H DOSY NMR (500 MHz, D_2O, 298 K) spectrum for tube complex **37** with corresponding log D, m^2s^{-1} = -9.71.

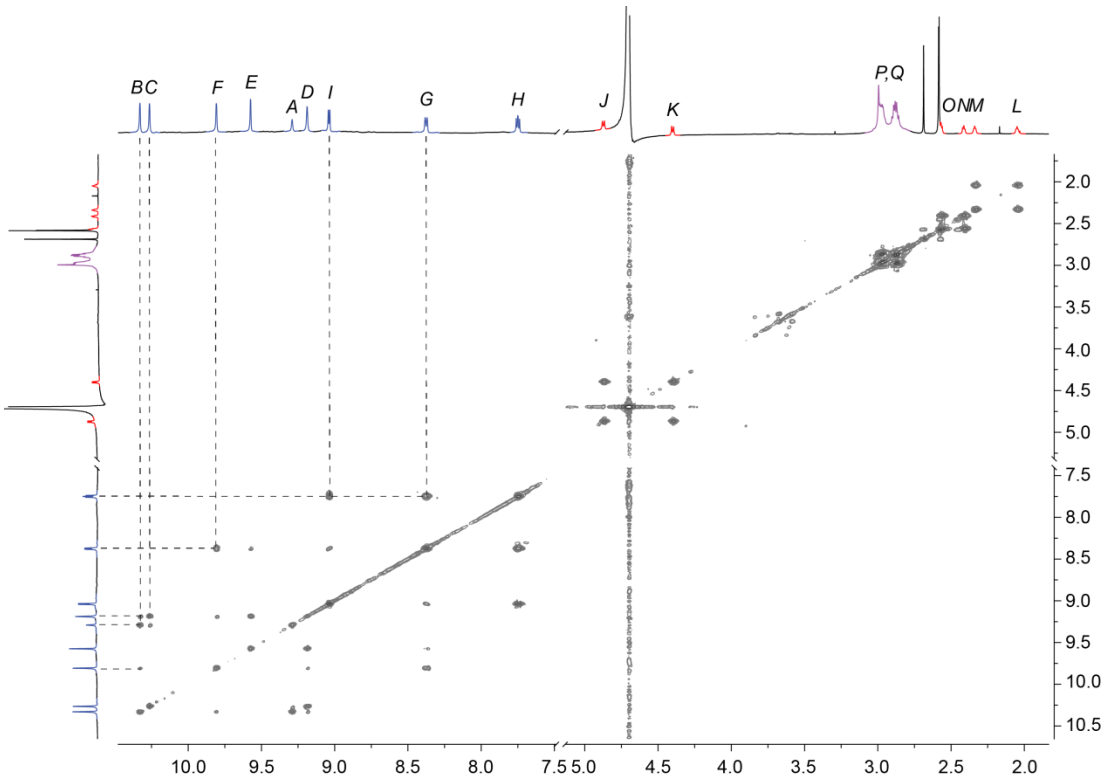

Figure 4.22 $^{1}H,^{1}H$-NOESY (500 MHz, D_2O, 298 K) of **37**.

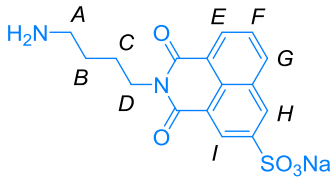

39

A flask was charged with 1,4-diaminobutane (0.60 mL, 6 mmol) and **20** (1.50 g, 5 mmol) and EtOH (10 mL). The suspension was refluxed for 16 h. The resulting solid was filtered, washed with cold EtOH and dried in air to get a light yellow solid (1.53 g, 83%). m.p. >350 °C, ^{1}H NMR (600 MHz, DMSO-d_6) δ 8.68 (dd, J = 12.6, 1.6 Hz, 2H, H_{I+H}), 8.57 (dd, J = 8.3, 1.1 Hz, 1H, H_G), 8.50 (dd, J = 7.2, 1.1 Hz, 1H, H_E), 7.91 – 7.86 (m, 1H, H_F), 4.12 (t, J = 6.8 Hz, 2H, H_D), 2.82 (t, J = 7.5 Hz, 2H, H_A), 1.77 – 1.68 (m, 2H, H_C), 1.63-1.53 (m, 2H, H_B); ^{13}C NMR (150 MHz, DMSO-d_6) δ 163.5, 163.4, 147.1, 135.1, 131.0, 130.9, 129.9, 128.7, 127.6, 127.1, 122.0, 121.9, 62.8, 40.1, 24.8, 24.7; HR-ESIMS m/z 371.06820 $[M+H]^+$ (calc. for $C_{16}H_{16}O_5N_2NaS$ 371.06721).

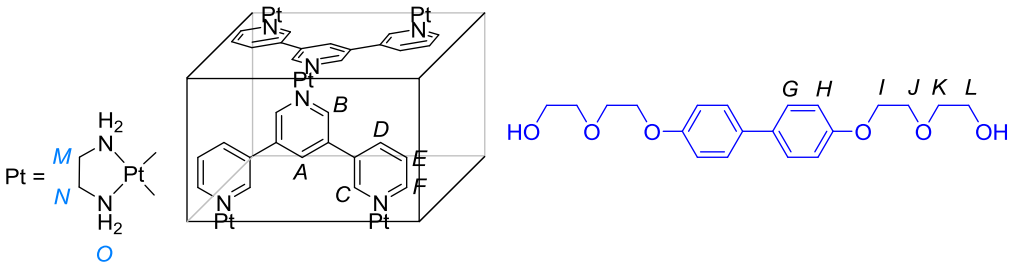

40

^{1}H NMR (500 MHz, D_2O); δ 9.88 (d, J = 2.4 Hz, 8H, H_C), 9.66 (d, J = 1.6 Hz, 8H, H_B), 9.15 (dd, J = 5.7, 1.4 Hz, 8H, H_F), 9.07 (t, appearing as apparent s, J = 1.8 Hz, 4H, H_A), 8.34 (dt, J = 8.2, 1.6 Hz, 8H, H_D), 7.82 (dd, J = 8.1, 5.9 Hz, 8H, H_E), 4.86 (d, J = 8.3 Hz, 4H, H_G), 4.48 (d, J = 8.5 Hz, 4H, H_H), 3.99 (t, J = 4.6 Hz, 4H, H_K), 3.85 (t, J = 4.6 Hz, 4H, H_L), 3.82 (t, J = 3.3 Hz, 4H, H_J), 2.99 – 2.89 (m, 16H, H_{M+I}), 2.86 (m, 12H, H_N), 2.69 (s, J (^{195}Pt) = 38.1 Hz, 24H, H_O); ^{13}C NMR (125 MHz, D_2O); δ 156.2, 153.3, 150.4, 150.1, 137.6, 134.6, 133.9, 132.4, 128.0, 127.9, 122.1, 112.9, 72.4, 68.4, 66.2, 60.7, 47.6, 46.8.

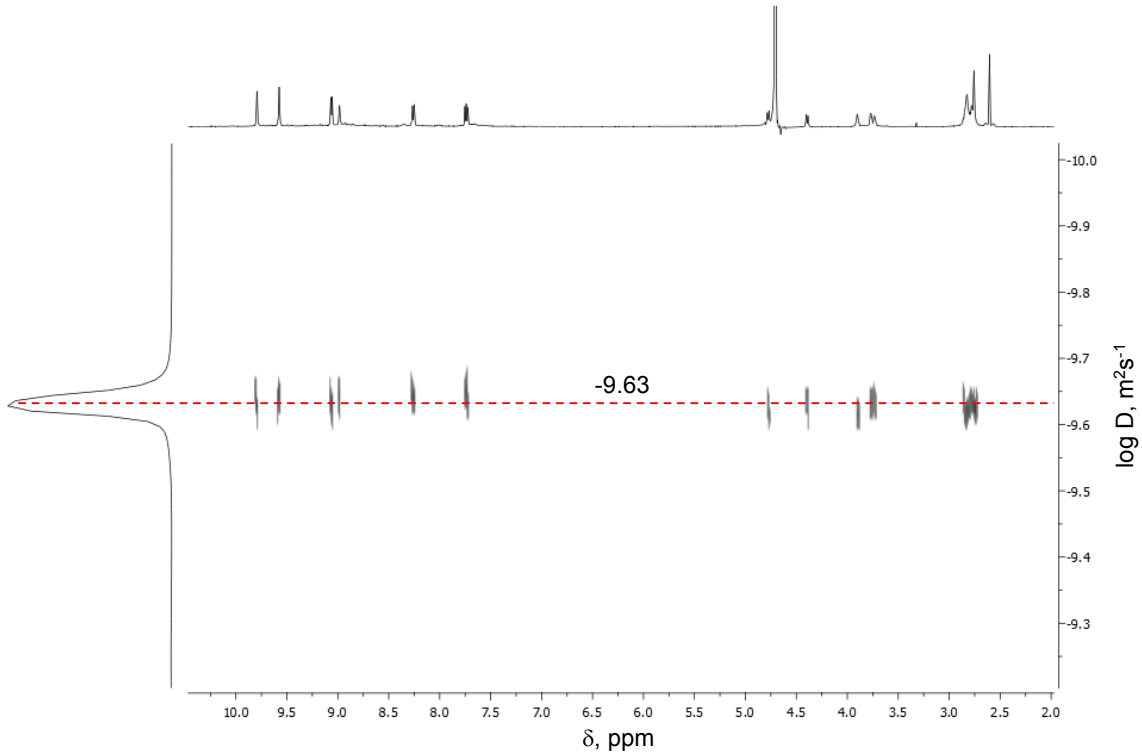

Figure 4.23 ^{1}H DOSY NMR (500 MHz, D_2O, 298 K) spectrum for tube complex **40** with corresponding log D, m^2s^{-1} = -9.63.

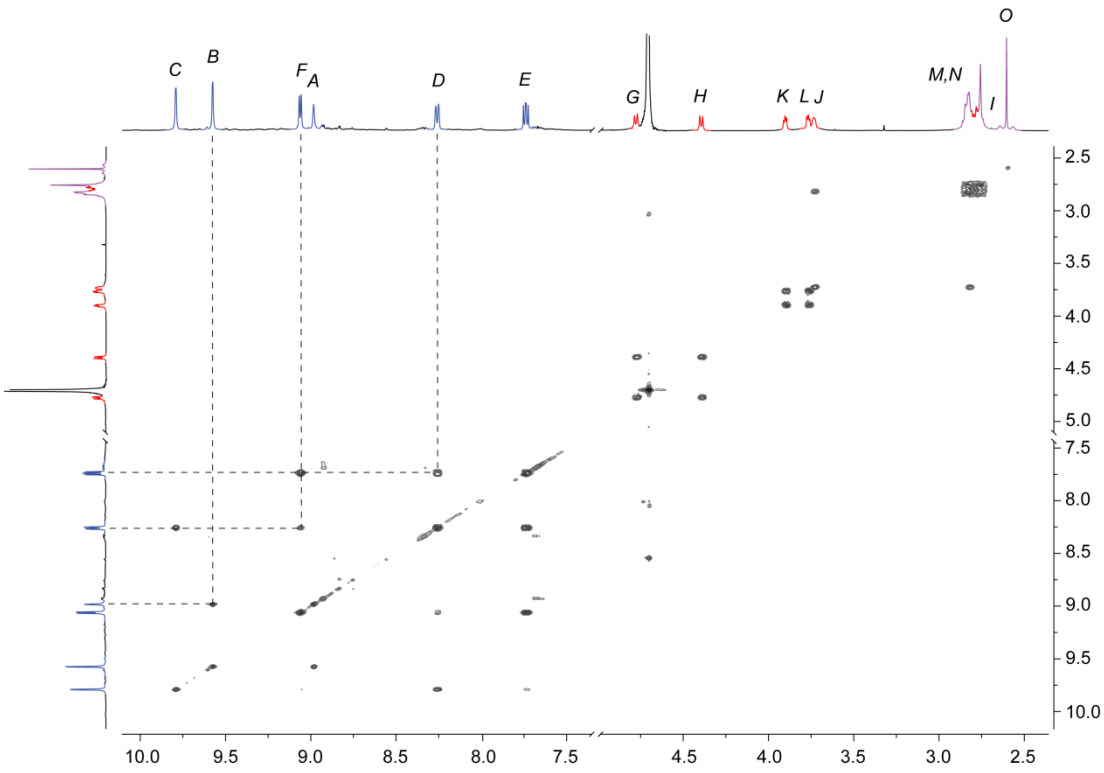

Figure 4.24 $^{1}H,^{1}H$-COSY (500 MHz, D_2O, 298 K) of **40**.

4.5 References

1. P. R. Symmers, M. J. Burke, D. P. August, P. I. T. Thomson, G. S. Nichol, M. R. Warren, C. J. Campbell and P. J. Lusby, *Chem. Sci.*, **2015**.
2. J. W. Steed and J. L. Atwood, *Supramolecular Chemistry*, 2 edn., Wiley, Chichester, 2009.
3. M. D. Ward and P. R. Raithby, *Chem. Soc. Rev.*, **2013**, *42*, 1619-1636.
4. (a) M. Fujita, S. Nagao and K. Ogura, *J. Am. Chem. Soc.*, **1995**, *117*, 1649-1650; (b) M. Fujita, D. Oguro, M. Miyazawa, H. Oka, K. Yamaguchi and K. Ogura, *Nature*, **1995**, *378*, 469-471; (c) P. Jacopozzi and E. Dalcanale, *Angew. Chem. Int. Ed. Engl.*, **1997**, *36*, 613-615; (d) N. Takeda, K. Umemoto, K. Yamaguchi and M. Fujita, *Nature*, **1999**, *398*, 794-796; (e) S. Leininger, J. Fan, M. Schmitz and P. J. Stang, *Proc. Natl. Acad. Sci.*, **2000**, *97*, 1380-1384; (f) S.-Y. Yu, T. Kusukawa, K. Biradha and M. Fujita, *J. Am. Chem. Soc.*, **2000**, *122*, 2665-2666; (g) U. Radhakrishnan, M. Schweiger and P. J. Stang, *Org. Lett.*, **2001**, *3*, 3141-3143; (h) Y. Yamanoi, Y. Sakamoto, T. Kusukawa, M. Fujita, S. Sakamoto and K. Yamaguchi, *J. Am. Chem. Soc.*, **2001**, *123*, 980-981; (i) T. Kusukawa and M. Fujita, *J. Am. Chem. Soc.*, **2002**, *124*, 13576-13582; (j) M. Yoshizawa, M. Nagao, K. Umemoto, K. Biradha, M. Fujita, S. Sakamoto and K. Yamaguchi, *Chem. Commun.*, **2003**, 1808-1809; (k) D. K. Chand, K. Biradha, M. Kawano, S. Sakamoto, K. Yamaguchi and M. Fujita, *Chem. Asian J.*, **2006**, *1*, 82-90; (l) K. Nakabayashi, Y. Ozaki, M. Kawano and M. Fujita, *Angew. Chem. Int. Ed.*, **2008**, *47*, 2046-2048; (m) T. Murase, K. Otsuka and M. Fujita, *J. Am. Chem. Soc.*, **2010**, *132*, 7864-7865; (n) Y.-R. Zheng, Z. Zhao, M. Wang, K. Ghosh, J. B. Pollock, T. R. Cook and P. J. Stang, *J. Am. Chem. Soc.*, **2010**, *132*, 16873-16882; (o) J. J. Henkelis, C. J. Carruthers, S. E. Chambers, R. Clowes, A. I. Cooper, J. Fisher and M. J. Hardie, *J. Am. Chem. Soc.*, **2014**, *136*, 14393-14396.
5. M. Fujita, J. Yazaki and K. Ogura, *J. Am. Chem. Soc.*, **1990**, *112*, 5645-5647.
6. M. Fujita, K. Umemoto, M. Yoshizawa, N. Fujita, T. Kusukawa and K. Biradha, *Chem. Commun.*, **2001**, 509-518.
7. (a) M. Fujita, *Chem. Soc. Rev.*, **1998**, *27*, 417-425; (b) M. Fujita, M. Tominaga, A. Hori and B. Therrien, *Acc. Chem. Res.*, **2005**, *38*, 369-378.
8. (a) M. Aoyagi, K. Biradha and M. Fujita, *J. Am. Chem. Soc.*, **1999**, *121*, 7457-7458; (b) M. Aoyagi, S. Tashiro, M. Tominaga, K. Biradha and M. Fujita, *Chem. Commun.*, **2002**, 2036-2037.
9. (a) S. Sakamoto, M. Fujita, K. Kim and K. Yamaguchi, *Tetrahedron*, **2000**, *56*, 955-964; (b) K. Yamaguchi, *J. Mass Spectrom.*, **2003**, *38*, 473-490.
10. (a) M. Tominaga, S. Tashiro, M. Aoyagi and M. Fujita, *Chem. Commun.*, **2002**, 2038-2039; (b) S. Tashiro, M. Tominaga, T. Kusukawa, M. Kawano, S. Sakamoto, K. Yamaguchi and M. Fujita, *Angew. Chem. Int. Ed.*, **2003**, *42*, 3267-3270; (c) M. Tominaga, M. Kato, T. Okano, S. Sakamoto, K. Yamaguchi and M. Fujita, *Chem. Lett.*, **2003**, *32*, 1012-1013; (d) T. Yamaguchi, S. Tashiro, M. Tominaga, M. Kawano, T. Ozeki and M. Fujita, *J. Am. Chem. Soc.*, **2004**, *126*, 10818-10819.
11. (a) D. Cai, R. D. Larsen and P. J. Reider, *Tetrahedron Lett.*, **2002**, *43*, 4285-4287; (b) W. Li, D. P. Nelson, M. S. Jensen, R. S. Hoerrner, D. Cai, R. D. Larsen and P. J. Reider, *J. Org. Chem.*, **2002**, *67*, 5394-5397.

12. S. Gamsey and R. Wessling, A, Polyviologen Boronic Acid Quenchers for Use in Analyte Sensors, WO2009009756 (A2), **2009**.

13. C. E. Summer, B. J. Hitch and B. L. Bernard, Process for preparation of resorcinol bis(dihydroxyethyl)ether, **1991**.

14. S. A. Caldarelli, S. El Fangour, S. Wein, C. Tran van Ba, C. Périgaud, A. Pellet, H. J. Vial and S. Peyrottes, *J. Med. Chem.*, **2013**, *56*, 496-509.

15. D.-H. Qu, Q.-C. Wang, J. Ren and H. Tian, *Org. Lett.*, **2004**, *6*, 2085-2088.

16. S. Banerjee, E. B. Veale, C. M. Phelan, S. A. Murphy, G. M. Tocci, L. J. Gillespie, D. O. Frimannsson, J. M. Kelly and T. Gunnlaugsson, *Chem. Soc. Rev.*, **2013**, *42*, 1601-1618.

17. A. Shafir, P. A. Lichtor and S. L. Buchwald, *J. Am. Chem. Soc.*, **2007**, *129*, 3490-3491.

18. D. Fujita, A. Takahashi, S. Sato and M. Fujita, *J. Am. Chem. Soc.*, **2011**, *133*, 13317-13319.

19. (a) H. J. Shine, H. Zmuda, K. H. Park, H. Kwart, A. G. Horgan and M. Brechbiel, *J. Am. Chem. Soc.*, **1982**, *104*, 2501-2509; (b) J. K. Clegg, J. Cremers, A. J. Hogben, B. Breiner, M. M. J. Smulders, J. D. Thoburn and J. R. Nitschke, *Chem. Sci.*, **2013**, *4*, 68-76.

20. E. Cordova, R. A. Bissell and A. E. Kaifer, *J. Org. Chem.*, **1995**, *60*, 1033-1038.

21. (a) G. L. Johnson and T. A. Michelfeld, in *Inorganic Syntheses*, John Wiley & Sons, Inc., 1966, pp. 242-244; (b) M. Fujita, J. Yazaki and K. Ogura, *Chem. Lett.*, **1991**, *20*, 1031-1032.

22. (a) M. D. Levin and P. J. Stang, *J. Am. Chem. Soc.*, **2000**, *122*, 7428-7429; (b) B. Olenyuk, M. D. Levin, J. A. Whiteford, J. E. Shield and P. J. Stang, *J. Am. Chem. Soc.*, **1999**, *121*, 10434-10435.

23. (a) B. Jack Mccormick, E. N. Jaynes, R. I. Kaplan, H. C. Clark and J. D. Ruddick, in *Inorganic Syntheses*, John Wiley & Sons, Inc., 1972, pp. 216-218; (b) M. Morell Cerdà, B. Costisella and B. Lippert, *Inorg. Chim. Acta*, **2006**, *359*, 1485-1488.

24. A. Gegout, J. L. Delgado, J.-F. Nierengarten, B. Delavaux-Nicot, A. Listorti, C. Chiorboli, A. Belbakra and N. Armaroli, *New J. Chem.*, **2009**, *33*, 2174-2182.

25. A. E. Thompson, G. Hughes, A. S. Batsanov, M. R. Bryce, P. R. Parry and B. Tarbit, *J. Org. Chem.*, **2004**, *70*, 388-390.

26. W. Lin, X. Zhang, Z. He, Y. Jin, L. Gong and A. Mi, *Synth. Commun.*, **2002**, *32*, 3279-3284.

Conclusion and Outlook

The acid-base responsive switching between “3+1” and “2+2” cyclometallated platinum complexes has been explored in Chapter II. These types of externally addressable coordination complexes have the potential to be further developed into a bistable molecular shuttle.

In Chapter III, attempts to synthesise a platinum complexed-[2]rotaxane have been investigated. The CuAAC “click” rotaxane product failed to complex to platinum(II) which necessitated redesigns of the rotaxanes. A platinum complexed-macrocycle was then used to carry out ligand exchange reactions with series of 3,5-disubstituted pyridine based-thread. Still, the instability of the rotaxane precursor and difficulties in separation were encountered. The conditions that can overcome these reactivity problems without disturbing the macrocycle-thread interactions and the suitable separation procedure are yet to be determined and a further redesign will be required to finish the rotaxane. Once the rotaxane is realised, studies of acid-base stimuli-responsive bistable platinum-complexed [2]rotaxane can be explored as suggested from the positive results of the “3+1” to “2+2” interconversion of non-interlocked platinum C^N^C macrocyclic compounds in Chapter II.

In Chapters IV, the metal-directed self-assembly of tubular complexes were studied. The self-assembly of tris- and pentakis(3,5-pyridine) with [(en)Pd(NO_3)$_2$] in the presence of biphenyl with ethyleneoxide side chain was successful in forming tubular structures. The stoppered template, however, did not give any evidence of rotaxane formation. A variety of rod-like templates also showed no positive template effect, including azobenzene, stilbene, anthracene, 4,4’-bipyridine, alkyl chain functionalized biphenol, benzidine. Different metal building blocks including [(en)Pt(NO_3)$_2$] and [Co(12ane[S_4])(ClO_4)$_2$] were used to determine the self-assembly. The Pt^{II} analogue tube only formed a tris(3,5-pyridine) tube after a week at 100 °C, whereas the cobalt-thiacrown ether complexes did not form any discrete tube. More detailed studies of the non-covalent interactions between the template molecule and host framework need to be undertaken to improve the better system design. Another obvious area for investigation would be the use of alternative non-anionic stoppers. A self-assembled rotaxane would be a potential tool for molecular machines studies as the complex organic synthesis has been circumvented.

Appendix: Published paper

"Acid-base responsive switching between "3+1" and "2+2" platinum complexes" D. Sooksawat, S. J. Pike, A. M. Z. Slawin, P. J. Lusby, *Chem. Commun.,* **2013**, *49*, 11077-11079.

ChemComm

RSC Publishing

COMMUNICATION

View Article Online
View Journal | View Issue

Acid–base responsive switching between "3+1" and "2+2" platinum complexes†

Cite this: *Chem. Commun.*, 2013, **49**, 11077

Received 28th August 2013,
Accepted 15th October 2013

DOI: 10.1039/c3cc46587j

www.rsc.org/chemcomm

Dhassida Sooksawat,[a] Sarah J. Pike,[a] Alexandra M. Z. Slawin[b] and Paul J. Lusby*[a]

We report that the acid–base induced changes to a cyclometallated platinum complex can be used to drive the exchange of accompanying ligands with different denticities.

Central to the development of synthetic molecular machines is the discovery of new externally addressable, switchable molecular or supramolecular elements.[1] Bistable rotaxanes and catenanes which utilise transition metal–ligand interactions are particularly attractive,[2–5] not least because their inherent strength can be used for purposes such as ratcheting.[6] Another desirable feature of switchable systems is that they should exhibit a large thermodynamic bias in both states. In this regard, the benchmark for systems where the metal ion remains integrated during operation[4] is still Sauvage's exploitation of the preferred coordination differences of Cu(I) and Cu(II), which was first described nearly twenty years ago.[2a] Herein, we describe cyclometallated platinum motifs which are able to exchange monodentate and bidentate ligands with excellent selectivity in response to acid–base stimuli.

We recently reported that 2,6-diphenylpyridine ($H_2\mathbf{L^1}$) can coordinate to platinum(II) either as a doubly anionic tridentate or monoanionic bidentate ligand, and that this can be exploited to assemble–disassemble metallosupramolecular architectures based on *cis*-coordinating multitopic pyridyl ligands.[7] As well as accepting two monodentate ligands, we envisaged that a platinum complex where $H\mathbf{L^1}$ coordinates in a η^2 C^N fashion would be able to accommodate a neutral bidentate ligand. Thus, when [$\mathbf{L^1}$Pt(DMSO)] was treated with a mixture of *para*-toluene sulfonic acid (TsOH) and 5,5′-dimethyl-2,2′-bipyridine (dmbipy) in CH_2Cl_2, a compound was isolated which spectroscopic data indicated was the "2+2" complex, [$H\mathbf{L^1}$Pt(dmbipy)]OTs. For instance, the ^{1}H NMR spectrum (see ESI†) showed that the two pyridyl "halves" of the dmbipy ligand resonate quite differently, fully consistent with the occupation of the *trans*-to-nitrogen and *trans*-to-phenylato coordination sites, the latter which experiences pronounced shielding from the non-coordinating phenyl group of $H\mathbf{L^1}$. The structure of [$H\mathbf{L^1}$Pt(dmbipy)]OTs, confirmed by X-ray crystallography (Fig. 1a) using crystals grown from diisopropyl ether and chloroform, shows that while platinum adopts a near planar geometry (the Pt ion sits just 0.078 Å above the mean N_3C coordination plane) there is significant distortion and twisting of the ligands to alleviate steric clash between the non-coordinating phenyl group and the adjacent dmbipy ligand such that the complex adopts an overall helical twist.[8] In the solid state, both *P* and *M* enantiomers are observed, although in solution at room temperature the interconversion appears to be rapid.[9]

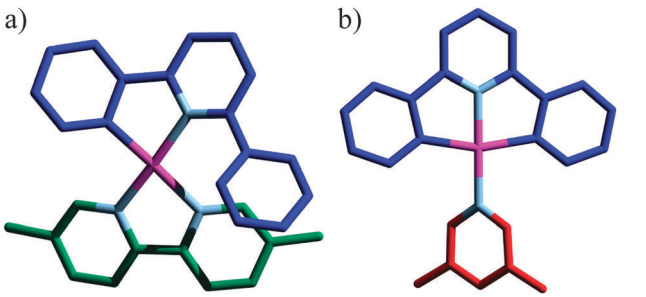

Fig. 1 X-ray crystal structures of (a) [$H\mathbf{L^1}$Pt(dmbipy)]OTs and (b) [$\mathbf{L^1}$Pt(3,5-lut)]. Colour code: C($\mathbf{L^1}$/$H\mathbf{L^1}$), blue; C(3,5-lut), red; C(dmbipy), green; N, light blue; Pt, magenta. Counter anion and solvent molecules have been removed for clarity.

To explore whether other neutral monodentate ligands would be similarly displaced, experiments starting with [$\mathbf{L^1}$Pt(py)], [$\mathbf{L^1}$Pt(3,5-lut)] and [$\mathbf{L^1}$Pt(DMAP)] (py = pyridine; 3,5-lut = 3,5-lutidine; DMAP = 4-dimethylaminopyridine) have been undertaken (Scheme 1). In the absence of TsOH, ^{1}H NMR spectroscopy shows that, in all cases, dmbipy does not displace the monodentate ligand and remains uncoordinated (see the ESI,† Fig. S1–S3). For [$\mathbf{L^1}$Pt(py)], the addition of a slight excess (1.3 eq.) of TsOH to the charge neutral complex and dmbipy results in the rapid displacement of the monodentate ligand and concomitant generation of [$H\mathbf{L^1}$Pt(dmbipy)]OTs (Scheme 1 and Fig. S1, ESI†). When similar ligand exchange experiments were carried out with [$\mathbf{L^1}$Pt(3,5-lut)] and [$\mathbf{L^1}$Pt(DMAP)], it was found that the addition of over two equivalents of TsOH was required in order to

[a] *EaStCHEM School of Chemistry, University of Edinburgh, The King's Buildings, West Mains Road, Edinburgh, EH9 3JJ, UK. E-mail: Paul.Lusby@ed.ac.uk; Fax: +44-131-6506453; Tel: +44-131-6504832*

[b] *School of Chemistry, University of St. Andrews, Purdie Building, St. Andrews, Fife, UK KY16 9ST*

† Electronic supplementary information (ESI) available: This includes all synthetic procedures, compound characterisation, ligand exchange experiments and crystallographic data. CCDC 956076–956078. For ESI and crystallographic data in CIF or other electronic format see DOI: 10.1039/c3cc46587j

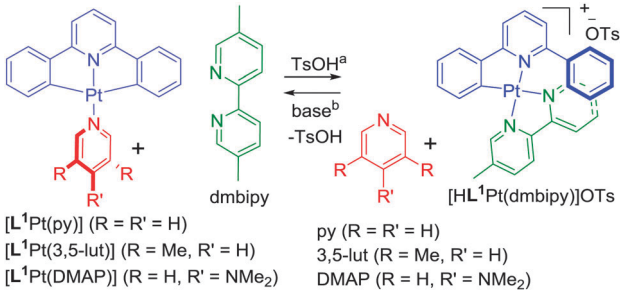

Scheme 1 Acid–base interconversion between ''3+1'' and ''2+2'' cyclometallated Pt complexes. Conditions: [a] 1.3–2.7 eq. TsOH, CD_2Cl_2, 298 K, 5 min; [b] P_1-^{t}Bu, CD_2Cl_2, 298 K, 1.5–2 h.

generate the "2+2" complex (Fig. S2 and S3, ESI†). We attribute this difference to two main factors – (i) the increased basicity of the liberated 3,5-lut and DMAP heterocycles, which leads to partial re-cyclometallation and (ii) the formation of more stable "2+1+1" intermediates (*e.g.* [HL^{1}Pt(DMAP)OTs] and [HL^{1}Pt(3,5-lut)OTs]), from which the chelate-driven displacement of DMAP/3-5-lut and tosylate ligands by dmbipy requires additional proton-assistance (for further discussion of these processes, see the ESI†).

As the pyridyl-based ligands are not replaced in the absence of acid, we predicted that simply adding base to a mixture of [HL^{1}Pt(dmbipy)]-OTs and monodentate moiety would reverse the coordinative bias. We have previously used the phosphazene base, P_1-^{t}Bu, to affect (re)cyclometallation.[7] Thus, when P_1-^{t}Bu was added to the mixture of [HL^{1}Pt(dmbipy)]OTs and monodentate pyridyl ligand (py, 3,5-lut or DMAP), the gradual disappearance of signals due to [HL^{1}Pt(dmbipy)]-OTs and re-appearance of [L^{1}Pt(py)], [L^{1}Pt(3,5-lut)] and [L^{1}Pt(DMAP)] followed 1.5–2 h at room temperature (Scheme 1 and Fig. S1–S3, ESI†).

To develop the system further, and with a stimuli-responsive molecular shuttle in mind, the macrocyclic C^N^C Pt complex, [L^{2}Pt(DMSO)], has been prepared. The free macrocycle, H_2L^2, was obtained in an excellent 80% from 2,6-di-(4-hydoxyphenyl)pyridine[10] and a bisphenol A derived dialkylbromide,[11] while insertion of platinum also occurs in an highly respectable 80% yield (see ESI†). From [L^{2}Pt(DMSO)], [L^{2}Pt(3,5-lut)] was prepared by exchange of the coordinated DMSO for 3,5-lut (Scheme 2, step a). The structure of [L^{2}Pt(3,5-lut)] has been confirmed by X-ray crystallography using single crystals grown from slow diffusion of diethyl ether into a saturated dichloromethane solution (Fig. 2). In solution, the ^{1}H NMR spectrum of [L^{2}Pt(3,5-lut)] (Fig. 3a) exhibits coordinated *ortho* lutidine signals (H_a) with characteristic ^{195}Pt satellites, while the *para* site (H_b) is significantly upfield shifted with respect to the free heterocycle, most likely due to shielding by the bisphenol A unit.

The TsOH induced formation of a "2+2" complex from [L^{2}Pt(DMSO)], this time using the unsymmetrical bidentate 2-(1-ethyl-phenyl-1*H*-1,2,3-triazol-4-yl)-5-bromopyridine (L^3) was also carried out (Scheme 2, step b). The ^{1}H NMR spectrum of the product revealed several interesting features (Fig. 3e). Firstly, when it could be reasonably expected that a mixture of both geometric isomers would result, only one – *trans*-[HL^{2}Pt(L^3)]OTs (see the ESI† for details of assignment using NOESY) – is produced. As the NMR of this product did not change over time, we would suggest that this product is both the kinetically and thermodynamically favoured isomer, as it has been previously observed that platinum isomers which feature cyclometallated ligands undergo sluggish rearrangement.[12] The second thing to note from the ^{1}H NMR

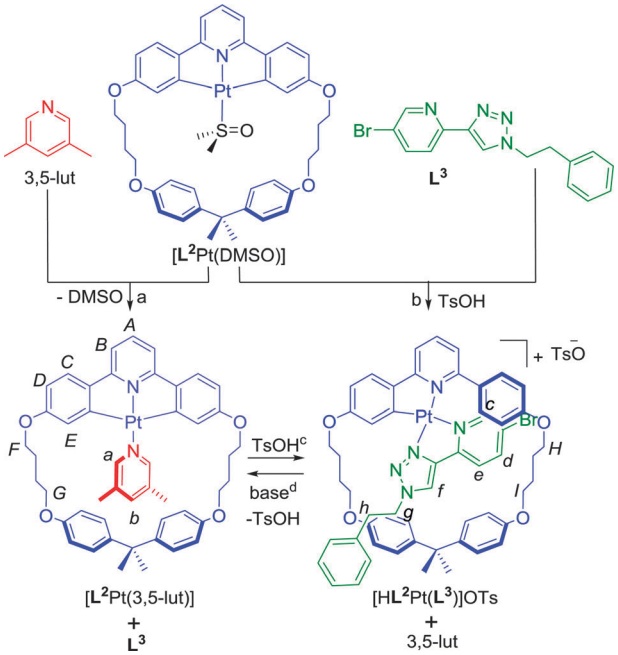

Scheme 2 Synthesis of, and acid–base responsive interconversion between, ''3+1'' and ''2+2'' macrocyclic cyclometallated Pt complexes. Conditions: [a] CH_2Cl_2, 313 K, 16 h, 37%; [b] CH_2Cl_2, 298 K, 1 h, 34%; [c] 1.7 eq. TsOH, CD_2Cl_2, 298 K, 5 min; [d] 5 eq. P_1-^{t}Bu, CD_2Cl_2, 298 K, 48 h.

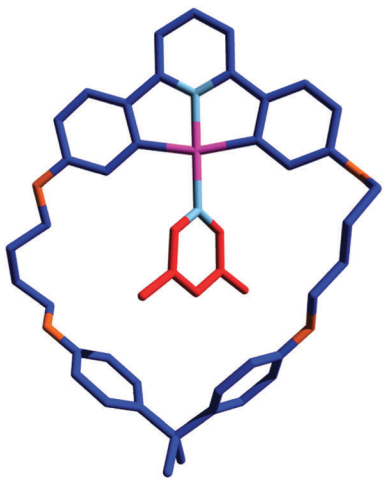

Fig. 2 X-ray crystal structure of [L^{2}Pt(3,5-lut)]. Colour code: C(L^2), blue; C(3,5-lut), red; N, light blue; O, orange; Pt, magenta. Solvent molecules have been removed for clarity.

spectrum of [HL^{2}Pt(L^3)]OTs (Fig. 3e) is the sterically congested nature of the complex, as the four triplets that arise from the H_F, H_G, H_g and H_h environments in the [L^{2}Pt(3,5-lut)] and L^3 precursors have been replaced by a complex diastereotopic pattern of signals.

Finally, the "3+1" to "2+2" interconversion between [L^{2}Pt(3,5-lut)] and [HL^{2}Pt(L^3)]OTs was examined using ^{1}H NMR spectroscopy (Scheme 2 and Fig. 3b–d). When L^3 was mixed with [L^{2}Pt(3,5-lut)] in CD_2Cl_2, only signals which are attributable to those two species were apparent (Fig. 3b). Upon the addition of 1.7 eq. of TsOH, the NMR spectrum changed to give a set of signals that were virtually indistinguishable from those of *trans*-[HL^{2}Pt(L^3)]OTs (Fig. 3c). As with the acyclic system, this change occurred within the time taken to record a subsequent spectrum. This rapid generation coupled to

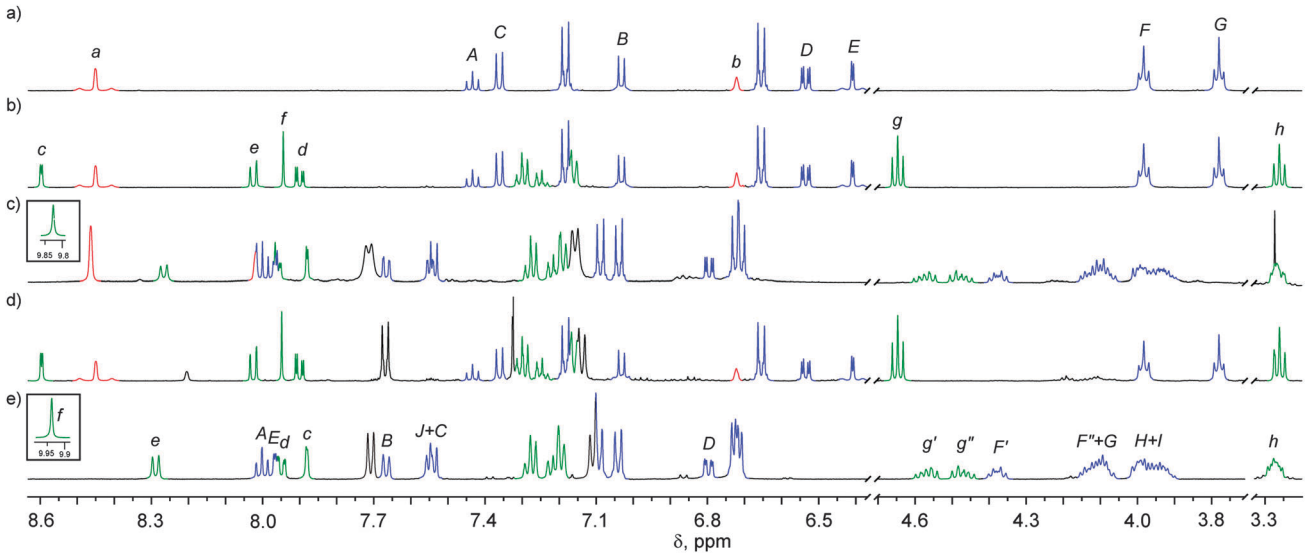

Fig. 3 Partial ^{1}H NMR spectra (CD_2Cl_2, 500 MHz, 300 K) showing interconversion between "3+1" and "2+2" macrocyclic cyclometallated Pt complexes. (a) [$\mathbf{L}^2$Pt(3,5-lut)]; (b) a 1 : 1 mixture of [$\mathbf{L}^2$Pt(3,5-lut)] and $\mathbf{L}^3$; (c) a 1 : 1 mixture of [$\mathbf{L}^2$Pt(3,5-lut)] and $\mathbf{L}^3$, 5 minutes after the addition of TsOH (1.7 eq.); (d) 48 h after the addition of P_1-^{t}Bu (5 eq.) to a solution of [H$\mathbf{L}^2$Pt($\mathbf{L}^3$)]OTs and 3,5-lut; (e) [H$\mathbf{L}^2$Pt($\mathbf{L}^3$)]OTs. Macrocycle signals are shown in blue, 3,5-lut in red and $\mathbf{L}^3$ in green. The assignments correspond to the lettering shown in Scheme 2.

the lack of observation of another isomer further supports that *trans*-[H$\mathbf{L}^2$Pt($\mathbf{L}^3$)]OTs is the kinetic (and thermodynamic) product, irrespective of the neutral monodentate ligand in the starting "3+1" complex. When five eq. of P_1-^{t}Bu was added to the NMR sample containing [H$\mathbf{L}^2$Pt($\mathbf{L}^3$)]OTs and free lutidine, the signals due to the "2+2" complex and monodentate ligand started to disappear, accompanied by the appearance of signals due to [$\mathbf{L}^2$Pt(3,5-lut)] and free $\mathbf{L}^3$. After 48 h, only signals due to [$\mathbf{L}^2$Pt(3,5-lut)] and free $\mathbf{L}^3$ could be observed (Fig. 3d). The sluggishness of this reaction in comparison to the same process for the acyclic complexes is almost certainly due to an increased steric barrier. We are currently investigating methods of lowering this by employing different bases/anions and/or using light to accelerate ligand exchange.[12a]

In summary, a rare example of a metallosupramolecular switch which can be alternated with excellent selectivity between different states using acid–base inputs has been described. We envisage that these types of externally addressable coordination complexes will continue to play a significant role in the development of molecular machines.

This work was supported by the EPSRC and The Royal Society. P.J.L. is a Royal Society University Research Fellow.

Notes and references

1 E. R. Kay, D. A. Leigh and F. Zerbetto, *Angew. Chem., Int. Ed.*, 2007, **46**, 72.
2 For interlocked systems which are able to switch between two transition metal-bound states, see (*a*) A. Livoreil, C. O. Dietrich-Buchecker and J.-P. Sauvage, *J. Am. Chem. Soc.*, 1994, **116**, 9399; (*b*) D. J. Cárdenas, A. Livoreil and J.-P. Sauvage, *J. Am. Chem. Soc.*, 1996, **118**, 11980; (*c*) A. Livoreil, J.-P. Sauvage, N. Armaroli, V. Balzani, L. Flamigni and B. Ventura, *J. Am. Chem. Soc.*, 1997, **119**, 12114; (*d*) N. Armaroli, V. Balzani, J.-P. Collin, P. Gaviña, J.-P. Sauvage and B. Ventura, *J. Am. Chem. Soc.*, 1999, **121**, 4397; (*e*) J.-P. Collin, F. Durola, J. Lux and J.-P. Sauvage, *Angew. Chem., Int. Ed.*, 2009, **48**, 8532; (*f*) J.-P. Collin, F. Durola, J. Lux and J.-P. Sauvage, *New J. Chem.*, 2010, **34**, 34; (*g*) J. D. Crowley, D. A. Leigh, P. J. Lusby, R. T. McBurney, L.-E. Perret-Aebi, C. Petzold, A. M. Z. Slawin and M. D. Symes, *J. Am. Chem. Soc.*, 2007, **129**, 15085; (*h*) D. A. Leigh, P. J. Lusby, R. T. McBurney and M. D. Symes, *Chem. Commun.*, 2010, **46**, 2382.
3 For interlocked systems which switch between a transition metal bound state and one other state, see (*a*) P. Mobian, J.-M. Kern and J.-P. Sauvage, *Angew. Chem., Int. Ed.*, 2004, **43**, 2392; (*b*) J.-P. Collin, D. Jouvenot, M. Koizumi and J.-P. Sauvage, *Eur. J. Inorg. Chem.*, 2005, 1850; (*c*) M. J. Barrell, D. A. Leigh, P. J. Lusby and A. M. Z. Slawin, *Angew. Chem., Int. Ed.*, 2008, **47**, 8036; (*d*) Z. Xue and M. F. Mayer, *J. Am. Chem. Soc.*, 2010, **132**, 3274.
4 For interlocked systems which switch between different transition metal-bound states through transmetallation, see (*a*) M. C. Jiménez, C. Dietrich-Buchecker and J.-P. Sauvage, *Angew. Chem., Int. Ed.*, 2000, **39**, 3284; (*b*) J. D. Crowley, K. D. Hänni, D. A. Leigh and A. M. Z. Slawin, *J. Am. Chem. Soc.*, 2010, **132**, 5309; (*c*) D. A. Leigh, P. J. Lusby, A. M. Z. Slawin and D. B. Walker, *Chem. Commun.*, 2012, **48**, 5826.
5 For non-interlocked metallosupramolecular (mechanical) switches, see (*a*) L. Fabbrizzi, F. Gatti, P. Pallavicini and E. Zambarbieri, *Chem.–Eur. J.*, 1999, **5**, 682; (*b*) S. Akine, S. Hotate and T. Nabeshima, *J. Am. Chem. Soc.*, 2011, **133**, 13868; (*c*) G. Tsekouras, O. Johansson and R. Lomoth, *Chem. Commun.*, 2009, 3425; (*d*) K. A. McNitt, K. Parimal, A. I. Share, A. C. Fahrenbach, E. H. Witlicki, M. Pink, D. K. Bediako, C. L. Plaisier, N. Le, L. P. Heeringa, D. A. V. Griend and A. H. Flood, *J. Am. Chem. Soc.*, 2009, **131**, 1305; (*e*) X. Su, T. F. Robbins and I. Aprahamian, *Angew. Chem., Int. Ed.*, 2011, **50**, 1841; (*f*) M. Schmittel, S. De and S. Pramanik, *Angew. Chem., Int. Ed.*, 2012, **51**, 3832; (*g*) C. W. Machan, M. Adelhardt, A. A. Sarjeant, C. L. Stern, J. Sutter, K. Meyer and C. A. Mirkin, *J. Am. Chem. Soc.*, 2012, **134**, 16921.
6 (*a*) M. N. Chatterjee, E. R. Kay and D. A. Leigh, *J. Am. Chem. Soc.*, 2006, **128**, 4058; (*b*) V. Serreli, C.-F. Lee, E. R. Kay and D. A. Leigh, *Nature*, 2007, **445**, 523; (*c*) A. Carlone, S. M. Goldup, N. Lebrasseur, D. A. Leigh and A. Wilson, *J. Am. Chem. Soc.*, 2012, **134**, 8321.
7 P. J. Lusby, P. Müller, S. J. Pike and A. M. Z. Slawin, *J. Am. Chem. Soc.*, 2009, **131**, 16398.
8 C. Deuschel-Cornioley, H. Stoeckli-Evans and A. von Zelewsky, *J. Chem. Soc., Chem. Commun.*, 1990, 121.
9 *In situ* generated [H$\mathbf{L}^1$Pt(dmbipy)]CSA (CSA = camphorsulfonate) only shows a single set of ^{1}H NMR resonances in CD_2Cl_2, a solvent in which tight ion pairing could be expected. Similarly, the addition of TRISPHAT to [H$\mathbf{L}^1$Pt(dmbipy)]OTs in CD_2Cl_2 does not show any signal splitting. See the ESI† for details. The low energy interconversion between diastereoisomers would suggest a mechanism which doesn't involve decoordination of dmbipy.
10 V. Aucagne, J. Berná, J. D. Crowley, S. M. Goldup, K. D. Hänni, D. A. Leigh, P. J. Lusby, V. E. Ronaldson, A. M. Z. Slawin, A. Viterisi and D. B. Walker, *J. Am. Chem. Soc.*, 2007, **129**, 11950.
11 F. Durola, J.-P. Sauvage and O. S. Wenger, *Helv. Chim. Acta*, 2007, **90**, 1439.
12 (*a*) S. J. Pike and P. J. Lusby, *Chem. Commun.*, 2010, **46**, 8338; (*b*) O. Chepelin, J. Ujma, P. E. Barran and P. J. Lusby, *Angew. Chem., Int. Ed.*, 2012, **51**, 4194.